

# Henry's Law Constant from Molecular Simulation: a Systematic Study of 95 Systems

Yow-Lin Huang<sup>1</sup>, Svetlana Miroshnichenko<sup>1</sup>, Hans Hasse<sup>2</sup>, Jadran Vrabec<sup>\*1</sup>

<sup>1</sup> Lehrstuhl für Thermodynamik und Energietechnik, Universität Paderborn, Warburger Straße 100, 33098 Paderborn, Germany

<sup>2</sup> Lehrstuhl für Thermodynamik, Technische Universität Kaiserslautern, Erwin-Schrödinger-Straße 44, 67663 Kaiserslautern, Germany

**Keywords** Henry's law constant; vapor-liquid equilibria; molecular mixture model; unlike interaction

## Abstract

A set of molecular models from prior work for 78 pure substances is taken as a basis for systematically studying the temperature dependence of the Henry's law constant in pure solvents. All 95 binary mixtures that can be formed out of these 78 components, and for which experimental Henry's law constant data are available, are investigated by molecular simulation. The mixture models are based on the modified Lorentz-Berthelot combining rule that contains one binary interaction parameter which is adjusted to the Henry's law constant at one temperature or, in preceding work, to the binary system vapor pressure. The predictions from the molecular models of the 95 binary mixtures are compared to available experimental data. In most cases, the molecular models yield good predictions for the gas solubility. It is found that the models are generally capable of yielding reliable data both at infinite dilution and at finite mole fractions.

---

\* corresponding author, tel.: +49-5251/60-2421, fax: +49-5251/60-3522,  
email: jadran.vrabec@upb.de

## 1 Introduction

Thermodynamic data on the distribution of the components in coexisting vapor and liquid phases are essential for a wide range of technical applications. A common classification distinguishes between mixtures in which the components have a similar volatility and mixtures in which the components have a strongly differing volatility. In the first case, for binary mixtures, considerable amounts of both components can be found in the coexisting phases, and the characterization of the equilibrium requires, for a given pair of temperature and pressure, both the liquid composition and the vapor composition. Depending on the mixture, a large variation in the distribution of the components is found, leading to qualitatively different forms of the two-phase envelope, such as for zeotropic or azeotropic systems. In the second case, the liquid overwhelmingly contains the component with low volatility (i.e., solvent), while the vapor is composed mainly of the volatile component (i.e., solute). The two-phase envelope is thus wide and has a characteristic shape. For example, it is observed at constant temperature that the solute mole fraction in the liquid increases approximately linearly with the pressure. This has given rise to a condensed characterization of the phase equilibrium in such cases through the Henry's law constant  $H_i$ . Considering a mixture of two components, classically the phase equilibrium condition for the solute  $i$  at a specified pair of temperature  $T$  and pressure  $p$  is then given by [1, 2]

$$H_i \exp \left\{ \frac{1}{k_B T} \int_{p_S^S}^p v_i^\infty dp \right\} x_i \gamma_i^* = p y_i \phi_i, \quad (1)$$

where  $x_i$  and  $y_i$  are the solute mole fractions in the saturated liquid and vapor phases, respectively,  $v_i^\infty$  is the partial molar volume of the solute at infinite dilution in the liquid, and  $k_B$  is the Boltzmann constant. Non-idealities of the liquid phase are considered by the activity coefficient normalized according to Henry's law  $\gamma_i^*$ , and of the vapor phase by the fugacity coefficient  $\phi_i$ . The exponential term, known as the Krichevski-Kasarnovski correction [3], accounts for the dependence of the chemical potential of the solute on the pressure  $p$ , where  $p_S^S$  stands for the pure solvent vapor pressure.

For the equilibrium condition of the solvent S, typically the extended form of Raoult's law is used [1, 2]

$$p_S^s \phi_S^s \exp \left\{ \frac{1}{k_B T} \int_{p_S^s}^p v_S dp \right\} x_S \gamma_S = p y_S \phi_S, \quad (2)$$

where  $\phi_S^s$  is the fugacity coefficient of the solvent at saturation,  $\gamma_S$  is the activity coefficient normalized according to Raoult's law, and  $v_S$  is the volume of the liquid solvent. Note that the exponential term is known as the Poynting correction.

Often the non-ideality of the phases and the Krichevski-Kasarnovski term as well as the Poynting correction are neglected, so that a very simple expression for the phase equilibrium remains, which only includes the pure substance solvent vapor pressure and the Henry's law constant.

The aim of this work is to predict the temperature dependence of the Henry's law constant in a systematic manner for a wide range of solutes and solvents by molecular modeling and simulation. The predictions are based on the polar two-center Lennard-Jones (2CLJ) potential that has been parameterized in previous work of our group for 78 components [4, 5]. These are 78 small molecules consisting of up to nine atoms that belong to different classes of fluids, including noble gases, alkanes, halogens, and numerous refrigerants. For many of the 78 molecules, the polar 2CLJ model is only a crude assumption. For example, the asymmetry of molecules is neglected, and the polar interaction is always aligned along the molecular axis. Also the polarizability, which is often assumed to be a crucial molecular property for thermodynamics, is only implicitly considered by Lennard-Jones interaction sites. Furthermore, the internal degrees of freedom are neglected, as the polar 2CLJ models are rigid.

Following a combinatorial approach, all binary mixtures for which experimental data on the Henry's law constant are available were studied here. This work extends a preceding publication on binary vapor-liquid equilibria (VLE) [6], where the same group of components has been regarded in the same combinatorial sense but at different conditions, i.e., at finite mole fractions. Such data are termed as VLE data in the following. Due

to the fact that for 29 binary combinations, both VLE [6] and Henry's law constant data are available, it was also investigated here whether molecular models are capable of yielding consistent results for both types of data.

Molecular modeling and simulation have been used for more than two decades for calculating the Henry's law constant. In the early works [7, 8, 9, 10], usually model mixtures of Lennard-Jones spheres without reference to real fluids were considered. Lotfi and Fischer [11] also simulated mixtures of Lennard-Jones spheres, however, they applied them to real fluid systems such as He in liquid CH<sub>4</sub> or Ne in liquid Kr. The influence of the unlike interaction between the two molecule species was also investigated by applying different combining rules [11].

Mixtures of real components became better accessible through the development of simulation methodology and computing infrastructure. For example, Boulougouris et al. [12] calculated the solubility of CH<sub>4</sub> in liquid C<sub>2</sub>H<sub>6</sub> and of the same solute in liquid water. Due to their technical importance, the solubility of larger hydrocarbons such as n-butane, n-hexane, cyclohexane, or benzene in liquid water was also studied [13, 14]. Other systems, including CO<sub>2</sub> in liquid water [15] or O<sub>2</sub> in liquid benzene [16], were investigated as well.

The Industrial Fluid Property Simulation Collective [17] challenged the molecular simulation community in 2004 to predict the Henry's law constant for Ar, N<sub>2</sub>, CH<sub>4</sub>, and C<sub>2</sub>H<sub>6</sub> in liquid ethanol. The submitted contributions have shown the capability of the molecular approach to determine this thermodynamic property [18, 19, 20, 21, 22].

In terms of simulation methodology, there is a variety of possibilities for determining the Henry's law constant. The most straightforward route is to sample the phase space of the solvent either by molecular dynamics or Monte-Carlo and to calculate the chemical potential of the solute at infinite dilution through insertions of test molecules by Widom's method [23]. However, if the density of the solvent is very high, e.g., in the case of liquid water around ambient conditions, successful test molecule insertions become highly unlikely, which deteriorates the statistics. Solutions to this problem are discussed in a recent review [1].

## 2 Experimental Database

In this work, experimental data were predominately retrieved using the Dortmunder Datenbank (DDB) [24]. Theoretically, out of the  $N = 78$  components modeled in [4, 5]  $N(N - 1)/2 = 3003$  binary mixtures can be formed, but of course, by far not all of these systems have been studied experimentally. For 95 systems, experimental Henry's law constant data were found in 72 publications [25]-[96]; thereof, for 29 binary mixtures experimental VLE data are also available [6].

The 95 binary systems studied here include 41 of the 78 pure components; cf. Table 1 for the full component list including their CAS RN numbers for proper identification. Please note that the ASHRAE nomenclature is used in the following due to its brevity, despite its deficiencies [97]. Of the 41 components, 20 act as solutes, 15 as solvents, and six as solutes and solvents, since they are studied in mixtures with less and more volatile components, cf. Table 1.

The 95 binary systems studied are listed in Table 2, together with a reference to the experimental  $H_i$  data, indicating the subgroup of 29 systems for which experimental VLE data are available as well.

## 3 Pure Fluid Models

In this work, 41 polar 2CLJ-based molecular models were used, taken from [4, 5]. These are five spherical non-polar (1CLJ) models for noble gases and CH<sub>4</sub>, one spherical dipolar (1CLJD) model for R30, furthermore 16 elongated dipolar (2CLJD) models which include CO and numerous refrigerants, and finally 19 elongated quadrupolar (2CLJQ) models, which include N<sub>2</sub>, O<sub>2</sub>, alkanes, refrigerants, and CO<sub>2</sub>.

A detailed description of the polar 2CLJ pair potential is provided in [6] and not repeated here. Generally, polar 2CLJ models have four parameters: size  $\sigma$ , energy  $\epsilon$ , elongation  $L$ , and dipole moment  $\mu$  or quadrupole moment  $Q$ ; Stockmayer models have a vanishing elongation, while the non-polar spherical LJ models have only two parameters:  $\sigma$  and  $\epsilon$ . Both their elongation and polarity are zero. Model parameters were adjusted in [4, 5]

to experimental pure fluid VLE data using global correlations of critical temperature, saturated liquid density, and vapor pressure as functions of these molecular parameters [98, 99]. These pure substance model parameters are not repeated here. Typically, the deviations between the molecular models and the experiment are below 1 % for the saturated liquid density and below 3 % for the vapor pressure [4, 5].

It should be noted that a wide range of polar moments are covered by the 41 pure substance models. Starting from a non-existent polar moment in the case of the noble gases and CH<sub>4</sub>, it ranges up to 1.5984 · 10<sup>-29</sup> Cm (4.7919 D) for the dipolar R130a and up to 5.3847 · 10<sup>-39</sup> Cm<sup>2</sup> (16.143 DÅ) for the quadrupolar R1110.

#### 4 Henry's Law Constant From Molecular Models

Several approaches have been proposed in the literature to obtain the Henry's law constant on the basis of molecular models. Here, a straightforward route was followed. The Henry's law constant  $H_i$  is related to the residual chemical potential of the solute  $i$  at infinite dilution in the solvent  $\mu_i^\infty$  [7, 18] by

$$H_i = \rho_S k_B T \exp(\mu_i^\infty / (k_B T)), \quad (3)$$

where  $\rho_S$  is the density of the solvent in its saturated liquid state.

In order to evaluate  $\mu_i^\infty$ , a molecular dynamics simulation applying Widom's test particle method [23] was used here. Therefore, test molecules representing the solute  $i$  were inserted into the pure saturated liquid solvent after each time step at random spatial coordinates, and the potential energy  $\psi_i$  between the solute test molecule  $i$  and all solvent molecules was calculated within the cut-off radius by

$$\mu_i^\infty = -k_B T \ln \langle V \exp(-\psi_i / (k_B T)) \rangle / \langle V \rangle, \quad (4)$$

where  $V$  is the volume and the brackets represent the  $NpT$  ensemble average.

The residual chemical potential at infinite dilution  $\mu_i^\infty$  and hence the Henry's law constant  $H_i$  is directly related to the unlike solvent-solute interaction and indirectly to the like solvent-solvent interaction which yields the configurations of the solvent molecules. In these configurations, the solute test molecules are inserted. The mole fraction of the solute in the solvent is exactly zero, as required for infinite dilution, since the test molecules are ghost particles that are removed after the potential energy calculation and thus do not affect the solvent molecules. Simulations were performed in the liquid state at a specified temperature, and the pressure was set to the pure substance vapor pressure of the solvent, as described by the molecular model.

Based on pairwise additive molecular models, the Henry's law constant is determined by two different interactions: firstly, the like interaction between solvent molecules and, secondly, the unlike interaction between solvent and solute molecules. While the like interaction is fully defined by the solvent model, the unlike interaction requires some discussion: the unlike polar contribution is defined in a physically straightforward manner, simply using the laws of electrostatics. To define the unlike Lennard-Jones contribution between solute  $i$  and solvent S molecules, the modified Lorentz-Berthelot combining rule [102] was used

$$\sigma_{iS} = \frac{\sigma_i + \sigma_S}{2}, \quad (5)$$

and

$$\epsilon_{iS} = \xi \cdot \sqrt{\epsilon_i \epsilon_S}, \quad (6)$$

where  $\xi$  is the binary interaction parameter that mainly accounts for the unlike dispersion. The Henry's law constant is sensitive to  $\xi$ , i.e., it decreases with increasing  $\xi$  [18]. This is physically reasonable, as a higher solubility due to stronger unlike dispersive attraction is expected.

For the 29 binary mixtures which were studied in [6] and also in this work, values for  $\xi$  are available. These were obtained in [6] by an adjustment to a single experimental vapor pressure  $p$  at some finite mole fraction

of the binary mixture. Such values are indicated by  $\xi_p$  in the following. On the basis of the binary interaction parameter  $\xi_p$ , the temperature dependence of the Henry's law constant was predicted here for the subgroup of 29 mixtures. As discussed below, in some cases significant deviations were encountered, in which case the binary interaction parameter was then readjusted to the experimental Henry's law constant data here, indicated by  $\xi_H$ . For the remaining 66 binary systems which were not studied in [6],  $\xi_H$  was adjusted in this work to  $H_i$  at some temperature, cf. Table 2.

In all simulations, 864 solvent molecules were used to evaluate the Henry's law constant. After an equilibration of 30,000 time steps, 200,000 production time steps of 1.5 fs were carried out inserting 3456 test molecules into the liquid solvent after each time step. The Lennard-Jones long-range interactions beyond the cut-off radius were corrected, employing angle averaging as proposed by Lustig [100]. The dipolar interactions were corrected using the reaction field method [101]. The cutoff radius was at least 17.5 Å. The quadrupolar and also the mixed dipolar-quadrupolar interactions need no long-range corrections, as their contributions disappear by orientational averaging.

As discussed above, Widom's method has its limitations. Often, the solute molecules are smaller than the solvent molecules which is advantageous for the calculation of  $H_i$ . However, when the temperature is low and thus the saturated liquid solvent density is very high, the probability of successful test molecule insertions becomes very low. Then, the  $H_i$  calculation shows large statistical uncertainties or even a complete failure of that method. Nonetheless, molecular dynamics simulation in combination with Widom's method was used here, because it works at higher temperatures, and simulation data over a larger temperature range allow for a reasonable temperature extrapolation.

## 5 Results and Discussion

For 95 binary mixtures, the Henry's law constant  $H_i$  was determined as a function of temperature. The results are presented in the electronic supplementary material for each individual system in graphical form that contains

the experimental data for comparison. There, it is distinguished graphically between the different experimental sources. The full numerical data set from simulation is provided in the electronic supplementary material as well, together with an estimate of the statistical uncertainty. Error bars were calculated by a block averaging method [103] and the error propagation law. Due to the fact that the error bars are predominantly within symbol size, they were omitted in the figures to achieve better visibility as the results for several binary mixtures are combined therein. In these figures, results for 37 of the 95 systems are shown as examples.

For this discussion, the 95 systems are grouped into six categories, cf. Table 2. The first category, containing 38 systems, is characterized by the presence of experimental data over a significant temperature range where a very good to excellent match with the simulation data was achieved. Eight such systems are shown in Figs. 1 and 2. The order of magnitude and also the temperature dependence of  $H_i$  vary. For example,  $H_i$  ranges from around 4 MPa for R1114 in R113, and increases with temperature, (Fig. 1), to around 450 MPa for N<sub>2</sub> in CS<sub>2</sub> and decreases with temperature, (Fig. 2). In the case of CH<sub>4</sub> in CS<sub>2</sub>, (Fig. 2),  $H_i$  changes little with temperature in the range considered.

For the second category, containing the six systems Ne in R113, Ar in R10, N<sub>2</sub> in R114, R1132 in R113, R116 in R113, and Xe in R113, the experimental data are also available over a significant temperature range, but the simulation results show a qualitatively different temperature dependence. Three typical systems are shown in Fig. 3. Due to the fact that the binary interaction parameter was adjusted to experimental  $H_i$  data for five of the six systems, the data sets from simulation and experiment intersect. For the remaining system, Ar in R10, cf. Fig. 3, the binary interaction parameter was adjusted in [6] to experimental VLE data at 348.15 K. Around this temperature, the predicted  $H_i$  from simulation compares well with the experimental data, however, the temperature trend differs.

For the 44 mixtures in the first and second categories a comparably broad experimental database is available for the present assessment. As in 38 of the 44 cases, the temperature dependence of  $H_i$  from simulation agrees well with the experiment, it can be stated that molecular modeling and simulation generally yield good results.

The third category, containing 20 systems, is characterized by the presence of a single experimental  $H_i$  data point that is part of the temperature range where simulation was feasible. Due to the adjustment of  $\xi$ , the simulation data coincide with experiment; however, the presented temperature extrapolation cannot be assessed on the basis of experimental data. Figure 4 shows four typical systems.

For most mixtures, experimental  $H_i$  data are available only at low temperatures, typically below 360 K. Particularly for the studied polar solvents, the saturated liquid state is then highly dense, so that the calculation of the chemical potential of the solute at infinite dilution by Widom's test particle method fails for low temperatures. This also depends on the nature of the solute; the larger and more polar the solute molecule is, the higher is the minimum temperature where such a calculation is feasible.

In 16 cases,  $H_i$  could not be determined in the temperature range where experimental data are present, which is the fourth category. However, as can be seen in Figs. 5 and 6 for seven selected mixtures, both the experimental and simulation data allow for an overlapping extrapolation which can be regarded as satisfactory. Note that the binary interaction parameter for the three systems R12 in R10, Cl<sub>2</sub> in R140, and R1140 in R140 was adjusted in [6] to experimental VLE data at 297.75 K, 313 K, and 346.15 K, respectively, cf. Figs. 5 and 6. Thus, for these systems, it can be stated that the molecular mixture models yield correct and consistent  $H_i$  and VLE data. With respect to Widom's method, it can be seen in Fig. 6 that the  $H_i$  calculation at 330 K was feasible for R13 in R10, while for R14 in the same solvent, it was not.

Furthermore, the fifth category is also characterized by non-overlapping temperature ranges, but experimental data are present only for a single temperature or a very narrow temperature range. For the respective 12 systems, only the simulation data allow for an extrapolation which was found to be in satisfactory agreement with experiment. Four selected examples are shown in Fig. 7.

As indicated above, for 29 systems both experimental VLE and  $H_i$  data are available. For these systems, the binary interaction parameter has been adjusted to the vapor pressure at finite mole fractions in prior work

[6], being indicated by  $\xi_p$ , leading to an excellent match between experiment and simulation with respect to the VLE data. For a subgroup of 20 systems, it was found here that these molecular mixture models are capable of yielding correct and consistent  $H_i$  and VLE data. Four such systems are shown in Fig. 8 as examples.

For the remaining nine systems, the predicted  $H_i$  data deviate from the experiment so that the binary interaction parameter was readjusted in these cases, labeled by  $\xi_H$ . This issue is illustrated in Figs. 9 and 10 for six systems. For example, in the case of CO<sub>2</sub> in CS<sub>2</sub>, cf. Fig. 9, the  $H_i$  values predicted on the basis of  $\xi_p$  are too low by around 30 %, but the temperature trend is satisfactory. Decreasing the binary interaction parameter by approximately 0.04 shifts  $H_i$  onto to the experimental data. For other systems, e.g., Ar in R113, cf. Fig. 10, the  $H_i$  values predicted on the basis of  $\xi_p$  are too high, so that  $\xi_H < \xi_p$ . It was observed that the influence of the binary interaction parameter on  $H_i$  is weaker for higher temperatures.

Fig. 11 lists the 29 systems where both experimental VLE and  $H_i$  data are available, comparing their optimal binary interaction parameters  $\xi_p$  from [6] and  $\xi_H$  from this work. As can be seen, only in a few cases, e.g., C<sub>2</sub>H<sub>2</sub> in R10 or R23 in R114, they strongly differ.

Finally, for the three mixtures Ne in R10, CO in R140a, and CO<sub>2</sub> in R150B2, constituting the sixth category, the present modeling approach did not yield reasonable results. The simulation data according to the Berthelot rule, i.e.,  $\xi = 1$ , were found to be very far off the experimental data which would require altering  $\xi$  by an unphysically large extent, e.g.,  $\xi > 2$  in the case of CO in R140a. It should be noted that the 1CLJ model for Ne performs poorly with respect to VLE data [6]. This is confirmed, as for both mixtures containing Ne studied here, i.e., Ne in R10 and Ne in R113 (wrong temperature dependence), unsatisfactory results were achieved.

Another aspect that can be studied on the basis of the present simulation data is the general temperature trend of the Henry's law constant for different solutes in a given solvent. For example, for the solvent R10, a total of 19 solutes was investigated. These simulation results are combined in Fig. 12, showing that the  $H_i$  values at low temperatures cover a band of around 130 MPa. With increasing temperature, the data sets for the

different solutes converge, covering a band of around 35 MPa at the critical temperature of the solvent. For the solvent CS<sub>2</sub>, where 15 solutes were investigated here, a similar behavior was found. Thus, it can be concluded that the Henry's law constant at high temperatures is less influenced by the solute properties through the unlike interaction, but mainly by the like solvent-solvent interaction.

## 6 Conclusion

It was shown that molecular simulation is a reliable method for investigating the Henry's law constant of gases dissolved in liquid solvents. To verify this issue, an extensive simulation effort was made to cover 95 binary mixtures in a combinatorial way. The molecular models employed in many cases oversimplify the molecular features of the substance that they represent. However, it was found that the molecular models are usually able to compensate such oversimplifications and adequately cover the gas solubility effects.

To optimally represent the phase behavior of all of the binary mixtures studied, the unlike dispersive energy parameter was adjusted to a single experimental Henry's law constant or the binary vapor pressure of each mixture. It was found that the Berthelot rule is a good choice. In 50 % of the cases studied, unlike dispersion was modified by 5 % or less. On average, unlike dispersion should be slightly weaker than the Berthelot rule suggests.

Based on these mixture models, the temperature dependence of the Henry's law constant was predicted and compared to the available experimental data. For the large majority of systems that can be assessed in this sense, good agreement was found. Furthermore, it was shown that the models are generally capable of yielding correct and consistent phase equilibrium data at infinite dilution and also at finite mole fractions.

For high temperatures, it was found for a given solvent that the Henry's law constant of different solutes converges to a narrow band. This indicates that this thermophysical property is then mainly determined by the solvent-solvent interaction.

Due to their numerical efficiency and accuracy, those molecular mixture models that were found to yield consistent data are also well suited to be used in simulations on a larger scale to investigate processes such as absorption, adsorption, evaporation flow, etc.

## **Acknowledgements**

We gratefully acknowledge Deutsche Forschungsgemeinschaft for funding this project. The presented research was conducted under the auspices of the Boltzmann-Zuse Society of Computational Molecular Engineering (BZS), and the simulations were performed on the national super computer NEC SX-8 at the High Performance Computing Center Stuttgart (HLRS) and on the HP X6000 super computer at the Steinbuch Centre for Computing, Karlsruhe.

We would like to thank Xijun Fu and Qingyun Li for handling numerous simulation runs and helping to prepare the material for publication.

## References

1. T. M. Letcher (Ed.), *Developments and Applications in Solubility*, (Cambridge, The Royal Society of Chemistry, 2007)
2. J. M. Smith, H. C. Van Ness, M. M. Abbott, *Introduction to Chemical Engineering Thermodynamics*, 5th ed. (New York, McGraw-Hill, 1996)
3. I. R. Krichevsky, J. S. Kasarnovsky, *J. Am. Chem. Soc.* **57**, 2168 (1935)
4. J. Vrabec, J. Stoll, H. Hasse, *J. Phys. Chem. B* **105**, 12126 (2001)
5. J. Stoll, J. Vrabec, H. Hasse, *J. Chem. Phys.* **119**, 11396 (2003)
6. J. Vrabec, Y.-L. Huang, H. Hasse, *Fluid Phase Equilib.* **279**, 120 (2009)
7. K. S. Shing, K. E. Gubbins, K. Lucas, *Mol. Phys.* **65**, 1235 (1988)
8. J. Stecki, A. Samborski, S. Toxvaerd, *Mol. Phys.* **70**, 985 (1990)
9. R. J. Sadus, *J. Phys. Chem. B* **101**, 3834 (1997)
10. S. Murad, S. Gupta, *Chem. Phys. Lett.* **319**, 60 (2000)
11. A. Lotfi, J. Fischer, *Mol. Phys.* **66**, 199 (1989)
12. G. C. Boulougouris, J. R. Errington, I. G. Economou, A. Z. Panagiotopoulos, D. N. Theodorou, *J. Chem. Phys. B* **104**, 4958 (2000)
13. G. C. Boulougouris, E. C. Voutsas, I. G. Economou, D. N. Theodorou, D. P. Tassios, *J. Chem. Phys. B* **105**, 7792 (2001)
14. I. G. Economou, *Fluid Phase Equilib.* **183-184**, 259 (2001)
15. M. Lísal, W. R. Smith, K. Aim, *Fluid Phase Equilib.* **228-229**, 345 (2005)
16. S. Murad, S. Gupta, *Fluid Phase Equilib.* **187-188**, 29 (2001)
17. F. Case, A. Chaka, D. G. Friend, D. Frurip, J. Golab, P. Gordon, R. Johnson, P. Kolar, J. Moore, R. D. Mountain, J. Olson, R. Ross, M. Schiller, *Fluid Phase Equilib.* **236**, 1 (2005)
18. T. Schnabel, J. Vrabec, H. Hasse, *Fluid Phase Equilib.* **233**, 134 (2005)
19. Y. Boutard, Ph. Ungerer, J. M. Teuler, M. G. Ahunbay, S. F. Sabater, J. Pérez-Pellitero, A. D. Mackie, E. Bourasseau, *Fluid Phase Equilib.* **236**, 25 (2005)
20. E. C. Cichowski, T. R. Schmidt, J. R. Errington, *Fluid Phase Equilib.* **236**, 58 (2005)
21. C. Wu, X. Li, J. Dai, H. Sun, *Fluid Phase Equilib.* **236**, 66 (2005)
22. L. Zhang, J. I. Siepmann, *Theor. Chem. Acc.* **115**, 391 (2006)
23. B. Widom, *J. Chem. Phys.* **39**, 2808 (1963)
24. J. Gmehling, J. Rarey, J. Menke, *Dortmunder Datenbank*, (Mixture Properties, Version 1.3.0.211, 2004)
25. W. F. Krieve, D. M. Mason, *J. Phys. Chem.* **60**, 374 (1956)
26. R. D. Ackley, K. J. Notz, *Distribution of Xenon between Gaseous and Liquid CO<sub>2</sub>*, (Technical Report ORNL-5122, Oak Ridge National Lab. TN, USA, 1976)
27. A. Fredenslund, J. Mollerup, O. Persson, *J. Chem. Eng. Data* **17**, 440 (1972)
28. J. C. Gjaldbaek, H. Niemann, *Acta Chem. Scand.* **12**, 611 (1958)
29. L. W. Reeves, J. H. Hildebrand, *J. Am. Chem. Soc.* **79**, 1313 (1957)
30. R. J. Powell, *J. Chem. Eng. Data* **17**, 302 (1972)
31. Y. Kobatake, J. H. Hildebrand, *J. Phys. Chem.* **65**, 331 (1961)
32. J. C. Gjaldbaek, J. H. Hildebrand, *J. Am. Chem. Soc.* **71**, 3147 (1949)
33. J. C. Gjaldbaek, *Acta Chem. Scand.* **6**, 623 (1952)
34. A. D. Raskina, V. I. Zetkin, E. V. Zakharov, I. M. Kolesnikov, V. I. Kosorotov, *J. Appl. Chem. (USSR)* **45**, 1374 (1972)
35. J. C. Gjaldbaek, *Acta Chem. Scand.* **7**, 537 (1953)
36. Y. Miyano, W. Hayduk, *Can. J. Chem. Eng.* **59**, 746 (1981)
37. A. Sahgal, H. M. La, W. Hayduk, *J. Chem. Eng.* **56**, 354 (1978)
38. G. Archer, J. H. Hildebrand, *J. Phys. Chem.* **67**, 1830 (1963)
39. Yu. P. Blagoi, N. A. Orobinskii, *Russ. J. Phys. Chem.* **39**, 1073 (1965)
40. H. C. Miller, L. S. Verdelli, J. F. Gall, *Ind. Eng. Chem.* **43**, 1126 (1951)
41. T. Tominaga, R. Battino, H. K. Gorowara, R. D. Dixon, E. Wilhelm, *J. Chem. Eng. Data* **31**, 175 (1986)
42. E. B. Graham, K. E. Weale, *Prog. Int. Res. Therm. Trans. Prop.*, 153 (1962)
43. F. Körösy, *Trans. Faraday Soc.* **33**, 416 (1937)
44. A. Lannung, J. C. Gjaldbaek, *Acta Chem. Scand.* **14**, 1124 (1960)

45. T. Akimoto, T. Nitta , T. Katayama, J. Chem. Eng. (Japan) **17**, 637 (1984)
46. V. M. Gorbachev, T. V. Tretyakov, Zavod. Lab. (USSR) **32**, 796 (1966)
47. J. K. Wolfe, Refrig. Eng. **59**, 704 (1951)
48. P. Luehring, A. Schumpe, J. Chem. Eng. Data **34**, 250 (1989)
49. N. K. Naumenko, *Investigation on the Solubility of Oxygen in Organic Solvents*, Thesis, 3 (1970)
50. P. Schlaepfer, T. Audykowski, A. Bukowiecki, Schweizer Archiv für Wiss. u. Technik **15**, 299 (1949)
51. E. Sinn, K. Matthes, E. Naumann, Wiss. Z. Friedrich-Schiller-Univ. Jena, Math.-Naturwiss. R. **16**, 523 (1967)
52. V. T. Vdovichenko, V. I. Kondratenko, Khim. Prom. (USSR) **43**, 290 (1967)
53. L. M. Kogan, N. S. Koltsov, N. D. Litvinov, Russ. J. Phys. Chem. **37**, 1040 (1963)
54. T. L. Smith, J. Phys. Chem. **59**, 188 (1955)
55. C. M. Blair, D. M. Yost, J. Am. Chem. Soc. **55**, 4489 (1933)
56. N. W. Taylor, J. H. Hildebrand, J. Am. Chem. Soc. **45**, 682 (1923)
57. G. Just, Z. Phys. Chem. **37**, 342 (1901)
58. M. Takahashi, Y. Kobayashi, H. Takeuchi, J. Chem. Eng. Data **27**, 328 (1982)
59. H. Hsu, D. Campbell, Aerosol Age **9**, 34 (1964)
60. H. Takeuchi, M. Fujine, T. Sato, K. Onda, J. Chem. Eng. (Japan) **8**, 252 (1975)
61. N. Brueckl, J. I. Kim, Z. Phys. Chem., Neue Folge **126**, 133 (1981)
62. R. Jadot, J. Chim. Phys. Phys.-Chim. Biol. **6**, 1036 (1972)
63. B. I. Konobeev, V. V. Lyapin, Khim. Prom. (USSR) **43**, 114 (1967)
64. W. Hayduk, S. C. Cheng, Can. J. Chem. Eng. **48**, 93 (1970)
65. E. Wilhelm, R. Battino, J. Chem. Thermodyn. **3**, 379 (1971)
66. R. G. Makitra, Ya. N. Pirig, T. I. Politanskaya, F. B. Moin, Russ. J. Phys. Chem. **55**, 424 (1981)
67. Anonymous, *Löslichkeit von F23 und HCl in verschiedenen Lösungsmitteln*, (Confident. Comp. Res. Rep. Rep. No. LC4912, 1970; cf. [24])
68. Anonymous, *Löslichkeit von HCl und F23 in verschiedenen Lösungsmitteln*, (Confident. Comp. Res. Rep., Rep. No. LC4914, 1970; cf. [24])
69. P. Sies, J. Krafczyk, Unpublished Data (1992); cf. [24]
70. J. Krafczyk, Unpublished Data (1991); cf. [24]
71. Yu. G. Mamedaliev, S. Musakhanly, Zh. Prikl. Khim. (USSR) **13**, 735 (1940)
72. J. Horiuti, Sci. Pap. Inst. Phys. Chem. Res. (Japan) **17**, 125 (1931)
73. R. G. Makitra, T. I. Politanskaya, F. B. Moin, Y. N. Pirig, T. S. Politanskaya, J. Appl. Chem. (USSR) **56**, 2048 (1984)
74. R. G. Makitra, F. B. Moin, T. I. Politanskaya, J. Phys. Chem. (USSR) **53**, 572 (1979)
75. M. Kriebel, H. J. Loeffler, Kältetechnik **18**, 34 (1966)
76. Anonymous, *Löslichkeit von gasförmigem F13, F22 und F23 in flüssigem F11*, (Confident. Comp. Res. Rep., Rep. No. LC4994, 1969; cf. [24])
77. T. Nitta, Y. Nakamura, H. Ariyasu, T. Katayama, J. Chem. Eng. (Japan) **13**, 97 (1980)
78. F. Fischer, G. Pfleiderer, Z. Anorg. Chem. **124**, 61 (1922)
79. N. F. Giles, L. C. Wilson, G. M. Wilson, W. V. Wilding, J. Chem. Eng. Data **42**, 1067 (1997)
80. F. H. Vonderheiden, J. W. Eldridge, J. Chem. Eng. Data **8**, 20 (1963)
81. K. E. Doering, FIZ Report, 1201 (1965)
82. R. G. Linford, J. H. Hildebrand, Trans. Faraday Soc. **66**, 577 (1970)
83. H. Hiraoka, J. H. Hildebrand, J. Phys. Chem. **68**, 213 (1964)
84. Y. P. Sokolov, A. I. Konshin, J. Appl. Chem. (USSR) **62**, 1310 (1989)
85. D. A. Armitage, R. G. Linford, D. G. T. Thornhill, Ind. Eng. Chem. Fundam. **17**, 362 (1978)
86. R. G. Linford, J. H. Hildebrand, J. Phys. Chem. **73**, 4410 (1969)
87. H. Jaster, P. G. Kosky, J. Chem. Eng. Data **21**, 66 (1976)
88. Yu. A. Sokolov, A. I. Konshin, S. V. Sokolov, J. Appl. Chem. (USSR) **60**, 2523 (1988)
89. V. D. Williams, J. Chem. Eng. Data **4**, 92 (1959)
90. O. V. Efstigneev, M. B. Santimova, S. G. Dunaev, S. B. Levanova, Khim. Prom. (USSR) **6**, 342 (1985)
91. R. G. Makitra, F. B. Moin , Ya. N. Pirig, T. I. Politanskaya, J. Appl. Chem. (USSR) **60**, 663 (1987)
92. R. G. Makitra, F. B. Moin, Ya. N. Pirig, T. I. Politanskaya, J. Appl. Chem. (USSR) **62**, 2567 (1990)
93. S. M. Danov, Yu. D. Golubev, Khim. Prom. (USSR) **44**, 116 (1968)
94. J. C. Gjaldbaek, E. K. Anderson, Acta Chem. Scand. **8**, 1398 (1954)
95. E. Otsuka, M. Takada, Nenryo-Kyokai-shi **42**, 229 (1963)

96. O. Y. Guzechak, V. N. Sarancha, I. M. Romanyuk, O. M. Yavorskaya, G. P. Churik, J. Appl. Chem. (USSR) **57**, 1662 (1985)
97. U. K. Deiters, Fluid Phase Equilib. **132**, 265 (1997)
98. J. Stoll, J. Vrabec, H. Hasse, J. Fischer, Fluid Phase Equilib. **179**, 339 (2001)
99. J. Stoll, J. Vrabec, H. Hasse, Fluid Phase Equilib. **209**, 29 (2003)
100. R. Lustig, Mol. Phys. **65**, 175 (1988)
101. M. P. Allen, D. J. Tildesley, *Computer Simulation of Liquids*, (Oxford, Clarendon Press, 1987)
102. T. Schnabel, J. Vrabec, H. Hasse, J. Mol. Liq. **135**, 170 (2007)
103. H. Flyvbjerg, H. G. Petersen, J. Chem. Phys. **91**, 461 (1989)

**Table 1** List of the 41 components studied in the present work, where *i* indicates solutes and S solvents. The model parameters were taken from [4, 5]

Fluid	CAS RN	Type	Fluid	CAS RN	Type
<b>Non-polar, 1CLJ</b>					
Ne	7440-37-1	<i>i</i>	N <sub>2</sub>	7727-37-9	<i>i</i>
Ar	13965-95-2	<i>i</i>	O <sub>2</sub>	7782-44-7	<i>i</i>
Kr	7439-90-9	<i>i</i>	Cl <sub>2</sub>	7782-50-5	<i>i/S</i>
Xe	7440-63-3	<i>i</i>	CO <sub>2</sub>	124-38-9	<i>i/S</i>
CH <sub>4</sub>	74-82-8	<i>i</i>	CS <sub>2</sub>	75-15-0	S
<b>Dipolar, 1CLJD</b>					
R30 (CH <sub>2</sub> Cl <sub>2</sub> )	75-09-2	S	C <sub>2</sub> H <sub>2</sub>	74-86-2	<i>i</i>
<b>Dipolar, 2CLJD</b>					
CO	630-08-0	<i>i</i>	Propylene (CH <sub>3</sub> —CH=CH <sub>2</sub> )	115-07-1	<i>i/S</i>
R11 (CFCl <sub>3</sub> )	75-69-4	S	SF <sub>6</sub>	2551-62-4	<i>i/S</i>
R12 (CF <sub>2</sub> Cl <sub>2</sub> )	75-71-8	<i>i</i>	R10 (CCl <sub>4</sub> )	56-23-5	S
R13 (CF <sub>3</sub> Cl)	75-72-9	<i>i</i>	R14 (CF <sub>4</sub> )	75-73-0	<i>i</i>
R20 (CHCl <sub>3</sub> )	67-66-3	S	R113 (CFCl <sub>2</sub> —CF <sub>2</sub> Cl)	76-13-1	S
R20B3 (CHBr <sub>3</sub> )	75-25-2	S	R114 (CF <sub>2</sub> Cl—CF <sub>2</sub> Cl)	76-14-2	S
R22 (CHF <sub>2</sub> Cl)	75-45-6	<i>i</i>	R116 (C <sub>2</sub> F <sub>6</sub> )	76-16-4	<i>i</i>
R23 (CHF <sub>3</sub> )	75-46-7	<i>i</i>	R150B2 (CH <sub>2</sub> Br—CH <sub>2</sub> Br)	106-93-4	S
R40 (CH <sub>3</sub> Cl)	74-87-3	<i>i/S</i>	R1110 (C <sub>2</sub> Cl <sub>4</sub> )	127-18-4	S
R130a (CH <sub>2</sub> Cl—CCl <sub>3</sub> )	630-20-6	S	R1114 (C <sub>2</sub> F <sub>4</sub> )	116-14-3	<i>i</i>
R140 (CHCl <sub>2</sub> —CH <sub>2</sub> Cl)	79-00-5	S	R1120 (CHCl=CCl <sub>2</sub> )	79-01-6	S
R140a (CCl <sub>3</sub> —CH <sub>3</sub> )	71-55-6	S			
R150a (CHCl <sub>2</sub> —CH <sub>3</sub> )	75-34-3	S			
R161 (CH <sub>2</sub> F—CH <sub>3</sub> )	74-96-4	<i>i</i>			
R1132 (CF <sub>2</sub> =CH <sub>2</sub> )	75-38-7	<i>i</i>			
R1140 (CHCl=CH <sub>2</sub> )	75-01-4	<i>i/S</i>			

**Table 2** Binary interaction parameter  $\xi_H$  adjusted to the Henry's law constant, experimental data used for the adjustment with reference, and simulation results with adjusted  $\xi_H$ . In cases where the experimental Henry's law constant is omitted,  $\xi_H$  was adjusted via temperature extrapolation. For an explanation of the categories, see sect. 5. The number in parentheses denotes the statistical uncertainty in the last digit

Mixture ( $i + S$ )	Category	$\xi_H$	$T$ (K)	$H_i^{\text{sim}}$ (MPa)	$H_i^{\text{exp}}$ (MPa)	Ref.
O <sub>2</sub> + Cl <sub>2</sub>	3	0.993	298	66.5 (4)	66.3	[25]
CO <sub>2</sub> + Cl <sub>2</sub> †	1	0.920	298.15	11.3 (1)	11.2	[25]
Xe + CO <sub>2</sub>	1	0.904	283.15	8.7 (2)	8.7	[26]
O <sub>2</sub> + CO <sub>2</sub> †	3	0.979	223.75	53.0 (5)	53.0	[27]
Ar + CS <sub>2</sub>	1	0.901	298.15	208.9 (3)	209.2	[28, 29]
Kr + CS <sub>2</sub>	3	0.966	298.15	57.2 (4)	57.7	[30]
Xe + CS <sub>2</sub>	3	0.999	298	9.8 (2)	9.7	[30]
CH <sub>4</sub> + CS <sub>2</sub>	1	0.984	298.15	78 (2)	80	[30, 31]
N <sub>2</sub> + CS <sub>2</sub>	1	0.905	298.15	463 (6)	456	[30, 31, 32]
O <sub>2</sub> + CS <sub>2</sub>	3	0.859	298.15	231 (2)	230	[33]
Cl <sub>2</sub> + CS <sub>2</sub>	1	0.991	298	0.93 (3)	0.96	[34]
CO + CS <sub>2</sub>	3	0.968	298	302 (4)	303	[33]
CO <sub>2</sub> + CS <sub>2</sub> †	1	0.877	306.36	34.1 (5)	33.6	[31, 35]
C <sub>2</sub> H <sub>2</sub> + CS <sub>2</sub>	1	0.942	288.15	17.5 (6)	17.5	[36]
C <sub>2</sub> H <sub>4</sub> + CS <sub>2</sub>	3	0.995	298	15.7 (5)	15.7	[37]
C <sub>2</sub> H <sub>6</sub> + CS <sub>2</sub>	3	0.992	298.15	9.8 (4)	9.4	[28, 30]
Propylene + CS <sub>2</sub>	3	0.870	298.15	20 (2)	19	[30]
SF <sub>6</sub> + CS <sub>2</sub>	1	0.862	288.29	117 (6)	110	[30, 31]
R14 + CS <sub>2</sub>	1	0.813	308	484 (14)	476	[38]
N <sub>2</sub> + Propylene†	4	0.959	180	52.1 (9)	-	[39]
N <sub>2</sub> + SF <sub>6</sub>	3	1.400	300.15	8.34 (3)	8.33	[40]
Ar + R10†	2	0.964	348.15	77.9 (5)	74.1	[29, 42]
Kr + R10	5	1.049	350	31.2 (2)	-	[41, 43]
CH <sub>4</sub> + R10	5	1.068	350	38.3 (3)	-	[44]
N <sub>2</sub> + R10	5	0.899	340	134 (1)	-	[45, 46, 47]
O <sub>2</sub> + R10	5	0.888	350	77.9 (4)	-	[46, 47, 48, 49, 50, 51]
Cl <sub>2</sub> + R10	1	0.972	344.15	2.0 (2)	2.0	[52, 53, 54, 55, 56]
CO <sub>2</sub> + R10	4	0.808	340	18.2 (1)	-	[35, 48, 57, 58, 59, 60]
C <sub>2</sub> H <sub>2</sub> + R10†	1	0.859	323.15	11.4 (1)	11.4	[36]

**Table 2** continued

Mixture ( $i + S$ )	Category	$\xi_H$	$T$ (K)	$H_i^{\text{sim}}$ (MPa)	$H_i^{\text{exp}}$ (MPa)	Ref.
C <sub>2</sub> H <sub>4</sub> + R10†	1	0.978	333.15	11.0 (4)	11.1	[37, 61, 62, 63]
C <sub>2</sub> H <sub>6</sub> + R10	5	1.043	350	8.3 (1)	-	[62, 64]
Propylene + R10†	1	1.005	333.15	2.8 (9)	2.8	[62, 63]
SF <sub>6</sub> + R10	4	0.834	361	26.6 (7)	-	[38, 41]
R12 + R10†	4	0.991	330	1.9 (10)	-	[65]
R13 + R10	4	0.943	330	12.6 (3)	-	[65]
R14 + R10	4	0.794	350	82 (1)	-	[38]
R22 + R10†	5	0.929	350	4.07 (7)	-	[66]
R23 + R10	5	0.725	380	32.3 (3)	-	[67, 68]
R40 + R10	4	0.925	350	2.23 (2)	-	[69, 70, 71, 72]
R161 + R10	4	0.959	350	2.34 (4)	-	[73, 74]
R13 + R11†	1	0.975	273.15	2.56 (7)	3.42	[75]
R22 + R11†	1	0.956	273.15	0.68 (2)	0.92	[75]
R23 + R11†	1	0.802	303.15	14.0 (1)	14.3	[67, 76]
N <sub>2</sub> + R20	3	0.905	298.15	196.9 (3)	196.1	[77]
O <sub>2</sub> + R20	3	0.833	289.65	140.8 (2)	140.7	[78]
Cl <sub>2</sub> + R20	1	0.985	298.15	0.6 (8)	0.7	[52]
C <sub>2</sub> H <sub>4</sub> + R20†	4	1.001	390	15.2 (2)	-	[63]
Propylene + R20†	4	0.975	390	6.79 (7)	-	[63]
R22 + R20	3	0.950	293.15	2 (2)	1.7	[66]
R40 + R20	3	0.991	298.15	0.4 (13)	0.5	[72]
R161 + R20	1	0.921	293.15	2 (2)	1.7	[73]
Kr + R20B3	3	0.956	295.15	61 (1)	61	[43]
CH <sub>4</sub> + R30	1	0.893	303.15	80.8 (8)	81.0	[79]
Cl <sub>2</sub> + R30	1	1.036	298.15	0.474(6)	0.483	[52]
CO <sub>2</sub> + R30†	1	0.868	310.93	10.38 (7)	10.38	[80]
CH <sub>4</sub> + R40	3	1.011	293.15	32.8 (3)	32.8	[81]
Ne + R113	2	0.928	298.15	116.9 (1)	116.9	[82]
Ar + R113†	1	1.027	298.06	32.7 (2)	32.7	[83]
Xe + R113	2	1.120	298.15	2.82 (3)	2.7	[82]
CH <sub>4</sub> + R113†	1	1.044	308.15	20.8 (1)	20.8	[83]
N <sub>2</sub> + R113	1	0.980	298.13	52.5 (4)	52.5	[83]

**Table 2** continued

Mixture ( $i + S$ )	Category	$\xi_H$	$T$ (K)	$H_i^{\text{sim}}$ (MPa)	$H_i^{\text{exp}}$ (MPa)	Ref.
CO <sub>2</sub> + R113	1	0.870	308.50	6.4 (5)	6.49	[83]
C <sub>2</sub> H <sub>4</sub> + R113	1	0.908	343.15	10.42 (6)	10.50	[84]
C <sub>2</sub> H <sub>6</sub> + R113	1	1.020	298.08	3.64 (4)	3.76	[82, 85, 86]
SF <sub>6</sub> + R113†	1	0.894	319	6.6 (1)	5.6	[38, 83, 87]
R14 + R113	1	0.858	278.40	18.5 (5)	18.5	[38]
R116 + R113	2	0.998	300.73	3 (2)	3.6	[82, 86]
R1114 + R113	1	0.946	298.15	3.3 (9)	3.4	[88]
R1132 + R113	2	0.978	363.15	6.2 (2)	6.2	[88]
N <sub>2</sub> + R114	2	1.196	313.15	18.6 (1)	18.6	[89]
SF <sub>6</sub> + R114†	1	1.050	277	0.7 (5)	1.02	[87]
R23 + R114†	3	0.732	303.15	9.45 (7)	9.44	[67]
Cl <sub>2</sub> + R130a†	1	0.915	373	4.2 (1)	4.2	[90]
Cl <sub>2</sub> + R140†	4	0.948	450	8.45 (3)	-	[90]
C <sub>2</sub> H <sub>2</sub> + R140	1	0.952	440	17.67 (8)	-	[91]
R1140 + R140†	4	0.980	450	5.25 (3)	-	[92]
Cl <sub>2</sub> + R140a†	1	0.930	281	0.7 (4)	0.5	[90]
CO <sub>2</sub> + R140a†	3	0.889	294.26	6.57 (6)	6.63	[59]
C <sub>2</sub> H <sub>2</sub> + R140a	1	0.914	323.15	8.86 (7)	7.52	[91]
R1140 + R140a	1	0.928	323.15	1.23 (3)	1.24	[91]
Cl <sub>2</sub> + R150a†	4	0.967	360	2.8 (2)	-	[90]
C <sub>2</sub> H <sub>2</sub> + R150a	4	0.965	360	9.18 (6)	-	[93]
Cl <sub>2</sub> + R150B2	3	0.994	313.15	0.8 (16)	0.9	[56]
CO + R150B2	3	0.909	298.15	369.1 (6)	370.7	[94]
O <sub>2</sub> + R1110	5	0.926	380	87.6 (2)	-	[50, 51]
Propylene + R1110†	4	1.011	380	5.4 (1)	-	[63]
R23 + R1110	5	0.664	380	60.0 (7)	-	[67, 68]
O <sub>2</sub> + R1120	5	0.961	340	88.3 (2)	-	[51]
CO <sub>2</sub> + R1120	5	0.829	310	16.3 (5)	-	[95]
C <sub>2</sub> H <sub>2</sub> + R1120	5	0.847	314	13.1 (6)	-	[95]
Propylene + R1120†	1	0.983	303.15	2.0 (2)	1.9	[63, 96]
C <sub>2</sub> H <sub>2</sub> + R1140	1	1.008	242.15	1.3 (11)	1.3	[93]

## List of Figures

**Fig. 1** Henry's law constant of N<sub>2</sub> (●), C<sub>2</sub>H<sub>4</sub> (■), R14 (◆) and R1114 (▲) in liquid R113. Full symbols represent simulation results, empty symbols are experimental data [38, 83, 84, 88].

**Fig. 2** Henry's law constant of Ar (●), CH<sub>4</sub> (■), N<sub>2</sub> (◆) and SF<sub>6</sub> (▲) in liquid CS<sub>2</sub>. Full symbols represent simulation results, empty symbols are experimental data [28, 30, 31].

**Fig. 3** Henry's law constant of Ar in liquid R10 (●), of Ne in liquid R113 (■) and of N<sub>2</sub> in liquid R114 (◆). Full symbols represent simulation results, empty symbols are experimental data [29, 82, 89].

**Fig. 4** Henry's law constant of Kr (●), O<sub>2</sub> (■), CO (◆) and C<sub>2</sub>H<sub>2</sub> (▲) in liquid CS<sub>2</sub>. Full symbols represent simulation results, empty symbols are experimental data [30, 33, 36].

**Fig. 5** Henry's law constant of Cl<sub>2</sub> (●), C<sub>2</sub>H<sub>2</sub> (■) and R1140 (◆) in liquid R140. Full symbols represent simulation results, empty symbols are experimental data [90, 91, 92].

**Fig. 6** Henry's law constant of SF<sub>6</sub> (●), R12 (■), R13 (◆) and R14 (▲) in liquid R10. Full symbols represent simulation results, empty symbols are experimental data [38, 41, 65].

**Fig. 7** Henry's law constant of CH<sub>4</sub> (●), N<sub>2</sub> (■), O<sub>2</sub> (◆) and C<sub>2</sub>H<sub>6</sub> (▲) in liquid R10. Full symbols represent simulation results, empty symbols are experimental data [44, 46, 48, 62].

**Fig. 8** Henry's law constant of R22 in liquid R10 (●), R22 in liquid R11 (■), C<sub>2</sub>H<sub>4</sub> in liquid R20 (◆) and CO<sub>2</sub> in liquid R140a (▲). Full symbols represent simulation results where the binary parameter  $\xi_p$  was adjusted to the vapor pressure in [6], empty symbols are experimental data [59, 63, 66, 75].

**Fig. 9** Henry's law constant for different binary systems. Full symbols represent simulation results where the binary parameter  $\xi_H$  was adjusted to the Henry's law constant in this work, semi-filled symbols represent simulation results where the binary parameter  $\xi_p$  was adjusted to the vapor pressure in [6], empty

symbols are experimental data: CO<sub>2</sub> in liquid CS<sub>2</sub> (●),  $\xi_H = 0.877$ ,  $\xi_p = 0.918$ , [28, 31, 57]; C<sub>2</sub>H<sub>4</sub> in liquid R10 (■),  $\xi_H = 0.978$ ,  $\xi_p = 1.003$ , [61, 63]; R13 in liquid R11 (◆),  $\xi_H = 0.953$ ,  $\xi_p = 0.975$ , [75].

**Fig. 10** Henry's law constant for different binary systems. Full symbols represent simulation results where the binary parameter  $\xi_H$  was adjusted to the Henry's law constant in this work, semi-filled symbols represent simulation results where the binary parameter  $\xi_p$  was adjusted to the vapor pressure in [6], empty symbols are experimental data: CO<sub>2</sub> in liquid Cl<sub>2</sub> (●),  $\xi_H = 0.920$ ,  $\xi_p = 0.936$ , [25]; Ar in liquid R113 (■),  $\xi_H = 1.027$ ,  $\xi_p = 1.012$ , [83]; CH<sub>4</sub> in liquid R113 (◆),  $\xi_H = 1.044$ ,  $\xi_p = 0.997$ , [83].

**Fig. 11** Comparison of the binary interaction parameter  $\xi_H$  that was adjusted to the Henry's law constant in this work (full bars) to the binary interaction parameter  $\xi_p$  that was adjusted to the vapor pressure in [6] (empty bars).

**Fig. 12** Henry's law constant of the 19 solutes Ar, Kr, CH<sub>4</sub>, N<sub>2</sub>, O<sub>2</sub>, Cl<sub>2</sub>, CO<sub>2</sub>, C<sub>2</sub>H<sub>2</sub>, C<sub>2</sub>H<sub>4</sub>, C<sub>2</sub>H<sub>6</sub>, Propylene, SF<sub>6</sub>, R12, R13, R14, R22, R23, R40 and R161 in liquid R10 from simulation (+). The dashed line indicates the critical temperature of the solvent.

Fig. 1.

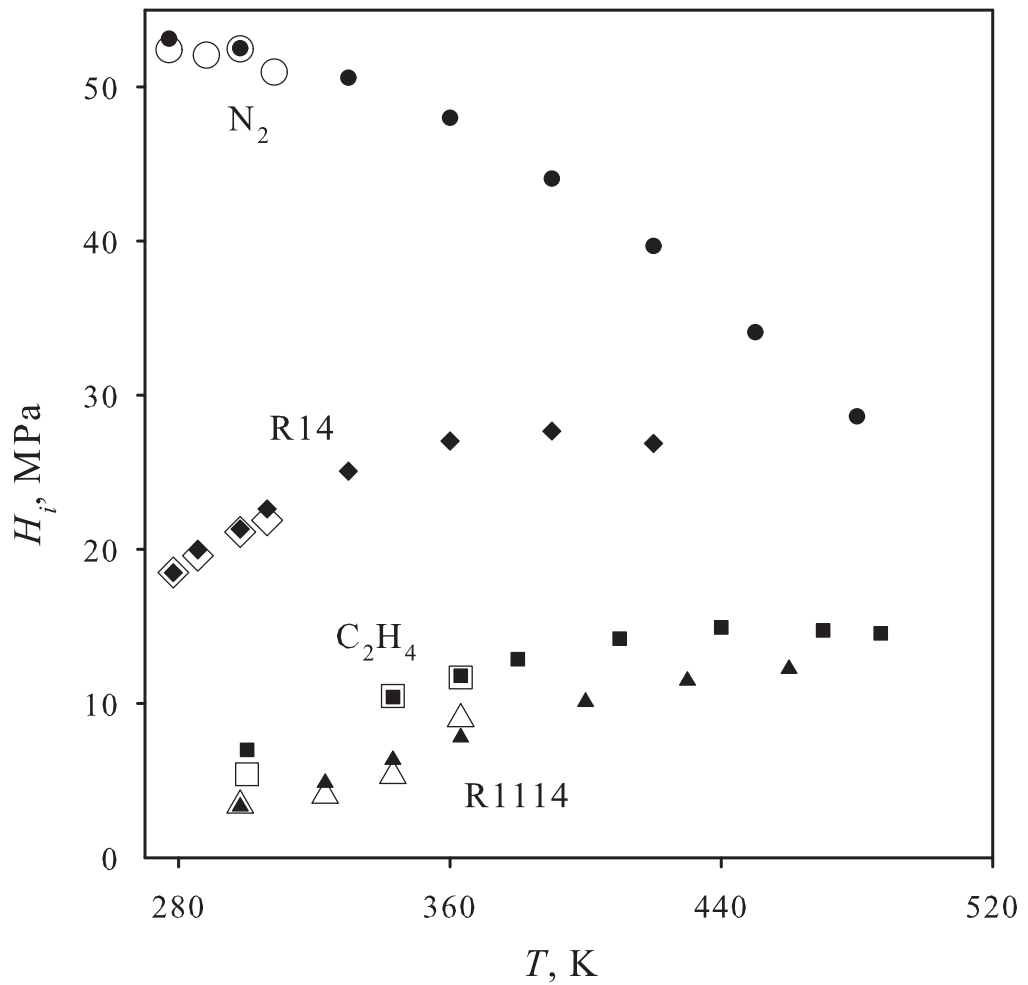


Fig. 2.

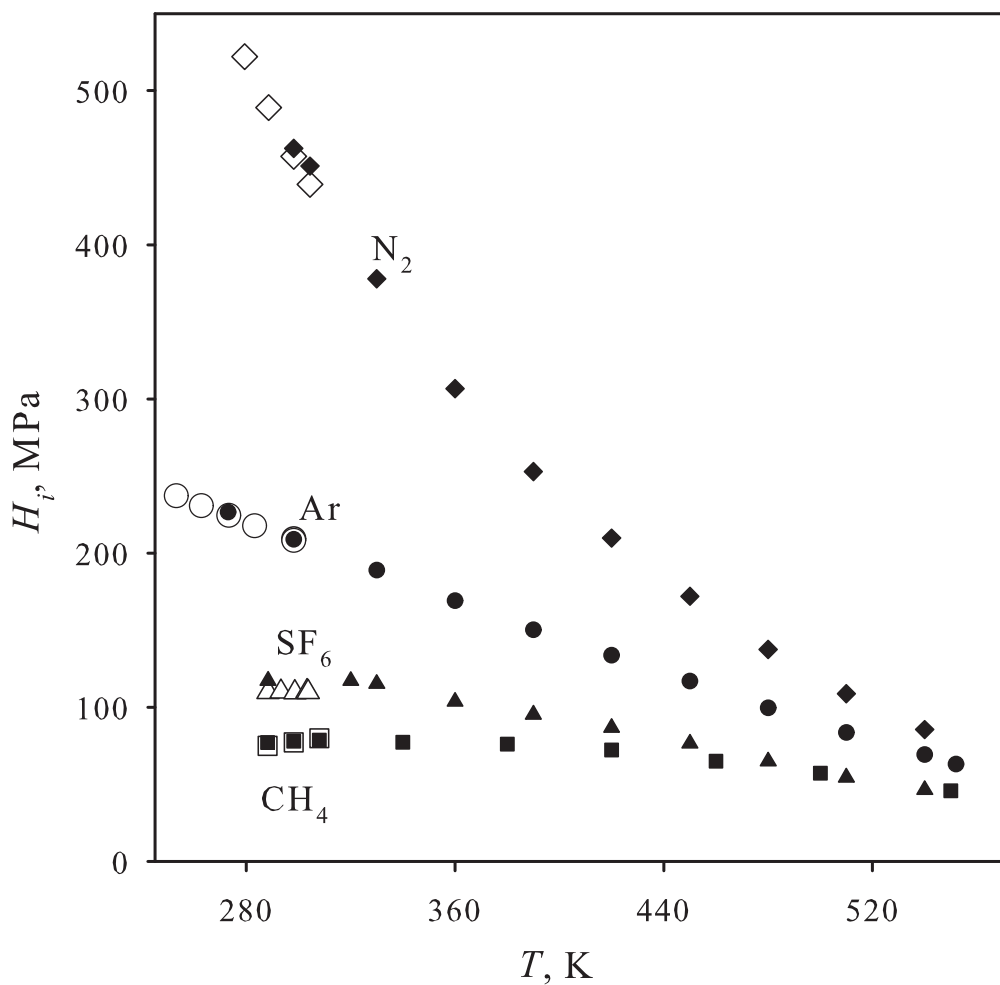


Fig. 3.

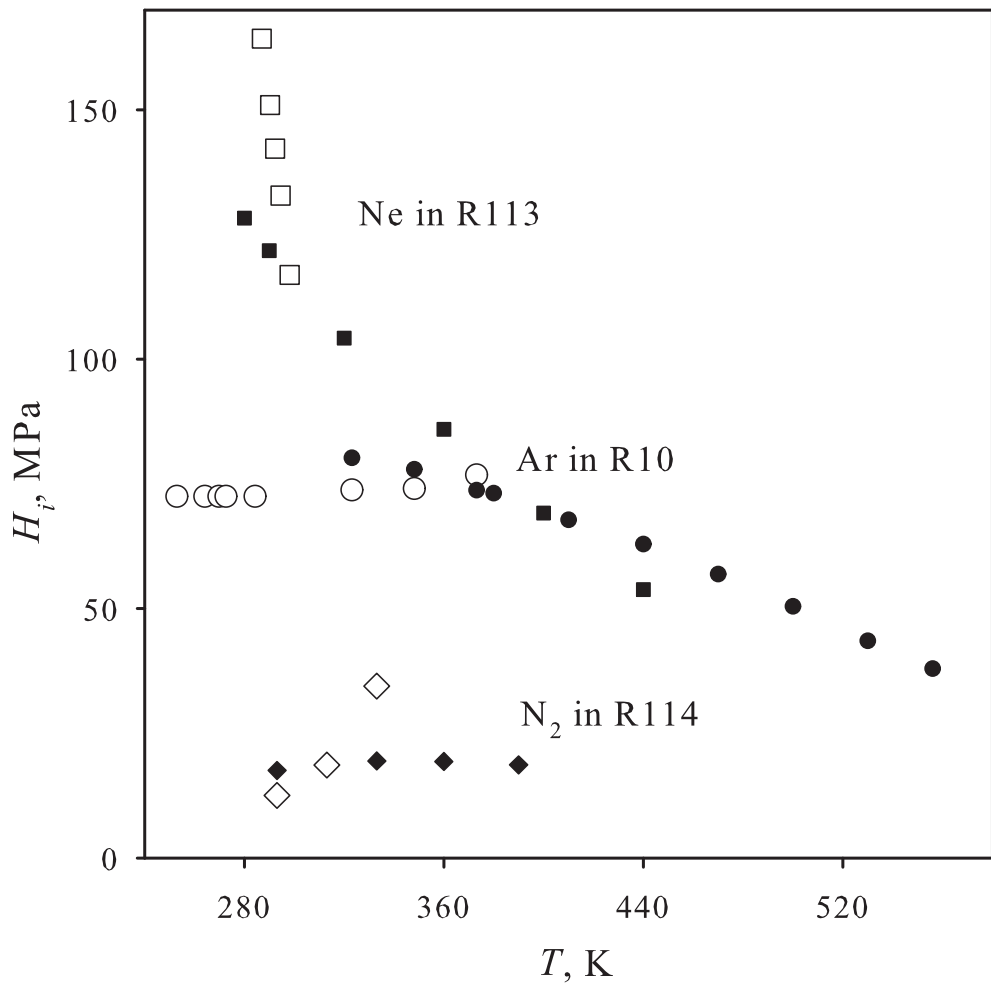


Fig. 4.

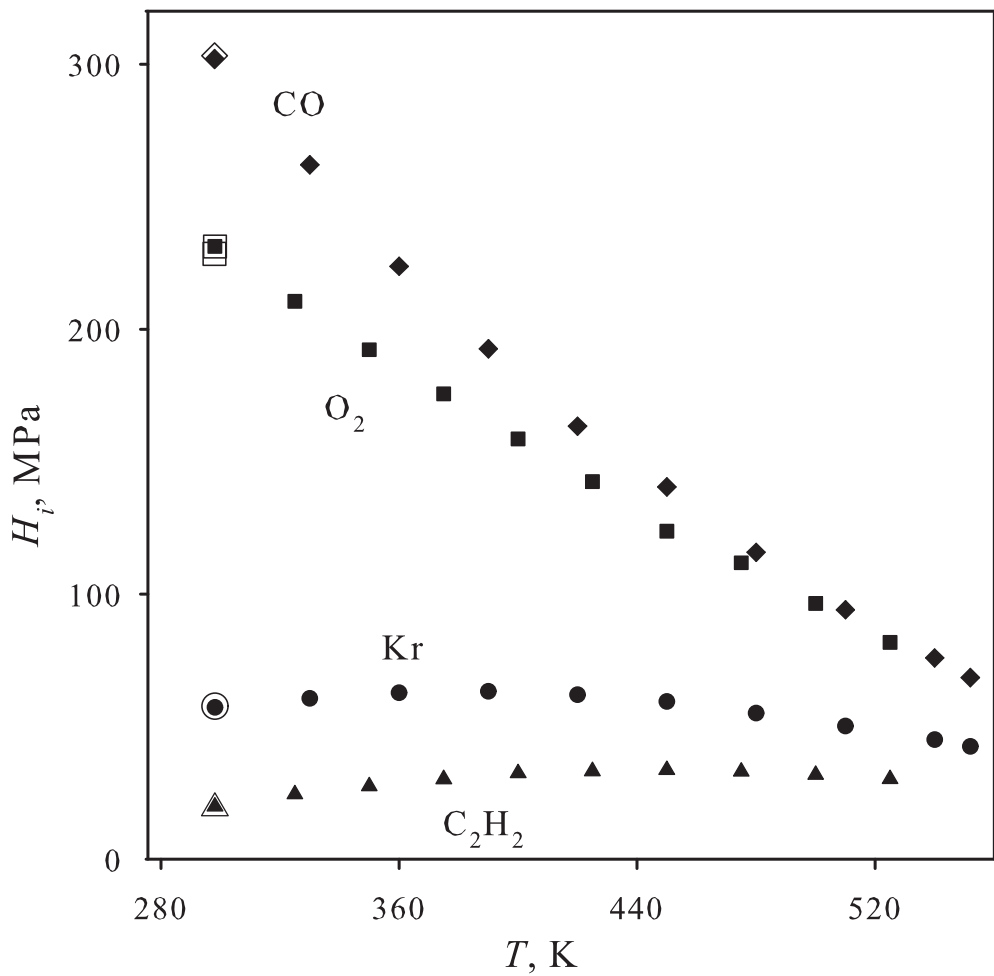


Fig. 5.

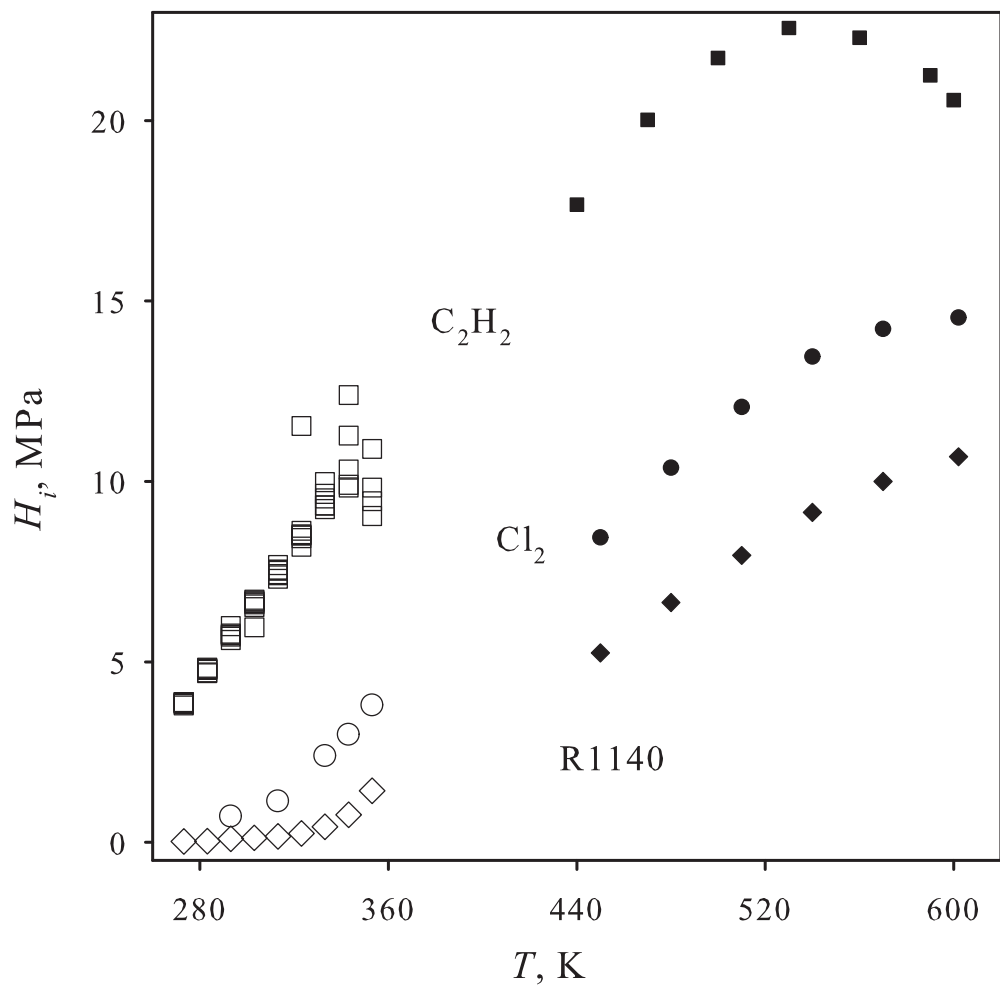


Fig. 6.

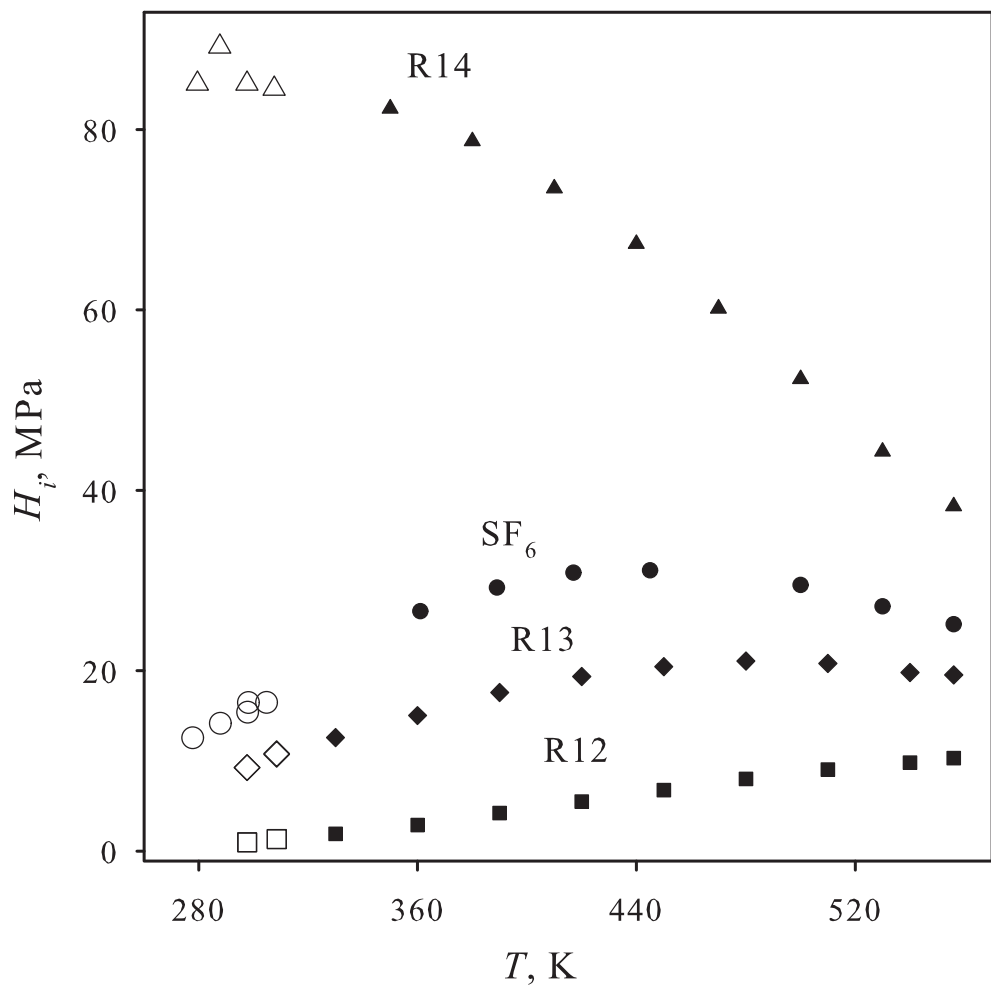


Fig. 7.

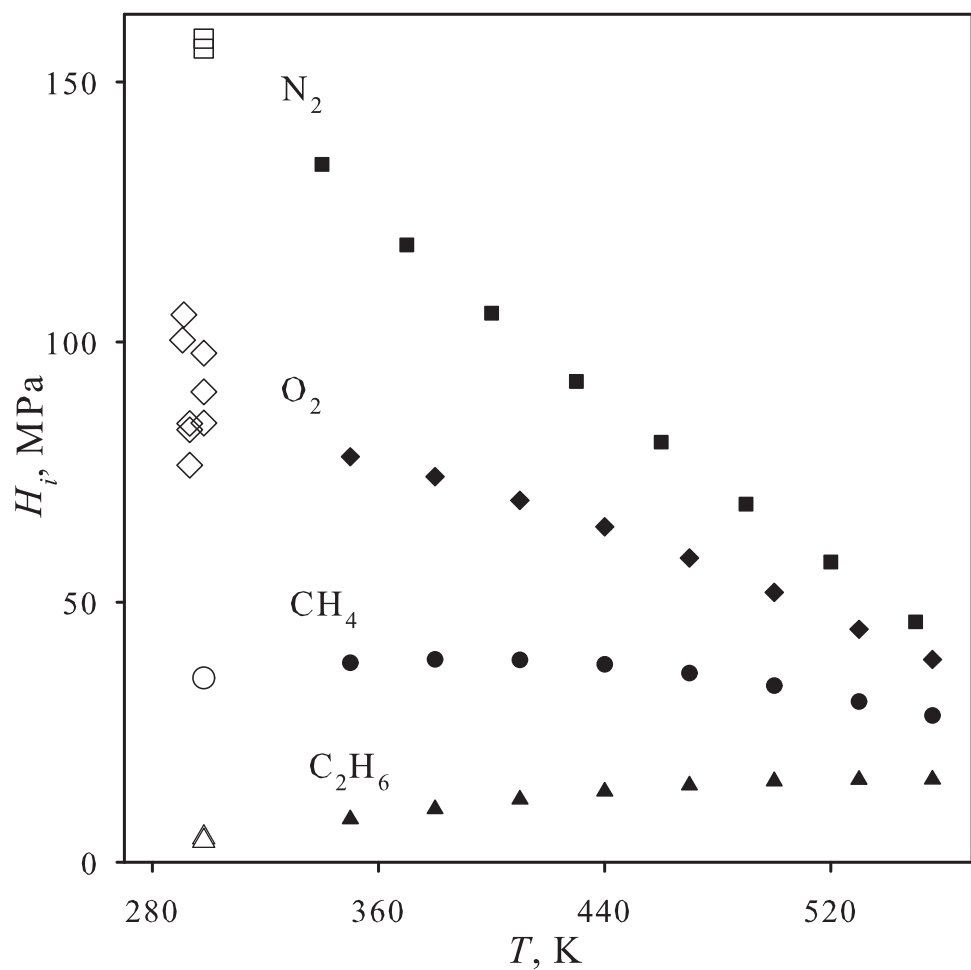


Fig. 8.

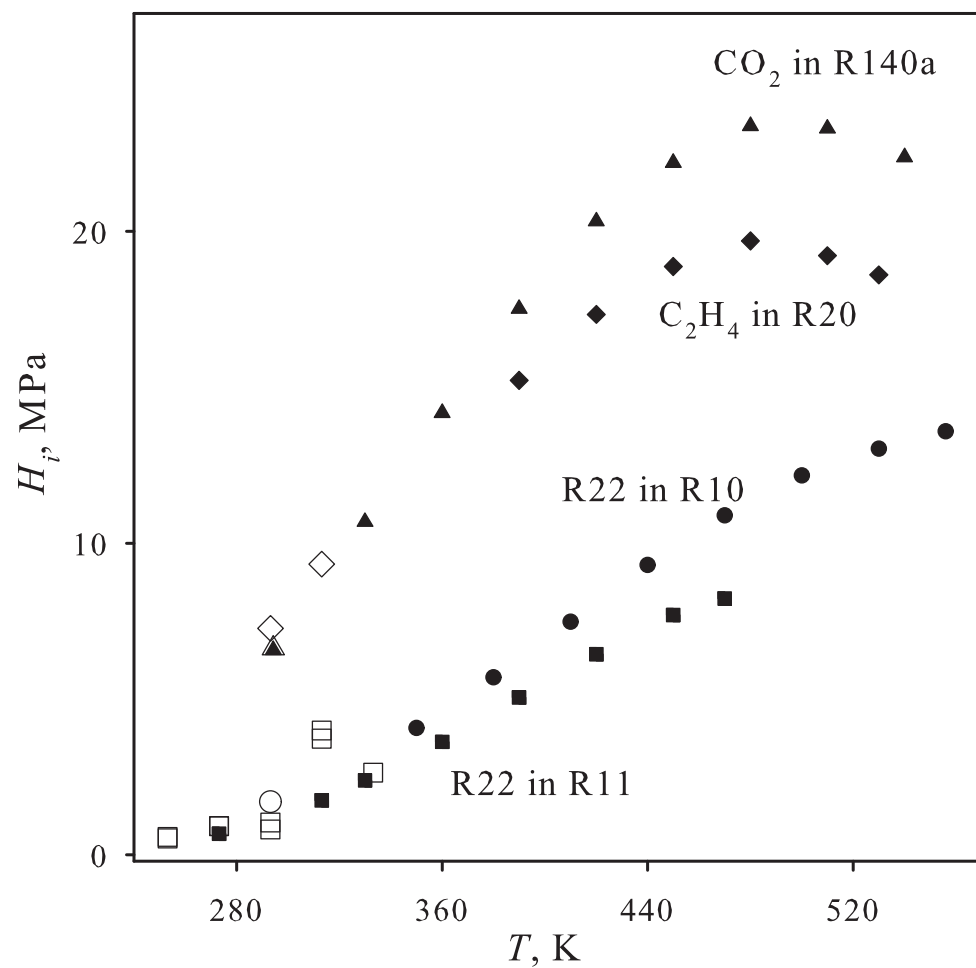


Fig. 9.

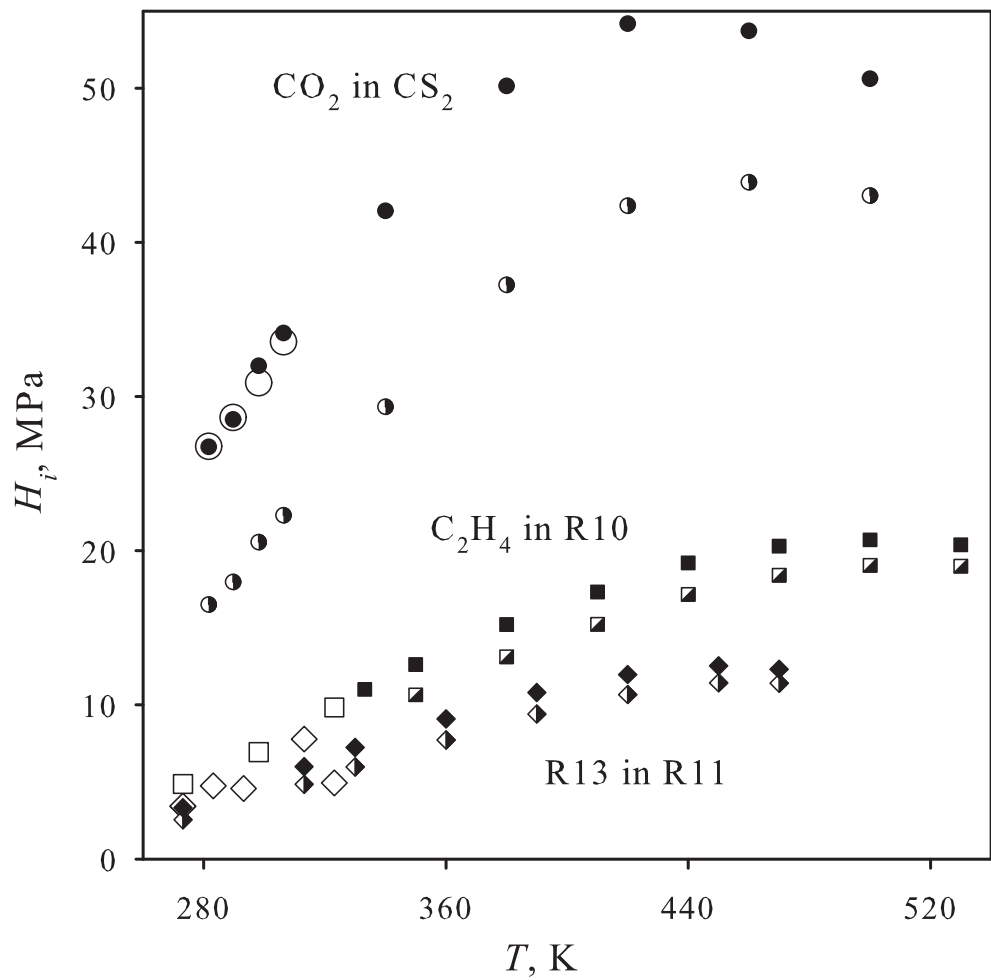


Fig. 10.

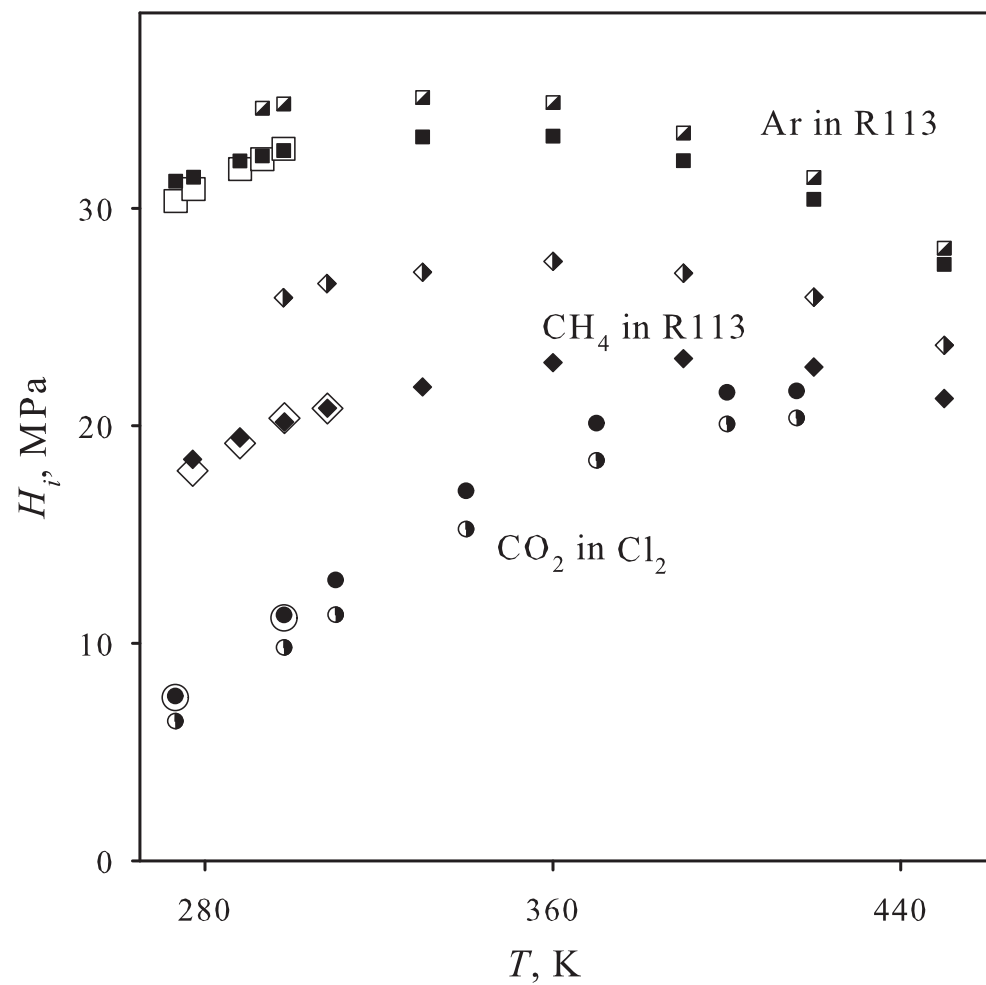


Fig. 11.

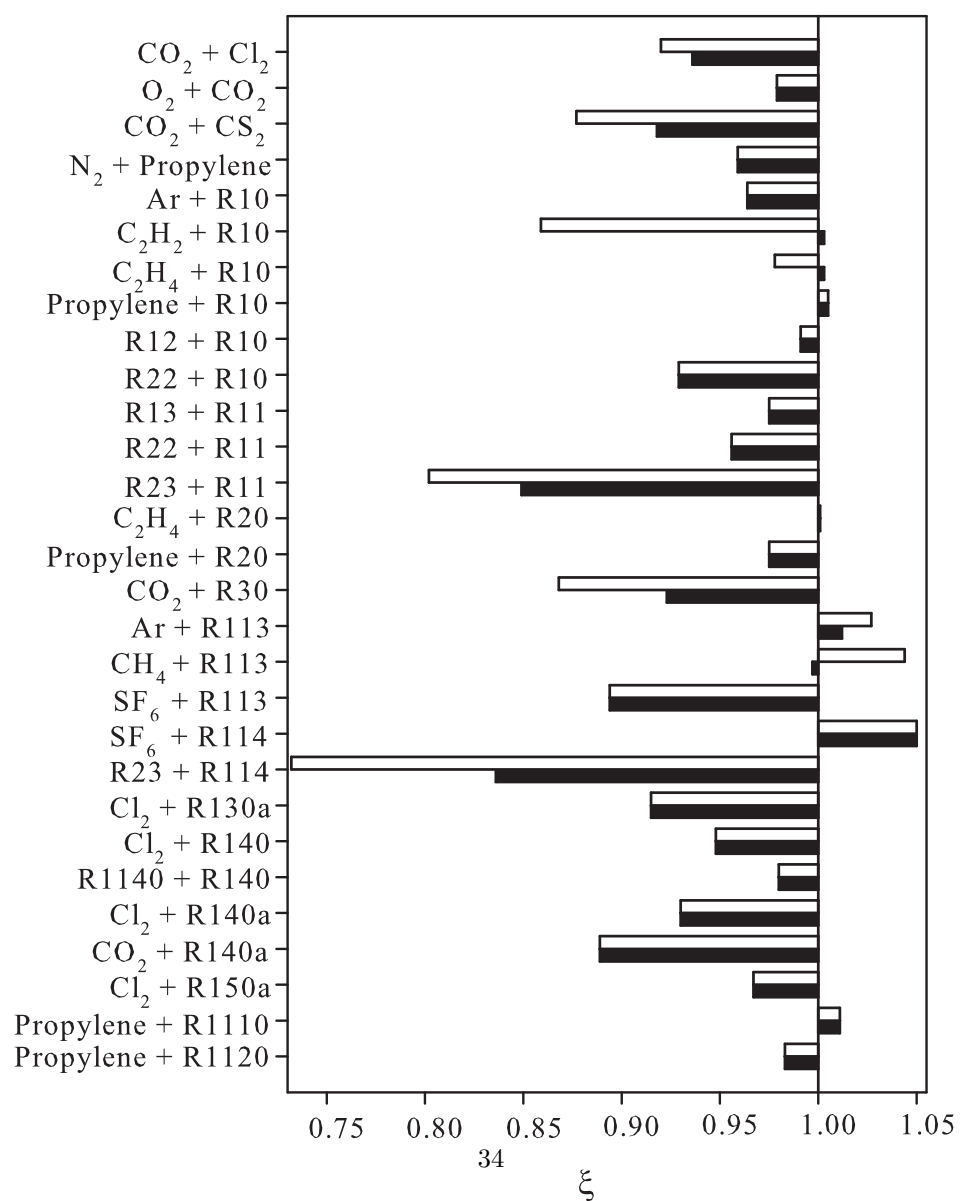
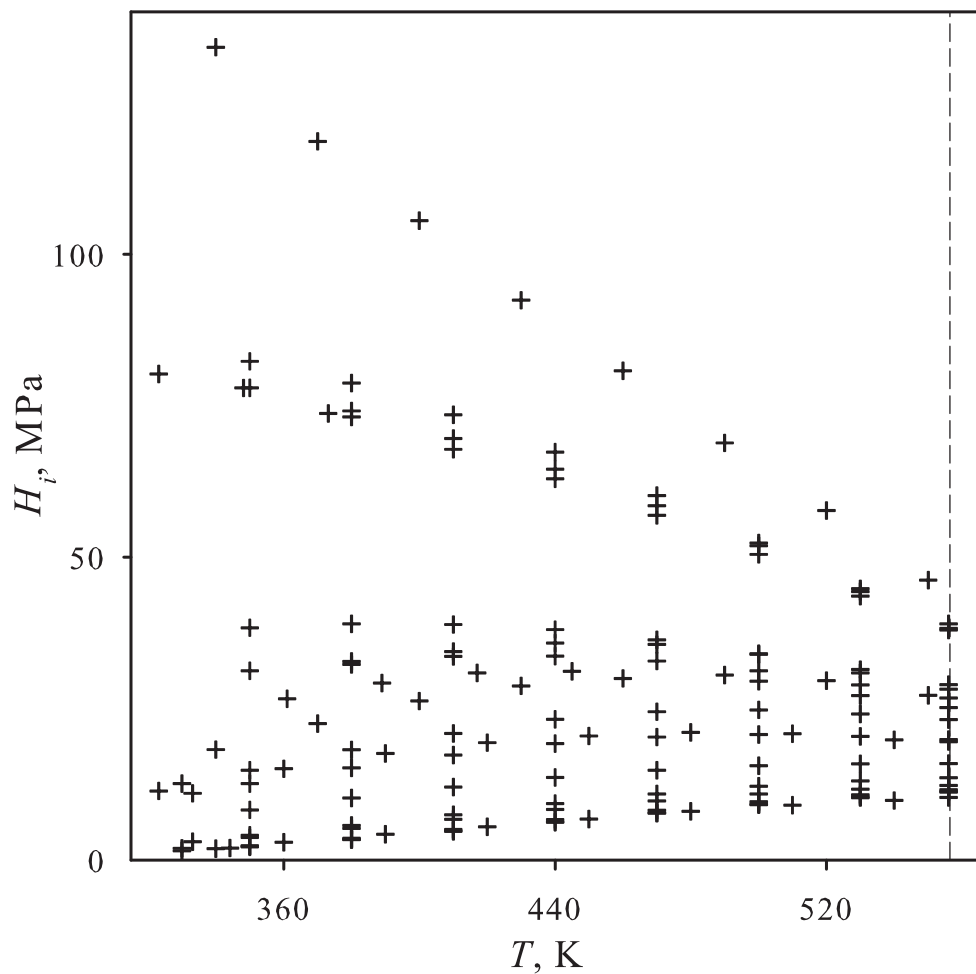


Fig. 12.



## **Supporting Information to:**

### **Henry's law constant from molecular simulation: a systematic approach regarding 95 systems**

Yow-Lin Huang<sup>1</sup>, Svetlana Miroshnichenko<sup>1</sup>, Hans Hasse<sup>2</sup>, Jadran Vrabec \*<sup>1</sup>

<sup>1</sup> Lehrstuhl für Thermodynamik und Energietechnik, Universität Paderborn, Warburger Straße 100, 33098  
Paderborn, Germany

<sup>2</sup> Lehrstuhl für Thermodynamik, Technische Universität Kaiserslautern, Erwin-Schrödinger-Straße 44,  
67663 Kaiserslautern, Germany

This supplementary material contains the full numerical simulation data for the Henry's law constant. Furthermore, the data is graphically compared to the available experimental data. Note that three systems are omitted due to the fact that they could not be simulated (Ne + R10, CO + R140a and CO<sub>2</sub> + R150B2).

---

\* corresponding author, tel.: +49-5251/60-2421, fax: +49-5251/60-3522,  
email: jadran.vrabec@upb.de

Table 1

Henry's law constant from simulation. For mixtures indicated by †, experimental VLE data is available, cf. [1].

$T$ K	$H_1$ MPa	$T$ K	$H_1$ MPa	$T$ K	$H_1$ MPa	$T$ K	$H_1$ MPa
$O_2 + Cl_2$		$CO_2 + Cl_2 \dagger$		$Xe + CO_2$		$O_2 + CO_2 \dagger$	
225	64 (1)	273.15	7.6 (1)	223.15	5.6 (6)	223.75	53.0 (5)
250	66.8 (7)	298.15	11.3 (1)	233.15	6.0 (5)	240	49.9 (4)
275	67.4 (5)	310	12.9 (1)	243.15	6.5 (4)	260	44.4 (3)
298	66.5 (4)	340	17.0 (1)	253.15	7.1 (3)	280	39.4 (2)
325	63.5 (4)	370	20.1 (1)	263.15	7.7 (2)	300	33.7 (2)
350	59.6 (3)	400	21.5 (1)	273.15	8.1 (2)		
375	54.2 (3)	416	21.6 (1)	283.15	8.7 (2)		
400	47.1 (3)			293.15	9.1 (2)		
410	43.6 (3)			298.15	9.3 (2)		
				303.15	9.7 (2)		
$Ar + CS_2$		$Kr + CS_2$		$Xe + CS_2$		$CH_4 + CS_2$	
273	227.0 (3)	298.15	57.2 (4)	298	9.8 (2)	288.16	77 (2)
298.15	208.9 (3)	330	60.7 (3)	325	12.5 (2)	298.15	78 (2)
330	188.9 (2)	360	62.8 (2)	350	15.0 (2)	307.95	79 (2)
360	169.1 (2)	390	63.3 (2)	375	17.7 (1)	340	77.3 (8)
390	150.2 (2)	420	62.0 (2)	400	19.9 (1)	380	76.2 (5)
420	133.7 (1)	450	59.5 (2)	425	21.8 (1)	420	72.2 (4)
450	117 (1)	480	55.1 (1)	450	23.4 (1)	460	65.1 (4)
480	99.6 (2)	510	50.2 (2)	475	24.4 (1)	500	57.3 (3)
510	83.6 (2)	540	45.1 (2)	500	25.0 (1)	550	45.8 (4)
540	69.3 (2)	552	42.5 (2)	525	25.0 (1)		
552	69.2 (2)						

**Table 1** continued.

<i>T</i> K	<i>H</i> <sub>1</sub> MPa	<i>T</i> K	<i>H</i> <sub>1</sub> MPa	<i>T</i> K	<i>H</i> <sub>1</sub> MPa	<i>T</i> K	<i>H</i> <sub>1</sub> MPa
N <sub>2</sub> + CS <sub>2</sub>		O <sub>2</sub> + CS <sub>2</sub>		Cl <sub>2</sub> + CS <sub>2</sub>		CO + CS <sub>2</sub>	
298.15	463 (6)	298.15	231 (2)	298	0.93 (3)	298	302 (4)
304.35	451 (5)	325	211 (2)	325	1.65 (3)	330	262 (2)
330	378 (3)	350	192 (1)	350	2.58 (3)	360	224 (1)
360	307 (2)	375	175.5 (9)	375	3.81 (3)	390	193 (1)
390	253 (2)	400	158.5 (8)	400	5.19 (4)	420	163.4 (1)
420	210 (1)	425	142.5 (7)	425	6.75 (4)	450	140.5 (8)
450	172 (1)	450	123.8 (6)	450	8.39 (4)	480	115.8 (6)
480	137.5 (8)	475	111.8 (5)	475	10.02 (4)	510	94.1 (7)
510	108.7 (8)	500	96.5 (5)	500	11.55 (4)	540	76 (6)
540	85.6 (7)	525	81.9 (6)	525	12.96 (5)	552	68.5 (7)
CO <sub>2</sub> + CS <sub>2</sub> †		C <sub>2</sub> H <sub>2</sub> + CS <sub>2</sub>		C <sub>2</sub> H <sub>4</sub> + CS <sub>2</sub>		C <sub>2</sub> H <sub>6</sub> + CS <sub>2</sub>	
281.65	26.7 (7)	288.15	17.5 (6)	298	15.7 (5)	298.15	9.8 (4)
289.70	28.5 (6)	325	23.9 (4)	325	19.4 (4)	325	12.3 (3)
298.15	32.0 (6)	350	27.8 (3)	350	22.5 (4)	350	15.1 (3)
306.36	34.1 (5)	375	31.6 (2)	375	25.7 (2)	375	18 (2)
340	42.0 (4)	400	34.2 (3)	400	27.9 (3)	400	20.3 (2)
380	50.1 (3)	425	36.2 (2)	425	29.7 (2)	425	22.3 (2)
420	54.2 (3)	450	37.3 (2)	450	30.9 (2)	450	23.9 (2)
460	53.7 (3)	475	37.4 (2)	475	31.2 (2)	475	24.8 (1)
500	50.6 (3)	500	36.6 (2)	500	30.8 (2)	500	25.2 (1)
550	42.8 (3)	525	35.0 (2)	525	29.9 (2)	525	25.0 (2)

**Table 1** continued.

<i>T</i> K	<i>H</i> <sub>1</sub> MPa	<i>T</i> K	<i>H</i> <sub>1</sub> MPa	<i>T</i> K	<i>H</i> <sub>1</sub> MPa	<i>T</i> K	<i>H</i> <sub>1</sub> MPa
Propylene + CS <sub>2</sub>		SF <sub>6</sub> + CS <sub>2</sub>		R14 + CS <sub>2</sub>		N <sub>2</sub> + Propylene†	
298.15	20 (2)	288.29	117 (6)	308	484 (14)	180	52.1 (9)
325	25 (1)	320	117 (2)	325	410 (11)	210	55.0 (5)
350	27.5 (8)	330	115 (2)	350	337 (6)	240	54.1 (3)
375	30.2 (5)	360	103.6 (9)	375	284 (3)	270	51.0 (3)
400	32.4 (5)	390	95.3 (6)	400	236 (3)	300	46.1 (2)
425	33.2 (4)	420	86.7 (4)	425	197 (2)	330	39.5 (2)
450	33.7 (3)	450	76.5 (4)	450	164 (1)	360	31.5 (2)
475	33.1 (2)	480	64.9 (3)	475	135 (1)		
500	31.9 (2)	510	54.5 (3)	500	109.5 (9)		
525	30.2 (2)	540	46.5 (3)	525	88.3 (8)		
N <sub>2</sub> + SF <sub>6</sub>		Ar + R10		Kr + R10†		CH <sub>4</sub> + R10	
240	4.92 (3)	323.15	80.2 (6)	350	31.2 (2)	350	38.3 (3)
260	6.23 (3)	348.15	77.9 (5)	380	32.8 (2)	380	39.0 (3)
280	7.43 (3)	373.15	73.7 (4)	410	33.6 (2)	410	38.9 (2)
300.15	8.34 (3)	380	73.1 (4)	440	33.6 (1)	440	38.0 (2)
318	8.84 (4)	410	67.8 (3)	470	32.8 (1)	470	36.3 (2)
		440	62.9 (2)	500	31.2 (1)	500	33.9 (1)
		470	56.9 (3)	530	28.9 (2)	530	30.9 (2)
		500	50.4 (2)	556	26.7 (2)	556	28.2 (2)
		530	43.5 (3)				
		556	38.0 (3)				

**Table 1** continued.

<i>T</i>	<i>H</i> <sub>1</sub>	<i>T</i>	<i>H</i> <sub>1</sub>	<i>T</i>	<i>H</i> <sub>1</sub>	<i>T</i>	<i>H</i> <sub>1</sub>
K	MPa	K	MPa	K	MPa	K	MPa
N <sub>2</sub> + R10		O <sub>2</sub> + R10		Cl <sub>2</sub> + R10		Cl <sub>2</sub> + R10	
340	134 (1)	350	77.9 (4)	330	1.53 (2)	500	9.11 (3)
370	118.6 (7)	380	74.1 (4)	340	1.86 (2)	530	10.30 (4)
400	105.6 (5)	410	69.6 (3)	344.15	2.0 (2)	556	11.19 (5)
430	92.4 (5)	440	64.5 (3)	350	2.18 (2)		
460	80.8 (4)	470	58.5 (3)	380	3.34 (2)		
490	68.8 (4)	500	51.9 (2)	410	4.72 (3)		
520	57.7 (4)	530	44.8 (3)	440	6.21 (3)		
550	46.2 (4)	556	39.0 (3)	470	7.70 (3)		
CO <sub>2</sub> + R10		C <sub>2</sub> H <sub>2</sub> + R10†		C <sub>2</sub> H <sub>4</sub> + R10†		C <sub>2</sub> H <sub>6</sub> + R10	
340	18.2 (1)	323.15	11.4 (1)	333.15	11.0 (4)	350	8.3 (1)
370	22.5 (1)	350	14.8 (1)	350	12.6 (1)	380	10.22 (9)
400	26.2 (1)	380	18.2 (1)	380	15.2 (1)	410	12.04 (9)
430	28.7 (1)	410	20.9 (1)	410	17.3 (1)	440	13.62 (7)
460	30.0 (1)	440	23.2 (1)	440	19.2 (1)	470	14.80 (8)
490	30.5 (1)	470	24.5 (1)	470	20.3 (1)	500	15.57 (7)
520	29.6 (2)	500	24.8 (1)	500	20.7 (1)	530	15.85 (8)
550	27.2 (2)	530	24.1 (1)	530	20.4 (1)	556	15.9 (1)
		556	23.1 (2)	556	19.9 (1)		

**Table 1** continued.

<i>T</i> K	<i>H</i> <sub>1</sub> MPa	<i>T</i> K	<i>H</i> <sub>1</sub> MPa	<i>T</i> K	<i>H</i> <sub>1</sub> MPa	<i>T</i> K	<i>H</i> <sub>1</sub> MPa
Propylene + R10†		SF <sub>6</sub> + R10		R12 + R10†		R13 + R10	
333.15	2.8 (9)	361	26.6 (7)	330	1.9 (10)	330	12.6 (3)
350	3.20 (6)	389	29.2 (4)	360	2.9 (5)	360	15.0 (2)
380	4.58 (5)	417	30.9 (3)	390	4.2 (3)	390	17.6 (2)
410	6.01 (6)	445	31.1 (3)	420	5.5 (2)	420	19.4 (2)
440	7.58 (5)	500	29.5 (2)	450	6.8 (2)	450	20.5 (2)
470	8.96 (6)	530	27.1 (2)	479.99	8.0 (1)	479.99	21.1 (1)
500	10.12 (5)	536	25.2 (3)	510	9.1 (1)	510	20.8 (1)
530	11.00 (5)			540	9.8 (2)	540	19.8 (2)
556	11.68 (7)			556	10.3 (2)	556	19.5 (2)
R14 + R10		R22 + R10†		R23 + R10†		R40 + R10	
350	82 (1)	350	4.07 (7)	380	32.3 (3)	350	2.23 (2)
380	78.7 (8)	380	5.70 (7)	410	34.4 (2)	380	3.39 (3)
410	73.5 (6)	410	7.48 (6)	440	35.8 (2)	410	4.79 (3)
440	67.3 (4)	440	9.30 (6)	470	35.6 (2)	440	6.31 (3)
470	60.2 (4)	470	10.89 (6)	500	34.1 (2)	470	7.82 (3)
500	52.3 (3)	500	12.17 (6)	530	31.4 (2)	500	9.23 (3)
530	44.3 (3)	530	13.03 (6)	556	28.9 (3)	530	10.42 (4)
556	38.2 (4)	556	13.59 (9)			556	11.30 (6)

**Table 1** continued.

<i>T</i> K	<i>H</i> <sub>1</sub> MPa	<i>T</i> K	<i>H</i> <sub>1</sub> MPa	<i>T</i> K	<i>H</i> <sub>1</sub> MPa	<i>T</i> K	<i>H</i> <sub>1</sub> MPa
R161 + R10		R13 + R11†		R22 + R11†		R23 + R11†	
350	2.34 (4)	273.15	2.56 (7)	273.15	0.68 (2)	273.15	10.1 (1)
380	3.56 (4)	313.15	4.84 (7)	313.15	1.75 (2)	303.15	14.0 (1)
410	5.05 (4)	330	5.97 (6)	330	2.39 (2)	313.15	15.2 (1)
440	6.64 (4)	360	7.72 (5)	360	3.63 (2)	330	17.2 (1)
470	8.21 (4)	390	9.41 (6)	390	5.05 (3)	360	19.6 (1)
500	9.63 (4)	420	10.67 (6)	420	6.44 (3)	390	21.2 (1)
530	10.77 (5)	450	11.43 (8)	450	7.69 (4)	420	21.6 (1)
556	11.62 (7)	470	11.41 (8)	470	8.23 (4)	450	20.6 (2)
						470	19.0 (2)
N <sub>2</sub> + R20		O <sub>2</sub> + R20		Cl <sub>2</sub> + R20		C <sub>2</sub> H <sub>4</sub> + R20†	
298	196.9 (3)	289.15	140.6 (3)	283.15	0.4 (1)	390	15.2 (2)
330	171.1 (2)	289.65	140.8 (2)	298.15	0.6 (8)	420	17.3 (1)
360	148.9 (2)	330	125.6 (2)	330	1.4 (4)	450	18.9 (1)
390	128.2 (2)	360	114.7 (2)	360	2.5 (3)	480	19.7 (1)
420	108.8 (2)	390	102.8 (1)	390	3.8 (2)	510	19.2 (1)
450	90.3 (2)	420	90.7 (1)	420	5.4 (1)	530	18.6 (1)
480	74.1 (2)	450	78.0 (1)	450	7.0 (1)		
510	57.2 (3)	480	66.1 (2)	480	8.7 (1)		
536	42.8 (4)	510	52.7 (3)	510	10.1 (1)		
		536	40.3 (4)	536.40	10.9 (2)		

**Table 1** continued.

<i>T</i> K	<i>H</i> <sub>1</sub> MPa	<i>T</i> K	<i>H</i> <sub>1</sub> MPa	<i>T</i> K	<i>H</i> <sub>1</sub> MPa	<i>T</i> K	<i>H</i> <sub>1</sub> MPa
Propylene + R20†		R22 + R20		R40 + R20		R161 + R20	
390	6.79 (7)	293.15	2 (2)	298.15	0.4 (13)	293.15	2 (2)
420	8.55 (6)	310	2 (1)	310	0.6 (8)	330	3.7 (8)
450	10.22 (7)	330	3.3 (9)	330	1.0 (5)	360	5.5 (5)
480	11.61 (7)	360	5.1 (5)	360	1.8 (4)	390	7.5 (3)
510	12.29 (7)	390	6.9 (3)	390	2.9 (2)	420	9.4 (2)
536	12.68 (9)	420	8.7 (2)	420	4.1 (2)	450	11.1 (2)
		450	10.3 (2)	450	5.5 (1)	480	12.5 (2)
		480	11.7 (2)	480	7.0 (1)	510	13.2 (2)
		510	12.5 (2)	510	8.3 (1)	536	13.1 (2)
		536	12.5 (2)	536	9.1 (1)		
Kr + R20B3		CH <sub>4</sub> + R30		Cl <sub>2</sub> + R30		CO <sub>2</sub> + R30†	
295.15	61 (1)	303.15	80.8 (8)	273.15	0.190 (4)	270.01	4.58 (6)
315	67 (1)	320	81.8 (7)	298.15	0.474 (8)	294.27	7.88 (6)
330	70 (1)	350	81.4 (5)	320	0.864 (7)	310.94	10.38 (7)
360	73.3 (7)	380	77.9 (5)	350	1.71 (5)	327.60	12.95 (8)
390	75.3 (6)	410	71.8 (4)	380	2.94 (5)	360	17.93 (9)
400	75.5 (6)	440	64.1 (4)	410	4.50 (4)	390	22.0 (1)
420	75.2 (5)	470	53.7 (4)	440	6.31 (4)	420.01	25.2 (1)
		500	44.3 (5)	470	8.15 (4)	450	27.0 (1)
		510	42.2 (4)	500	10.01 (5)	480	26.7 (2)
				510	10.60 (5)	510	26.1 (2)

**Table 1** continued.

<i>T</i> K	<i>H</i> <sub>1</sub> MPa	<i>T</i> K	<i>H</i> <sub>1</sub> MPa	<i>T</i> K	<i>H</i> <sub>1</sub> MPa	<i>T</i> K	<i>H</i> <sub>1</sub> MPa
CH <sub>4</sub> + R40		Ne + R113		Ar + R113†		Ar + R113†	
293.15	32.8 (3)	280	128.3 (1)	273.25	31.3 (2)	390	32.2 (1)
325	34.3 (2)	290	121.8 (1)	277.35	31.4 (2)	420	30.4 (1)
350	34.2 (2)	298.15	116.9 (1)	288.05	32.2 (2)	450	27.4 (1)
375	32.8 (2)	320	104.2 (1)	293.17	32.4 (2)	480	24.1 (2)
400	30.1 (2)	360	86.0 (1)	298.06	32.7 (2)		
416	28.1 (2)	400	69.2 (1)	330	33.3 (2)		
		440	53.8 (1)	360	33.3 (1)		
Xe + R113		CH <sub>4</sub> + R113†		N <sub>2</sub> + R113		CO <sub>2</sub> + R113	
280	2.2 (3)	277.15	18.5 (3)	277.15	53.1 (4)	308.5	6.4 (5)
290	2.5 (3)	288.05	19.4 (3)	298.13	52.5 (4)	330	8.7 (5)
298.15	2.8 (3)	298.24	20.2 (2)	330	50.6 (3)	350	10.6 (5)
340	4.6 (2)	308.15	20.8 (1)	360	48.0 (2)	380	13.1 (3)
380	6.4 (1)	330	21.8 (1)	390	44.1 (2)	400	14.4 (3)
400	7.2 (1)	360	22.9 (1)	420	39.7 (2)	440	16.2 (4)
		390	23.0 (1)	450	34.1 (2)	463	16.5 (5)
		420	22.7 (1)	480	28.6 (2)		
		450	21.3 (1)				
		480	19.4 (1)				

**Table 1** continued.

<i>T</i>	<i>H</i> <sub>1</sub>	<i>T</i>	<i>H</i> <sub>1</sub>	<i>T</i>	<i>H</i> <sub>1</sub>	<i>T</i>	<i>H</i> <sub>1</sub>
K	MPa	K	MPa	K	MPa	K	MPa
C <sub>2</sub> H <sub>4</sub> + R113		C <sub>2</sub> H <sub>6</sub> + R113		SF <sub>6</sub> + R113†		R14 + R113	
300.15	7.00 (7)	280	2.87 (4)	255	2.3(20)	278.40	18.5 (5)
343.15	10.42 (6)	290	3.24 (4)	266	3.1(12)	286.65	20.0 (5)
363.15	11.80 (7)	298.08	3.64 (4)	293	4.6 (7)	298.13	21.3 (4)
380	12.89 (6)	320	4.72 (4)	319	6.6 (4)	306.04	22.6 (3)
410	14.22 (7)	360	6.74 (4)	329	7.3 (4)	330	25.1 (3)
440	14.94 (7)			360	9.5 (2)	360	27.0 (2)
470	14.74 (8)			389.99	11.2 (2)	390	27.7 (2)
487	14.56 (9)			420	12.6 (1)	420	26.9 (2)
				450	13.0 (1)		
				480	13.0 (2)		
R116 + R113		R1114 + R113		R1132 + R113		N <sub>2</sub> + R114	
290	3 (2)	298.15	3.3 (9)	298.15	2.5 (5)	293.15	17.5 (2)
300.73	3 (2)	323.15	4.9 (6)	323.15	3.8 (3)	313.15	18.6 (1)
320	5 (1)	343.15	6.4 (3)	343.15	4.9 (3)	333.15	19.4 (1)
360	7.5 (5)	363.15	7.8 (2)	363.15	6.2 (2)	360	19.4 (1)
400	9.7 (2)	400	10.1 (2)	390	7.8 (2)	390	18.7 (1)
		430	11.5 (2)	420	9.4 (1)		
		460	12.2 (2)	450	10.5 (1)		
				480	11.1 (2)		
				487.25	11.2 (2)		

**Table 1** continued.

<i>T</i> K	<i>H</i> <sub>1</sub> MPa	<i>T</i> K	<i>H</i> <sub>1</sub> MPa	<i>T</i> K	<i>H</i> <sub>1</sub> MPa	<i>T</i> K	<i>H</i> <sub>1</sub> MPa
SF <sub>6</sub> + R114†		R23 + R114†		Cl <sub>2</sub> + R130a†		Cl <sub>2</sub> + R140†	
252	0.3 (10)	270	6.21 (8)	358	3.5 (2)	450	8.45 (3)
270	0.5 (9)	303.15	9.45 (7)	373	4.2 (1)	480	10.38 (4)
277	0.7 (5)	330	11.86 (7)	400	5.8 (1)	510	12.06 (4)
300	1.1 (3)	360	13.84 (7)	430	7.8 (1)	540	13.46 (5)
330	2.0 (2)	390	14.56 (8)	460	9.78 (9)	570	14.22 (6)
360	3.0 (1)	415	14.2 (1)			602	14.53 (9)
390	4.1 (1)						
410	4.8 (1)						
C <sub>2</sub> H <sub>2</sub> + R140		R1140 + R140†		Cl <sub>2</sub> + R140a†		CO <sub>2</sub> + R140a†	
440	17.67 (8)	450	5.25 (3)	281	0.7 (4)	294.26	6.57 (6)
470	20.02 (8)	480	6.65 (4)	293	0.9 (3)	330	10.68 (6)
500	21.73 (8)	510	7.95 (3)	303	1.2 (2)	360	14.18 (7)
530	22.56 (9)	540	9.14 (4)	313	1.5 (2)	390	17.52 (6)
560	22.3 (1)	570	10.00 (5)	328	2.0 (2)	420	20.32 (8)
590	21.3 (1)	602	10.68 (6)	360	3.4 (1)	450	22.20 (8)
600	20.6 (2)			390	4.9 (1)	480	23.4 (1)
				420	6.6 (1)	510	23.3 (1)
				450	8.27 (8)	540	22.4 (2)
				480	9.98 (8)		
				510	11.15 (8)		
				540	12.1 (1)		

**Table 1** continued.

<i>T</i> K	<i>H</i> <sub>1</sub> MPa	<i>T</i> K	<i>H</i> <sub>1</sub> MPa	<i>T</i> K	<i>H</i> <sub>1</sub> MPa	<i>T</i> K	<i>H</i> <sub>1</sub> MPa
C <sub>2</sub> H <sub>2</sub> + R140a		R1140 + R140a		Cl <sub>2</sub> + R150a†		C <sub>2</sub> H <sub>2</sub> + R150a	
323.15	8.86 (7)	323	1.23 (3)	360	2.8 (2)	360	9.18 (6)
350	11.67 (6)	350	2.03 (2)	390	4.3 (2)	390	11.92 (6)
380	14.60 (7)	380	3.11 (2)	420	5.95 (9)	420	14.39 (6)
410	17.29 (7)	410	4.37 (3)	450	7.61 (7)	450	16.13 (6)
440	19.36 (8)	440	5.75 (3)	480	9.11 (8)	480	17.02 (7)
470	20.64 (8)	470	7.06 (3)	510	10.29 (9)	510	16.2 (1)
500	21.1 (1)	500	8.27 (4)	520	10.67 (9)	523	13.7 (3)
530	20.5 (1)	530	9.22 (4)				
540	20.4 (1)	540	9.55 (5)				
Cl <sub>2</sub> + R150B2		CO + R150B2		O <sub>2</sub> + R1110		Propylene + R1110†	
313.15	0.8 (16)	298.15	369.1 (6)	380	87.6 (2)	380	5.4 (1)
330	1.2 (9)	330	321.9 (4)	410	83.6 (2)	410	7.2 (1)
360	2.1 (5)	360	279.1 (3)	440	78.0 (1)	440	9.15 (9)
390	3.3 (4)	390	240.2 (3)	470	72.5 (1)	470	10.90 (7)
420	4.9 (3)	420	211.1 (2)	500	66.4 (1)	500	12.41 (7)
450	6.6 (2)	450	182.8 (2)	530	60.4 (1)	530	13.71 (7)
480	8.4 (2)	480	158.9 (2)	560	53.7 (2)	560	14.64 (8)
510	10.3 (1)	510	138.6 (2)	590	46.4 (2)	590	15.03 (8)
540	12.1 (1)	540	120.1 (2)	620	39.8 (2)	620	15.25 (9)
570	13.6 (1)	570	101.6 (2)				

**Table 1** continued.

<i>T</i>	<i>H</i> <sub>1</sub>	<i>T</i>	<i>H</i> <sub>1</sub>	<i>T</i>	<i>H</i> <sub>1</sub>	<i>T</i>	<i>H</i> <sub>1</sub>
K	MPa	K	MPa	K	MPa	K	MPa
R23 + R1110		O <sub>2</sub> + R1120		CO <sub>2</sub> + R1120		C <sub>2</sub> H <sub>2</sub> + R1120	
380	60.0 (7)	340	88.3 (2)	310	16.3 (5)	314	13.1 (6)
410	62.5 (5)	370	84.1 (2)	340	22.1 (4)	342	17.3 (4)
440	62.6 (4)	400	78.8 (1)	370	27.8 (2)	371	21.7 (3)
470	61.0 (3)	430	72.7 (1)	400	32.1 (2)	400	25.2 (2)
500	58.0 (3)	460	66.7 (1)	430	35.0 (2)	430	27.8 (2)
530	54.3 (3)	490	60.4 (1)	460	36.9 (1)	460	29.5 (2)
560	49.3 (3)	520	52.7 (2)	471	37.1 (1)		
590	43.2 (3)	550	45.0 (3)				
620	37.5 (3)	571	39.3 (3)				
Propylene + R1120†		C <sub>2</sub> H <sub>2</sub> + R1140					
303.15	2.0 (2)	215.15	0.5 (20)				
323.15	3.5 (2)	220.65	0.6 (18)				
343.15	4.7 (1)	225.65	0.8 (16)				
360	5.8 (1)	231.65	0.9 (13)				
390	7.7 (1)	236.65	1.1 (13)				
420	9.50 (9)	242.15	1.3 (11)				
450	11.06 (9)	280	3.1 (4)				
480	12.44 (8)	320	5.8 (2)				
510	13.51 (8)	360	8.9 (1)				
540	14.07 (8)						
571	14.24 (9)						

Fig. 1. Henry's law constant of O<sub>2</sub> in liquid Cl<sub>2</sub>. Simulation data: ●; experimental data: + [3].

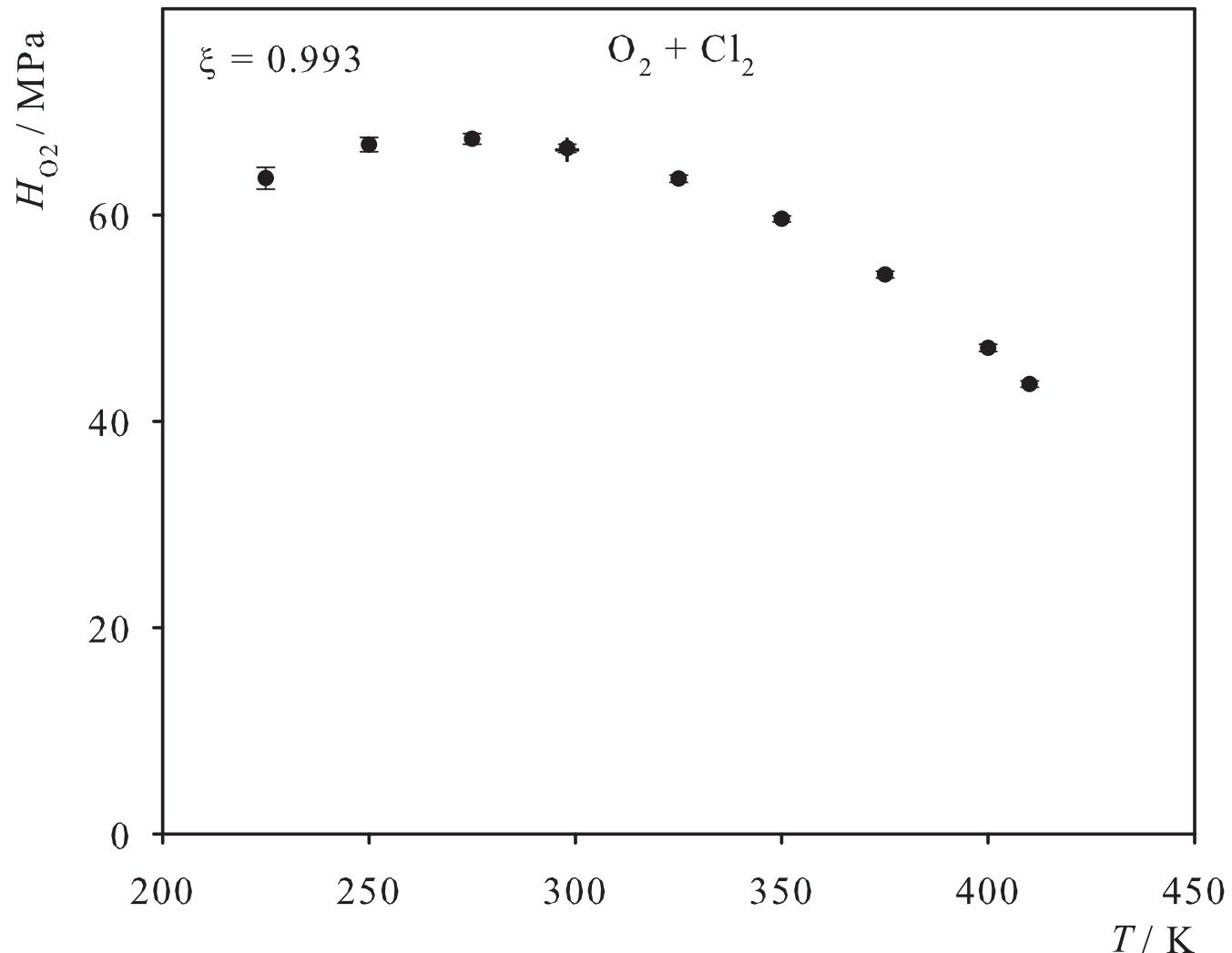


Fig. 2. Henry's law constant of CO<sub>2</sub> in liquid Cl<sub>2</sub>. Simulation data: ● ( $\xi=0.920$ ), ○ ( $\xi=0.936$ ); experimental data: + [3].

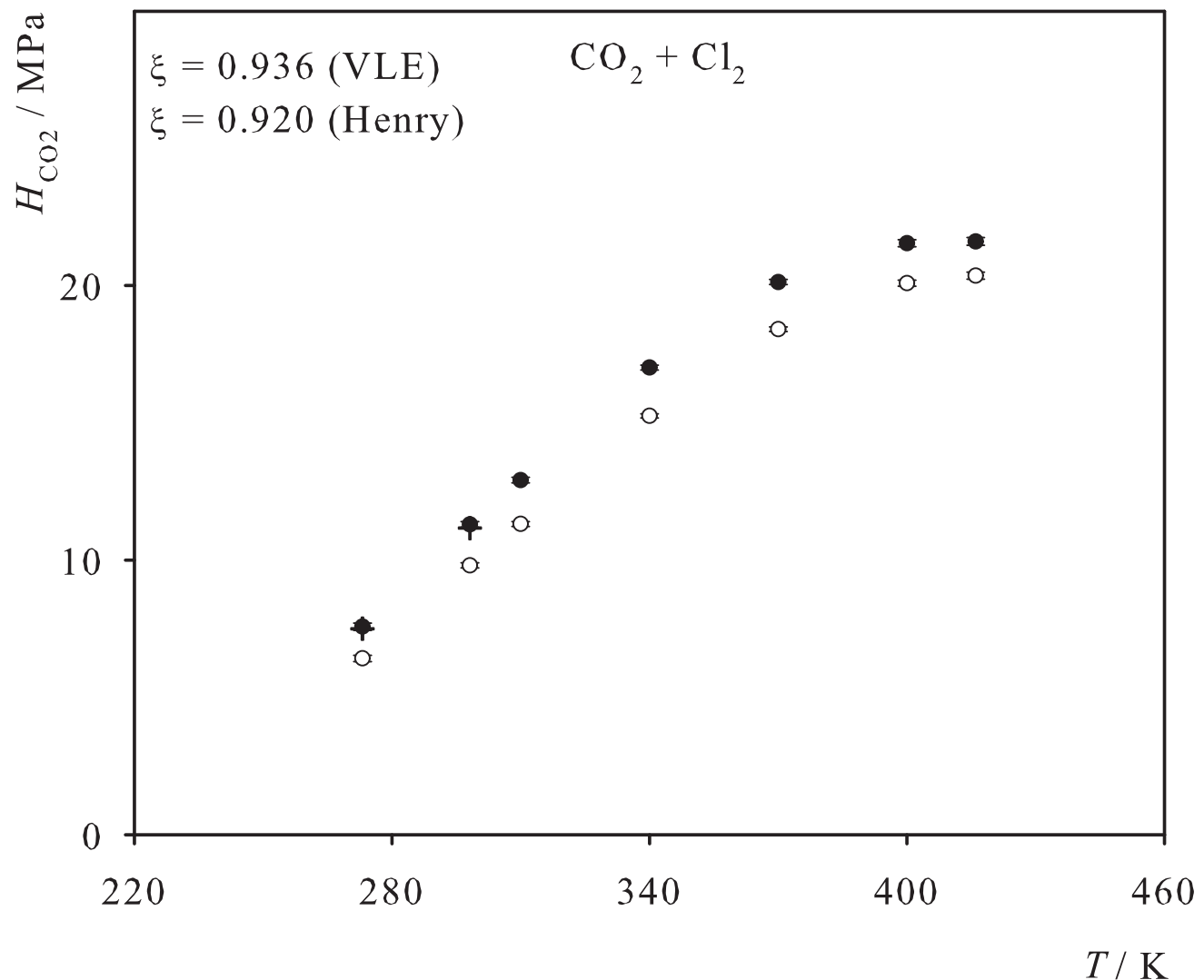


Fig. 3. Henry's law constant of Xe in liquid CO<sub>2</sub>. Simulation data: ●; experimental data: + [4].

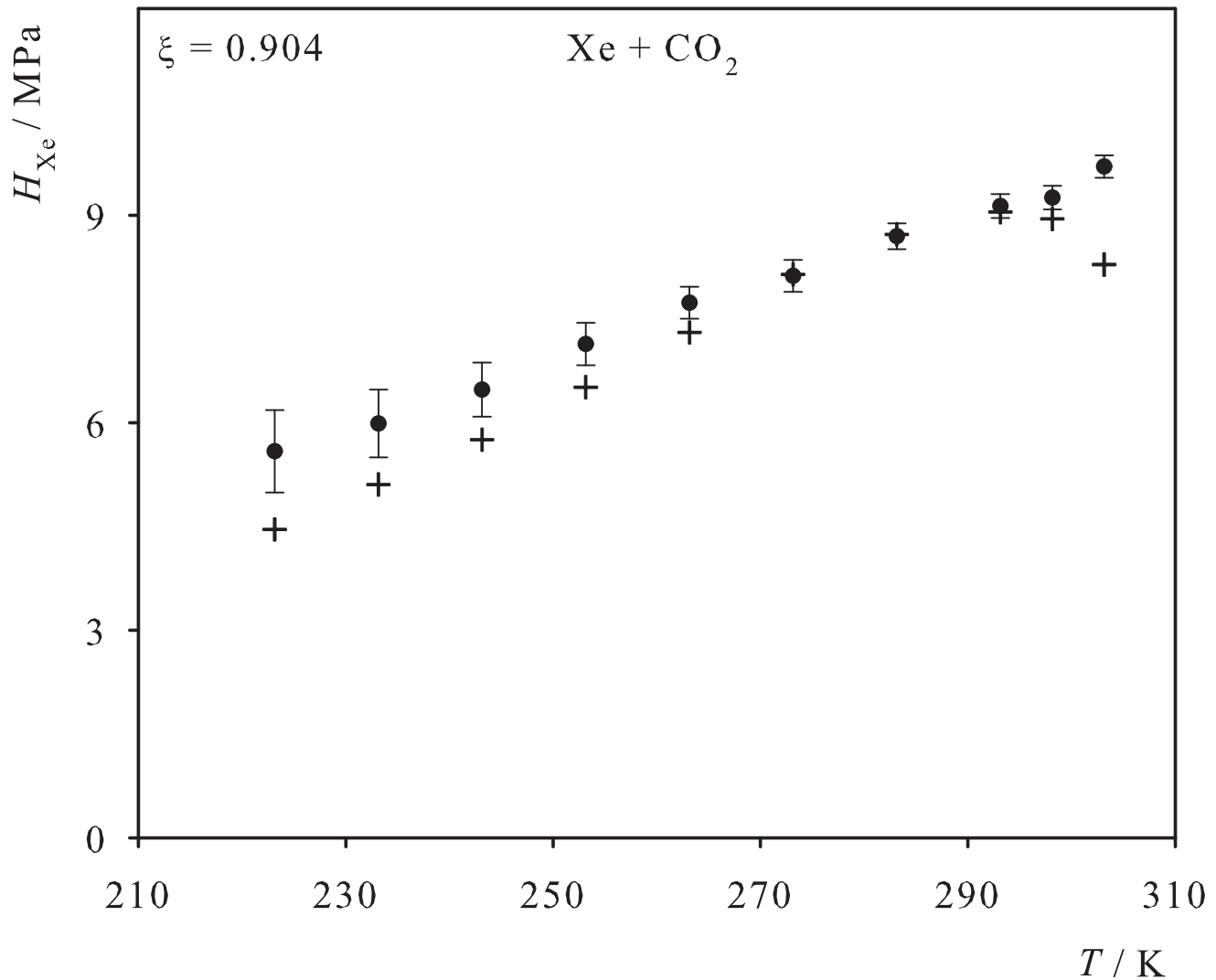


Fig. 4. Henry's law constant of O<sub>2</sub> in liquid CO<sub>2</sub>. Simulation data: ●; experimental data: + [5].

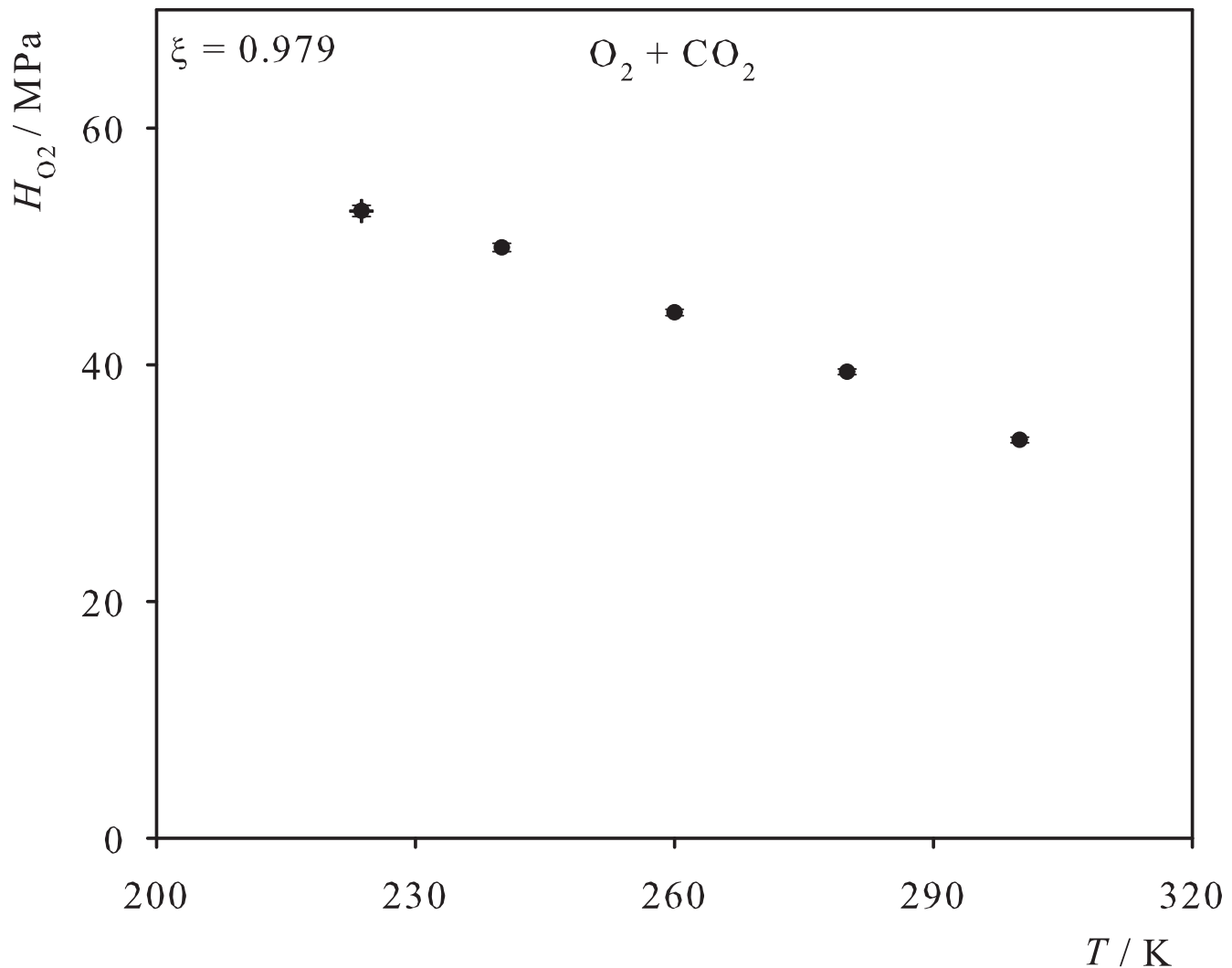


Fig. 5. Henry's law constant of Ar in liquid CS<sub>2</sub>. Simulation data: ●; experimental data: + [6], ■ [7].

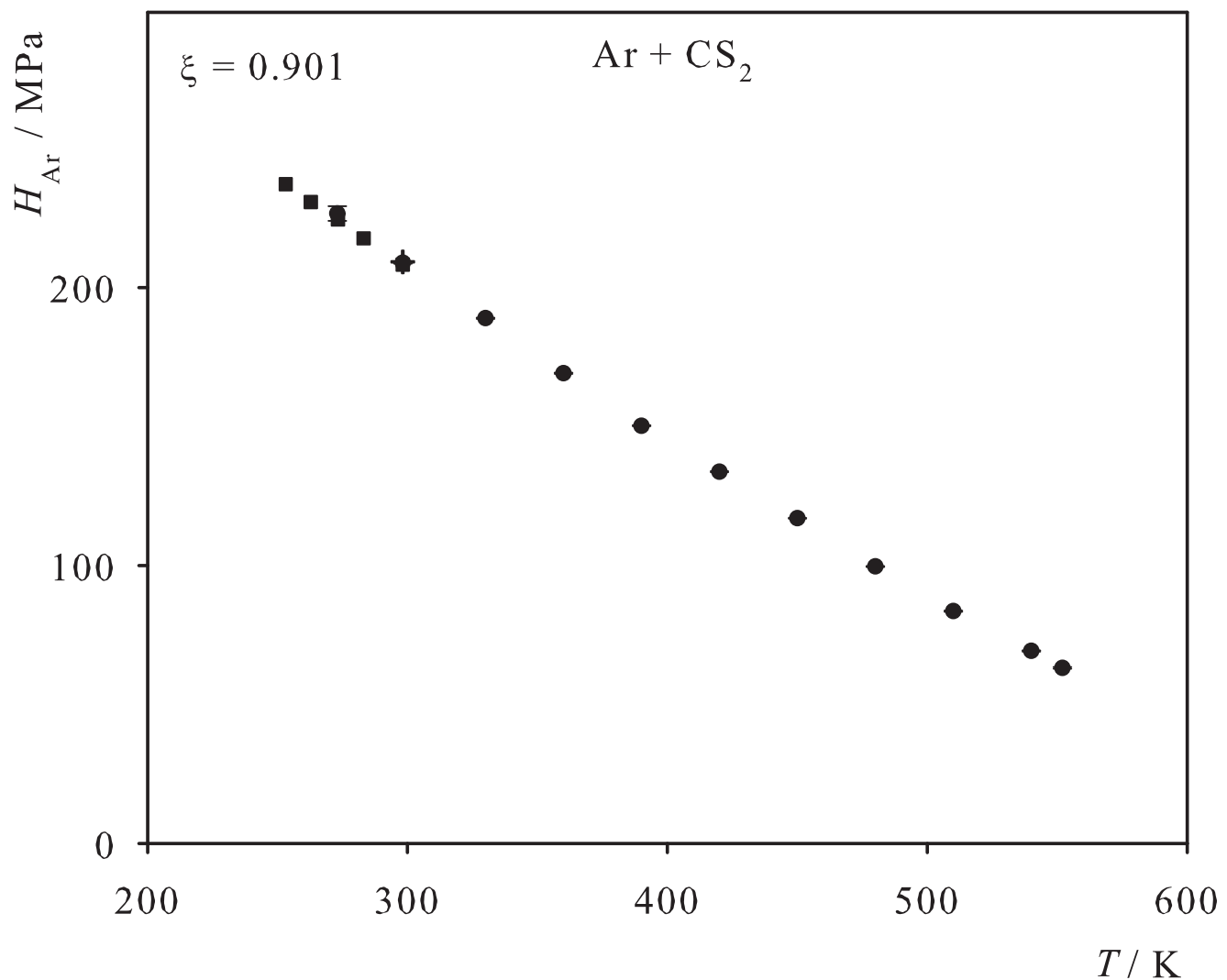


Fig. 6. Henry's law constant of Kr in liquid CS<sub>2</sub>. Simulation data: ●; experimental data: + [8].

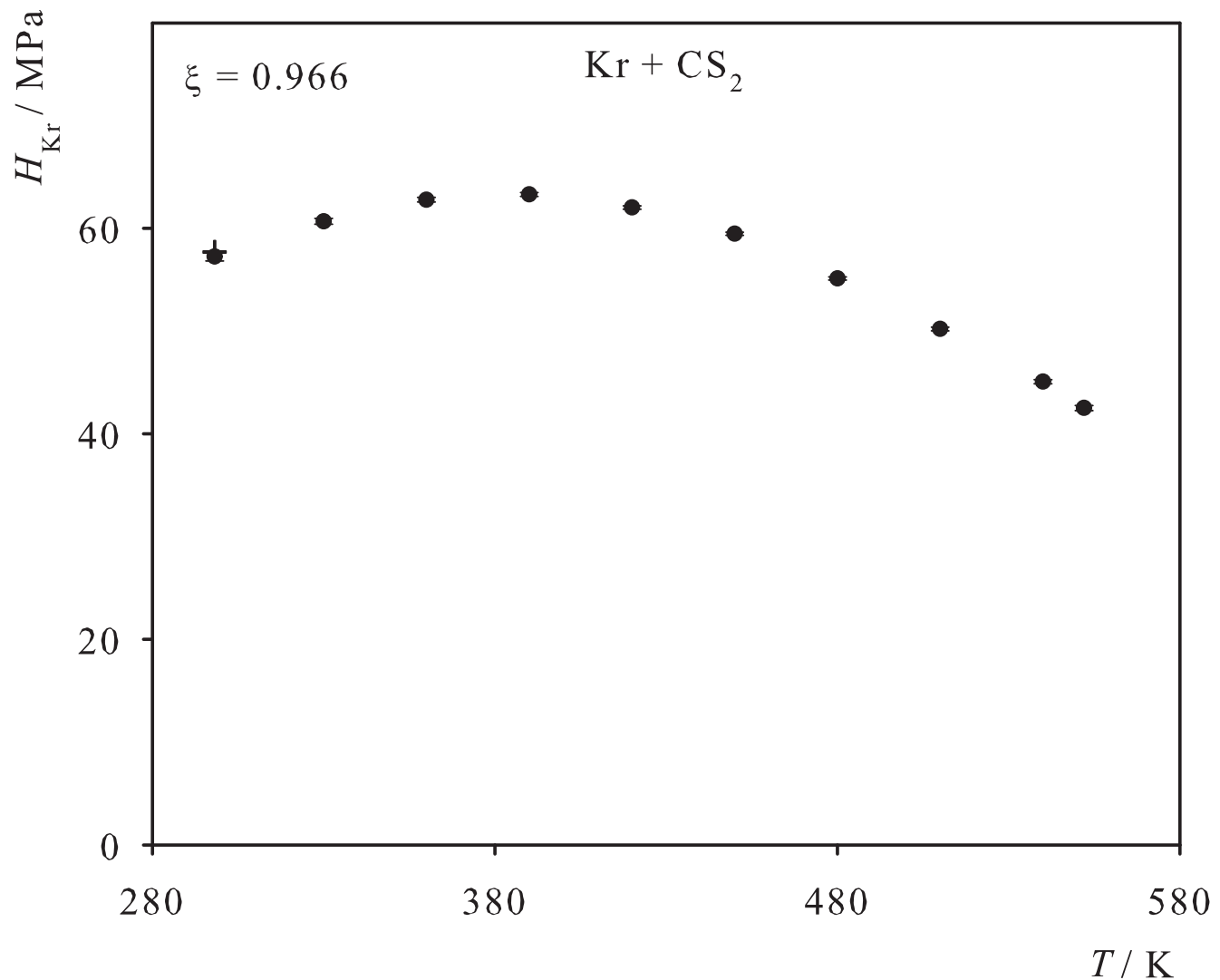


Fig. 7. Henry's law constant of Xe in liquid CS<sub>2</sub>. Simulation data: ●; experimental data: + [8].

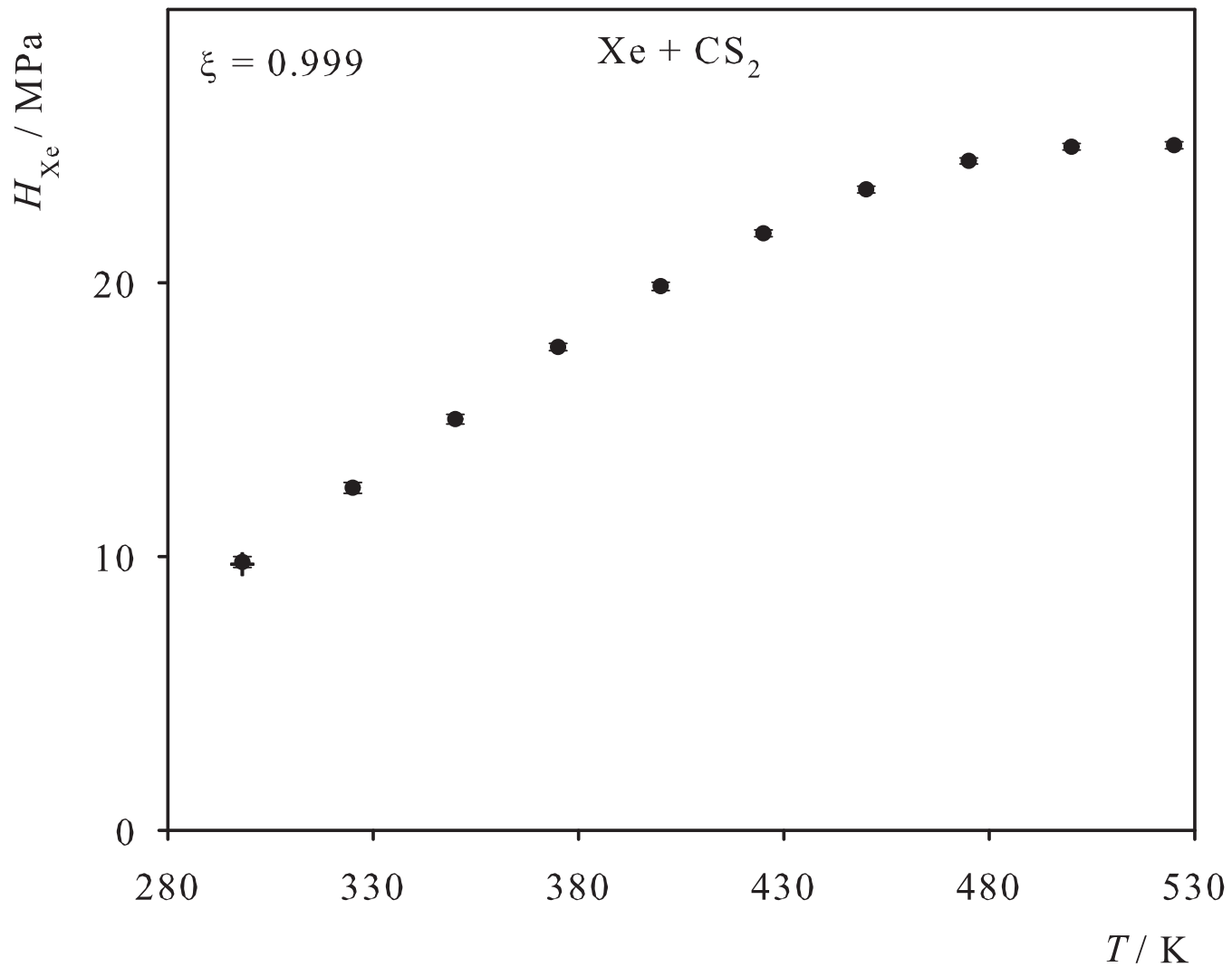


Fig. 8. Henry's law constant of CH<sub>4</sub> in liquid CS<sub>2</sub>. Simulation data: ●; experimental data: + [8], ■ [9].

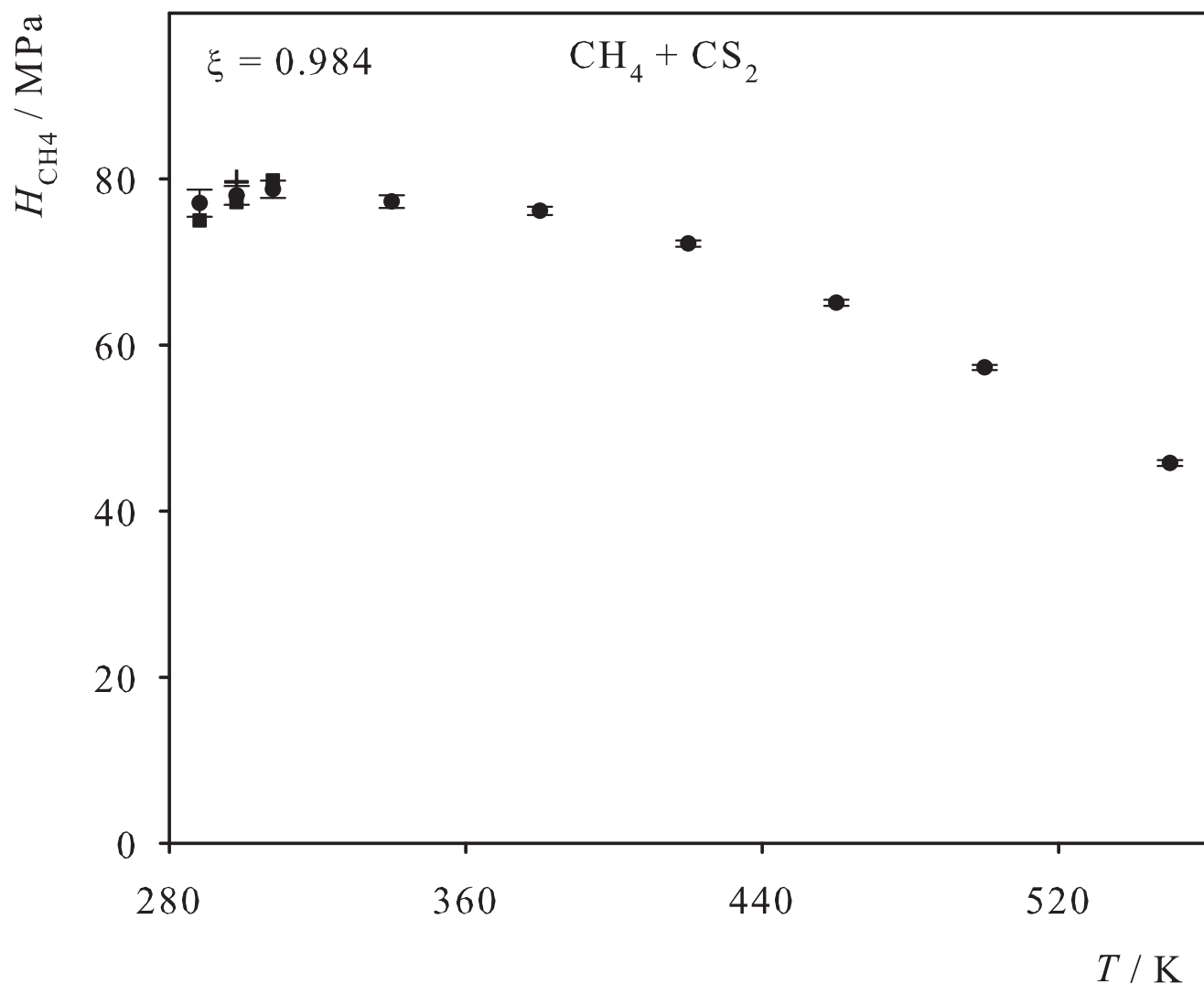


Fig. 9. Henry's law constant of N<sub>2</sub> in liquid CS<sub>2</sub>. Simulation data: ●; experimental data: + [8], ■ [9], ▲ [10].

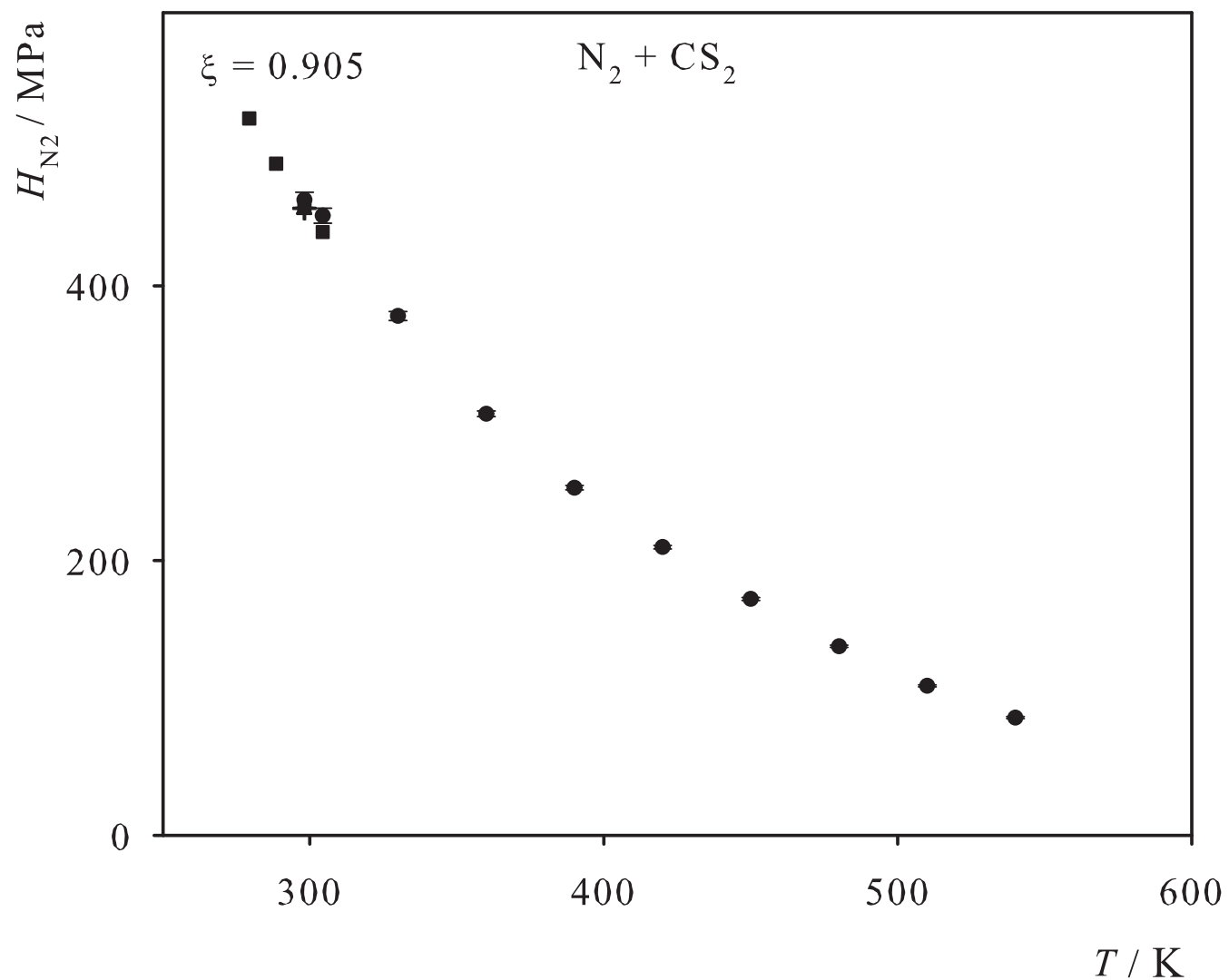


Fig. 10. Henry's law constant of O<sub>2</sub> in liquid CS<sub>2</sub>. Simulation data: ●; experimental data: + [11].

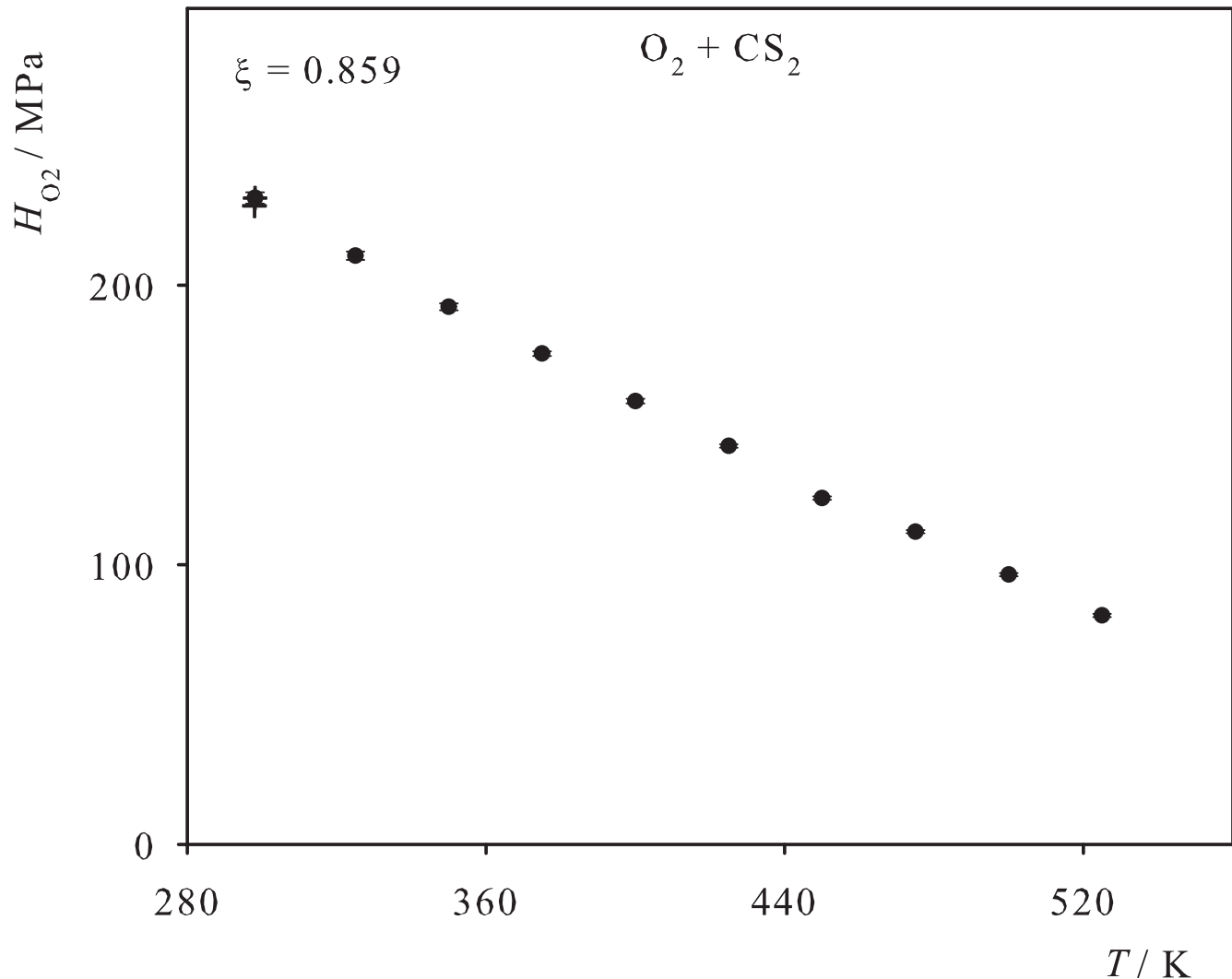


Fig. 11. Henry's law constant of  $\text{Cl}_2$  in liquid  $\text{CS}_2$ . Simulation data: ●; experimental data: + [12].

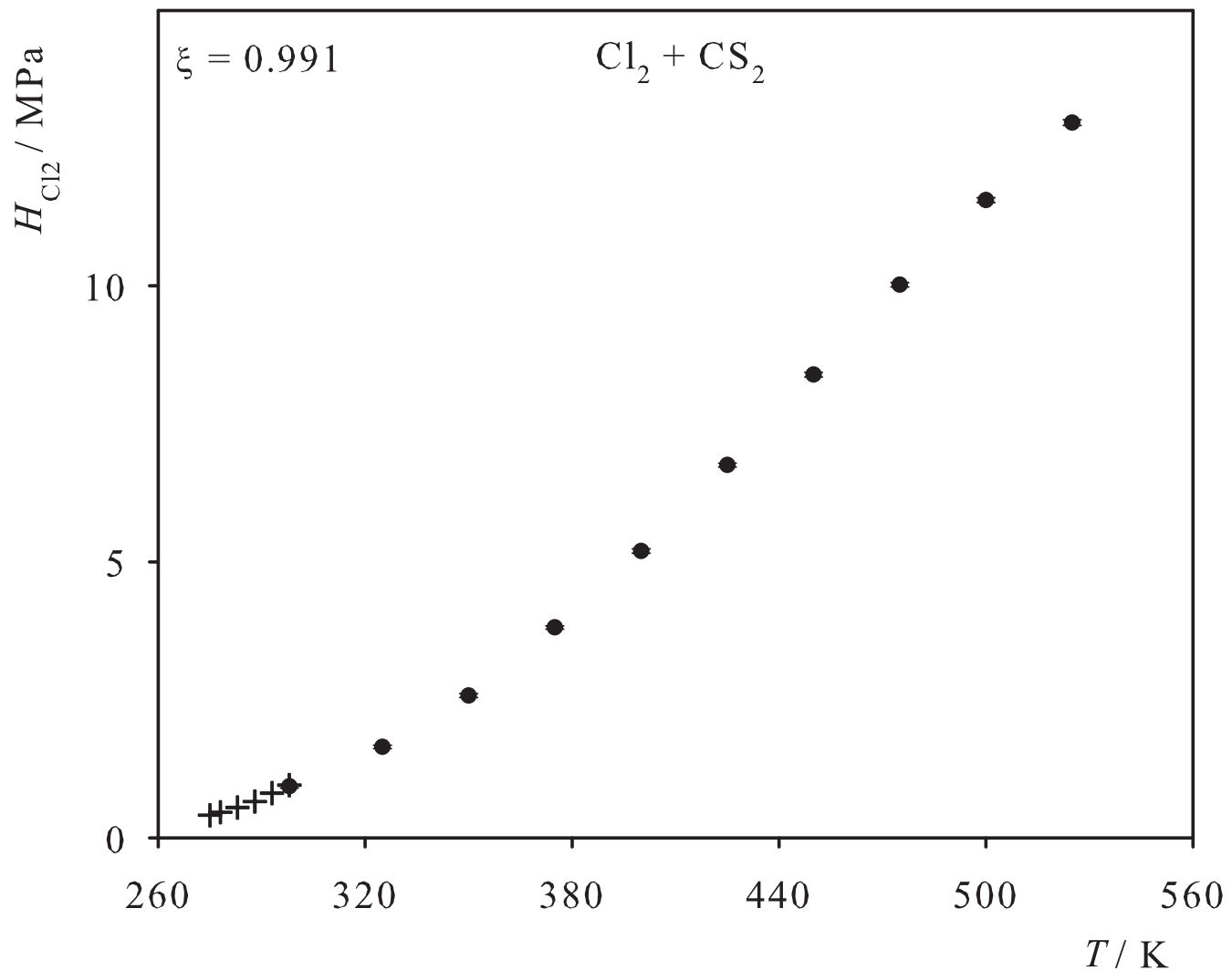


Fig. 12. Henry's law constant of CO in liquid CS<sub>2</sub>. Simulation data: ●; experimental data: + [11].

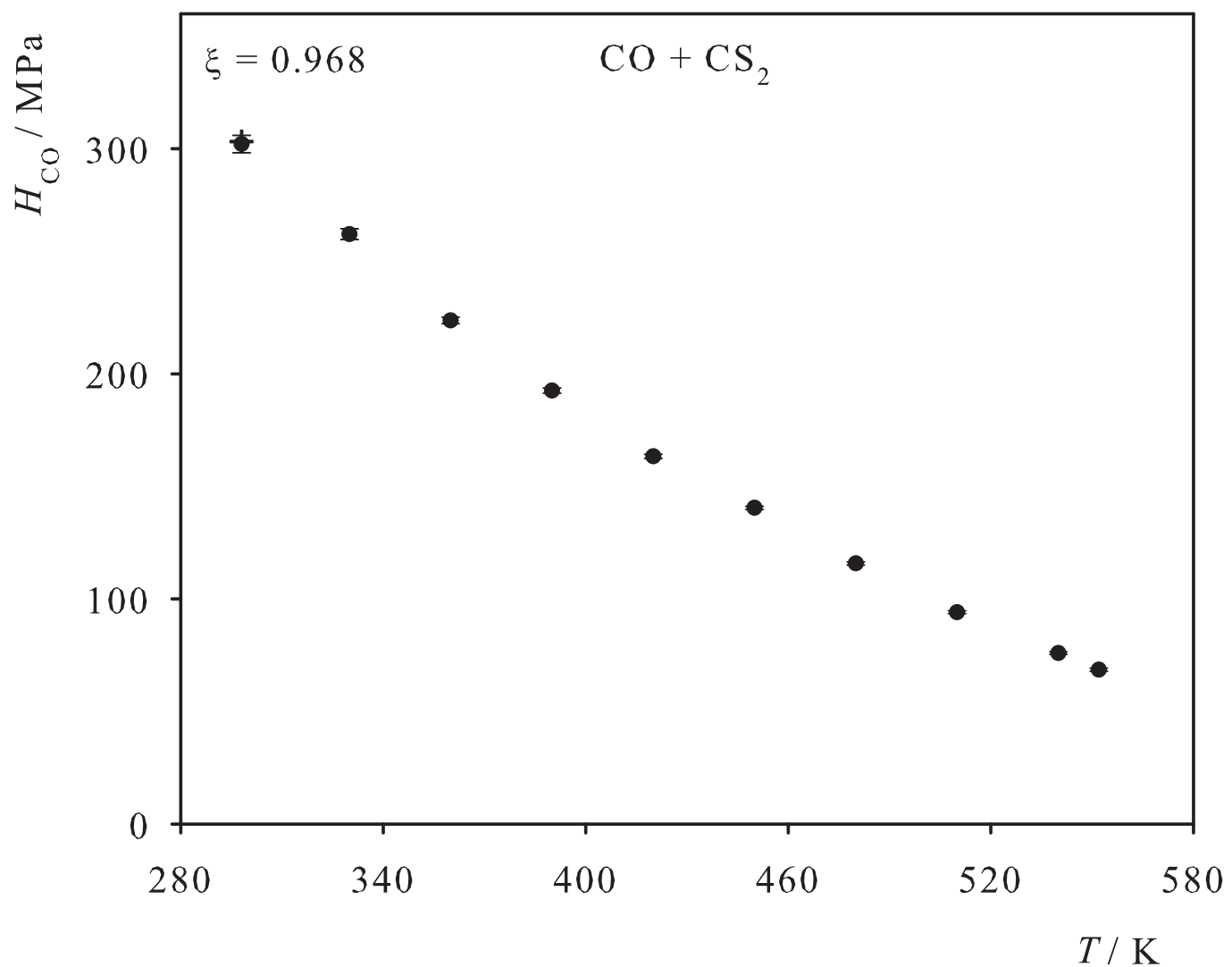


Fig. 13. Henry's law constant of CO<sub>2</sub> in liquid CS<sub>2</sub>. Simulation data: ● ( $\xi=0.877$ ), ○ ( $\xi=0.918$ ); experimental data: + [9], ■ [13].

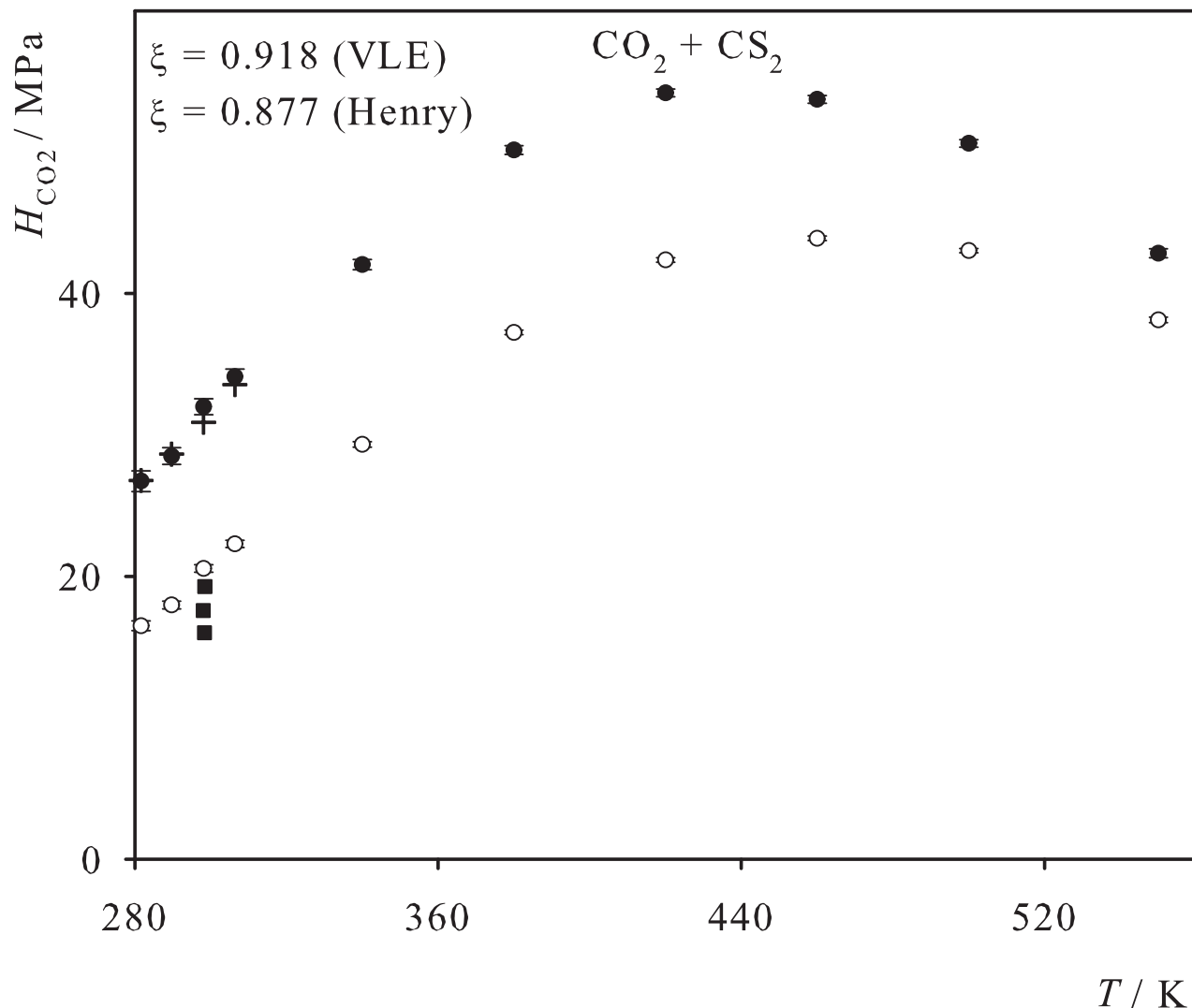


Fig. 14. Henry's law constant of C<sub>2</sub>H<sub>2</sub> in liquid CS<sub>2</sub>. Simulation data: ●; experimental data: + [14].

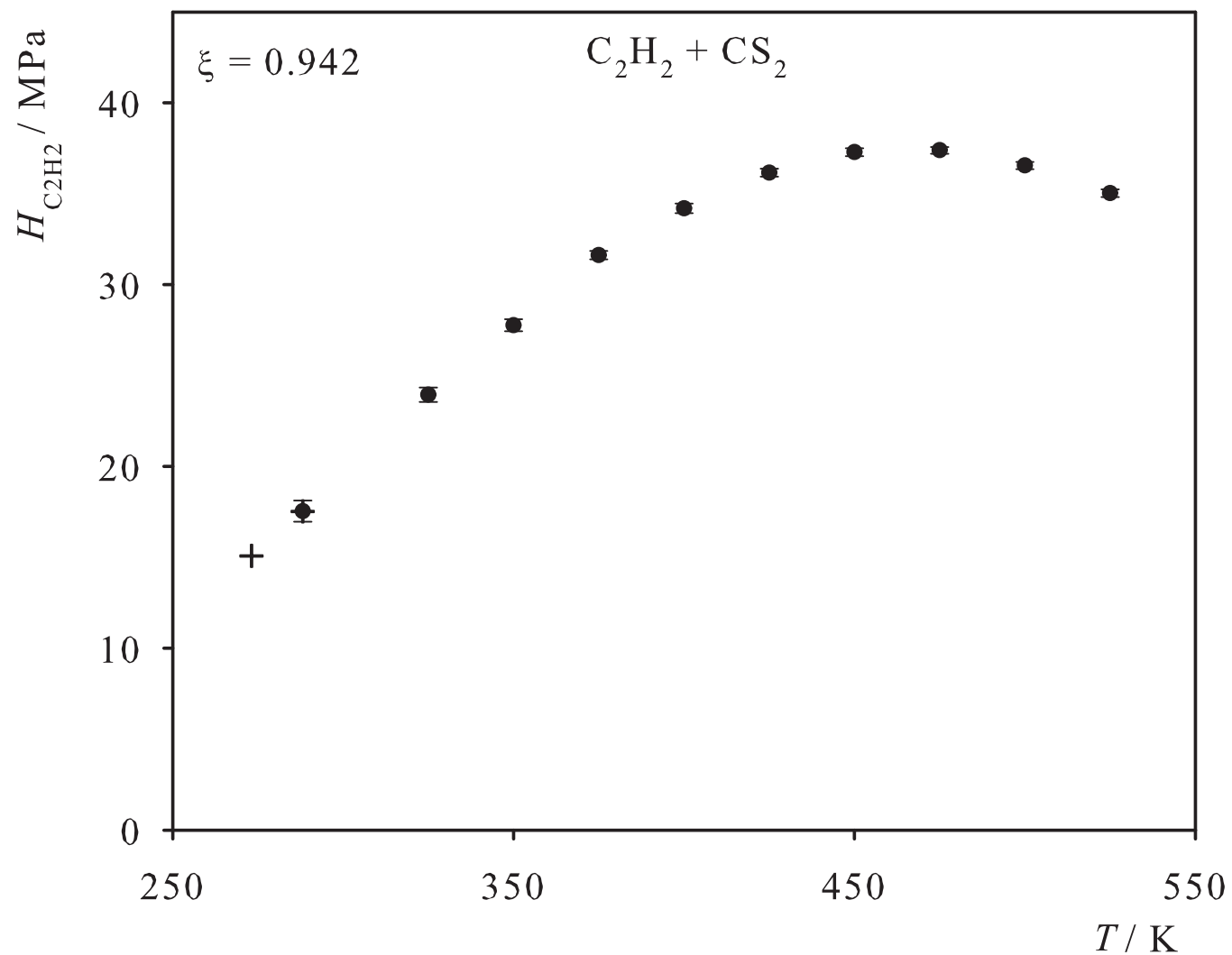


Fig. 15. Henry's law constant of C<sub>2</sub>H<sub>4</sub> in liquid CS<sub>2</sub>. Simulation data: ●; experimental data: + [15].

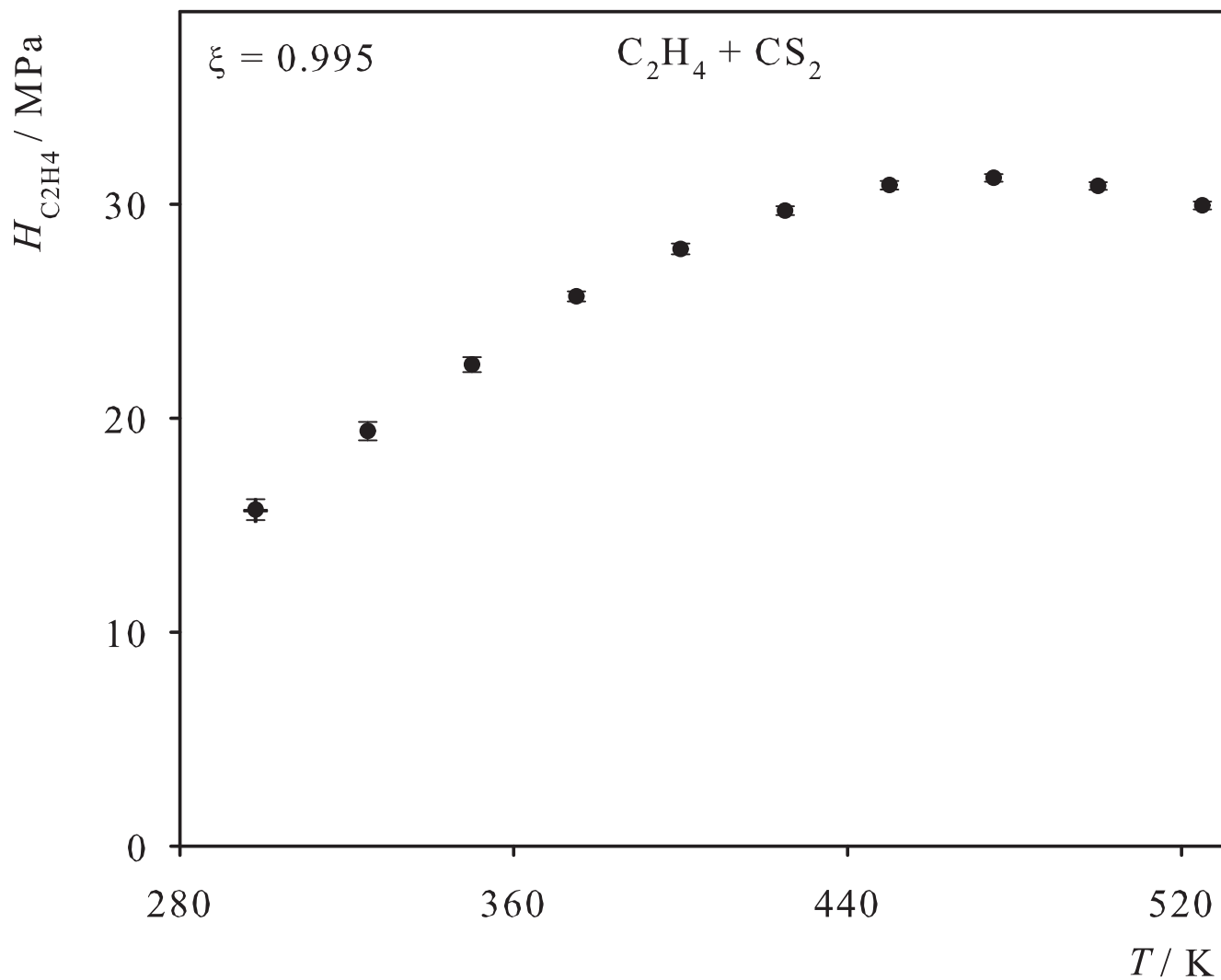


Fig. 16. Henry's law constant of C<sub>2</sub>H<sub>6</sub> in liquid CS<sub>2</sub>. Simulation data: ●; experimental data: + [8], ■ [6].

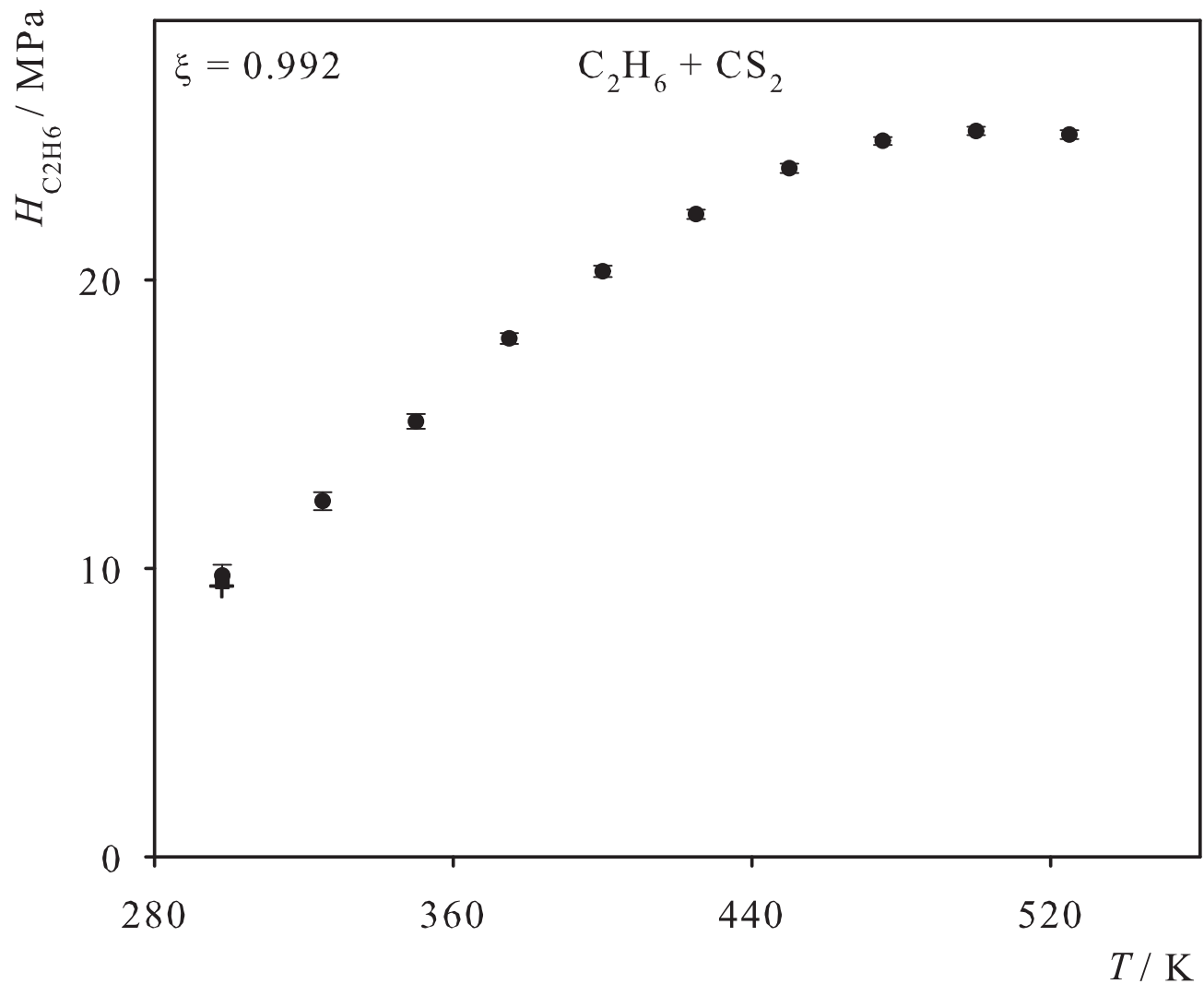


Fig. 17. Henry's law constant of Propylene in liquid CS<sub>2</sub>. Simulation data: ●; experimental data: + [8].

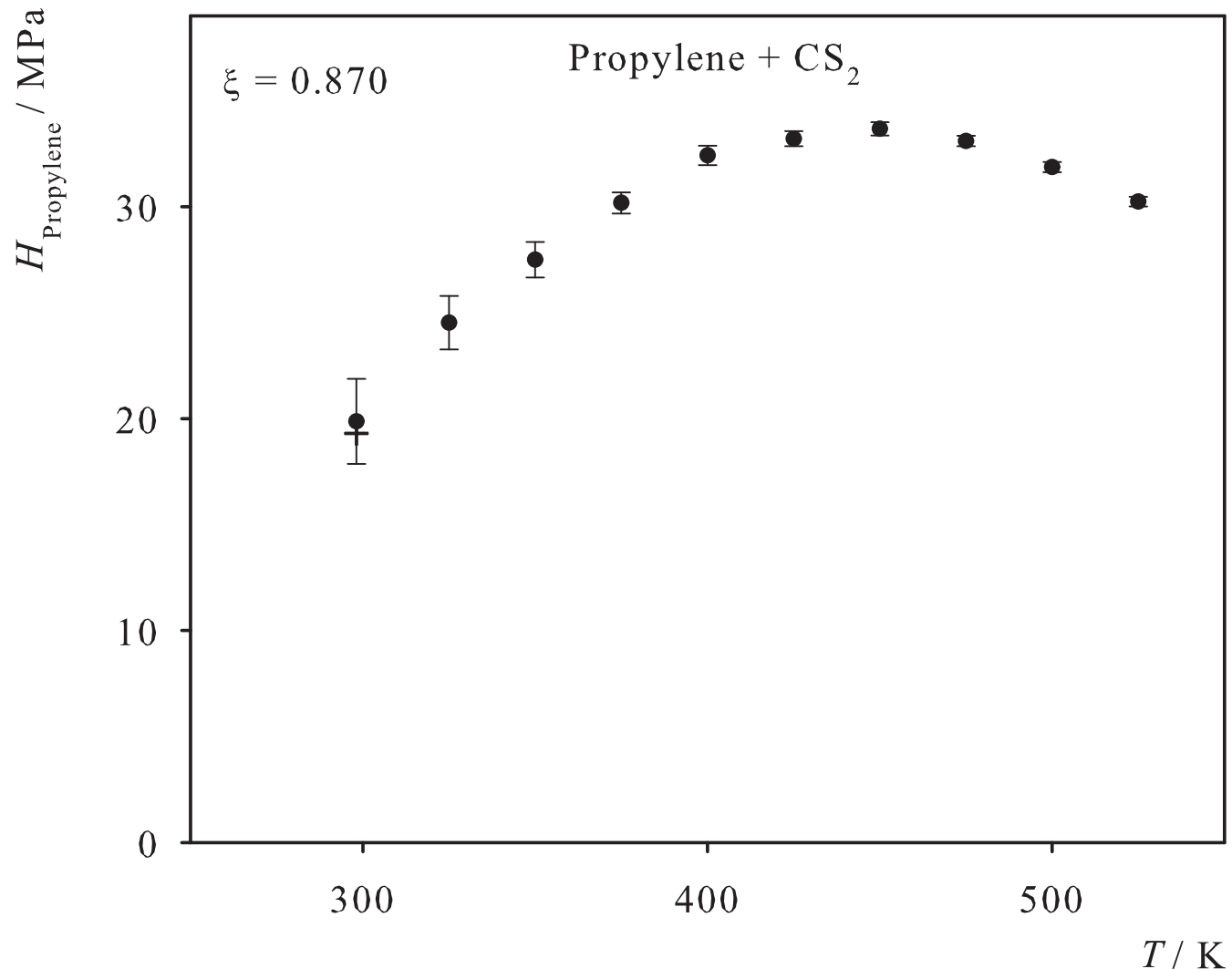


Fig. 18. Henry's law constant of SF<sub>6</sub> in liquid CS<sub>2</sub>. Simulation data: ●; experimental data: + [8], ■ [9].

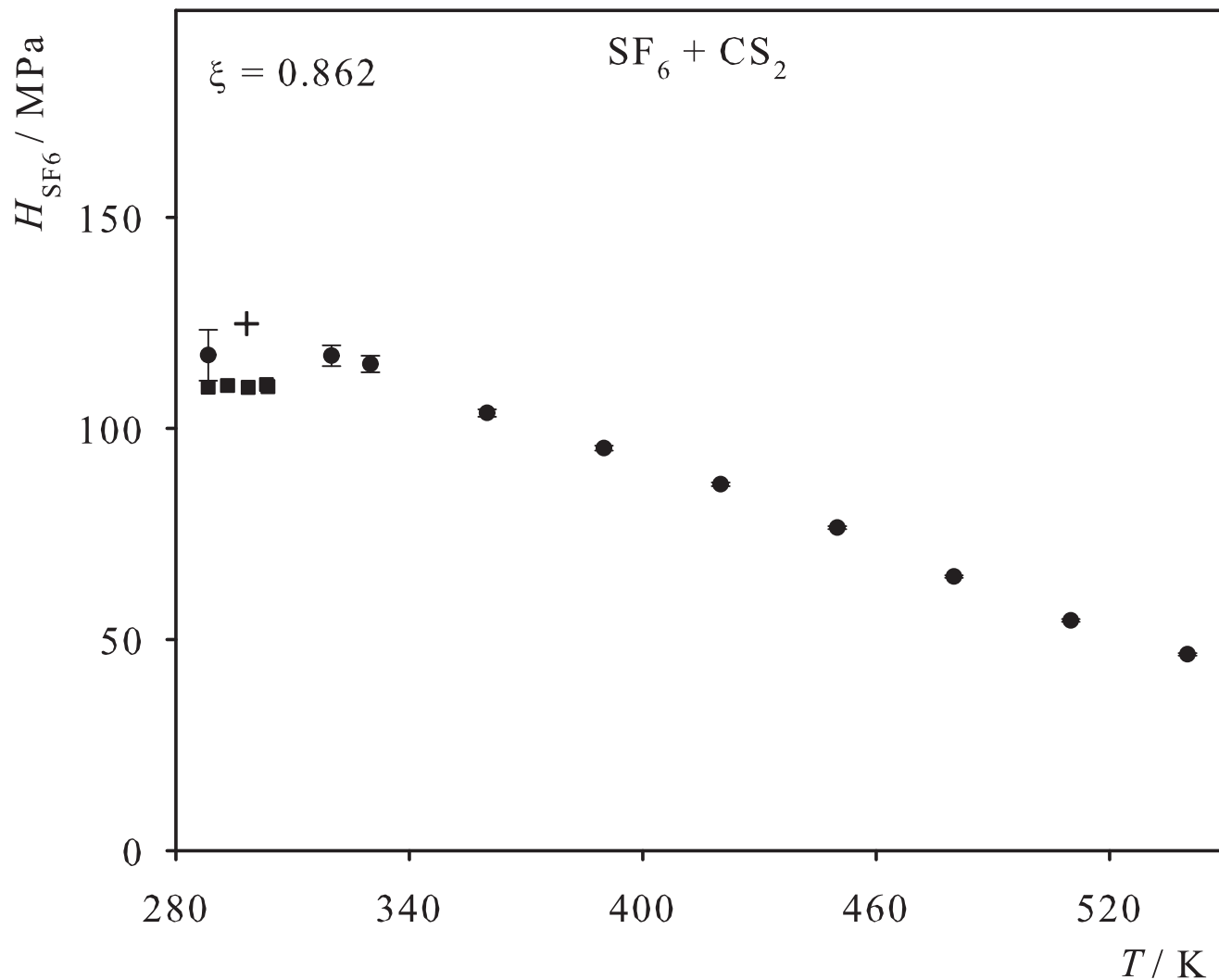


Fig. 19. Henry's law constant of R14 in liquid CS<sub>2</sub>. Simulation data: ●; experimental data: + [16].

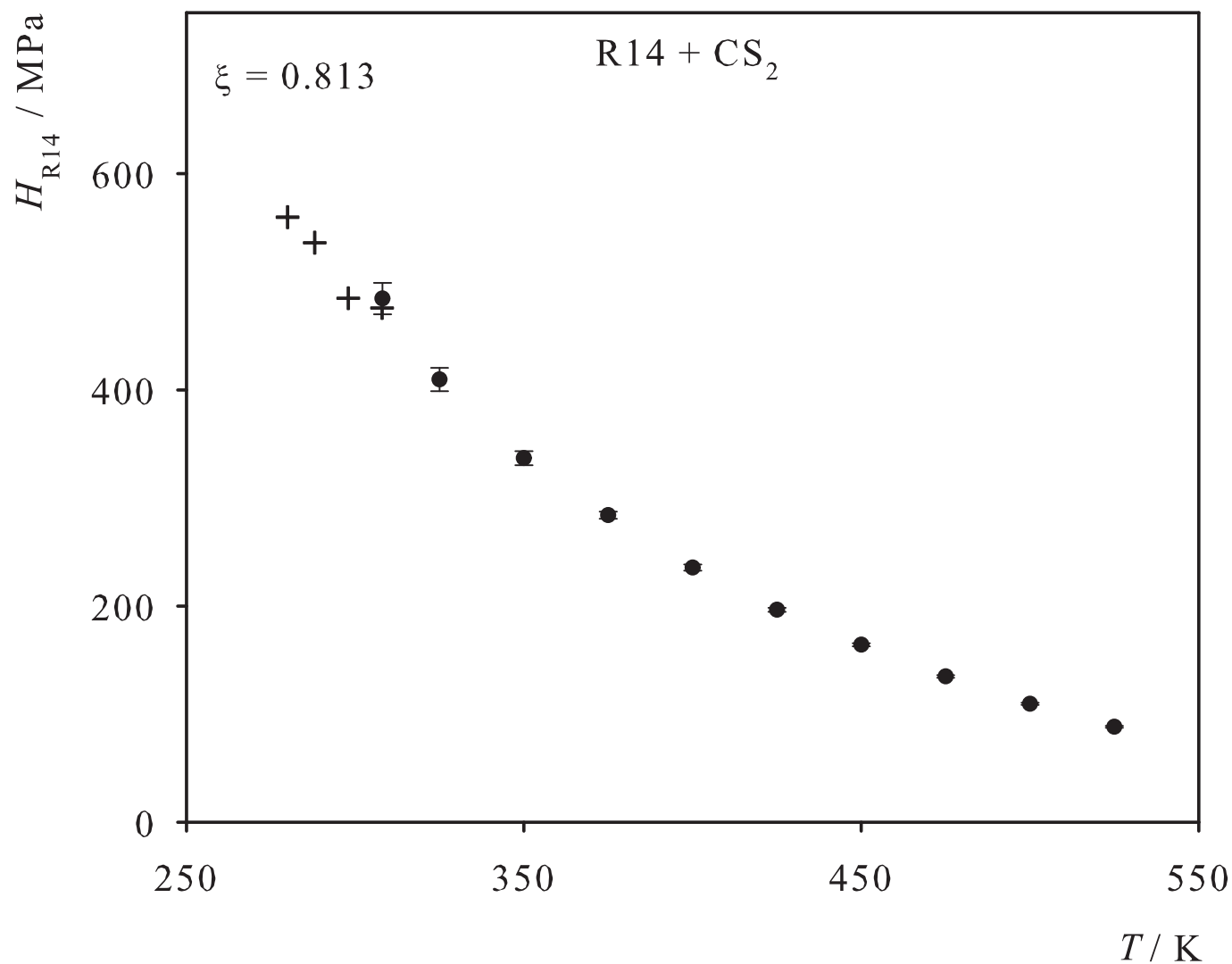


Fig. 20. Henry's law constant of N<sub>2</sub> in liquid Propylene. Simulation data: ●; experimental data: + [17].

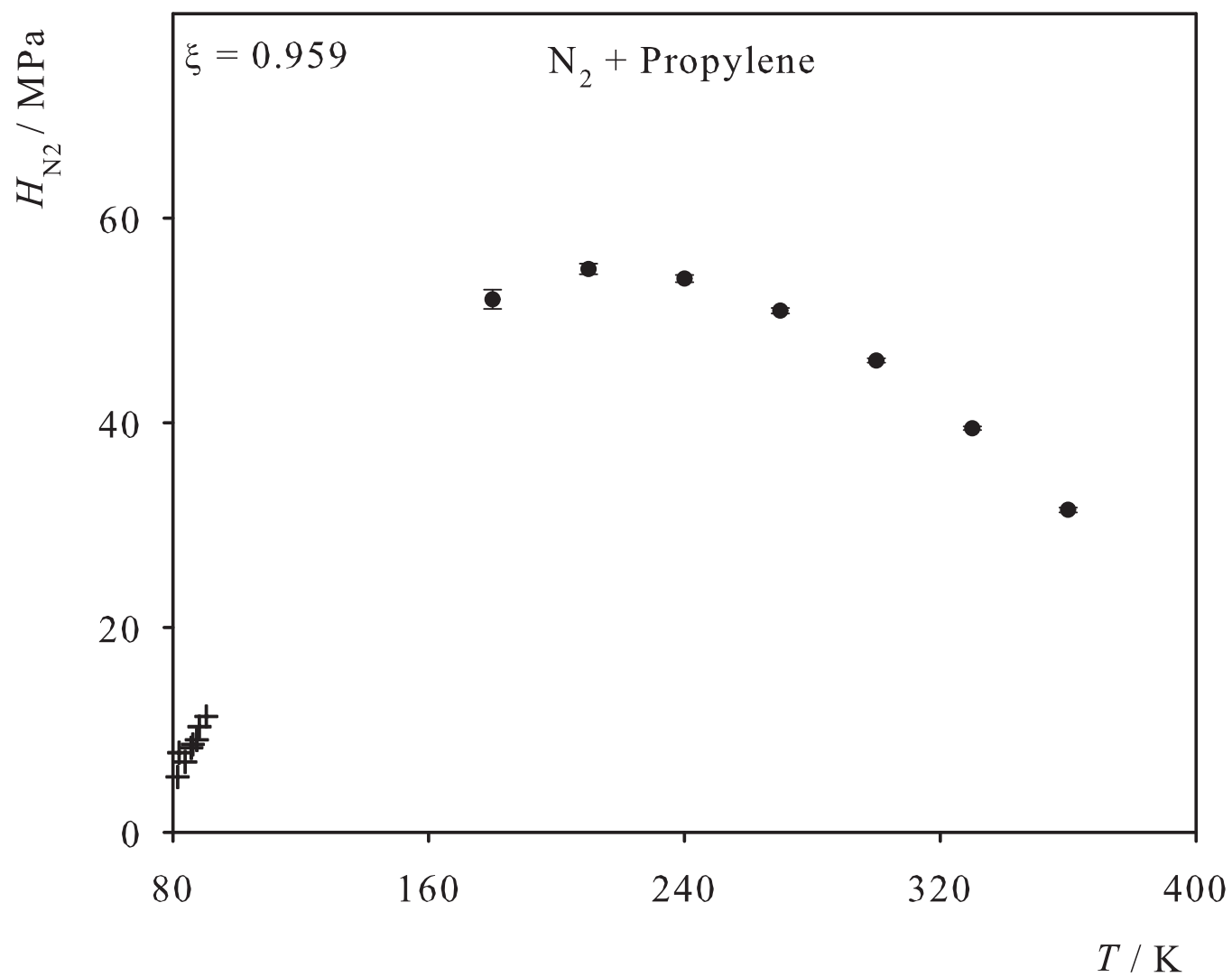


Fig. 21. Henry's law constant of N<sub>2</sub> in liquid SF<sub>6</sub>. Simulation data: ●; experimental data: + [18].

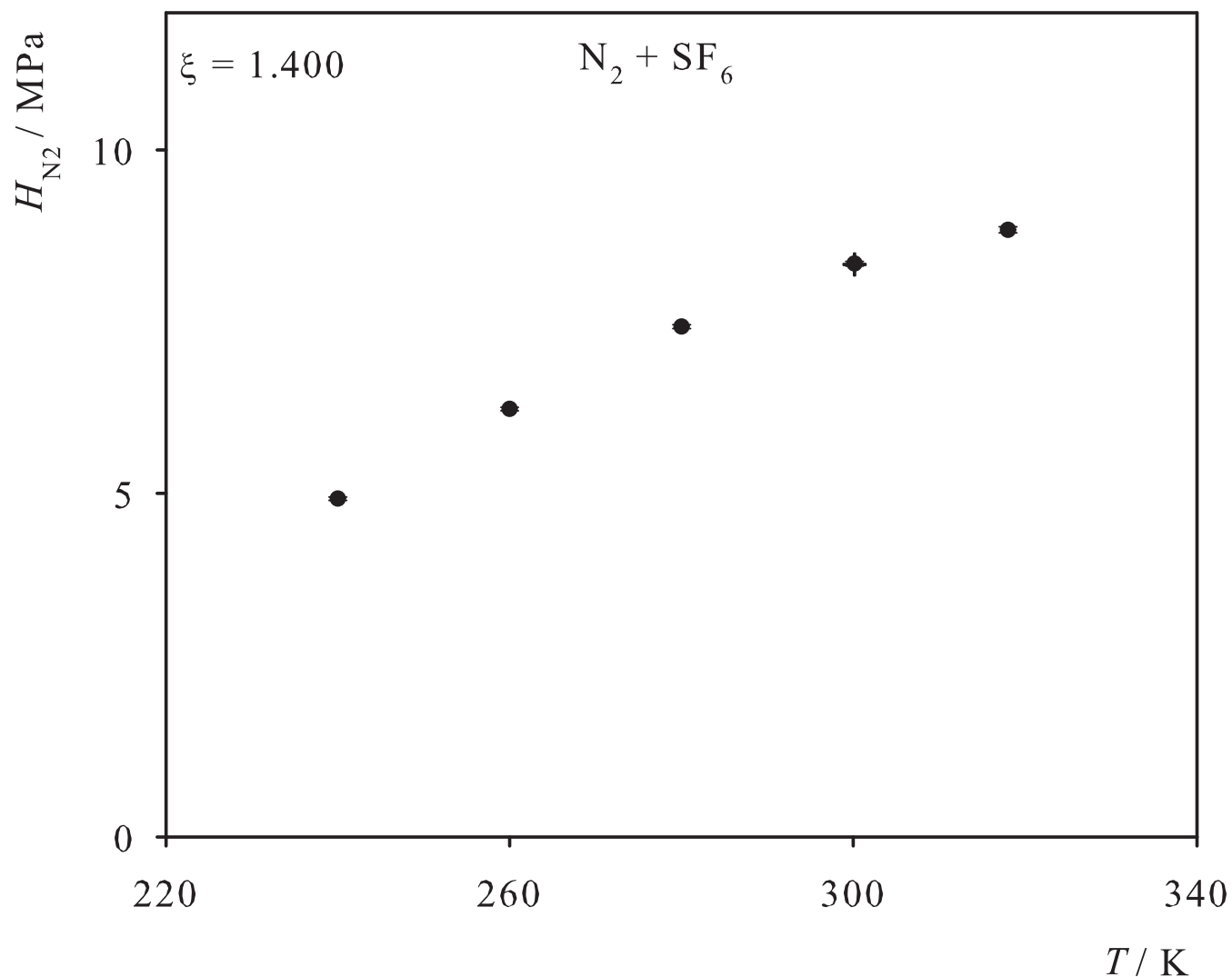


Fig. 22. Henry's law constant of Ar in liquid R10. Simulation data: ●; experimental data: + [20], ■ [7].

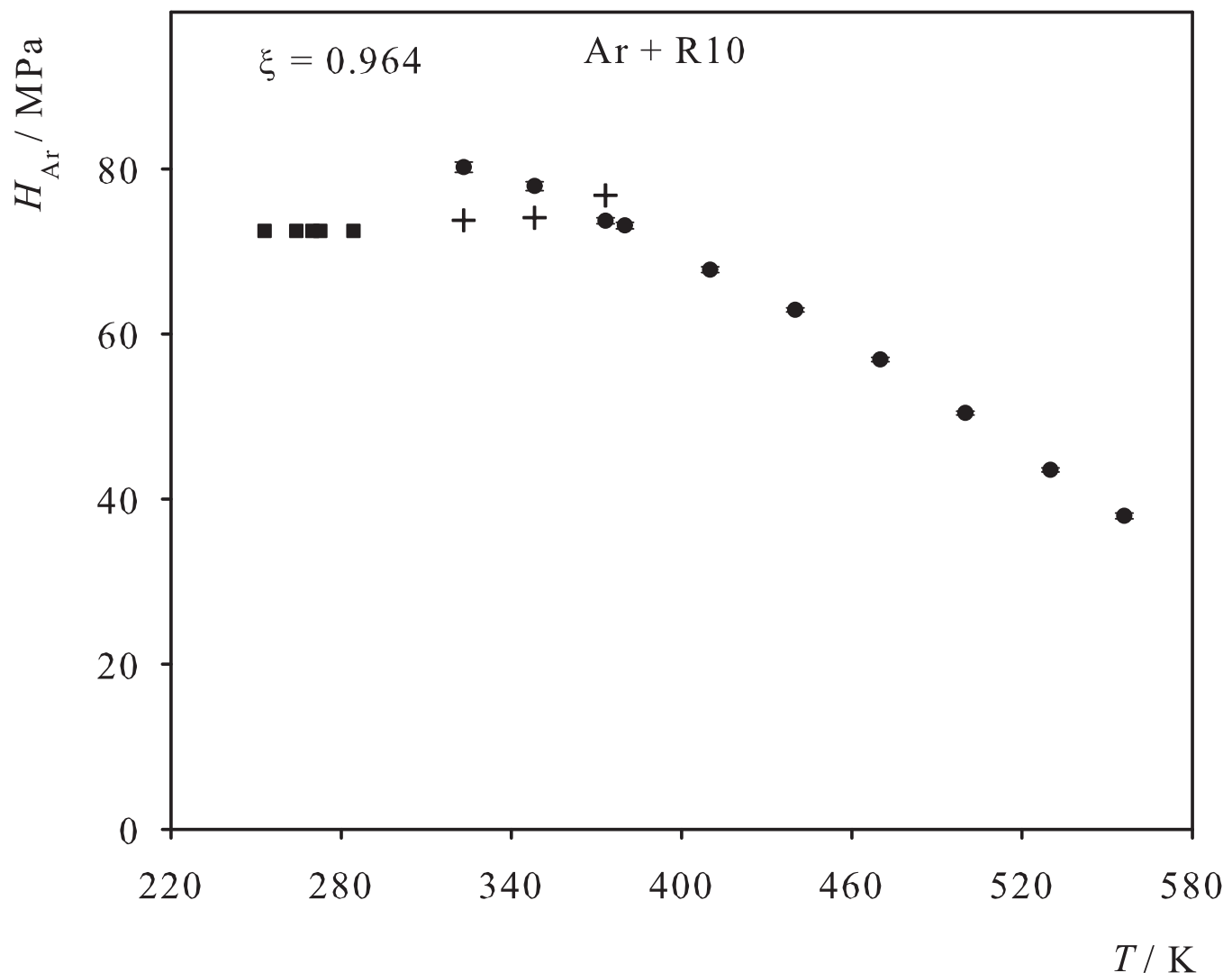


Fig. 23. Henry's law constant of Kr in liquid R10. Simulation data: ●; experimental data: + [19], ■ [21].

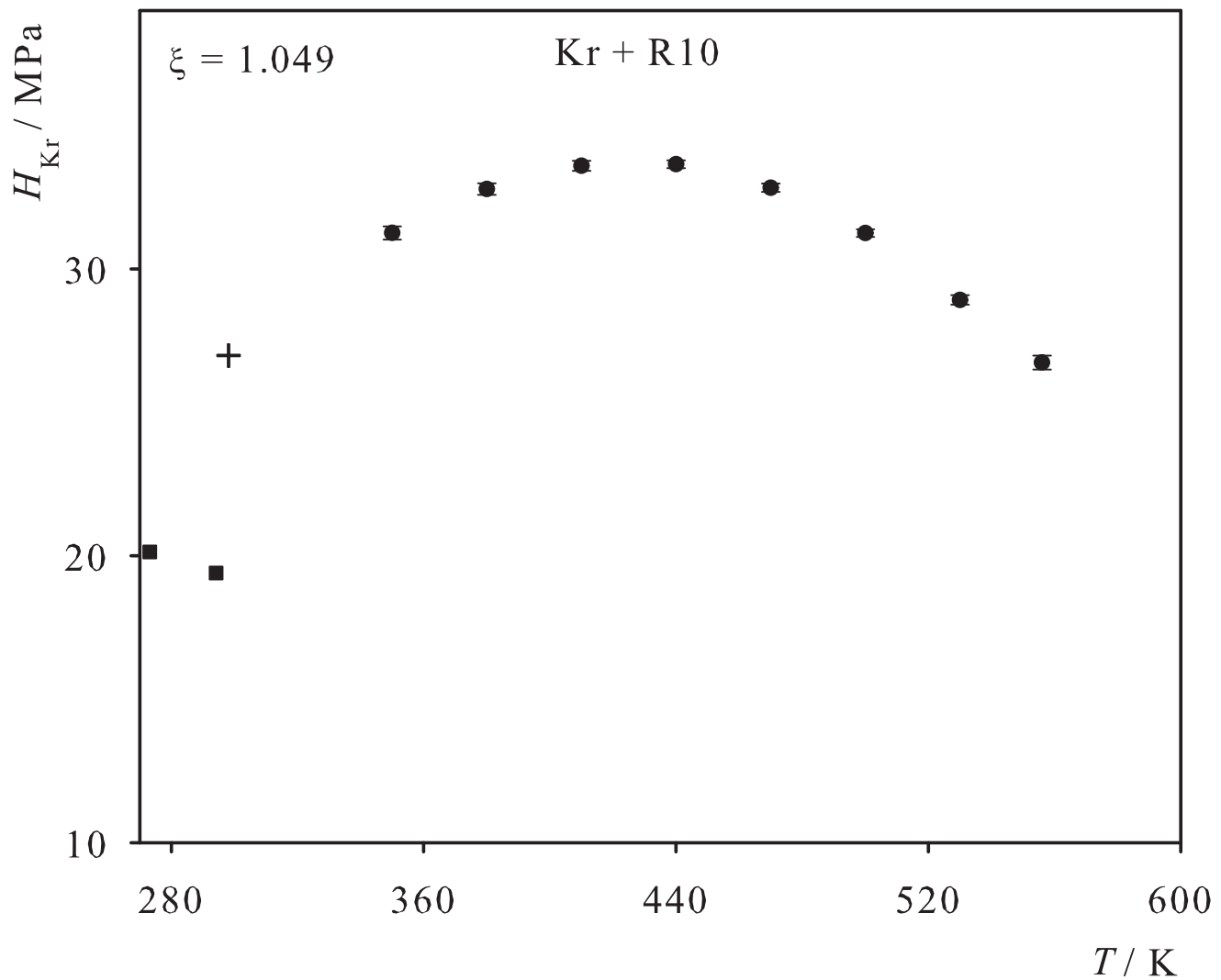


Fig. 24. Henry's law constant of CH<sub>4</sub> in liquid R10. Simulation data: ●; experimental data: + [22].

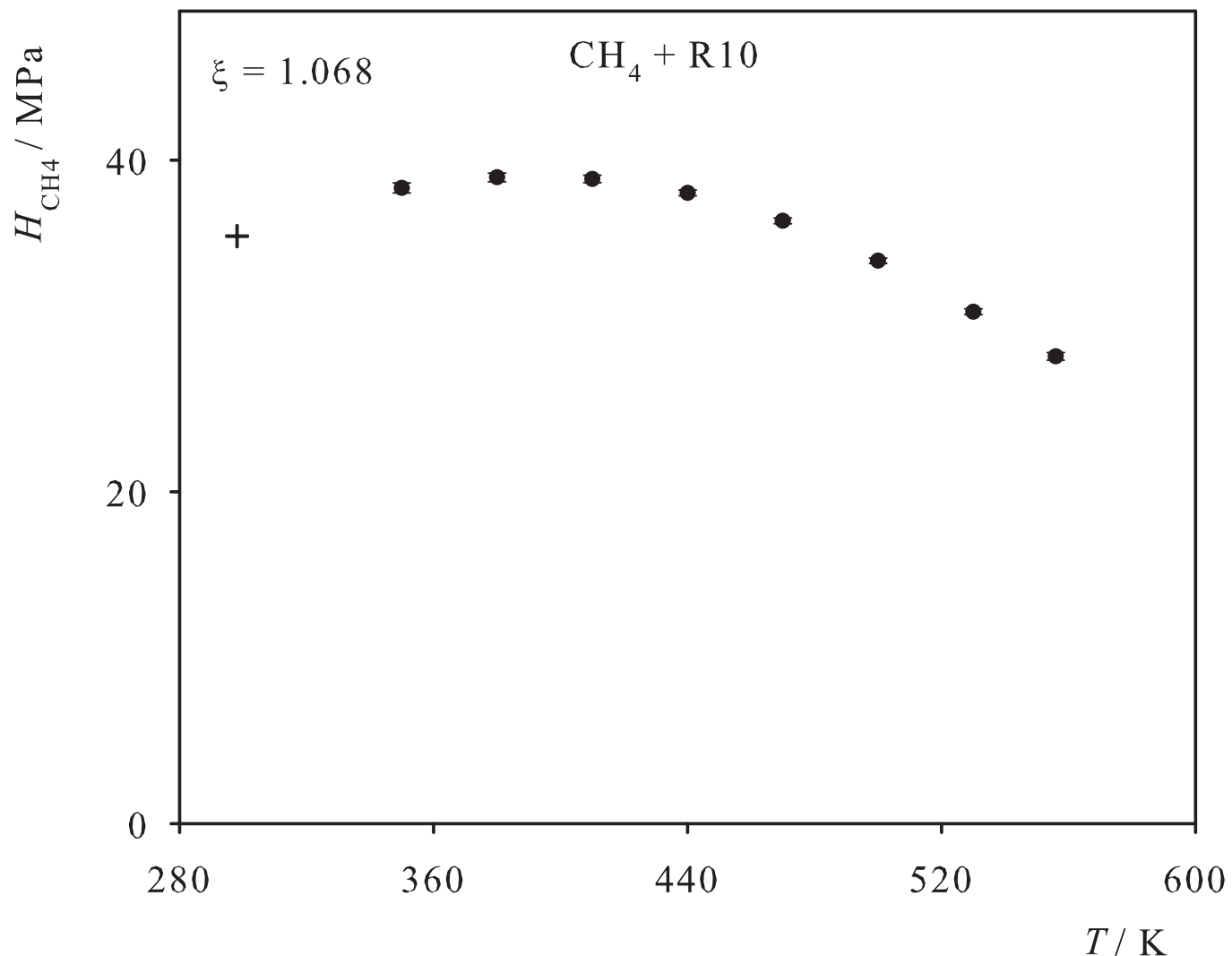


Fig. 25. Henry's law constant of N<sub>2</sub> in liquid R10. Simulation data: ●; experimental data: + [23], ■ [24], ▲ [25].

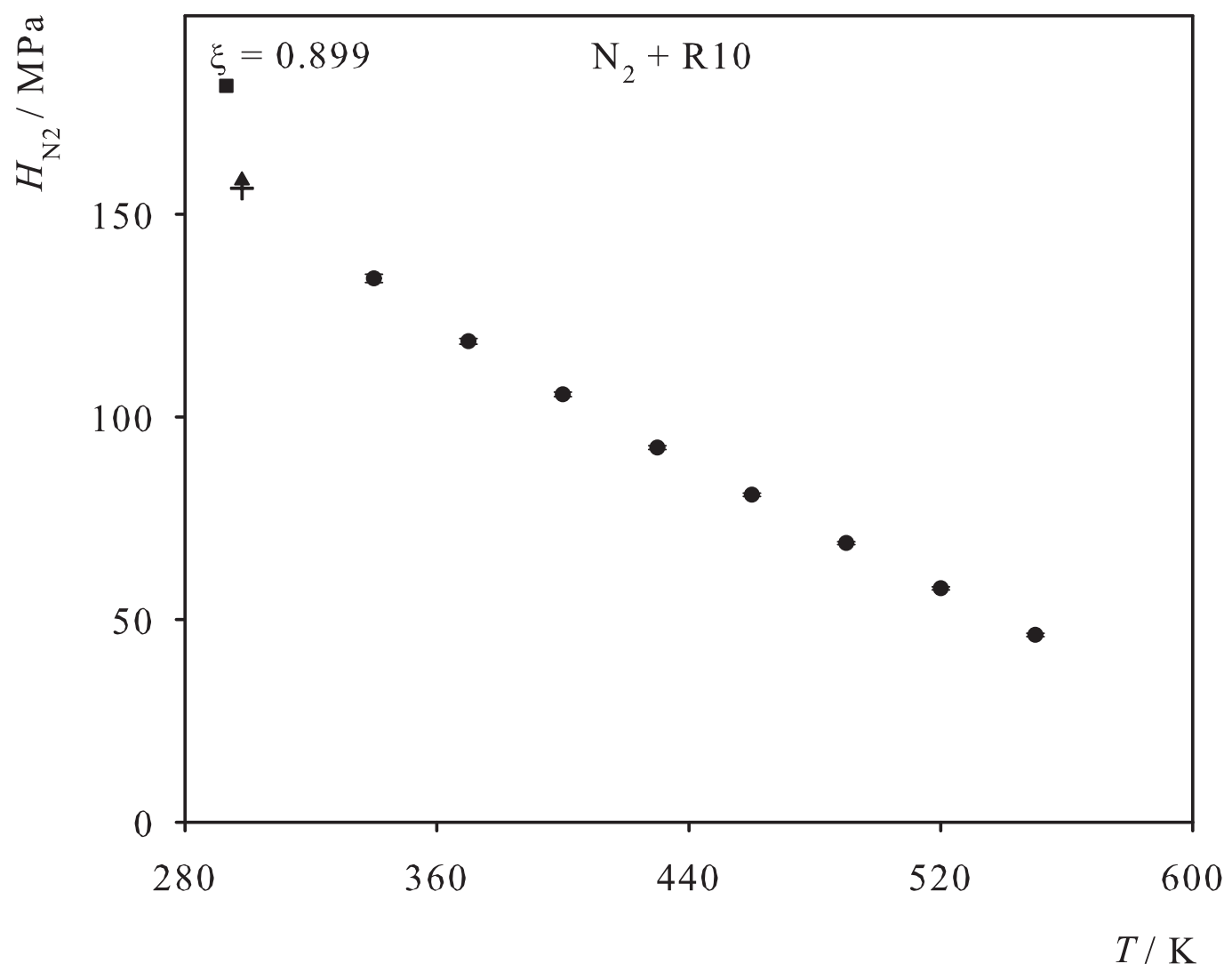


Fig. 26. Henry's law constant of O<sub>2</sub> in liquid R10. Simulation data: ●; experimental data: + [24], ■ [25], ▲ [26], ▼ [27], ♦ [28], ★ [29].

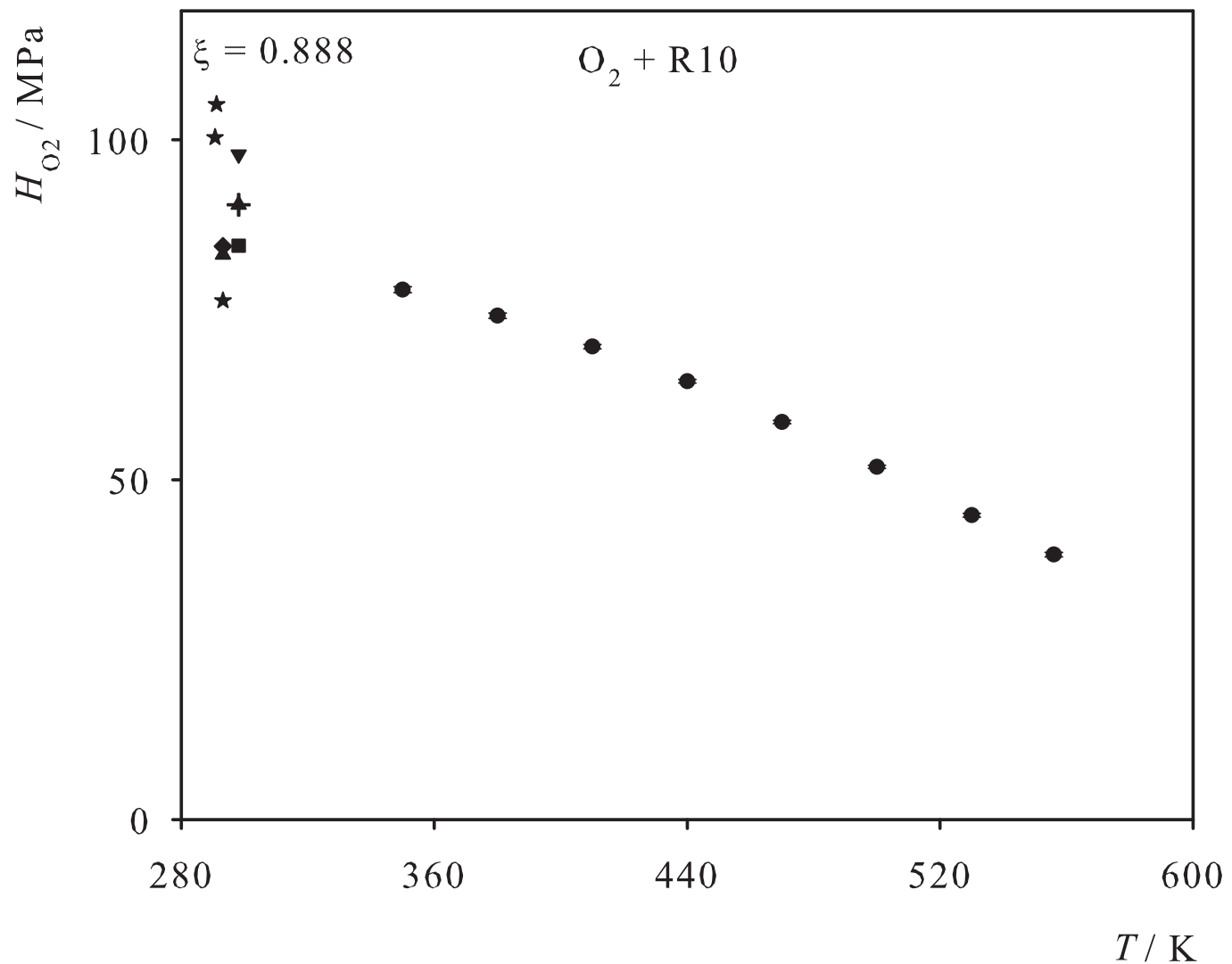


Fig. 27. Henry's law constant of  $\text{Cl}_2$  in liquid R10. Simulation data: ●; experimental data: + [30], ■ [31], ▲ [32], ▼ [33], ♦ [34].

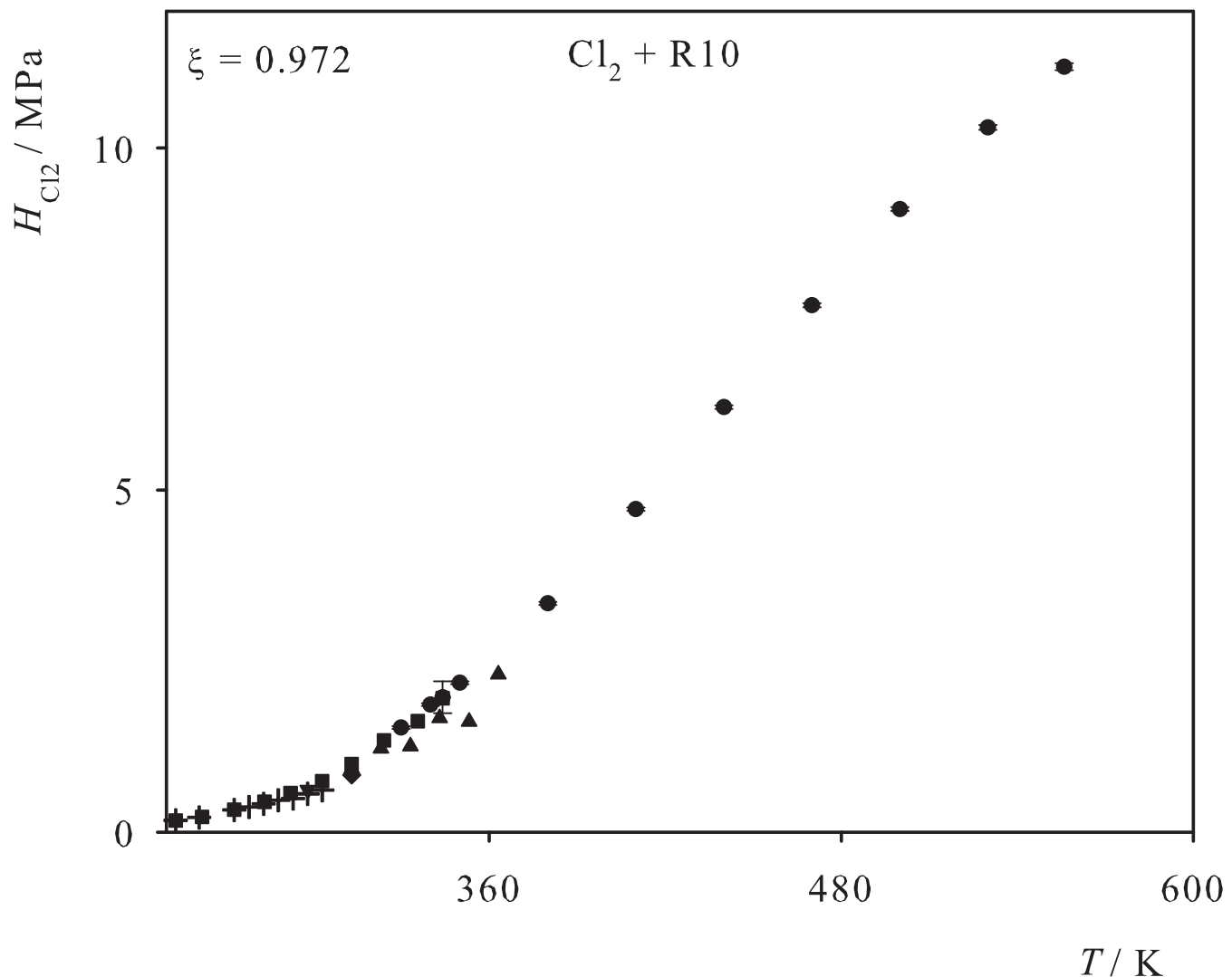


Fig. 28. Henry's law constant of CO<sub>2</sub> in liquid R10. Simulation data: ●; experimental data: + [13], ■ [26], ▲ [35], ▼ [36], ♦ [37], ★ [38].

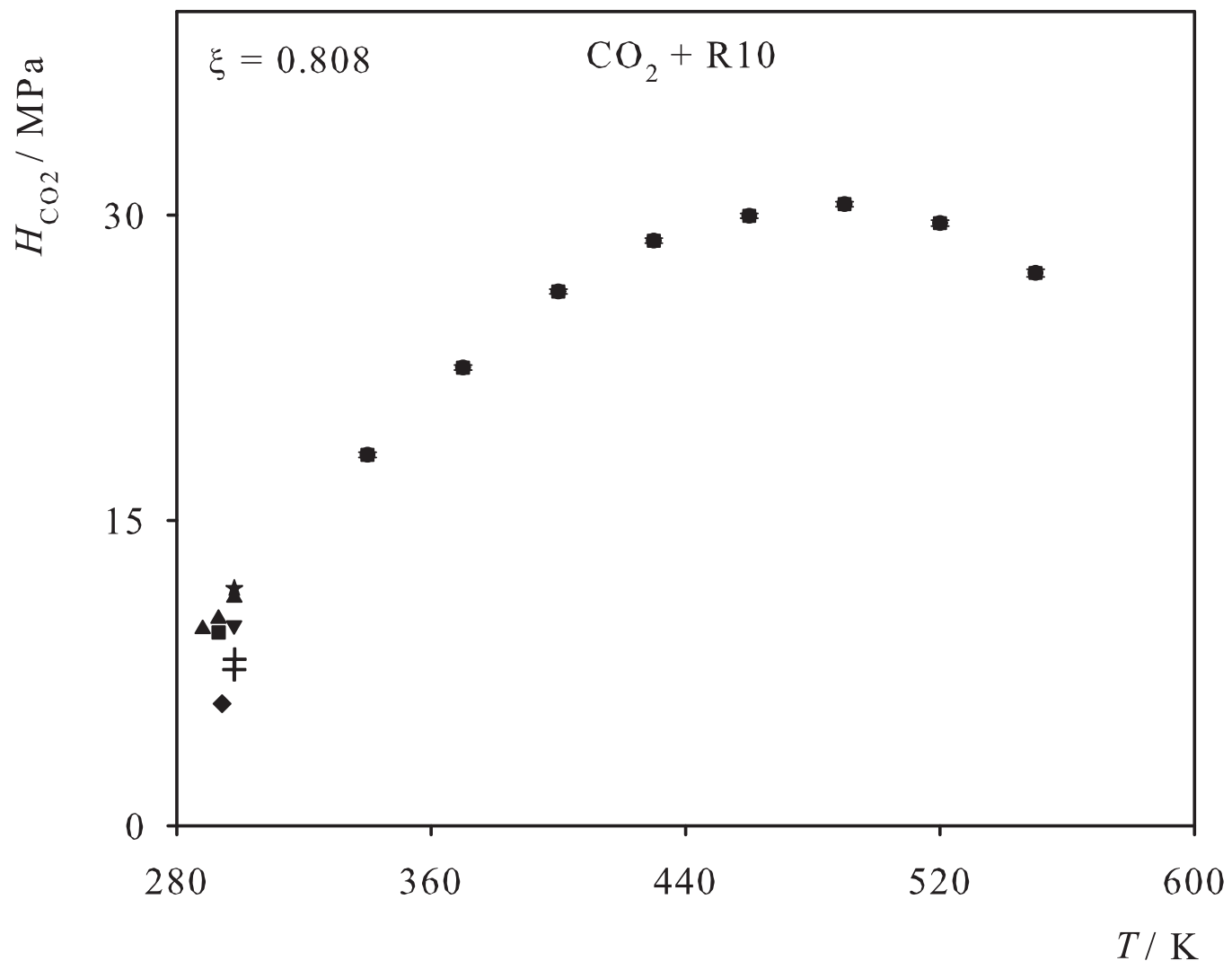


Fig. 29. Henry's law constant of C<sub>2</sub>H<sub>2</sub> in liquid R10. Simulation data: ● ( $\xi=0.859$ ), ○ ( $\xi=1.003$ ); experimental data: + [14].

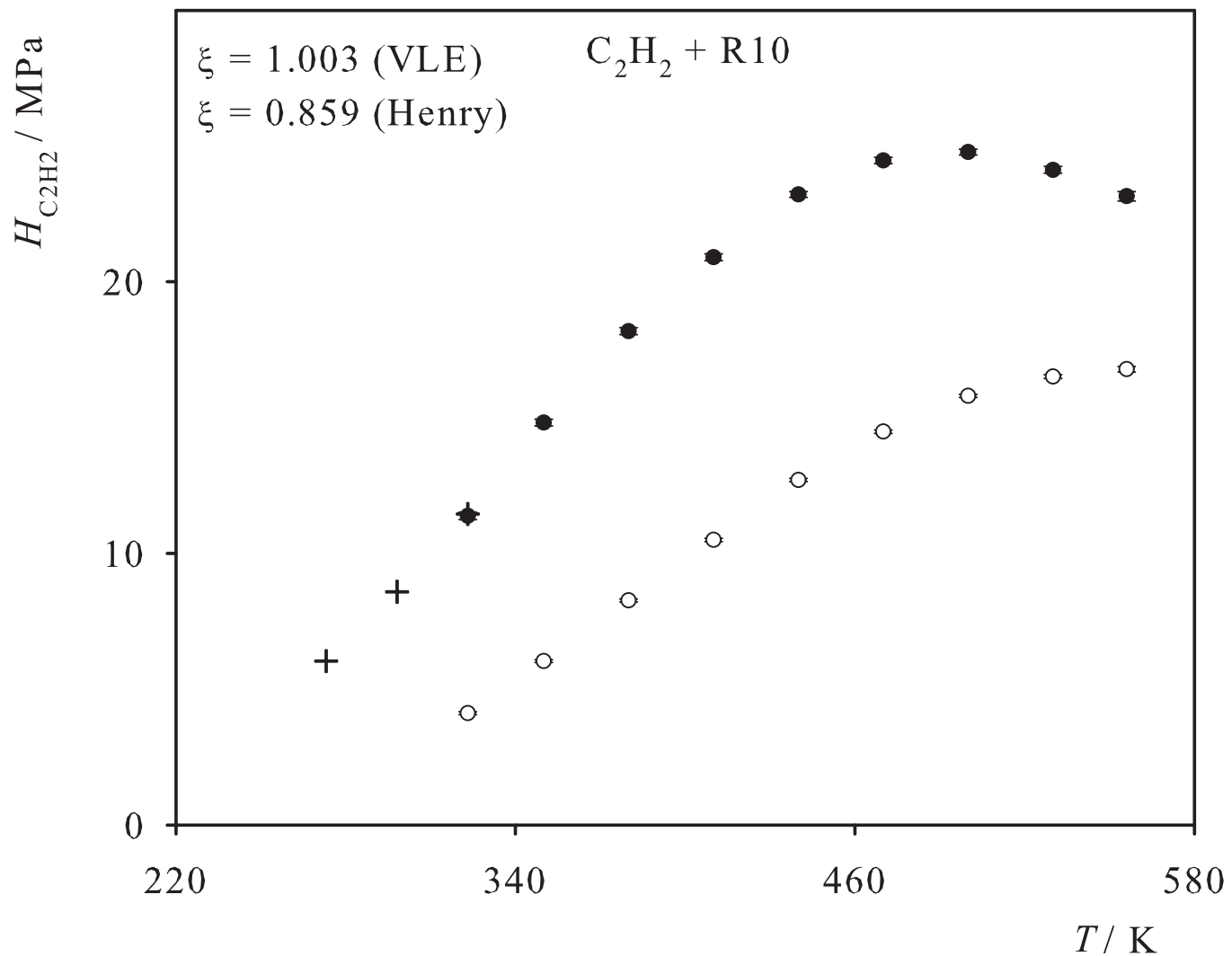


Fig. 30. Henry's law constant of C<sub>2</sub>H<sub>4</sub> in liquid R10. Simulation data: ● ( $\xi=0.978$ ), ○ ( $\xi=1.003$ ); experimental data: + [39], ■ [15], ▲ [40], ▼ [41].

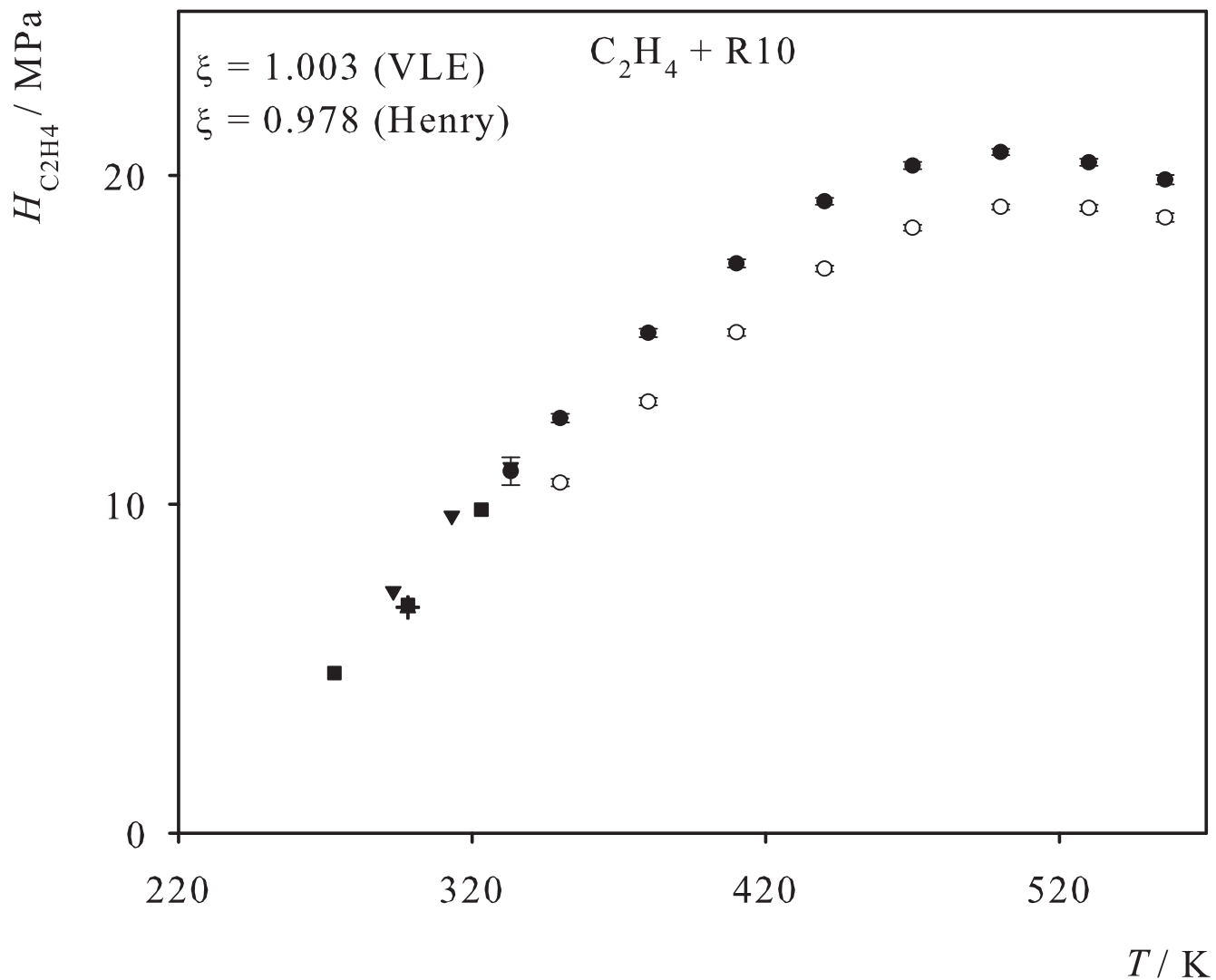


Fig. 31. Henry's law constant of C<sub>2</sub>H<sub>6</sub> in liquid R10. Simulation data: ●; experimental data: + [40], ■ [42].

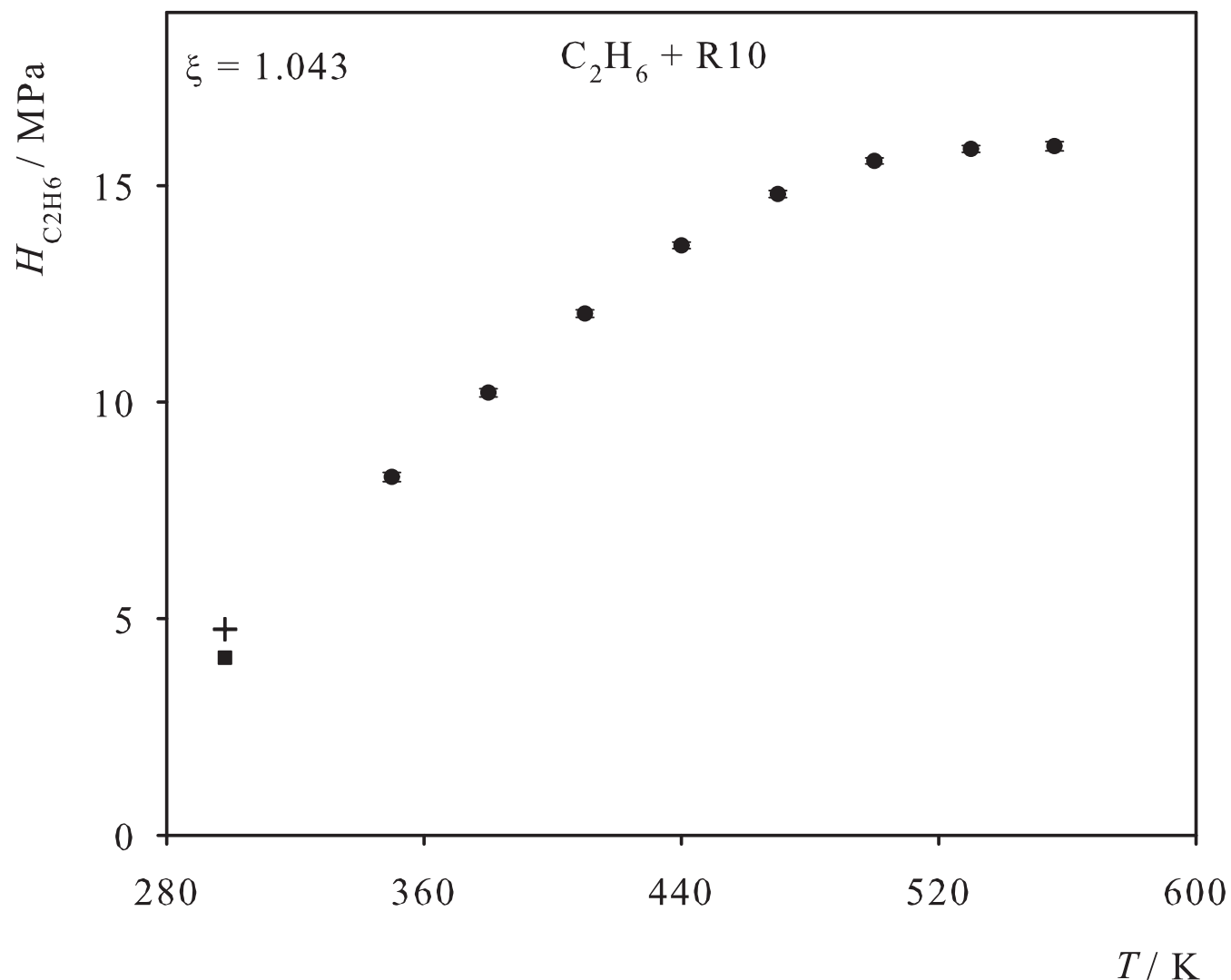


Fig. 32. Henry's law constant of Propylene in liquid R10. Simulation data: ●; experimental data: + [40], ■ [41].

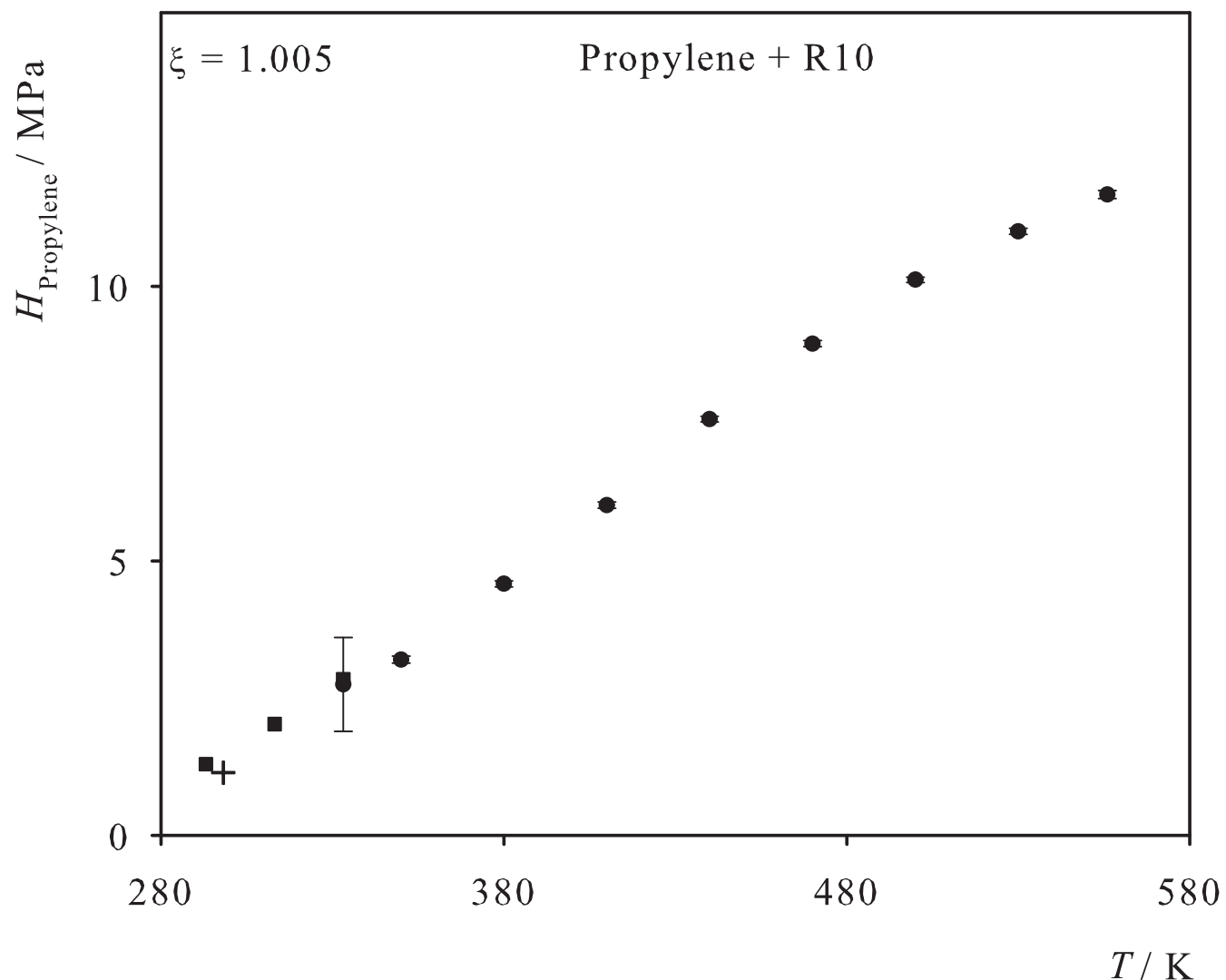


Fig. 33. Henry's law constant of SF<sub>6</sub> in liquid R10. Simulation data: ●; experimental data: + [16], ■ [19].

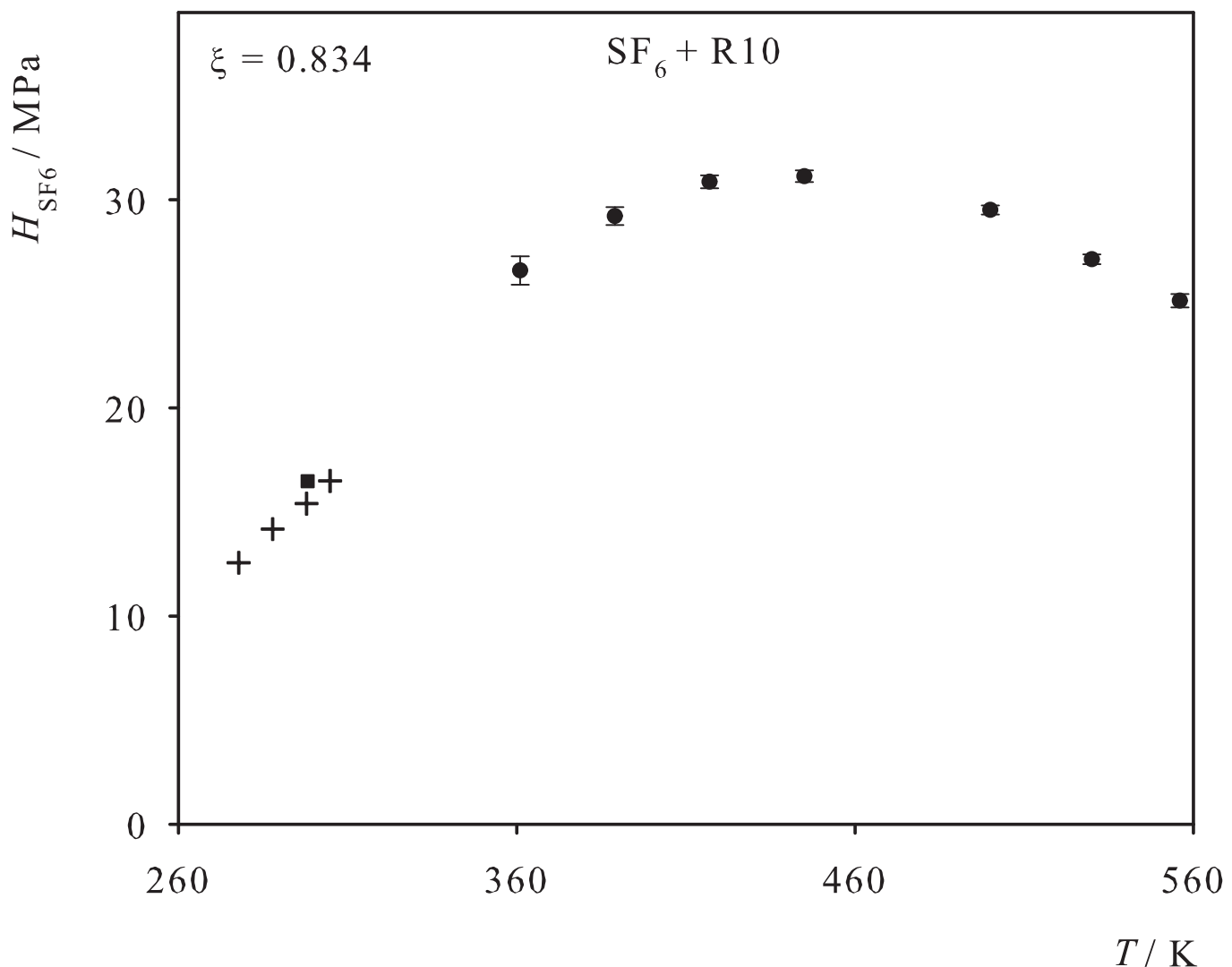


Fig. 34. Henry's law constant of R12 in liquid R10. Simulation data: ●; experimental data: + [43].

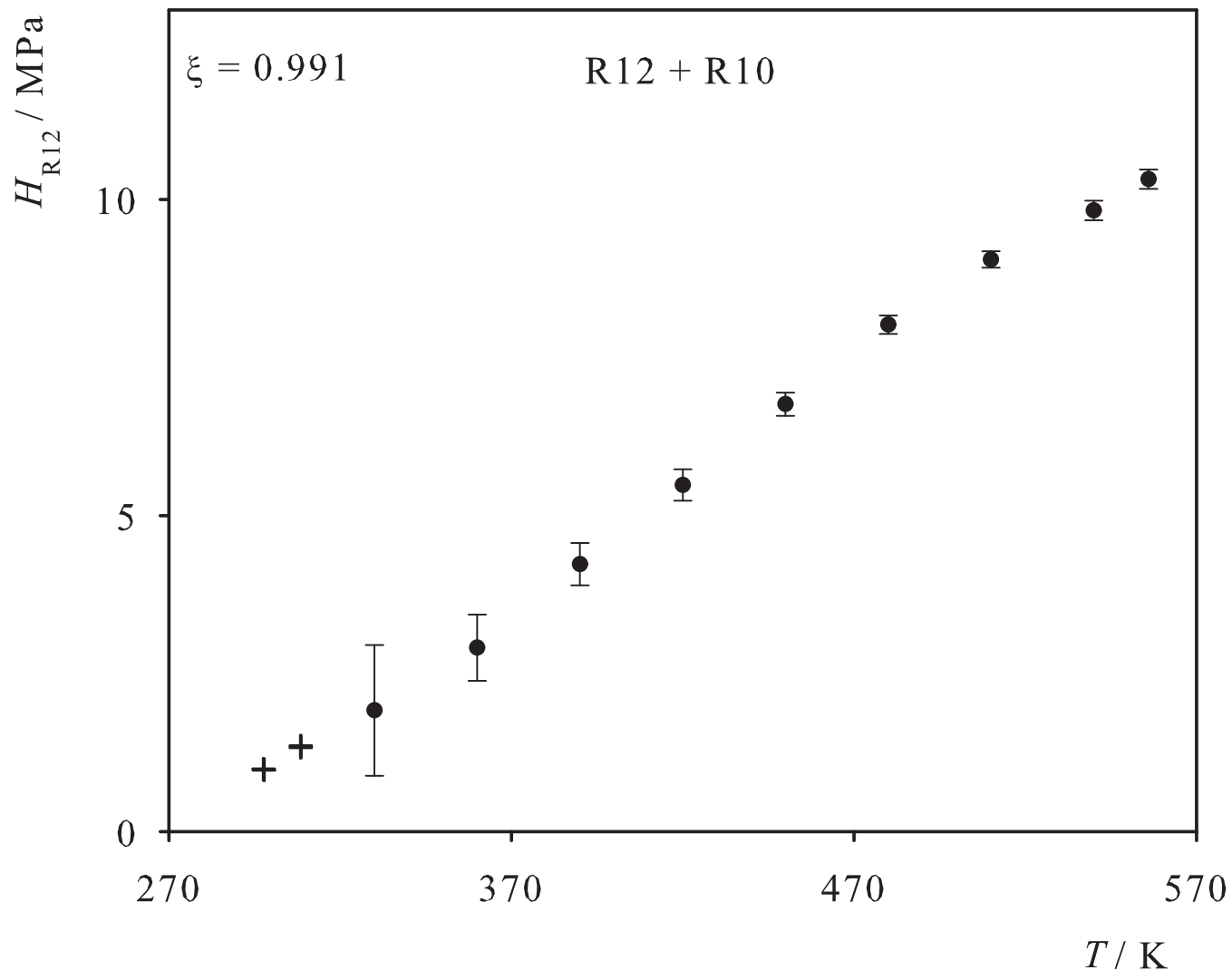


Fig. 35. Henry's law constant of R13 in liquid R10. Simulation data: ●; experimental data: + [43].

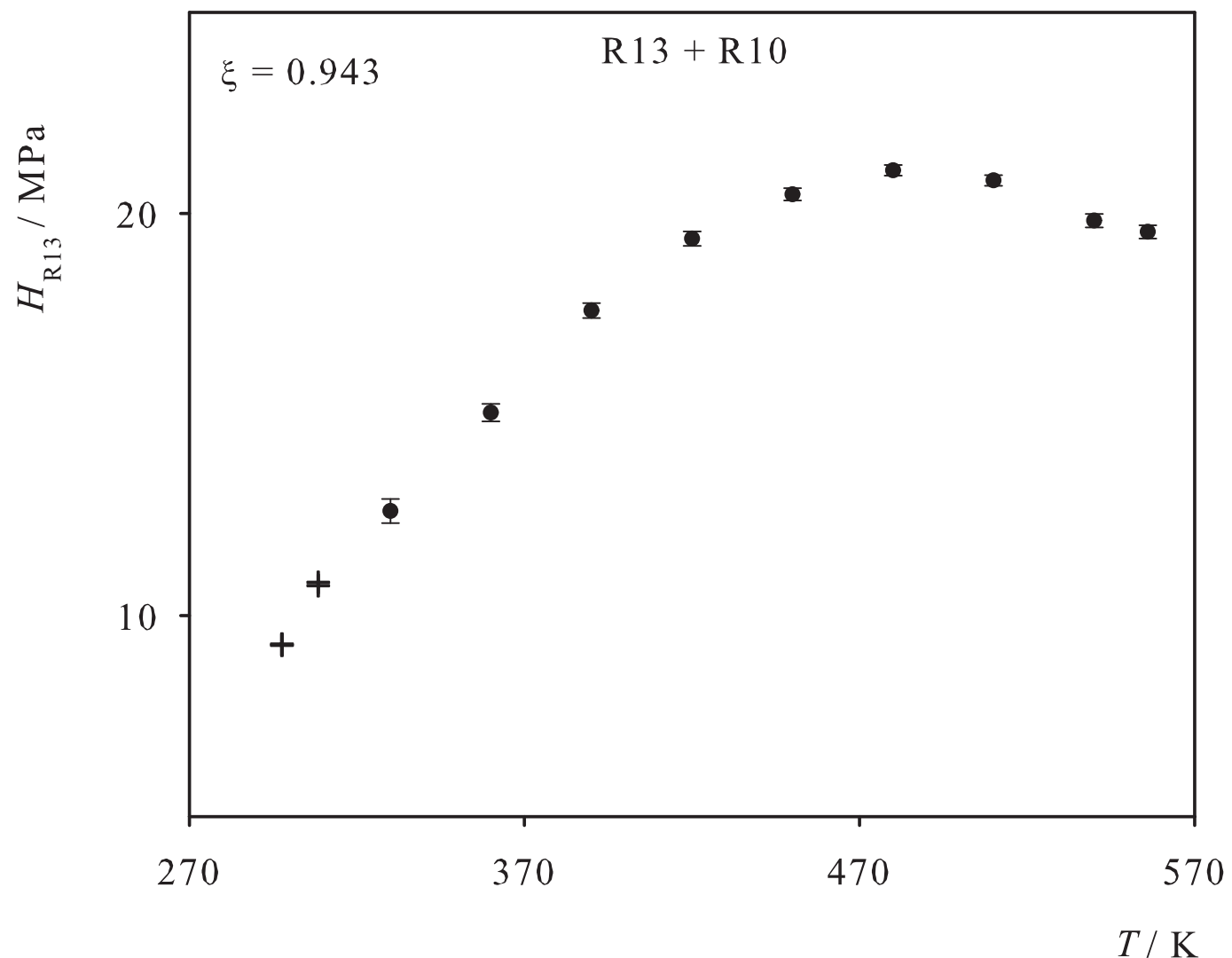


Fig. 36. Henry's law constant of R14 in liquid R10. Simulation data: ●; experimental data: + [16].

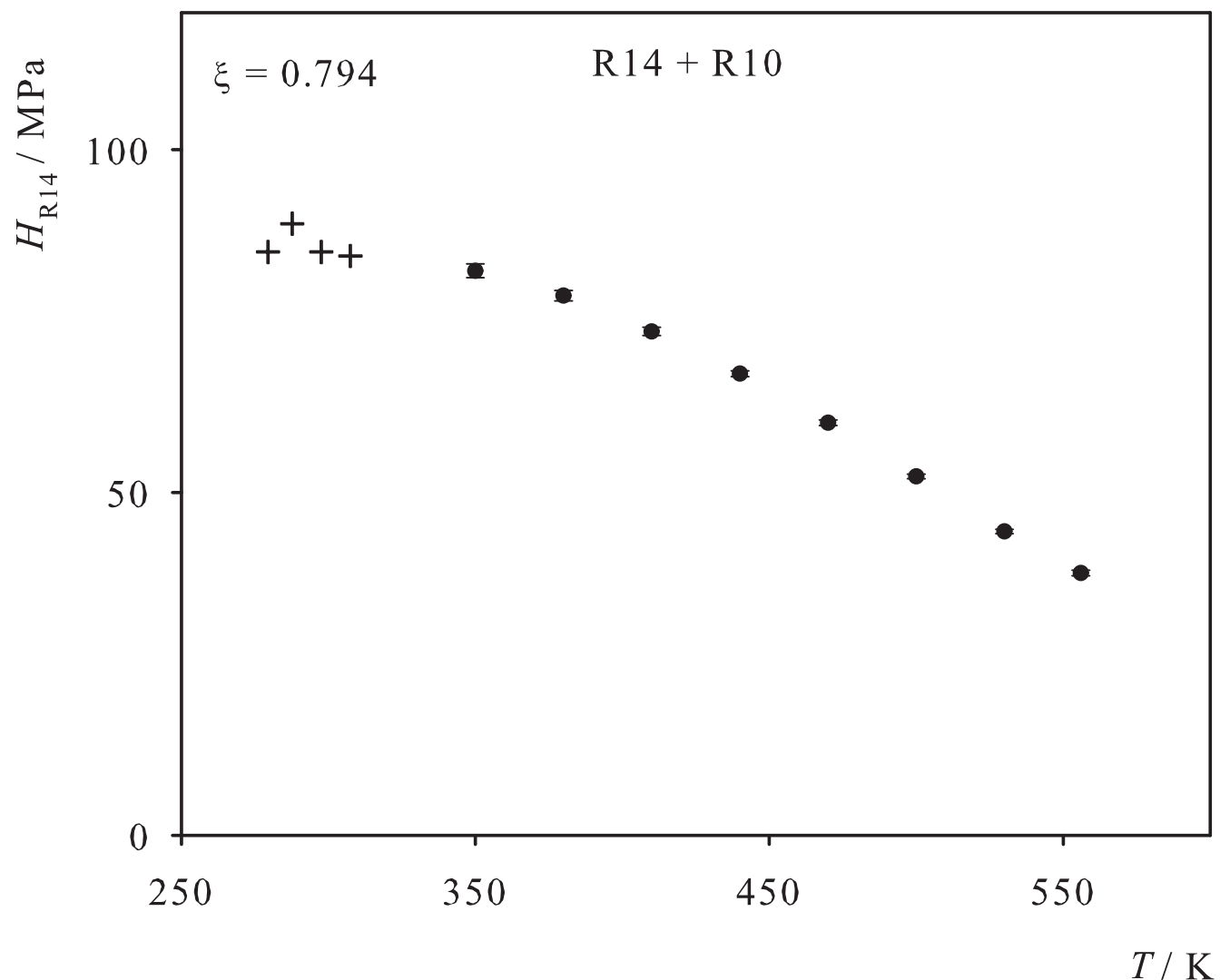


Fig. 37. Henry's law constant of R22 in liquid R10. Simulation data: ●; experimental data: + [44].

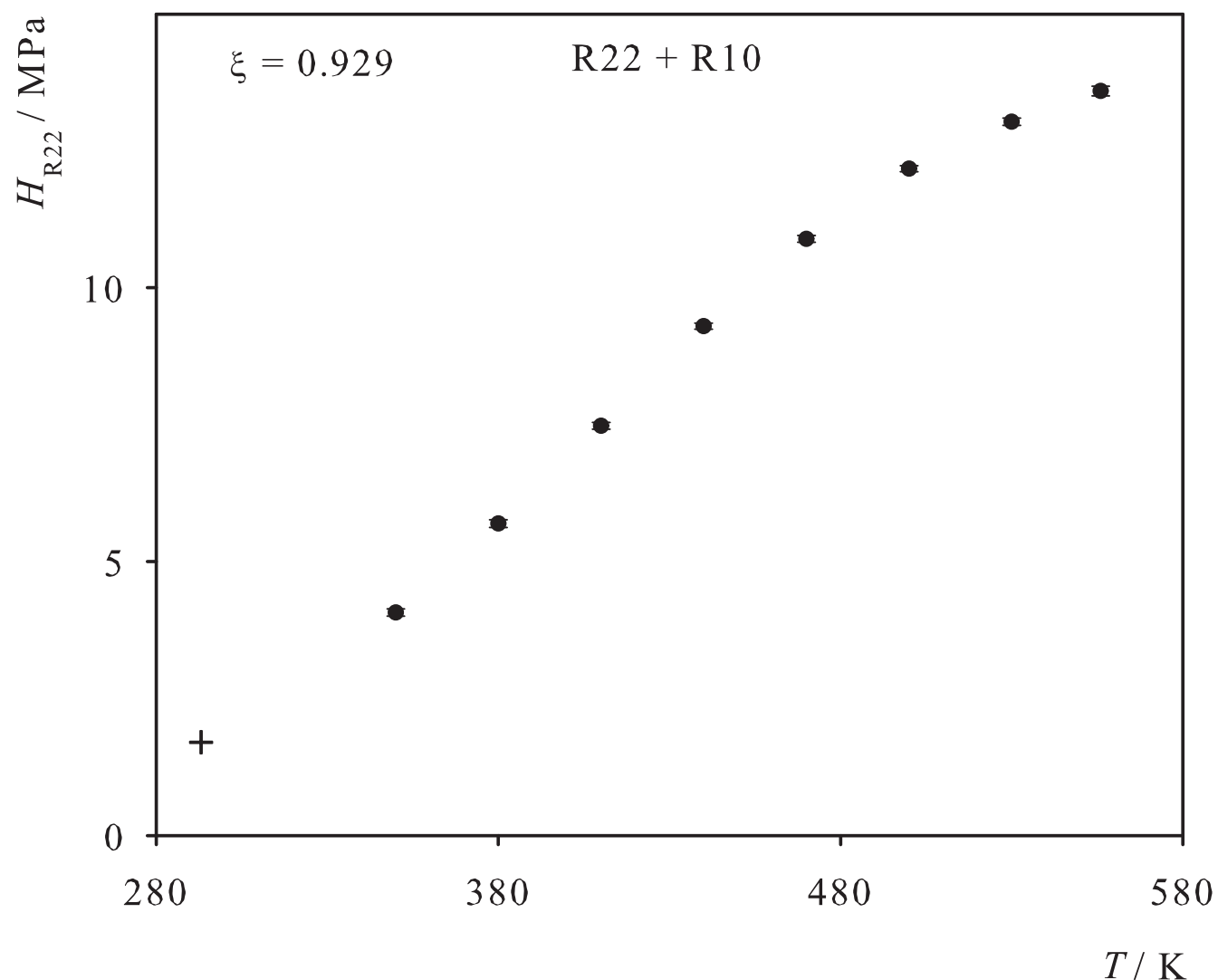


Fig. 38. Henry's law constant of R23 in liquid R10. Simulation data: ●; experimental data: + [45], ■ [46].

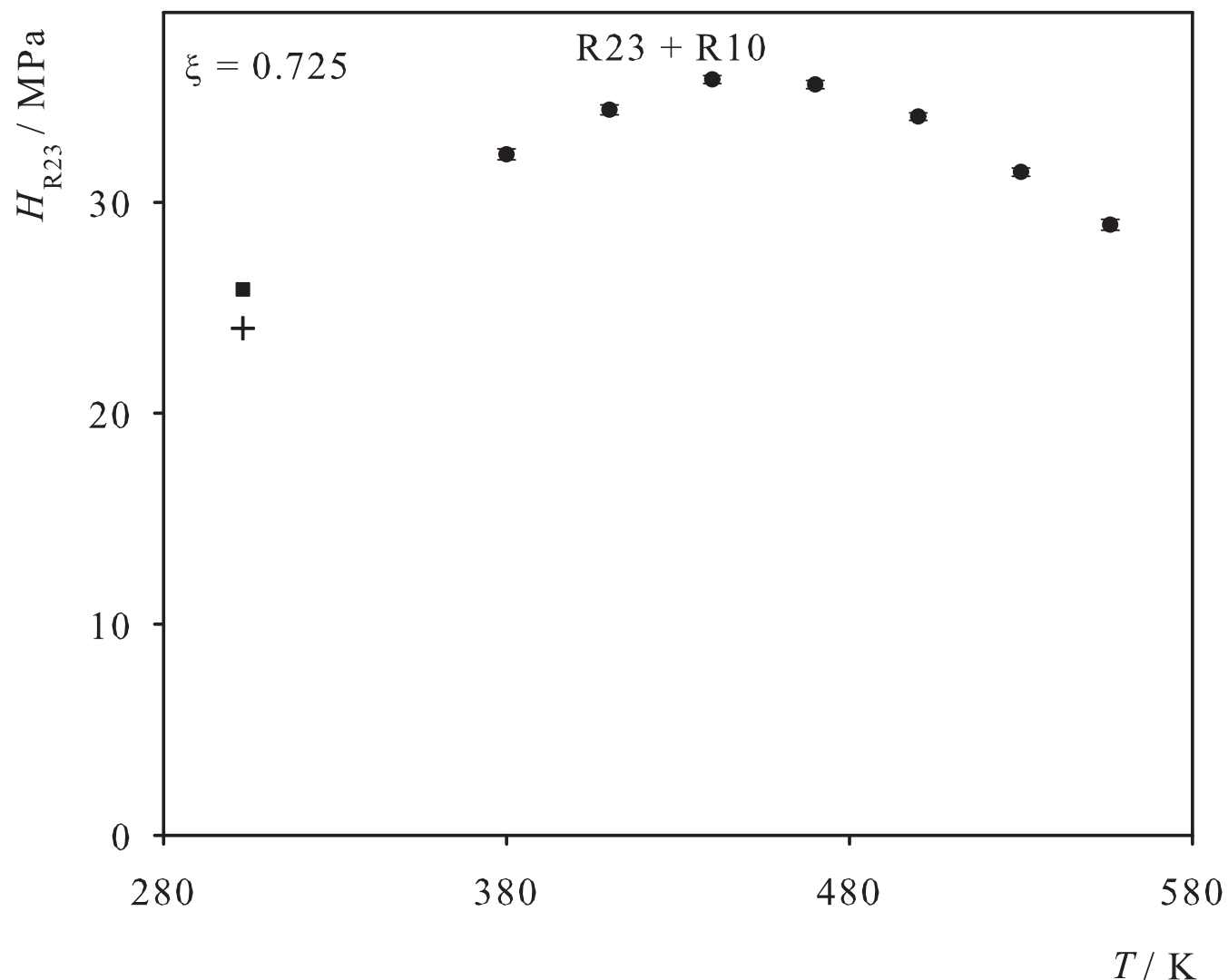


Fig. 39. Henry's law constant of R40 in liquid R10. Simulation data: ●; experimental data: + [47], ■ [48], ▲ [49], ▼ [50].

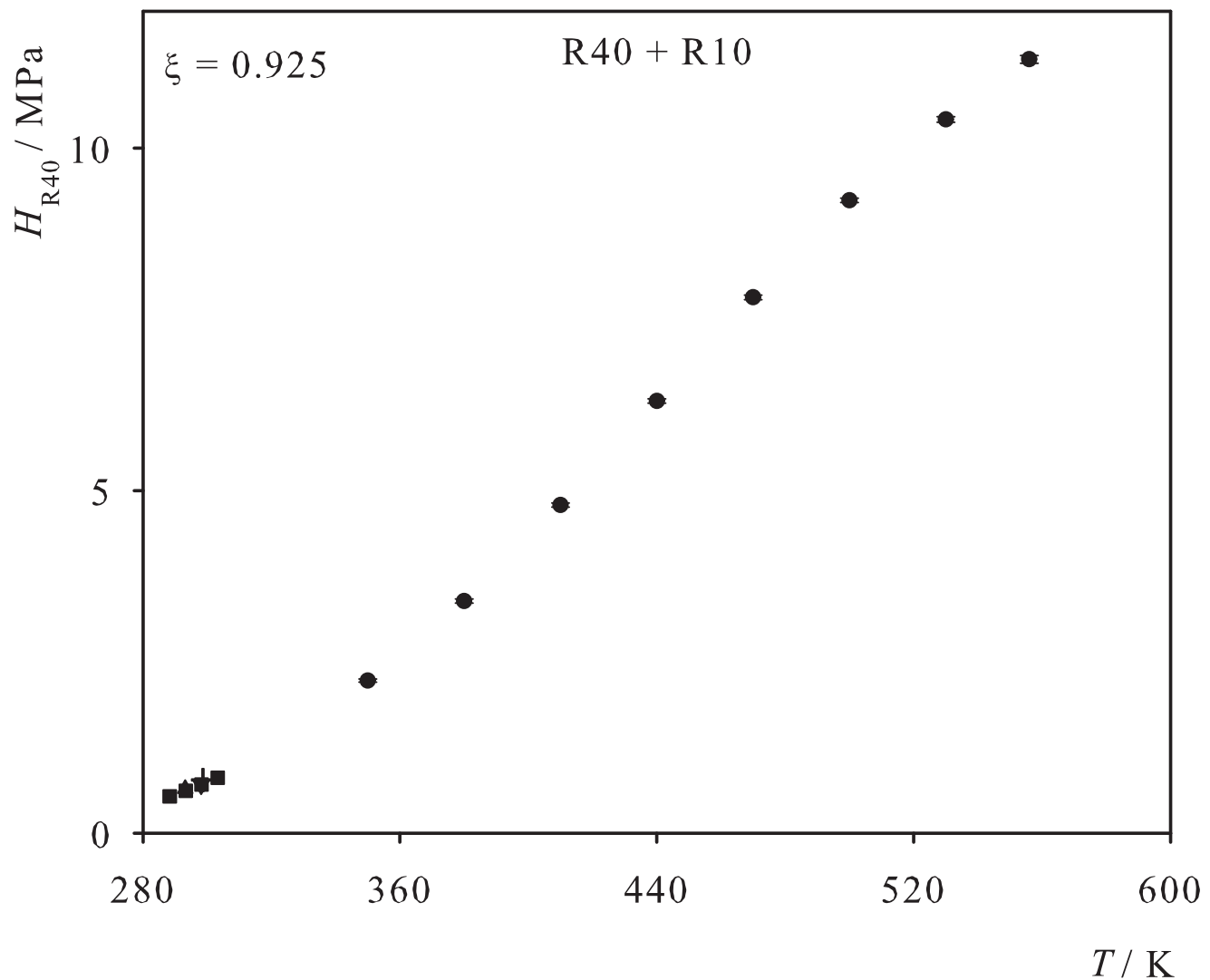


Fig. 40. Henry's law constant of R161 in liquid R10. Simulation data: ●; experimental data: + [51], ■ [52].

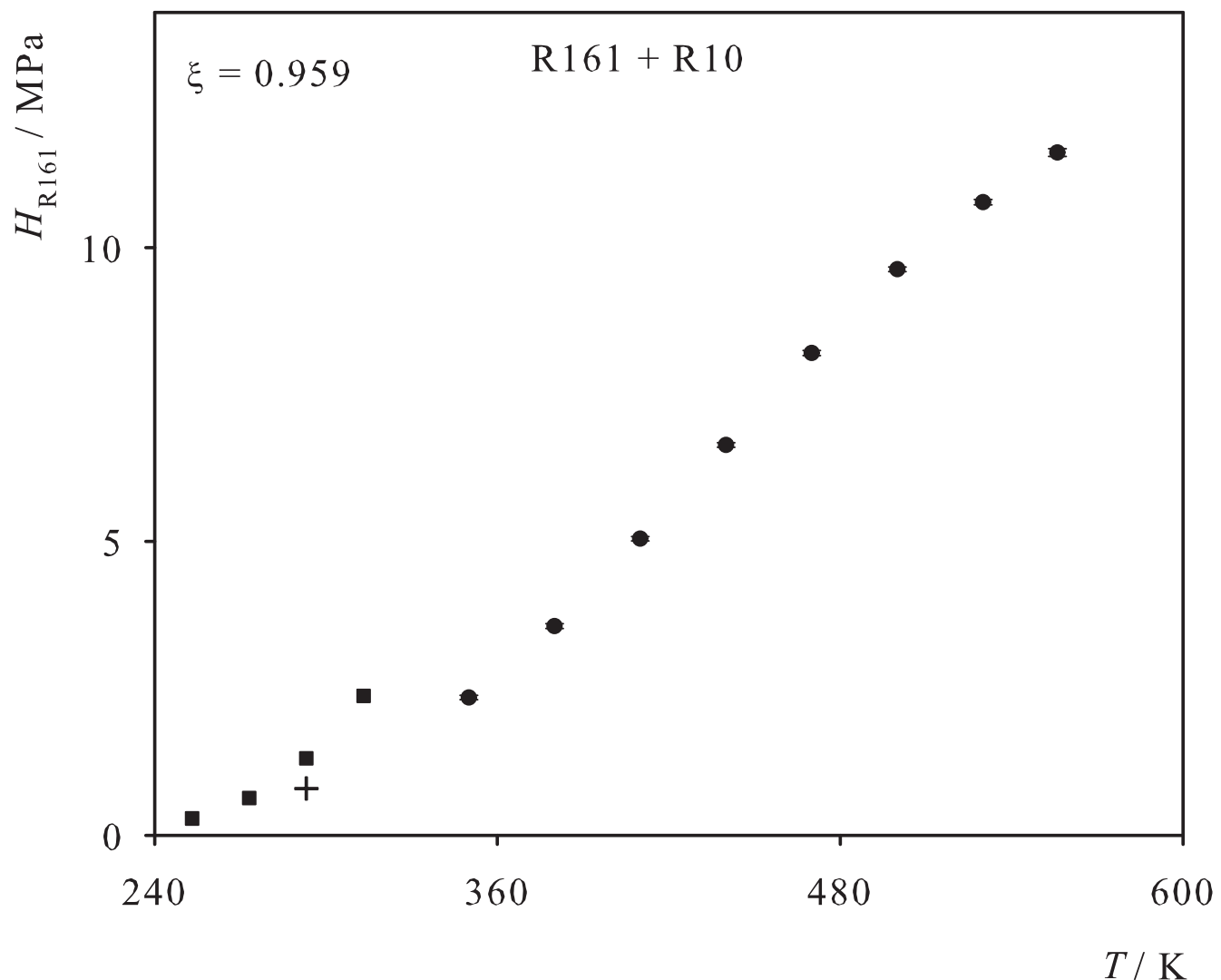


Fig. 41. Henry's law constant of R13 in liquid R11. Simulation data: ●; experimental data: + [53].

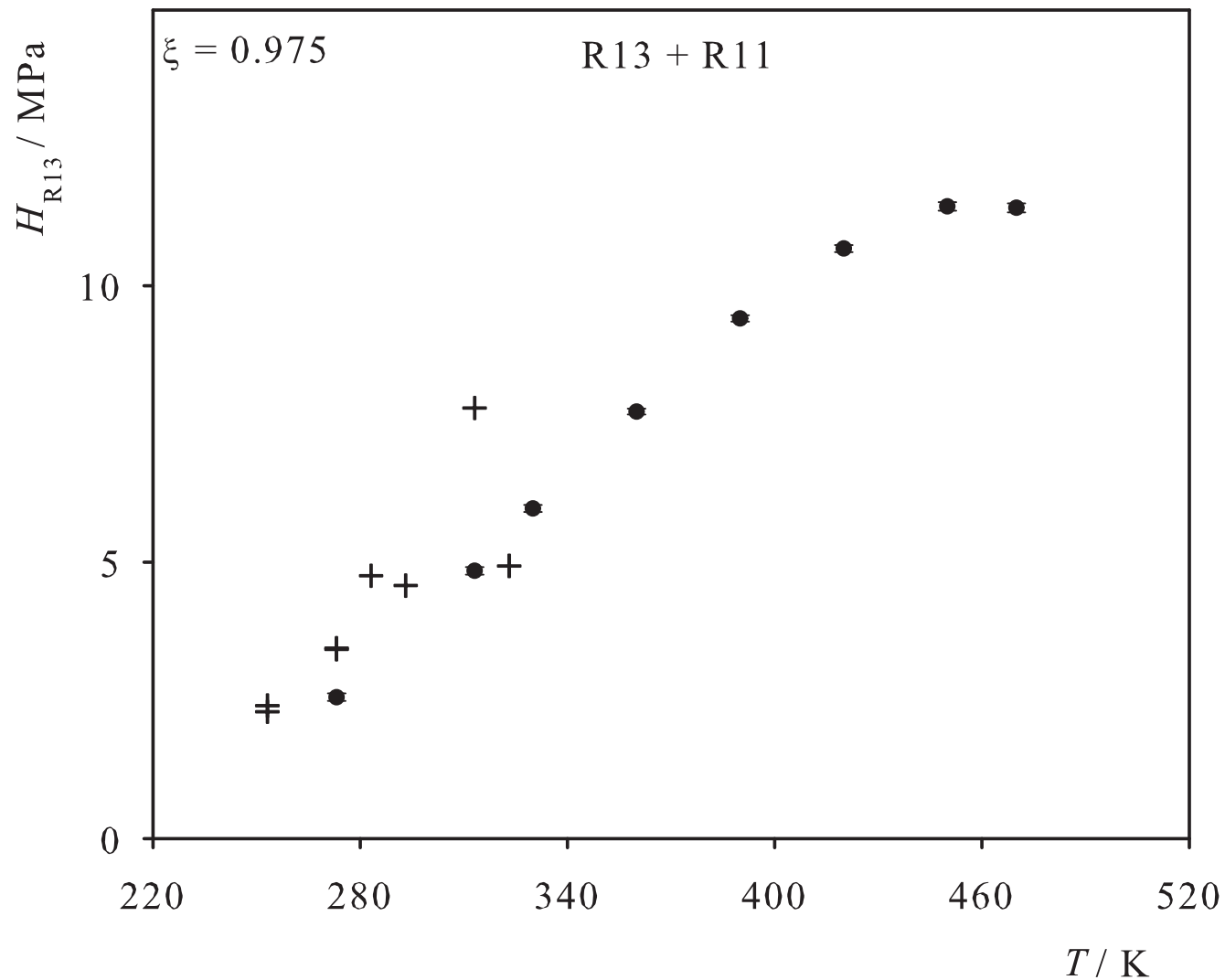


Fig. 42. Henry's law constant of R22 in liquid R11. Simulation data: ●; experimental data: + [53].

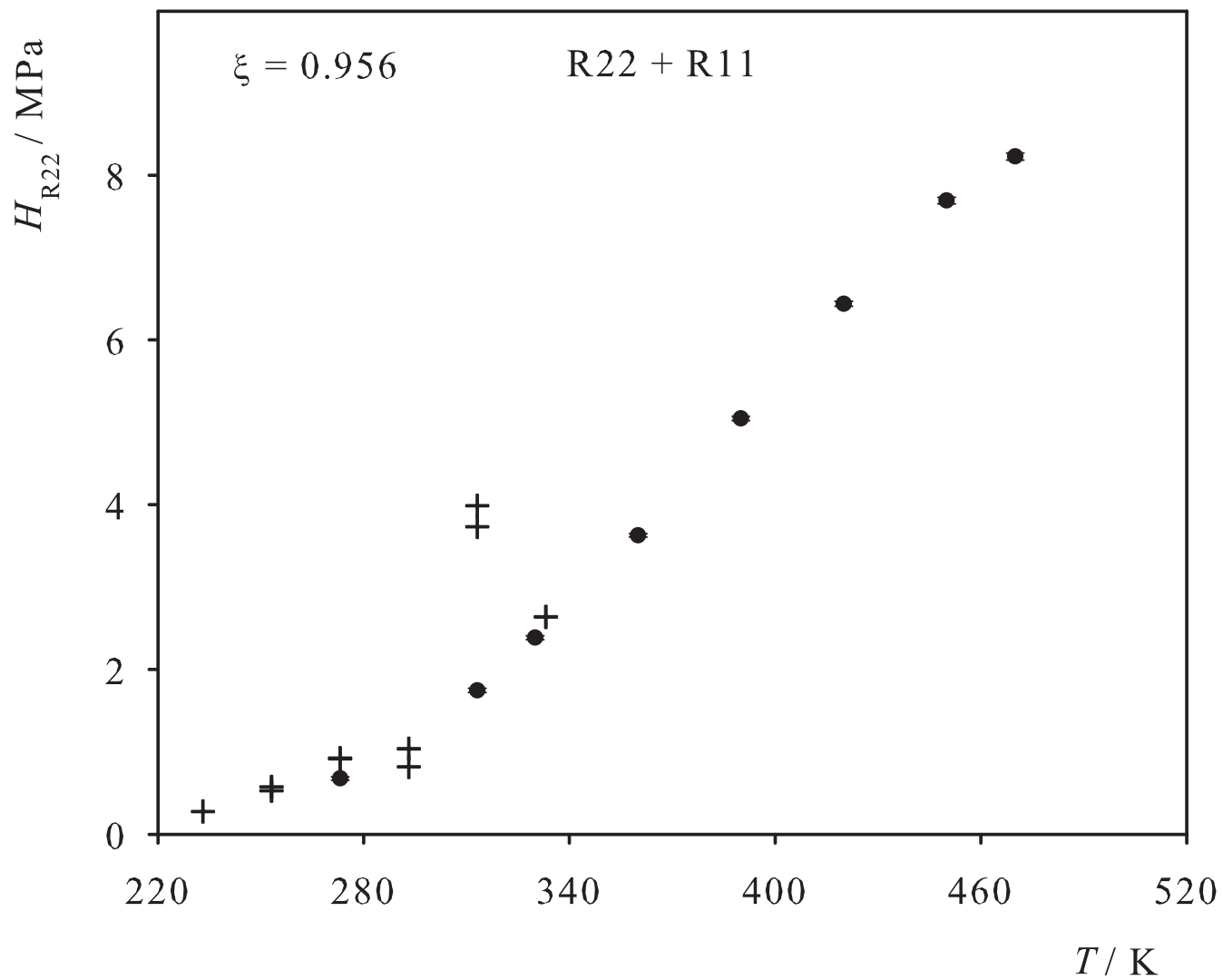


Fig. 43. Henry's law constant of R23 in liquid R11. Simulation data: ● ( $\xi=0.802$ ), ○ ( $\xi=0.849$ ); experimental data: + [45], ■ [54].

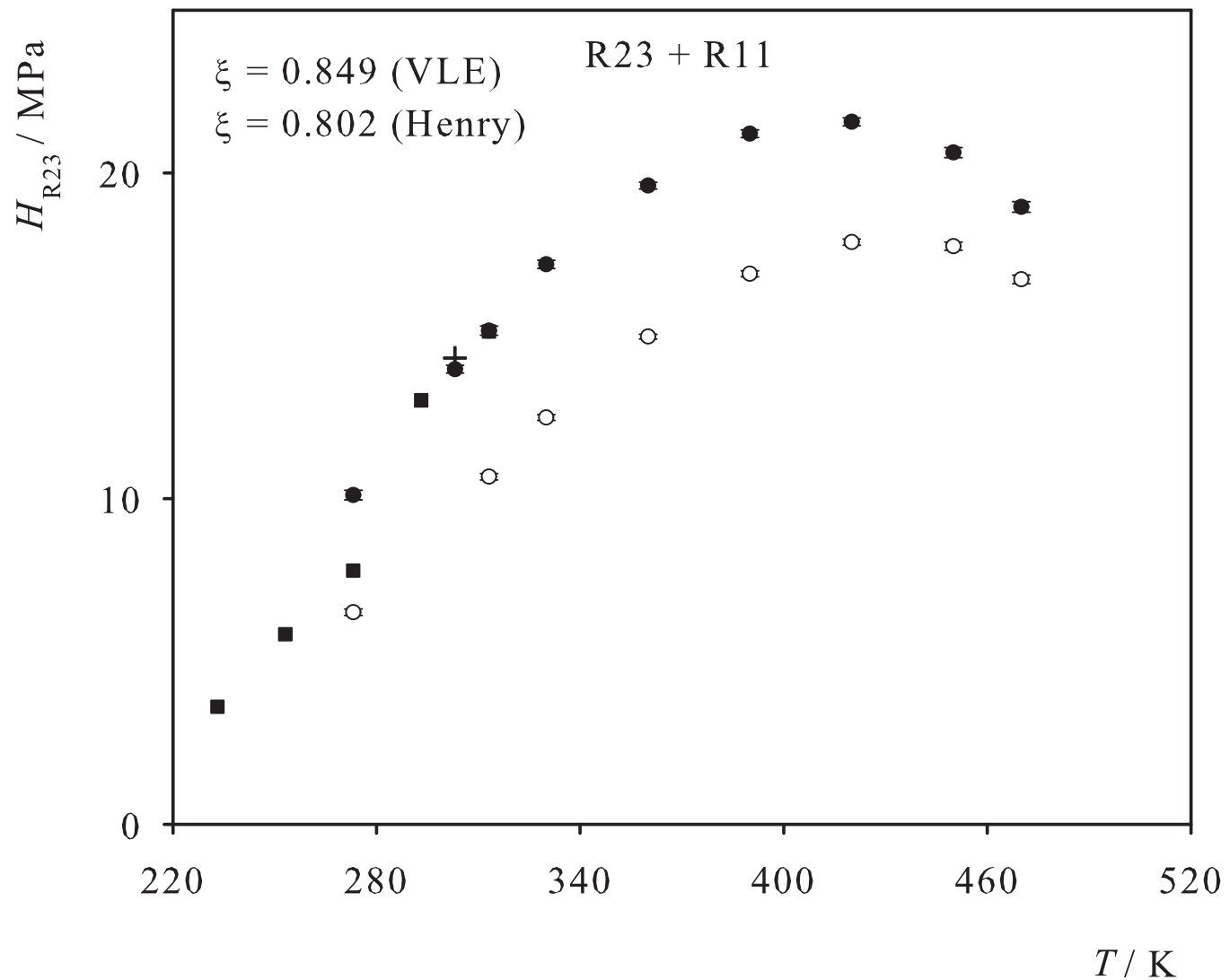


Fig. 44. Henry's law constant of N<sub>2</sub> in liquid R20. Simulation data: ●; experimental data: + [55].

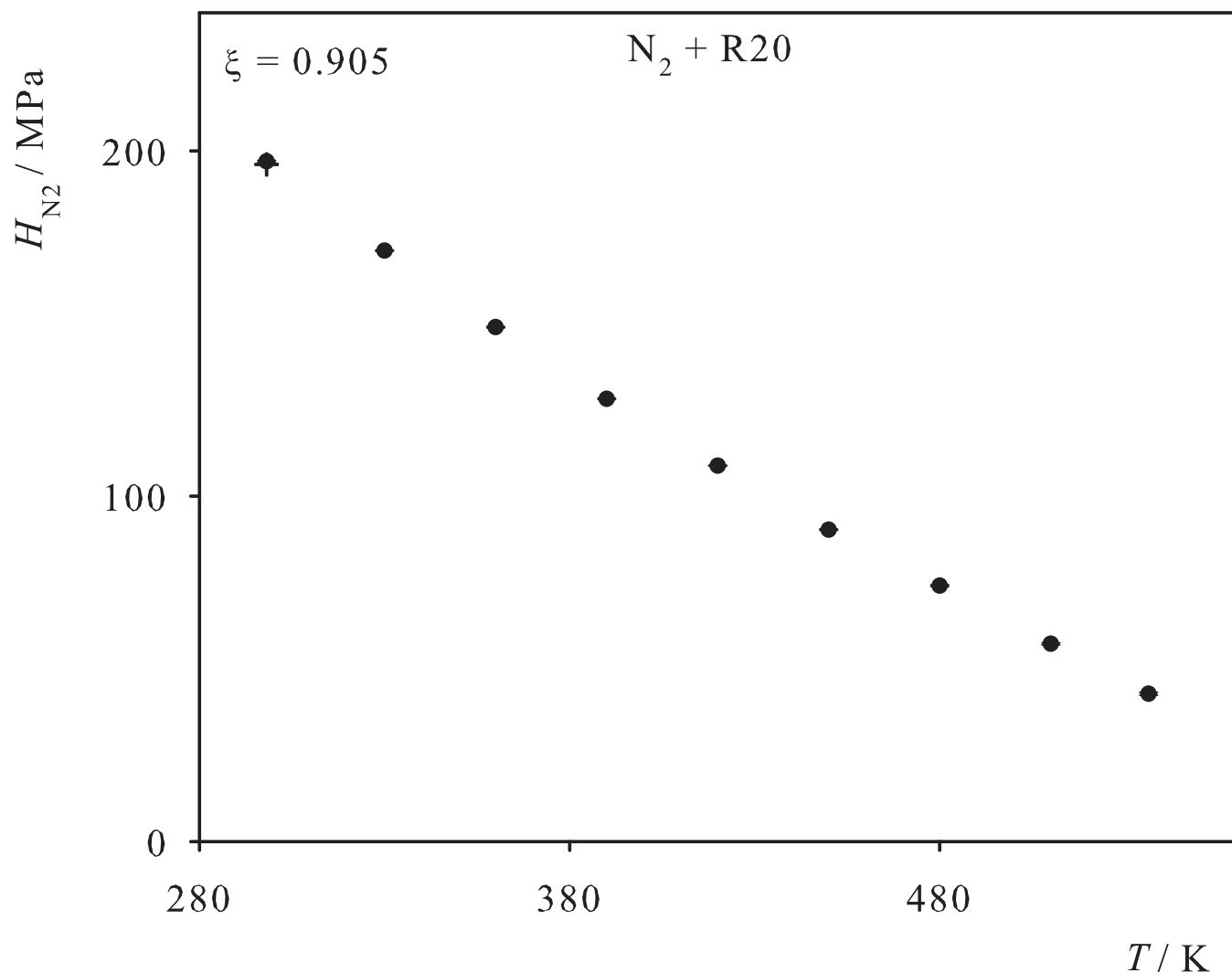


Fig. 45. Henry's law constant of O<sub>2</sub> in liquid R20. Simulation data: ●; experimental data: + [56].

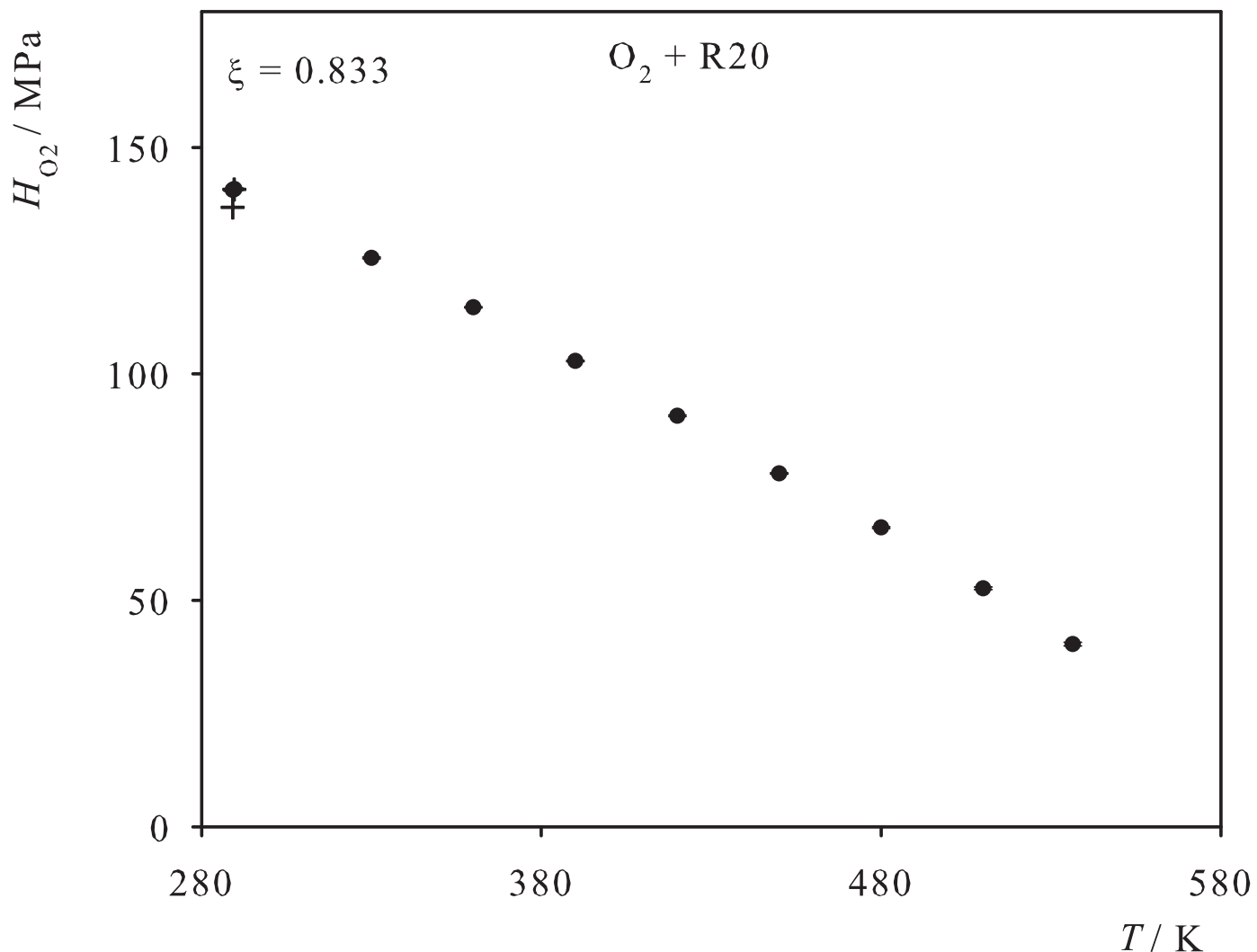


Fig. 46. Henry's law constant of  $\text{Cl}_2$  in liquid R20. Simulation data: ●; experimental data: + [30].

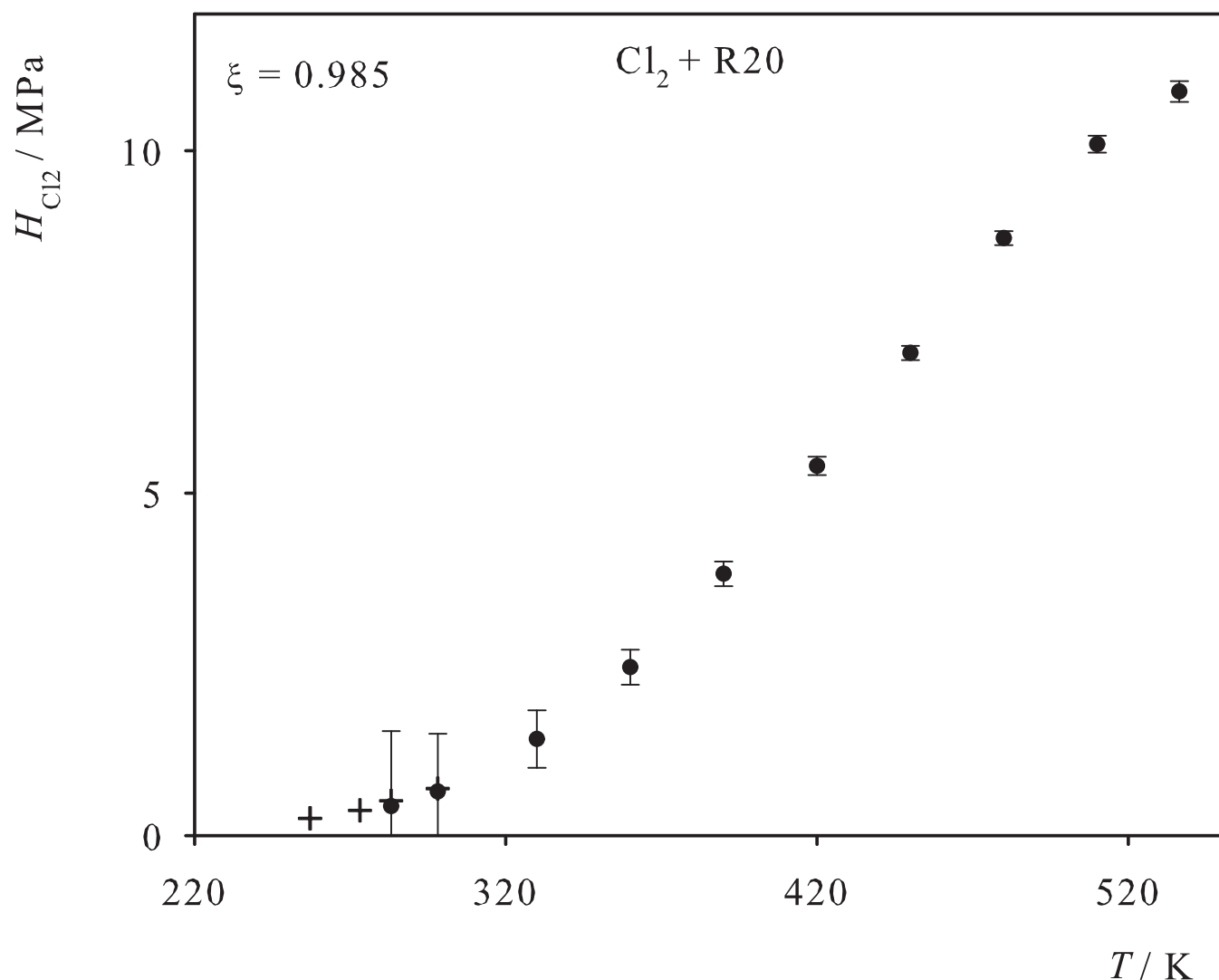


Fig. 47. Henry's law constant of C<sub>2</sub>H<sub>4</sub> in liquid R20. Simulation data: ●; experimental data: + [41].

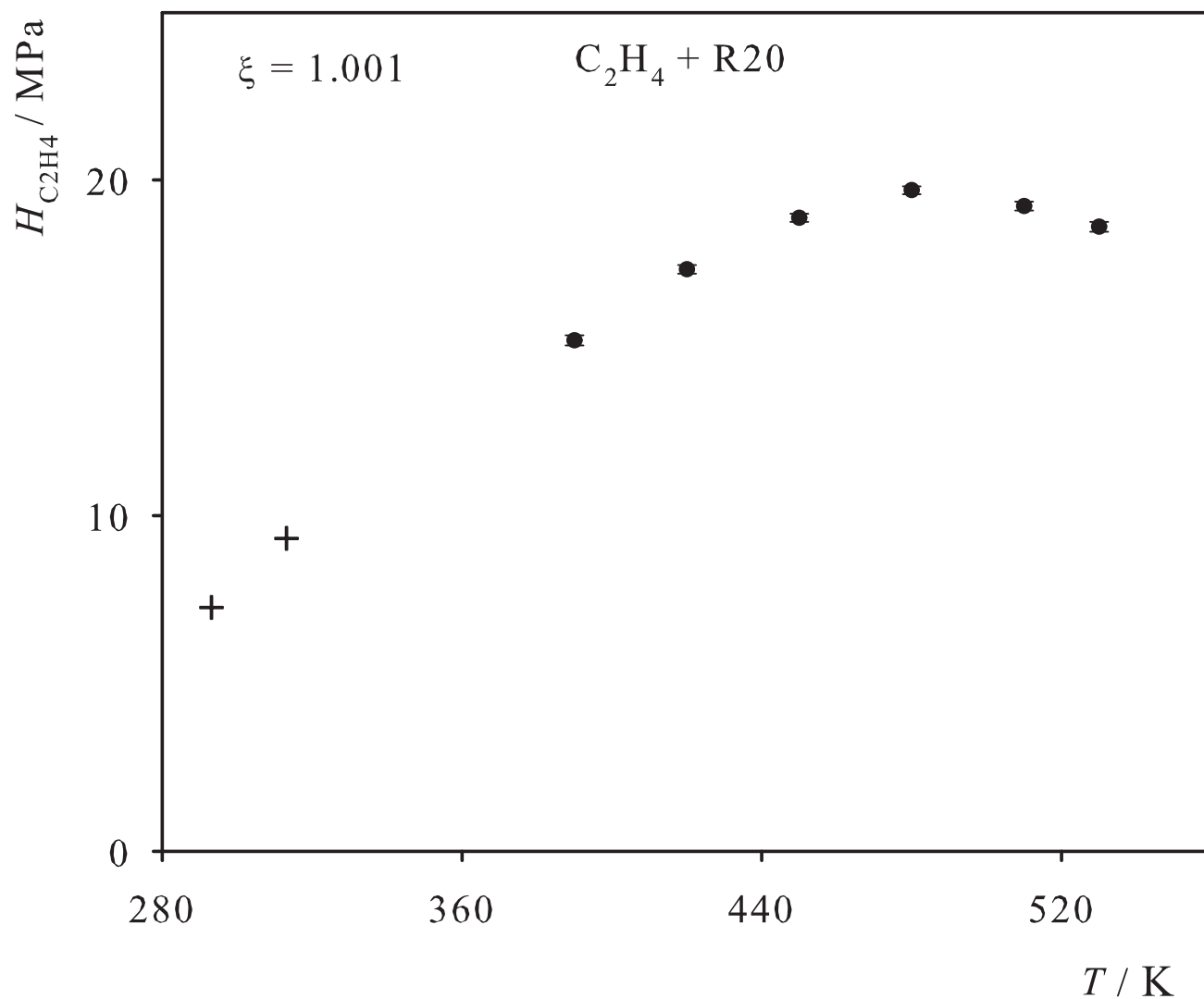


Fig. 48. Henry's law constant of Propylene in liquid R20. Simulation data: ●; experimental data: + [41].

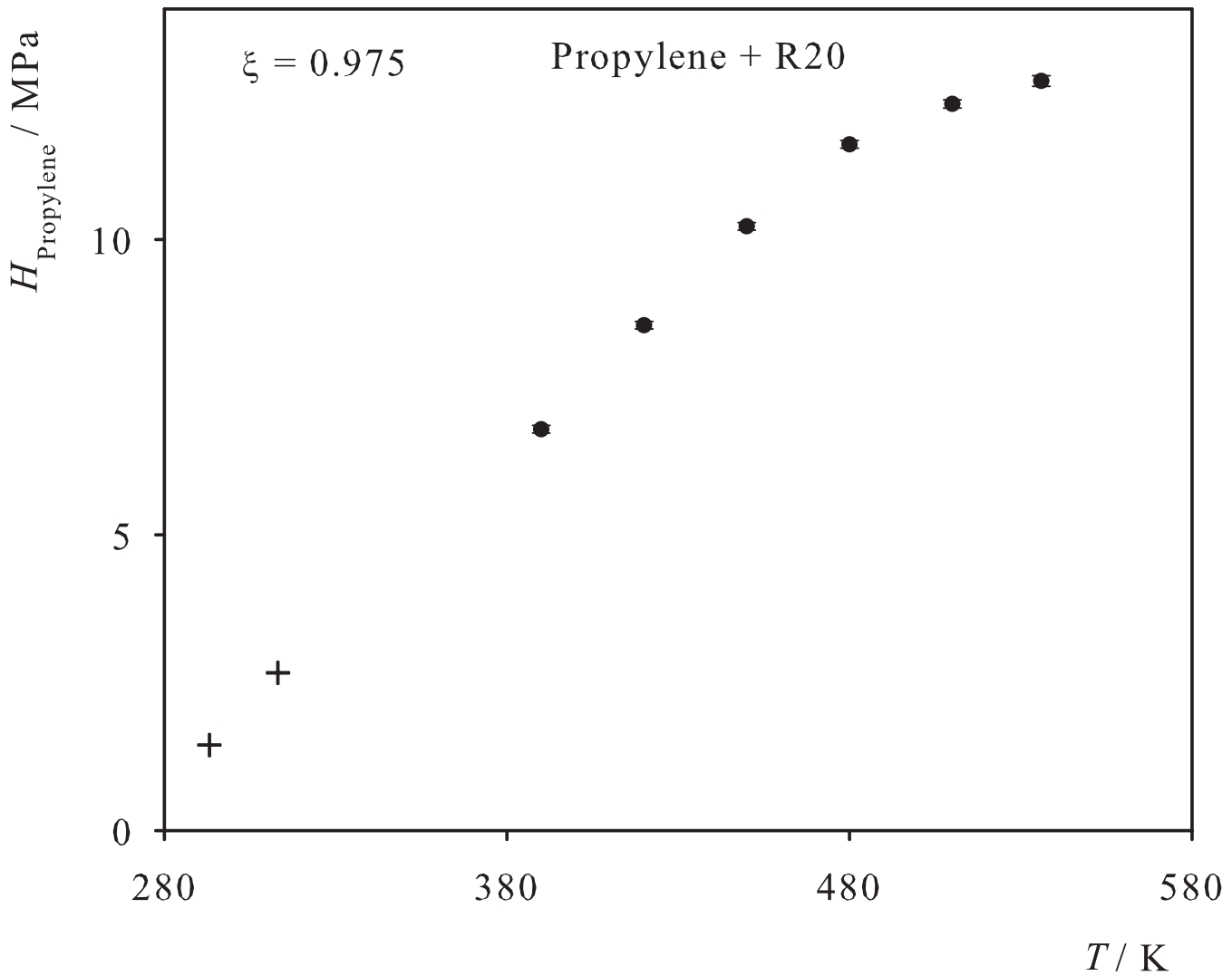


Fig. 49. Henry's law constant of R22 in liquid R20. Simulation data: ●; experimental data: + [44].

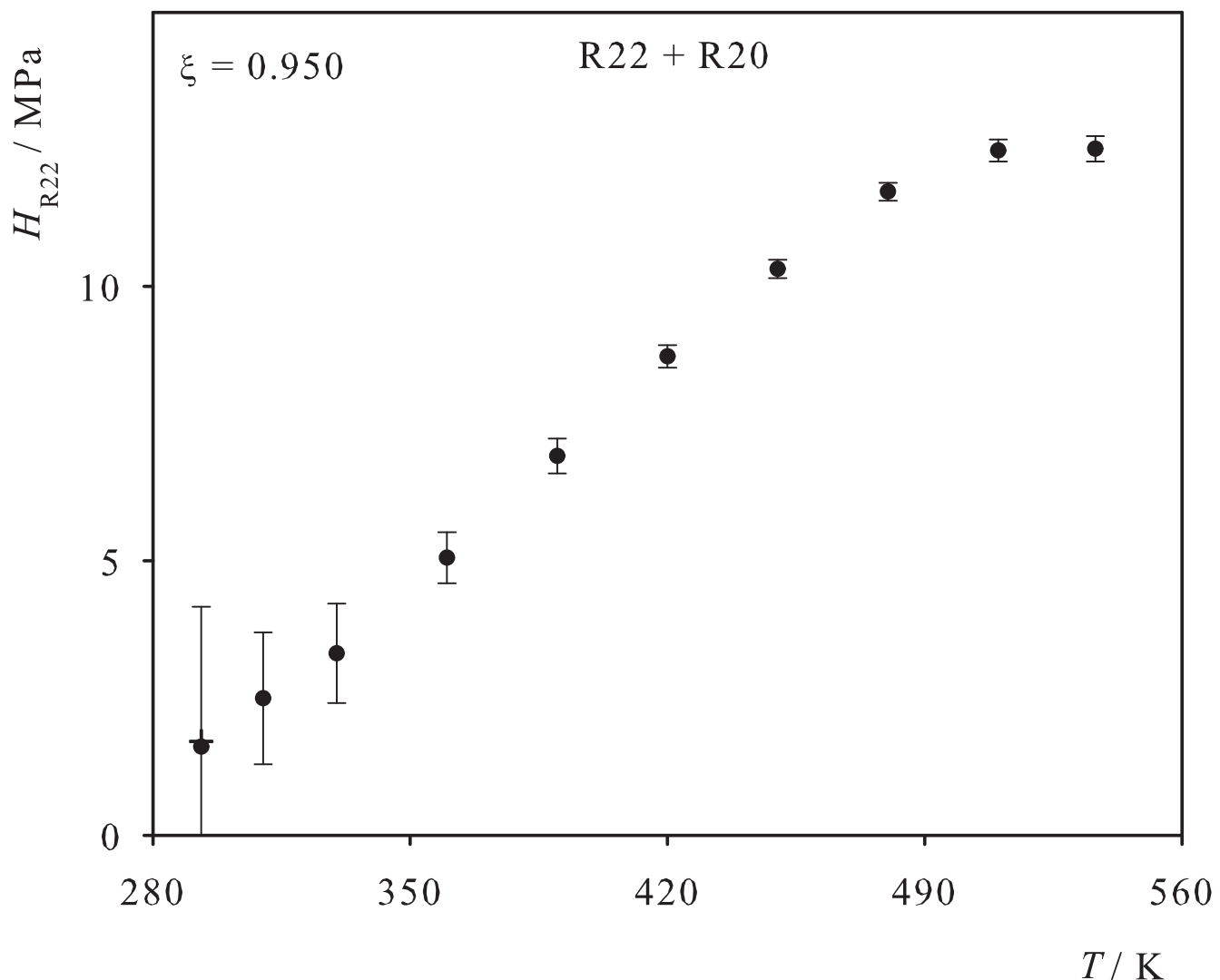


Fig. 50. Henry's law constant of R40 in liquid R20. Simulation data: ●; experimental data: + [50].

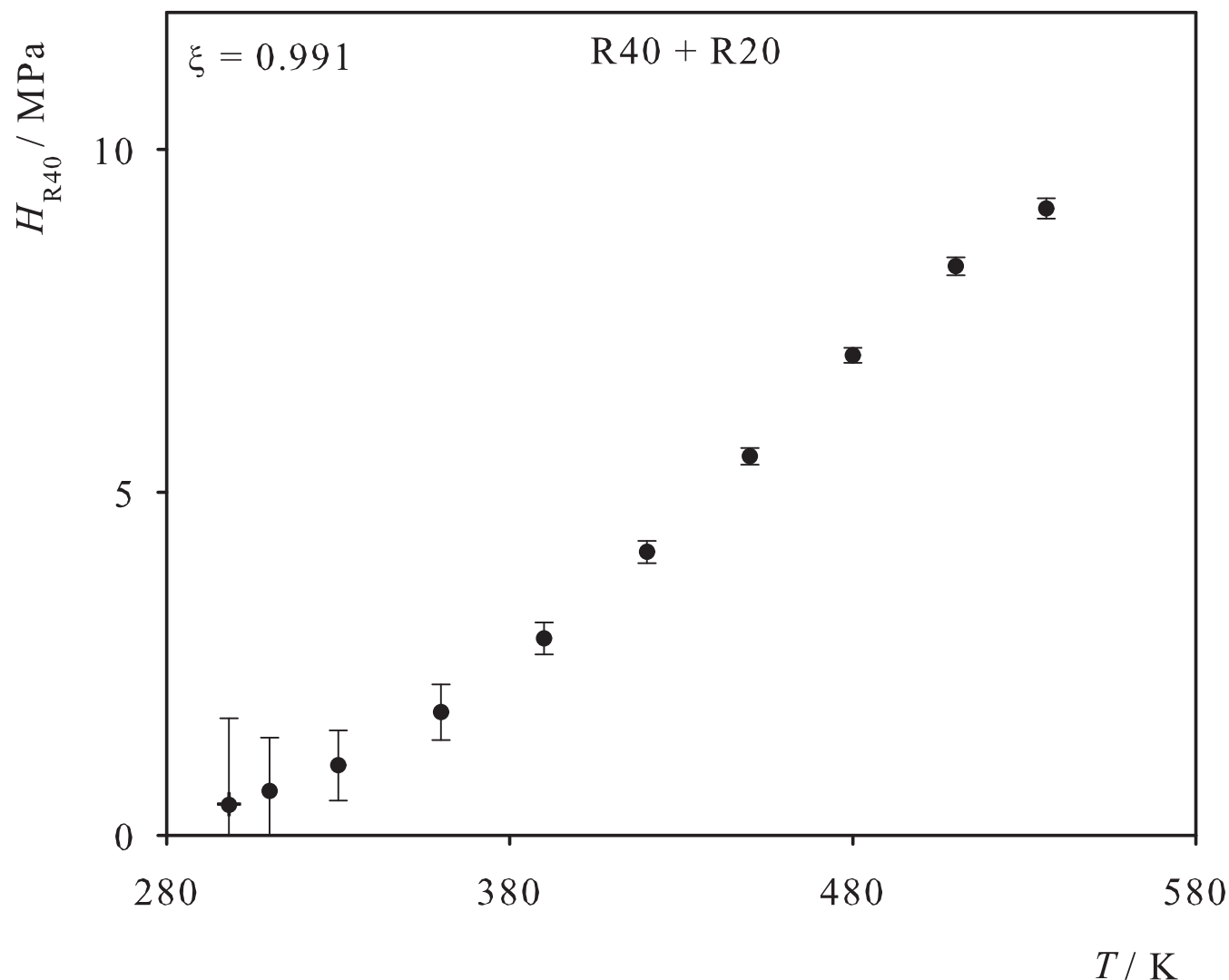


Fig. 51. Henry's law constant of R161 in liquid R20. Simulation data: ●; experimental data: + [51].

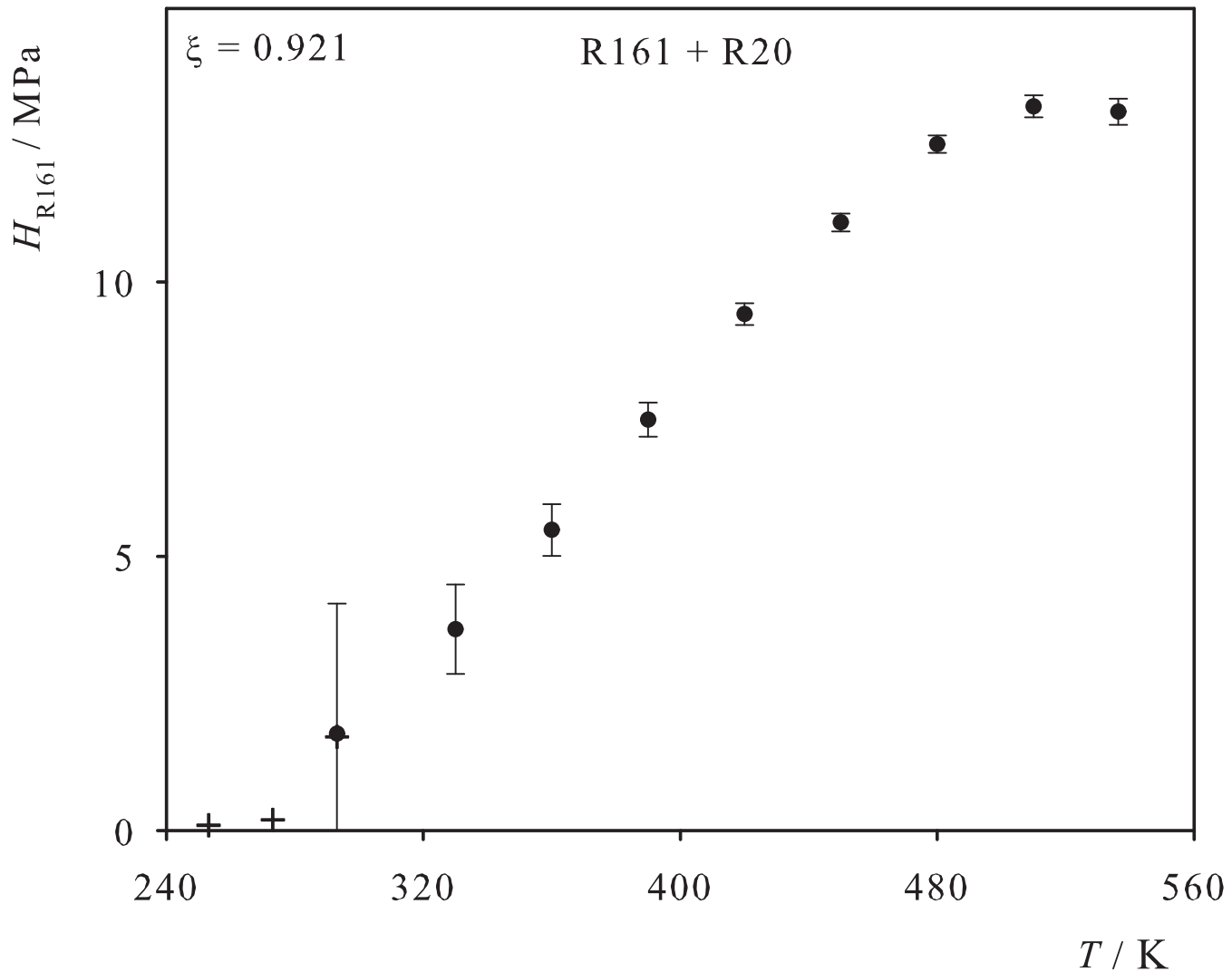


Fig. 52. Henry's law constant of Kr in liquid R20B3. Simulation data: ●; experimental data: + [21].

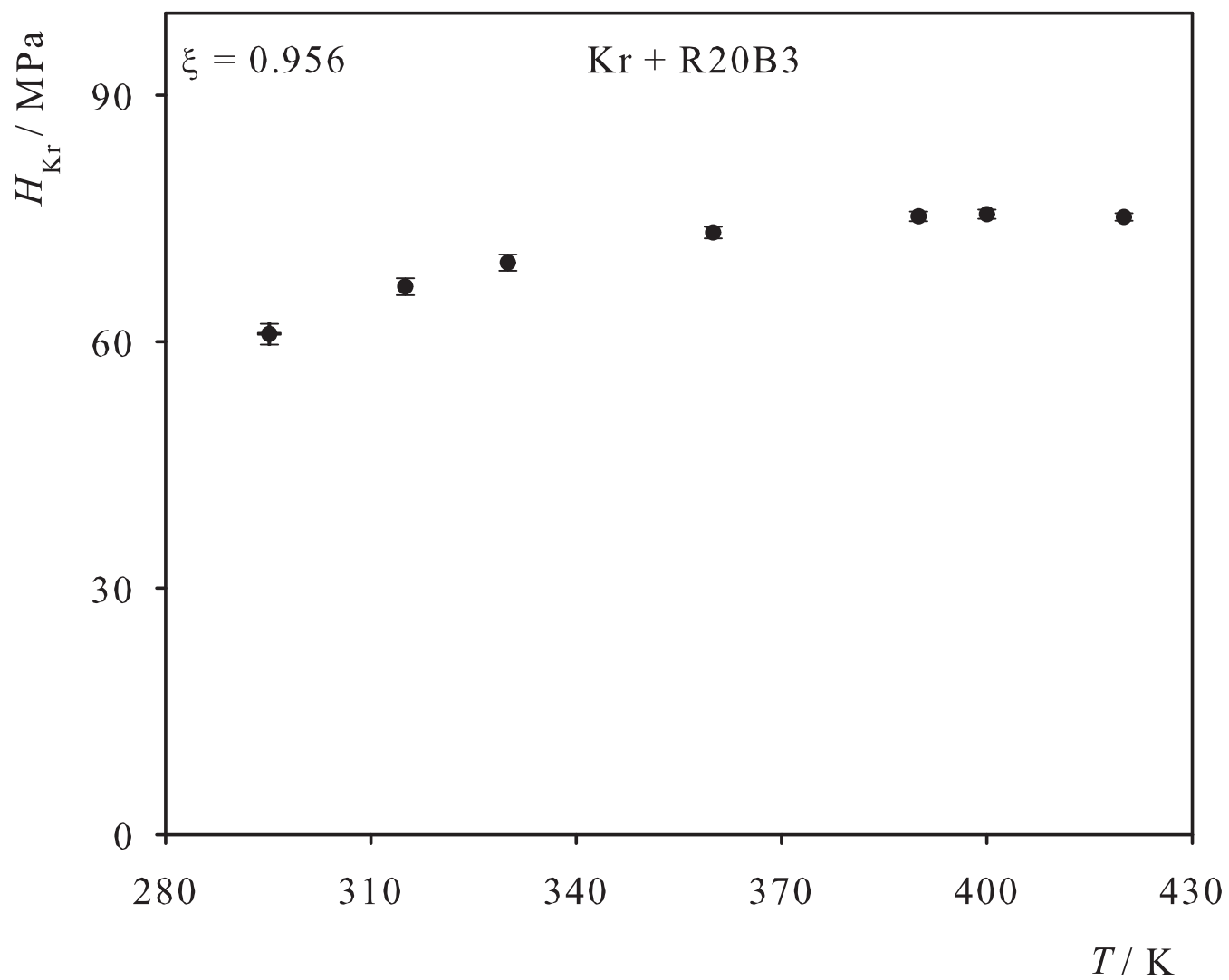


Fig. 53. Henry's law constant of CH<sub>4</sub> in liquid R30. Simulation data: ●; experimental data: + [57].

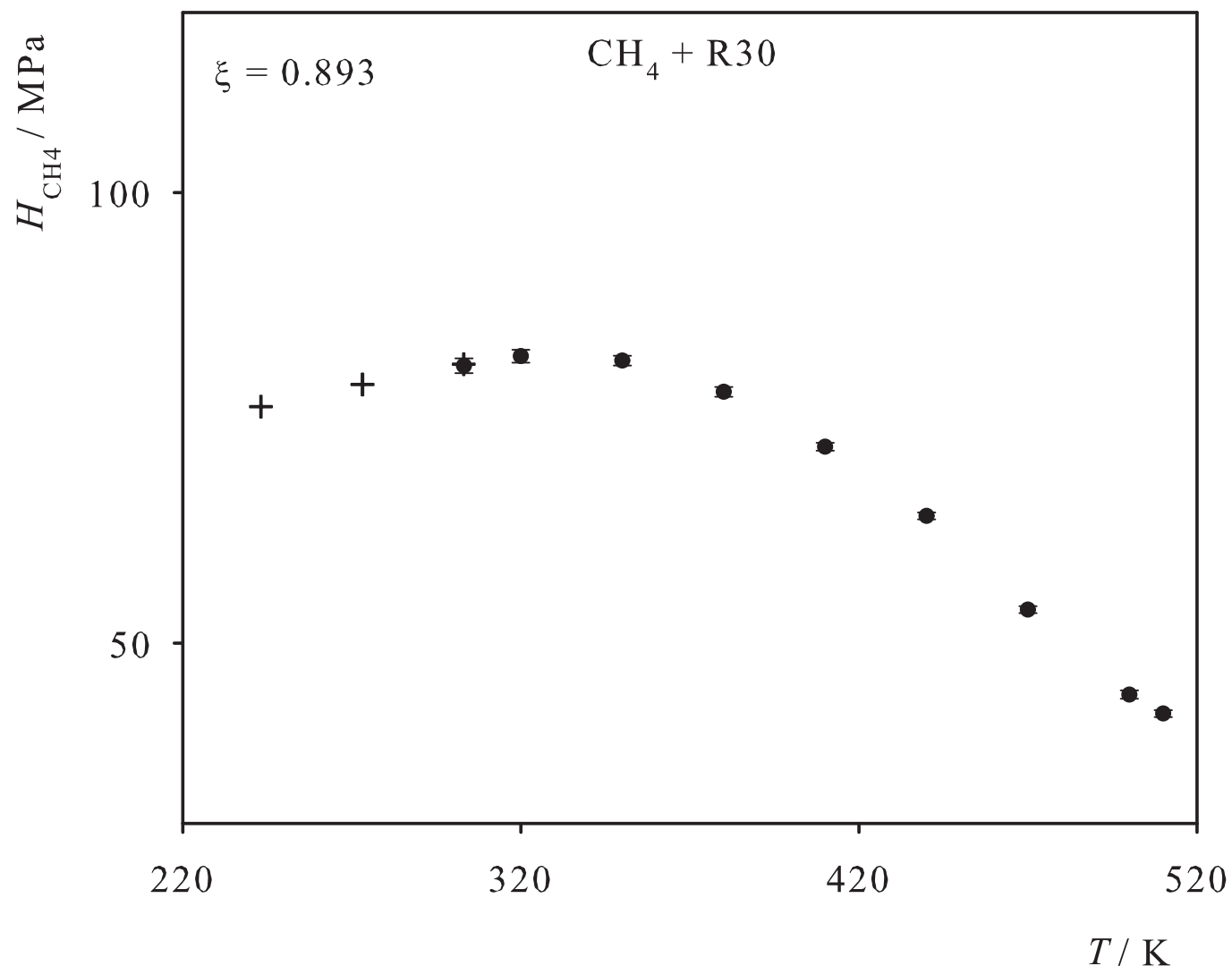


Fig. 54. Henry's law constant of  $\text{Cl}_2$  in liquid R30. Simulation data: ●; experimental data: + [30].

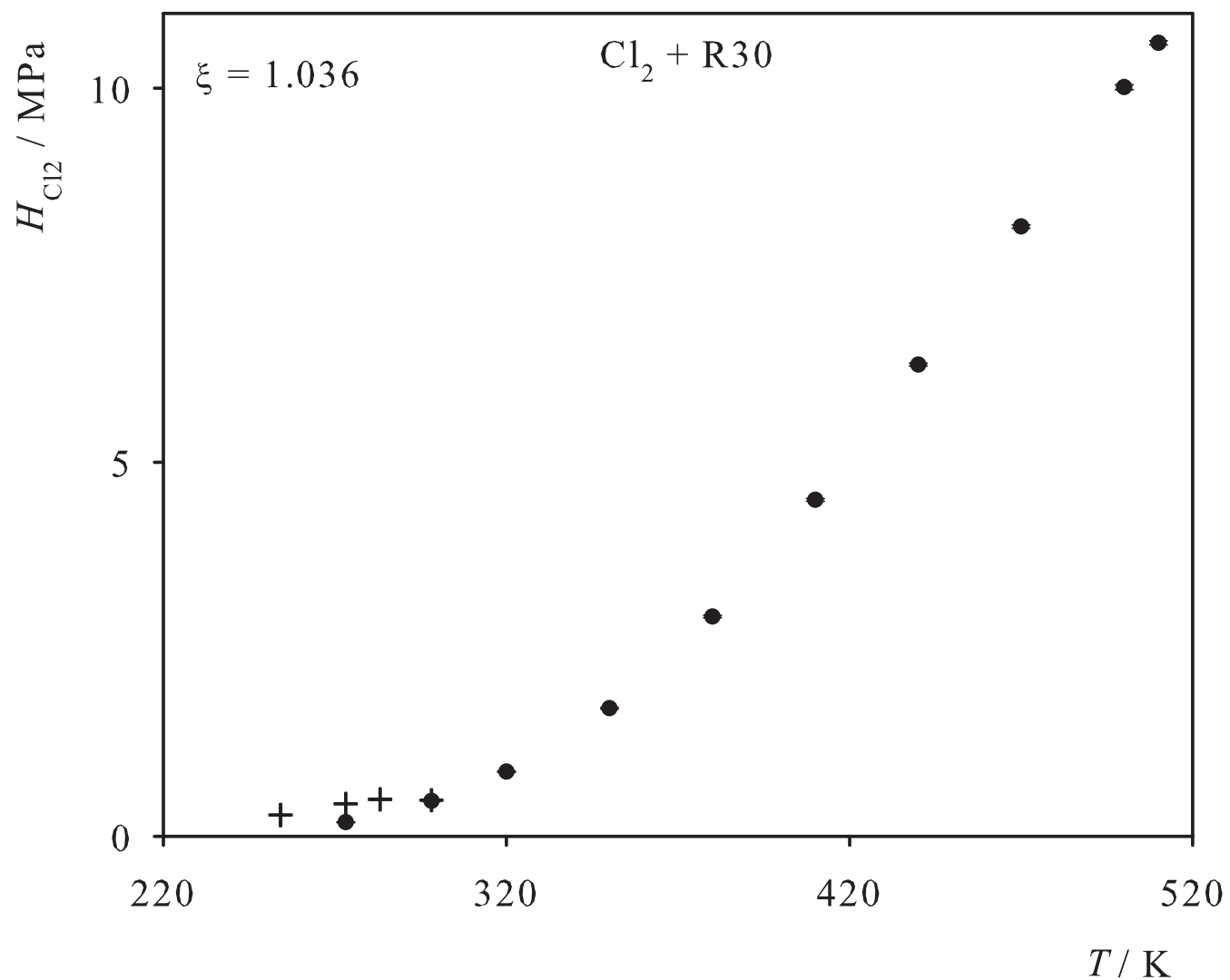


Fig. 55. Henry's law constant of CO<sub>2</sub> in liquid R30. Simulation data: ● ( $\xi=0.868$ ), ○ ( $\xi=0.923$ ); experimental data: + [58].

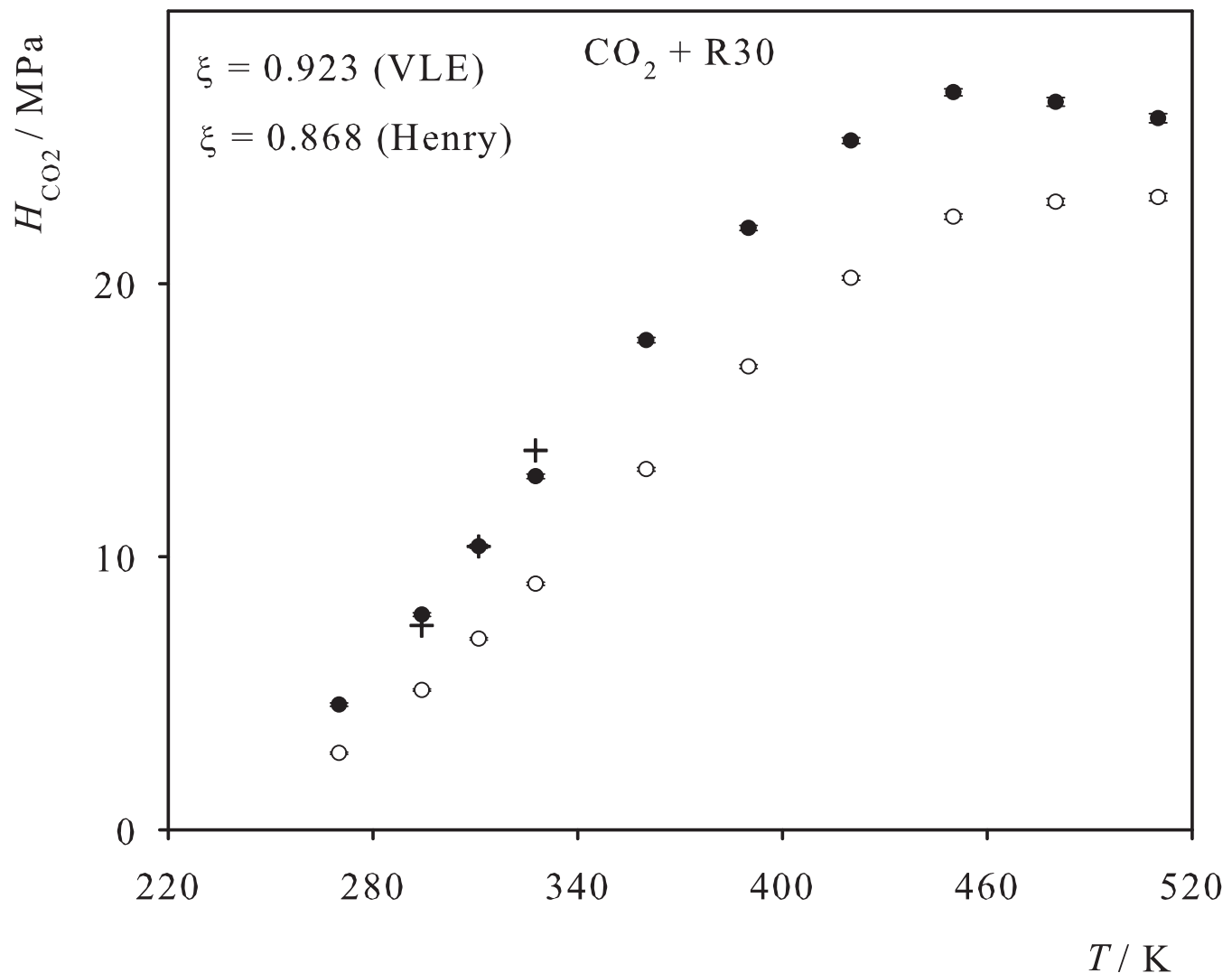


Fig. 56. Henry's law constant of CH<sub>4</sub> in liquid R40. Simulation data: ●; experimental data: + [59].

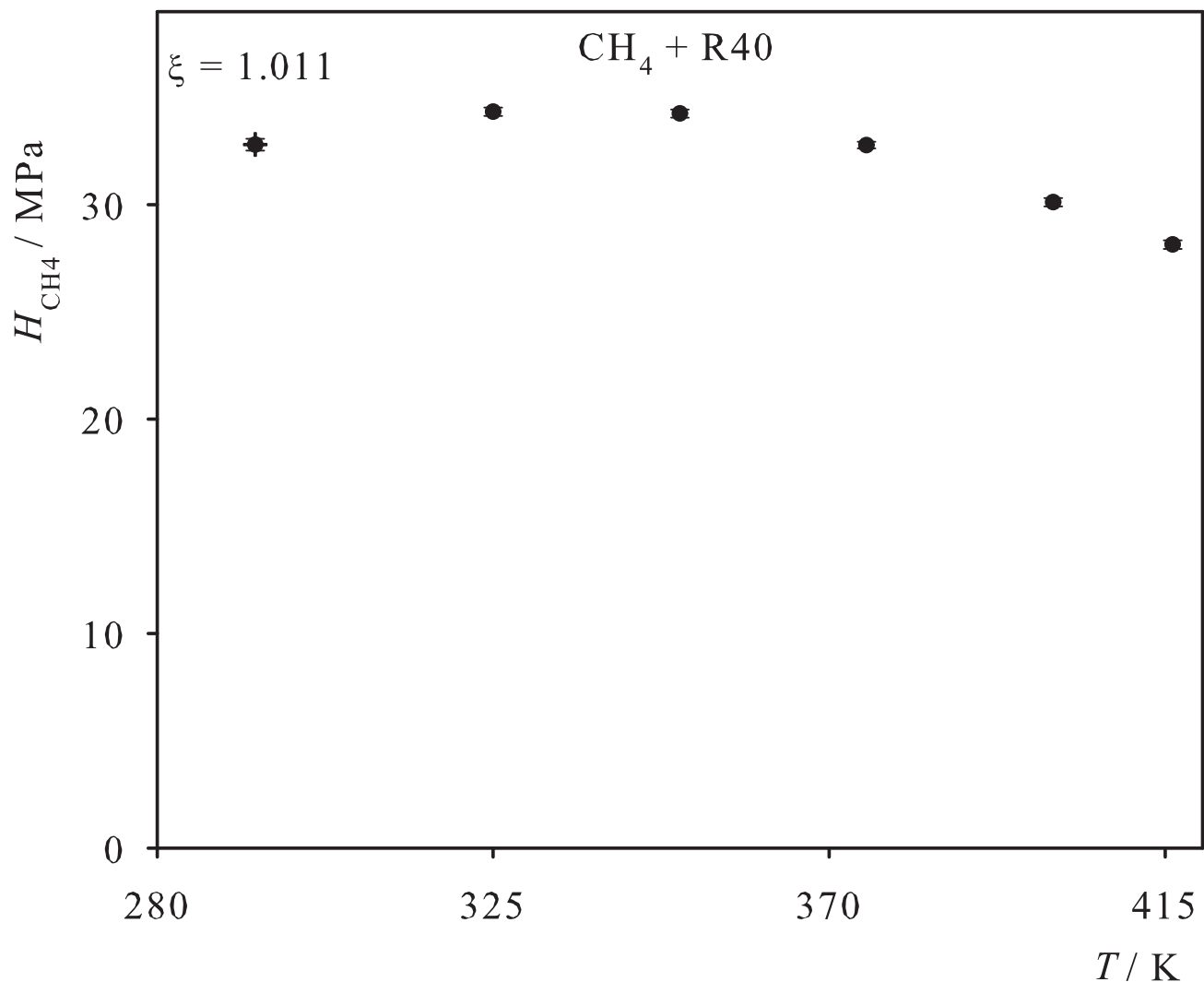


Fig. 57. Henry's law constant of Ne in liquid R113. Simulation data: ●; experimental data: + [60].

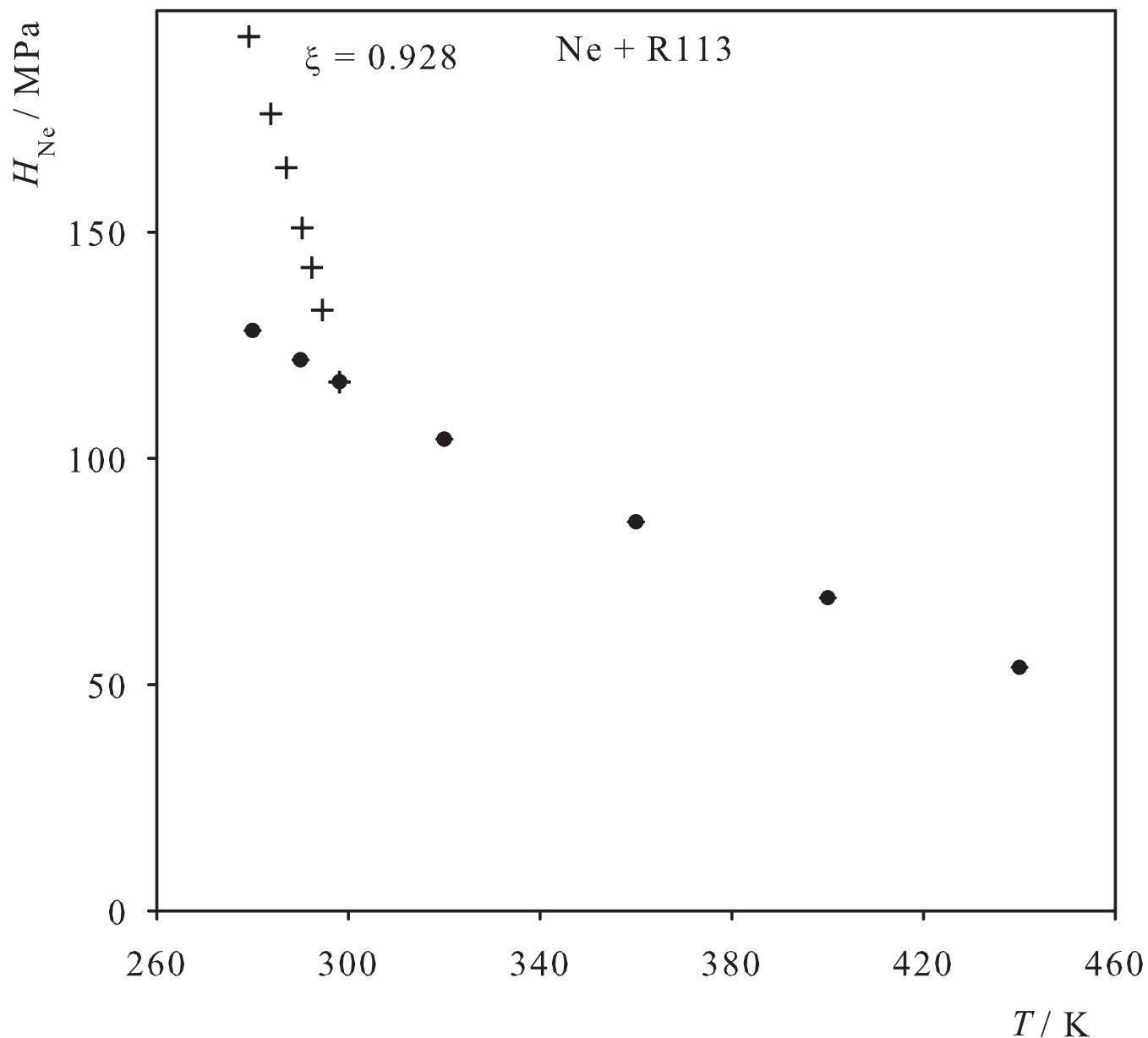


Fig. 58. Henry's law constant of Ar in liquid R113. Simulation data: ● ( $\xi=1.027$ ), ○ ( $\xi=1.012$ ); experimental data: + [61].

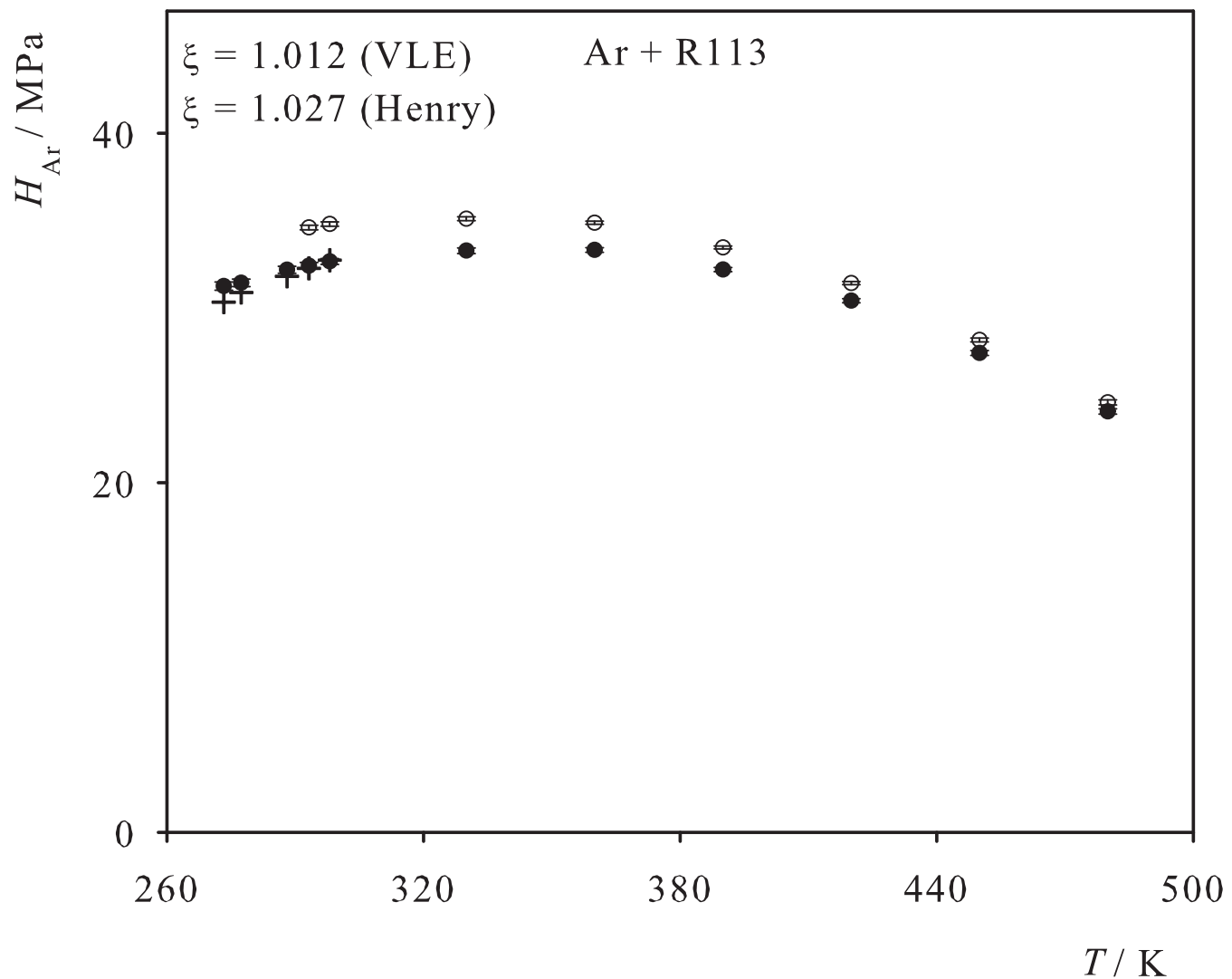


Fig. 59. Henry's law constant of Xe in liquid R113. Simulation data: ●; experimental data: + [60].

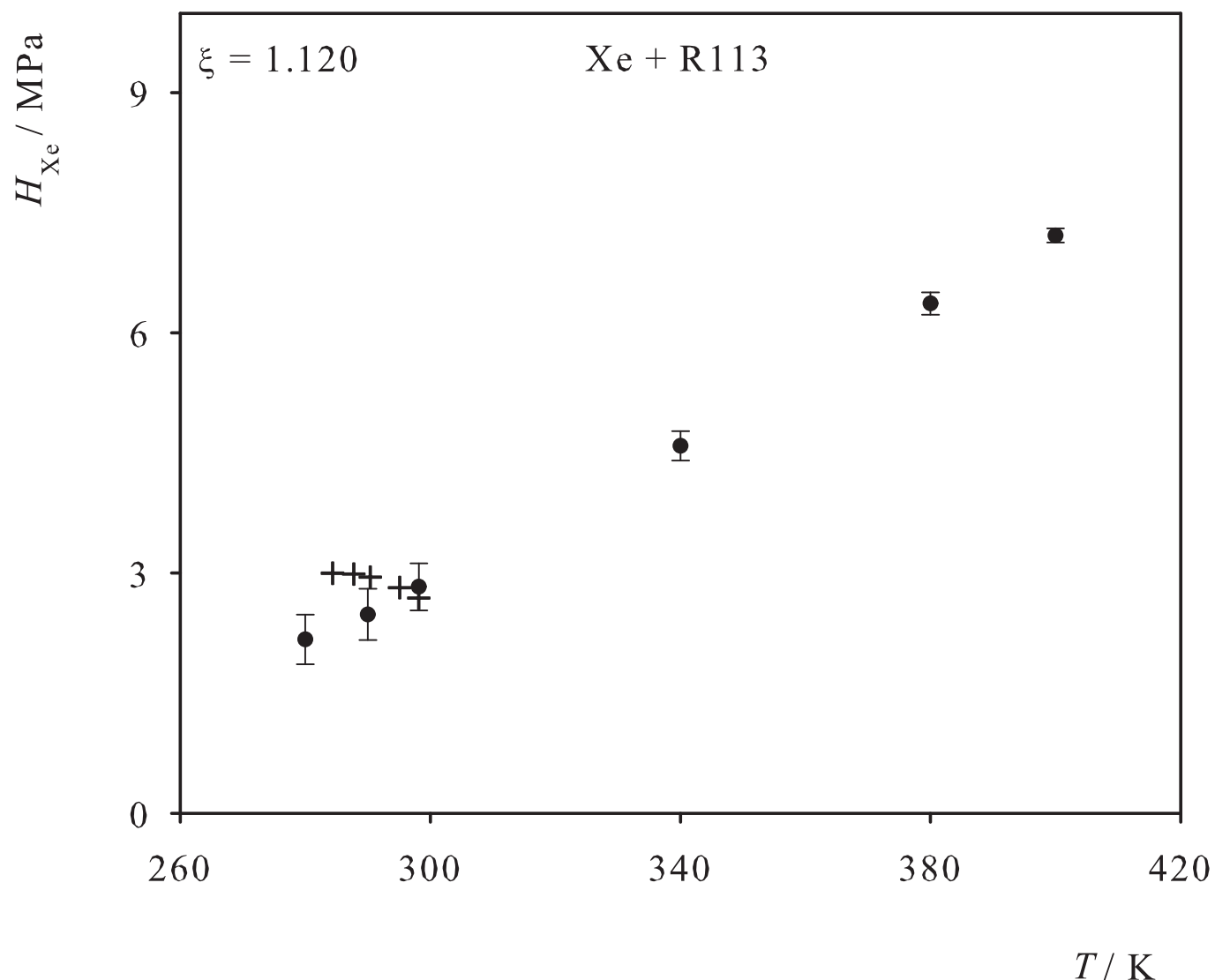


Fig. 60. Henry's law constant of CH<sub>4</sub> in liquid R113. Simulation data: ● ( $\xi=1.044$ ), ○ ( $\xi=0.997$ ); experimental data: + [61].

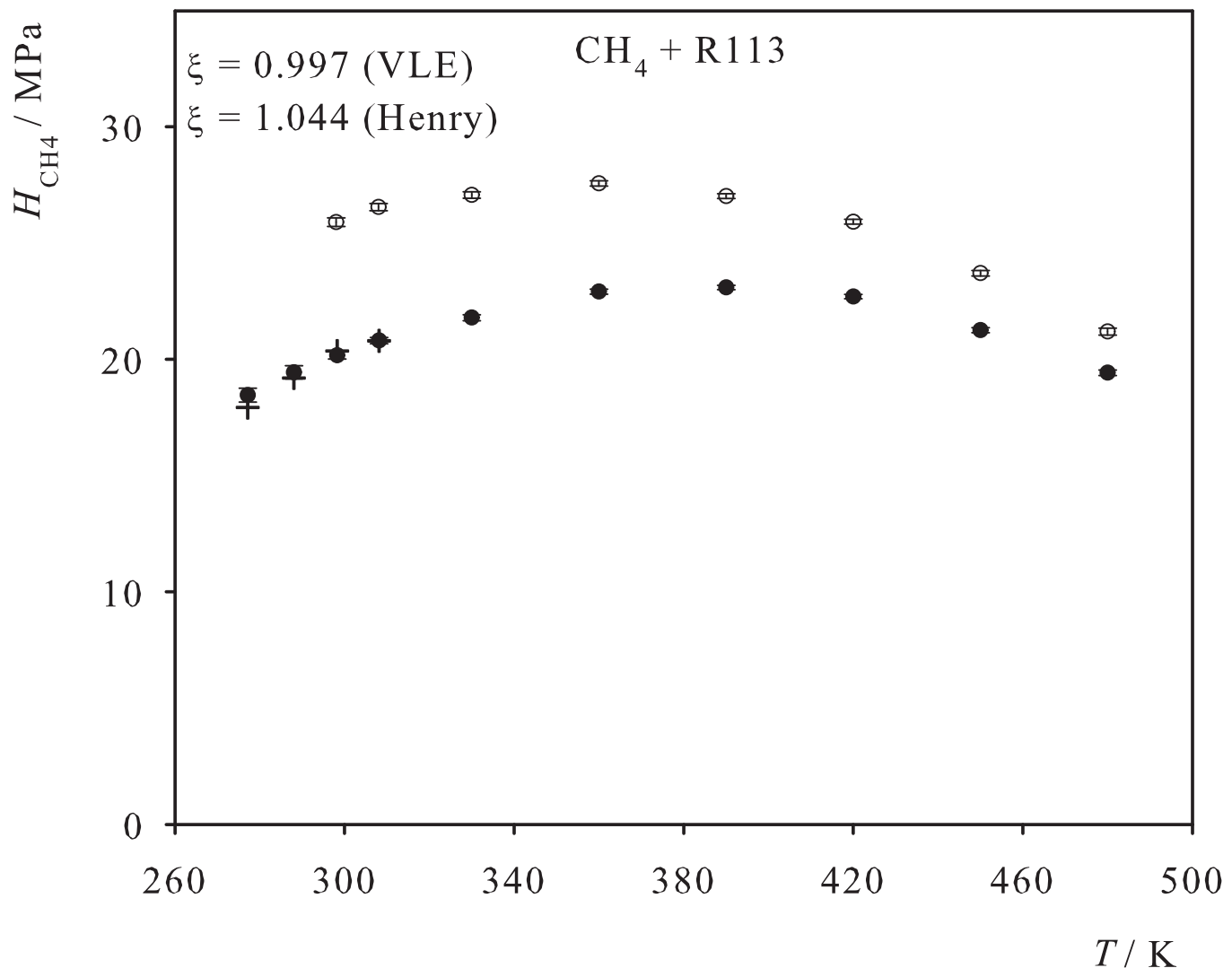


Fig. 61. Henry's law constant of N<sub>2</sub> in liquid R113. Simulation data: ●; experimental data: + [61].

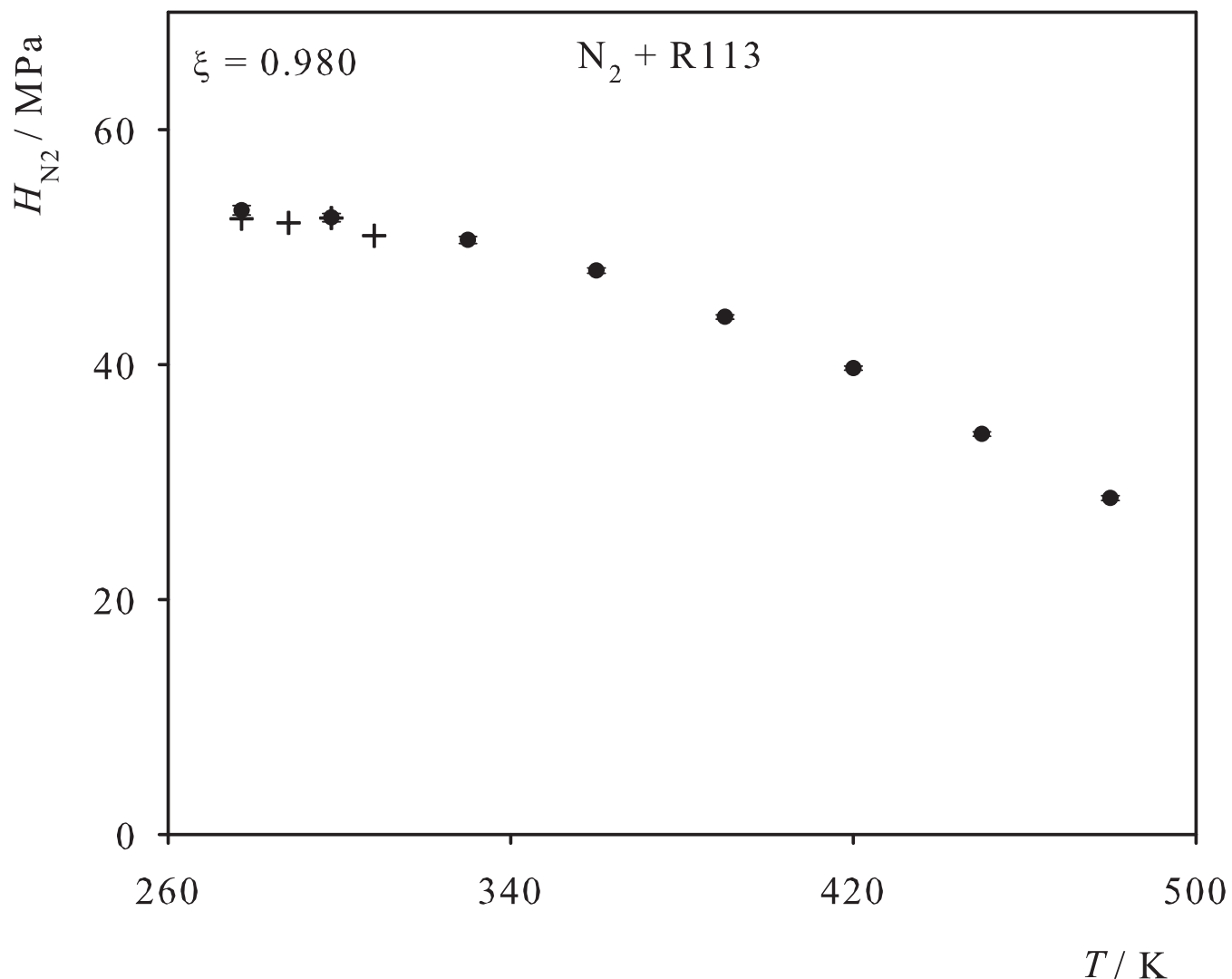


Fig. 62. Henry's law constant of CO<sub>2</sub> in liquid R113. Simulation data: ●; experimental data: + [61].

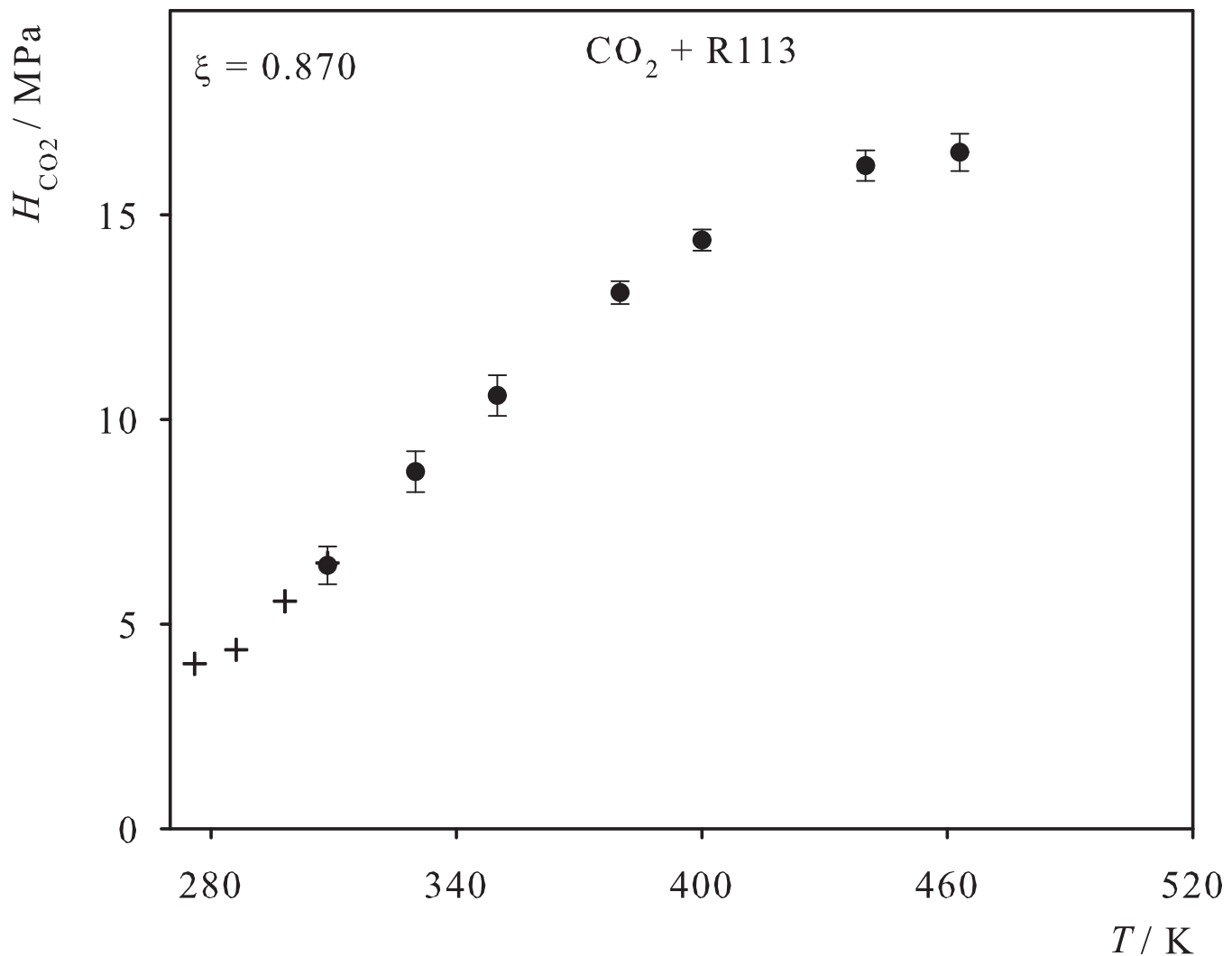


Fig. 63. Henry's law constant of C<sub>2</sub>H<sub>4</sub> in liquid R113. Simulation data: ●; experimental data: + [62].

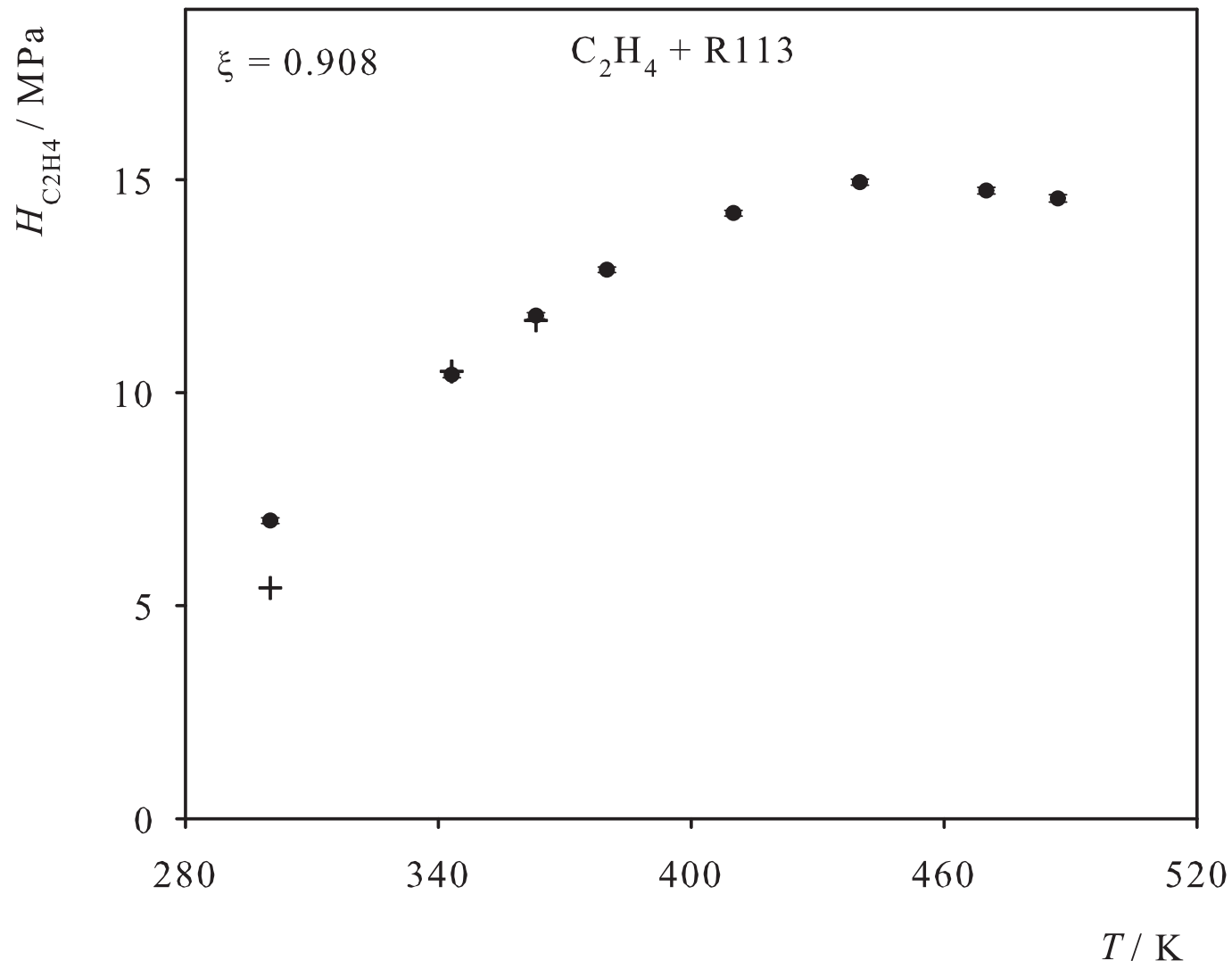


Fig. 64. Henry's law constant of C<sub>2</sub>H<sub>6</sub> in liquid R113. Simulation data: ●; experimental data: + [63], ■ [60], ▲ [64].

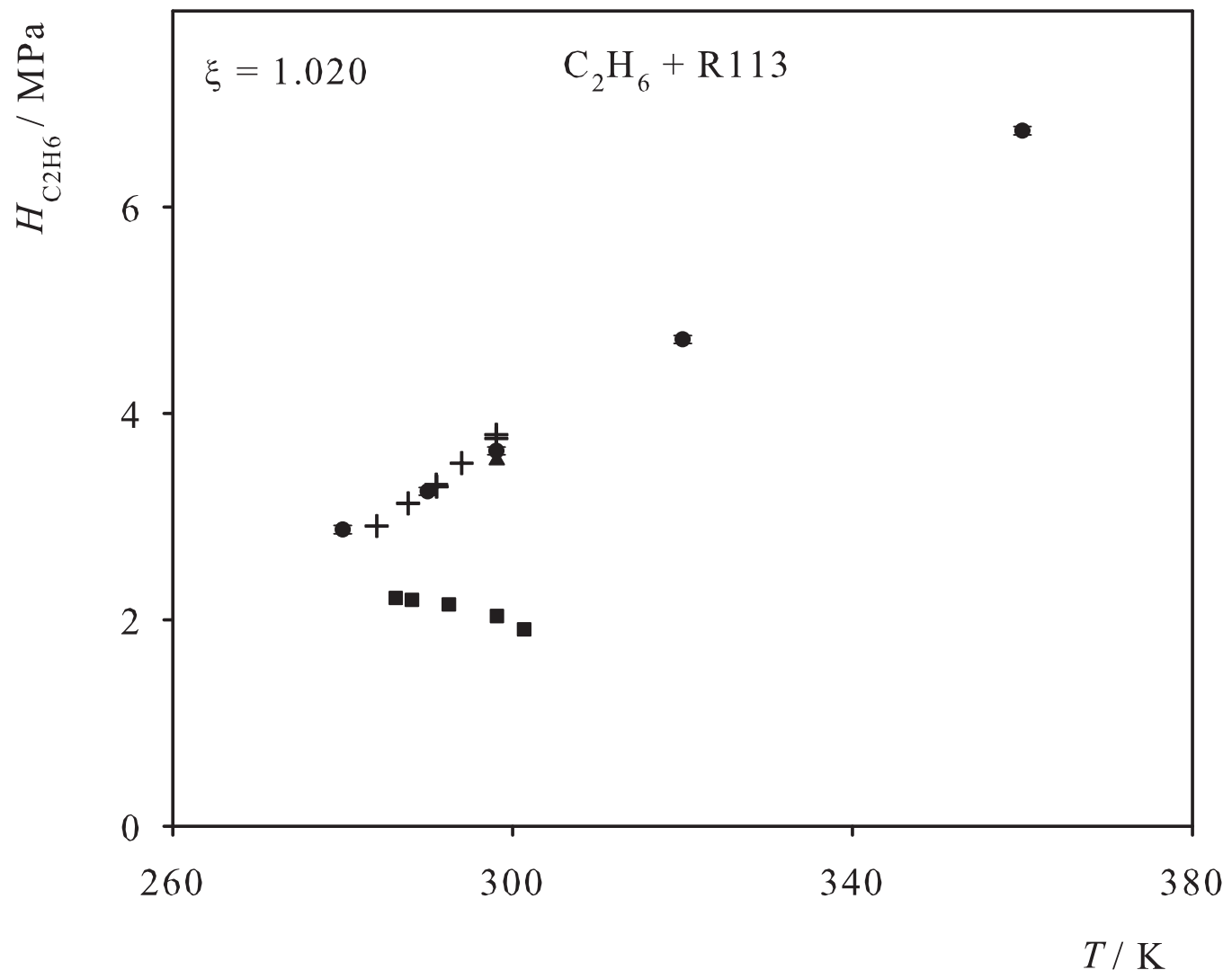


Fig. 65. Henry's law constant of SF<sub>6</sub> in liquid R113. Simulation data: ●; experimental data: + [65], ■ [16], ▲ [61].

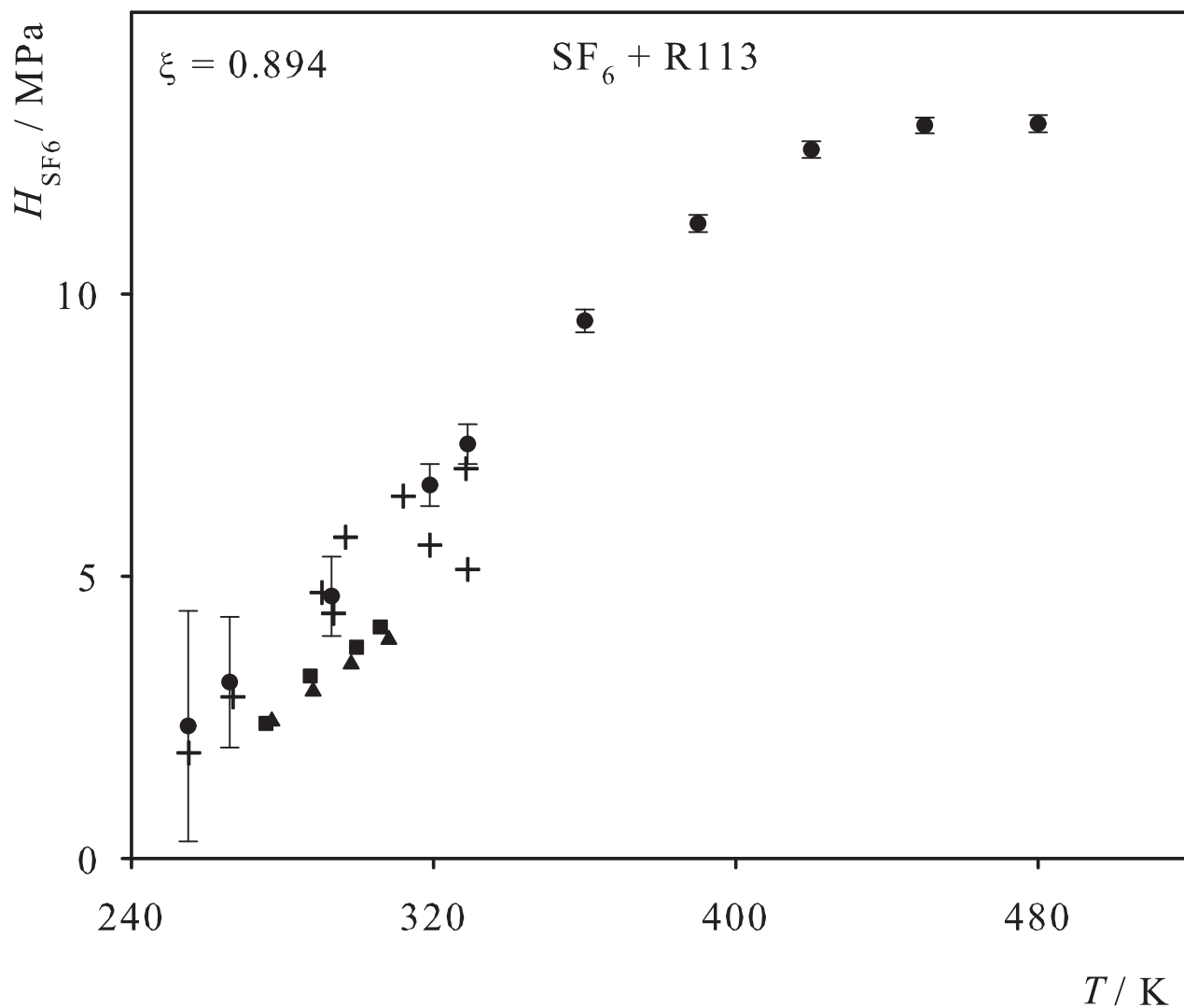


Fig. 66. Henry's law constant of R14 in liquid R113. Simulation data: ●; experimental data: + [16].

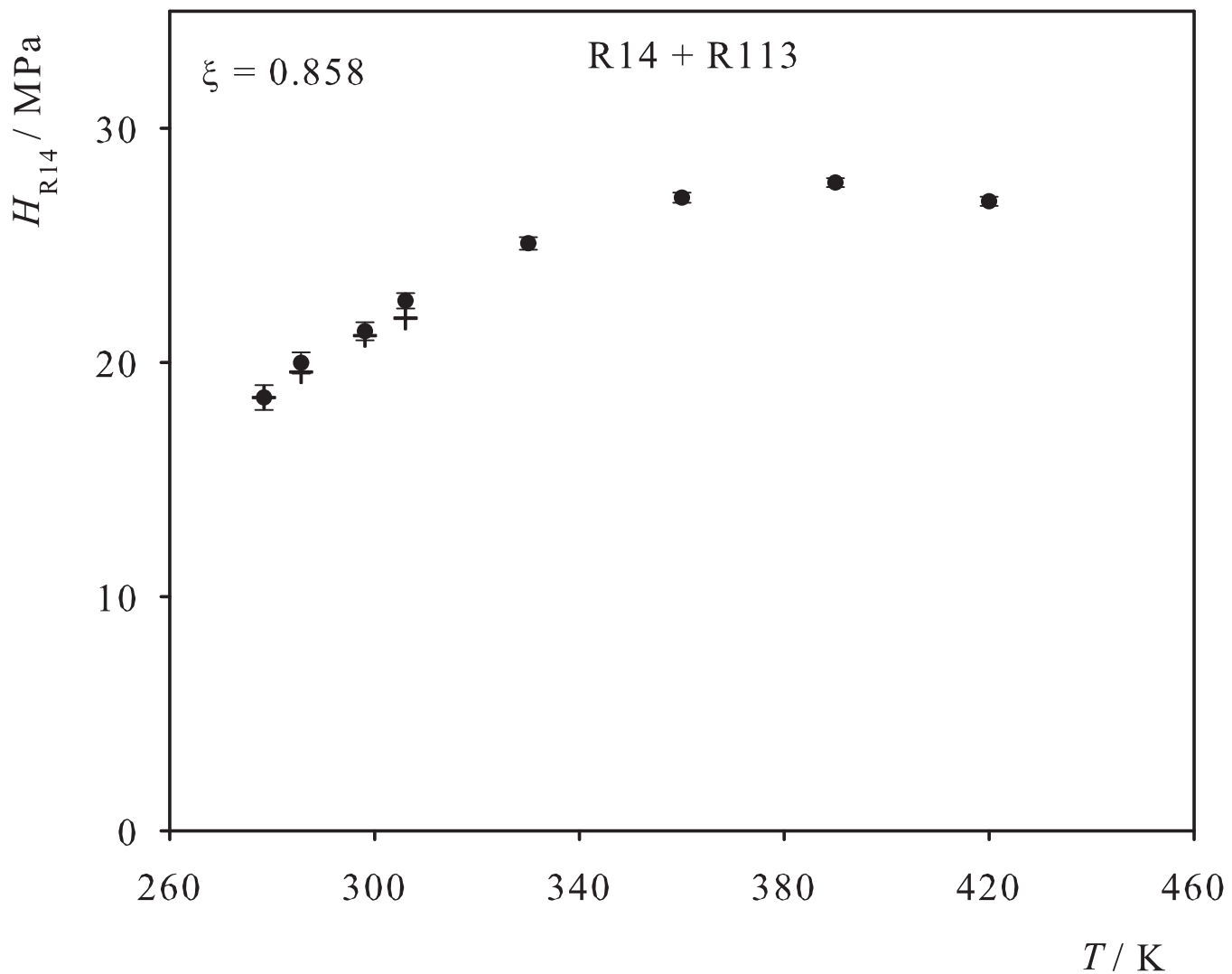


Fig. 67. Henry's law constant of R116 in liquid R113. Simulation data: ●; experimental data: + [60], ■ [64].

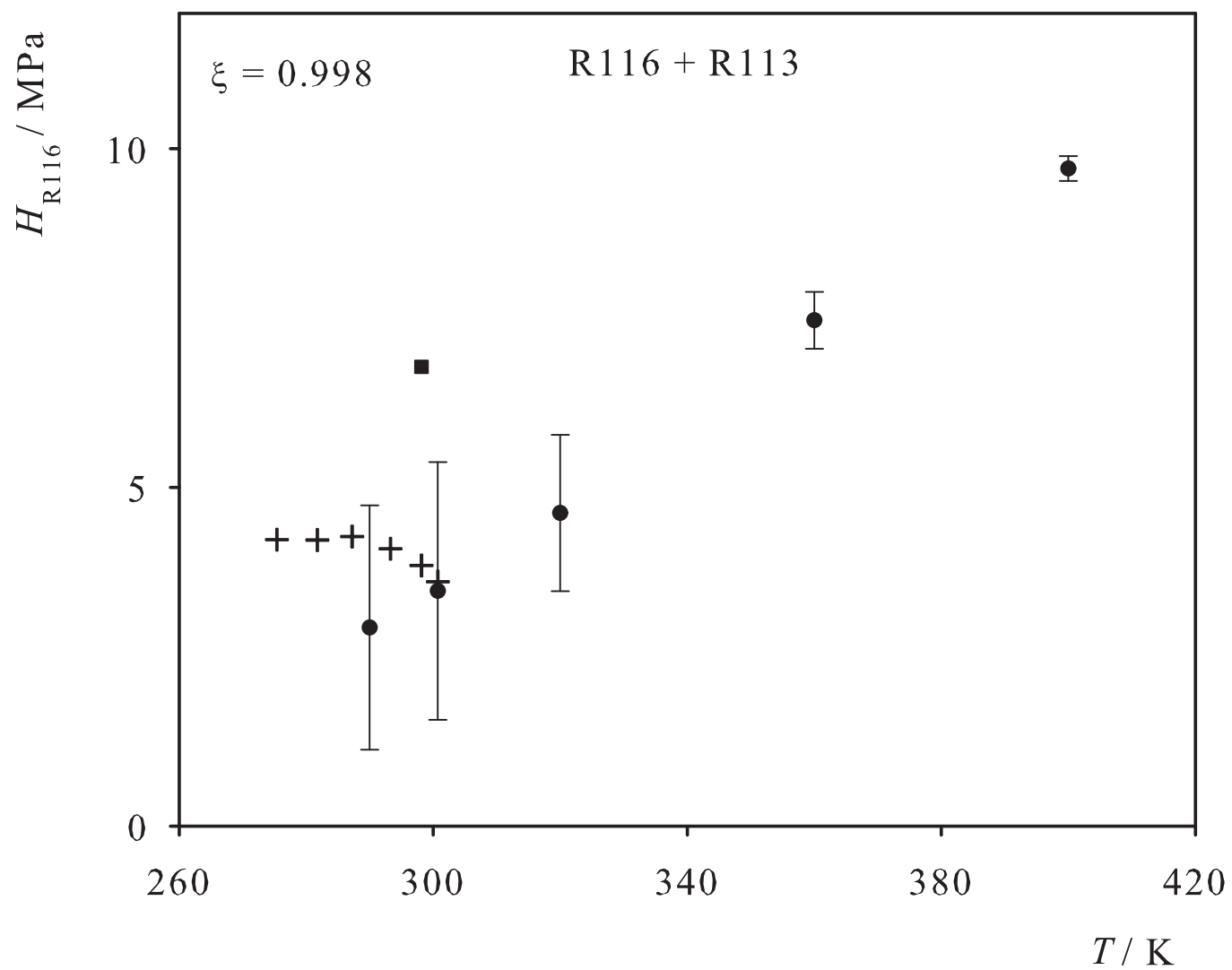


Fig. 68. Henry's law constant of R1114 in liquid R113. Simulation data: ●; experimental data: + [66].

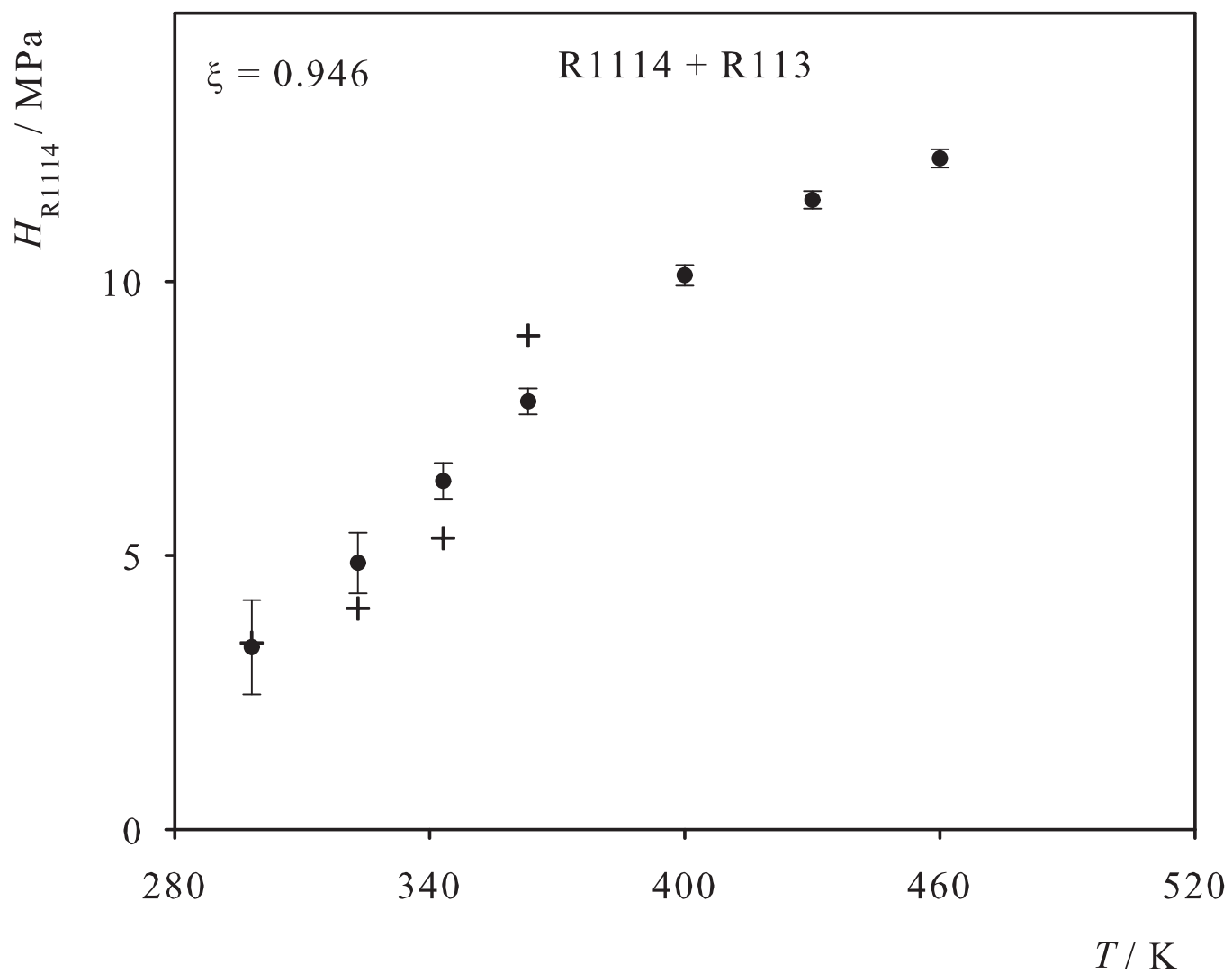


Fig. 69. Henry's law constant of R1132 in liquid R113. Simulation data: ●; experimental data: + [66].

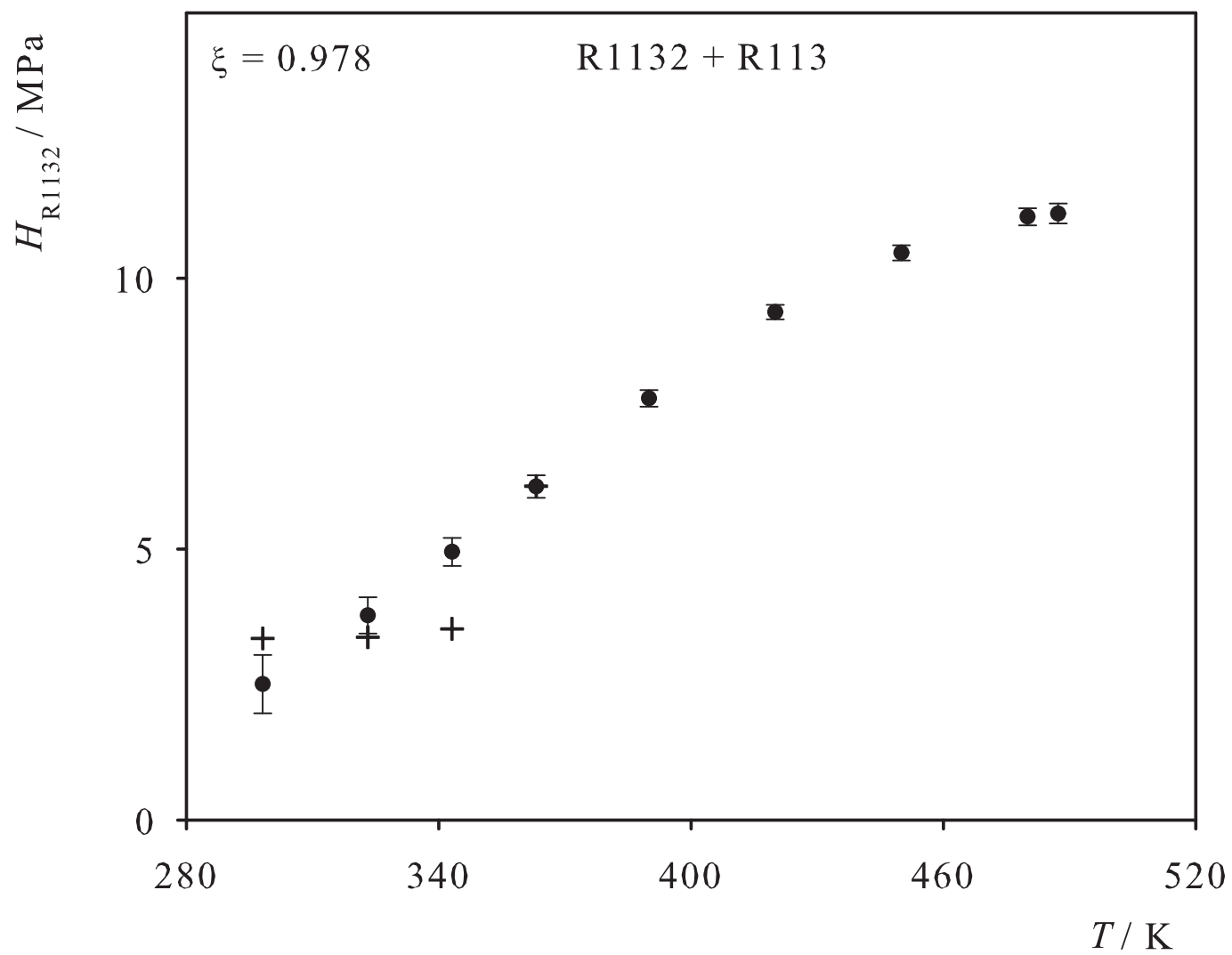


Fig. 70. Henry's law constant of N<sub>2</sub> in liquid R114. Simulation data: ●; experimental data: + [67].

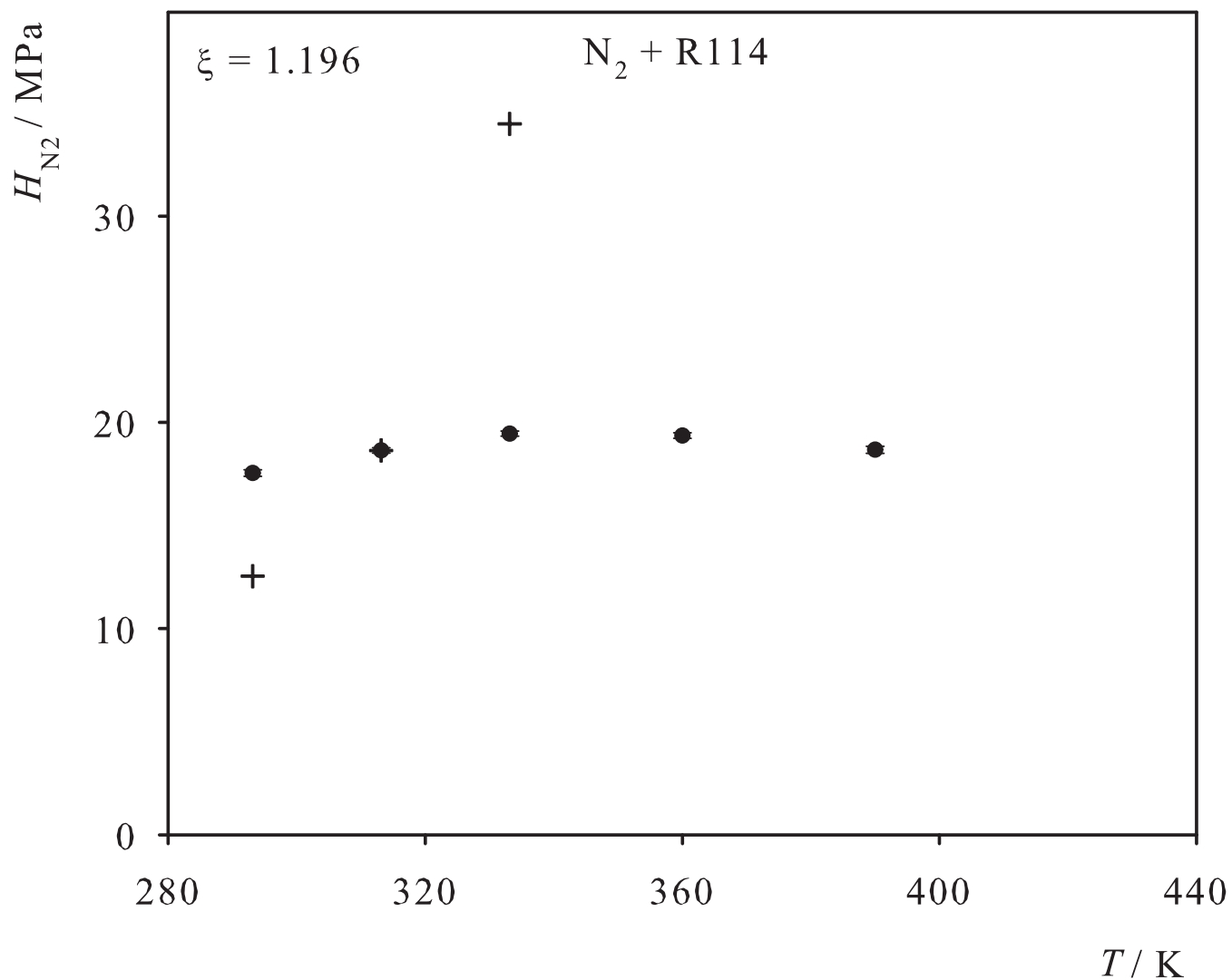


Fig. 71. Henry's law constant of SF<sub>6</sub> in liquid R114. Simulation data: ●; experimental data: + [65].

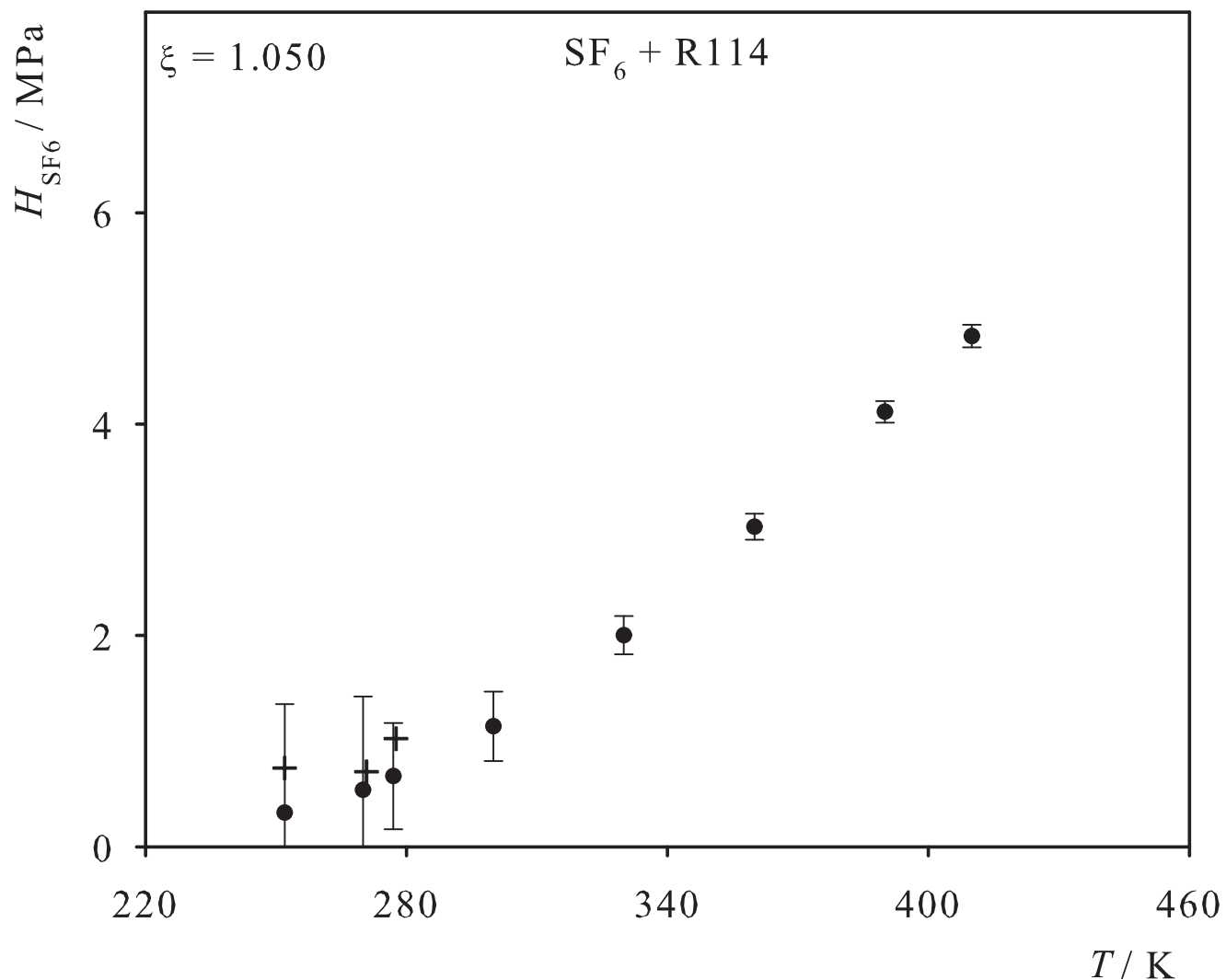


Fig. 72. Henry's law constant of R23 in liquid R114. Simulation data: ● ( $\xi=0.732$ ), ○ ( $\xi=0.836$ ); experimental data: + [45].

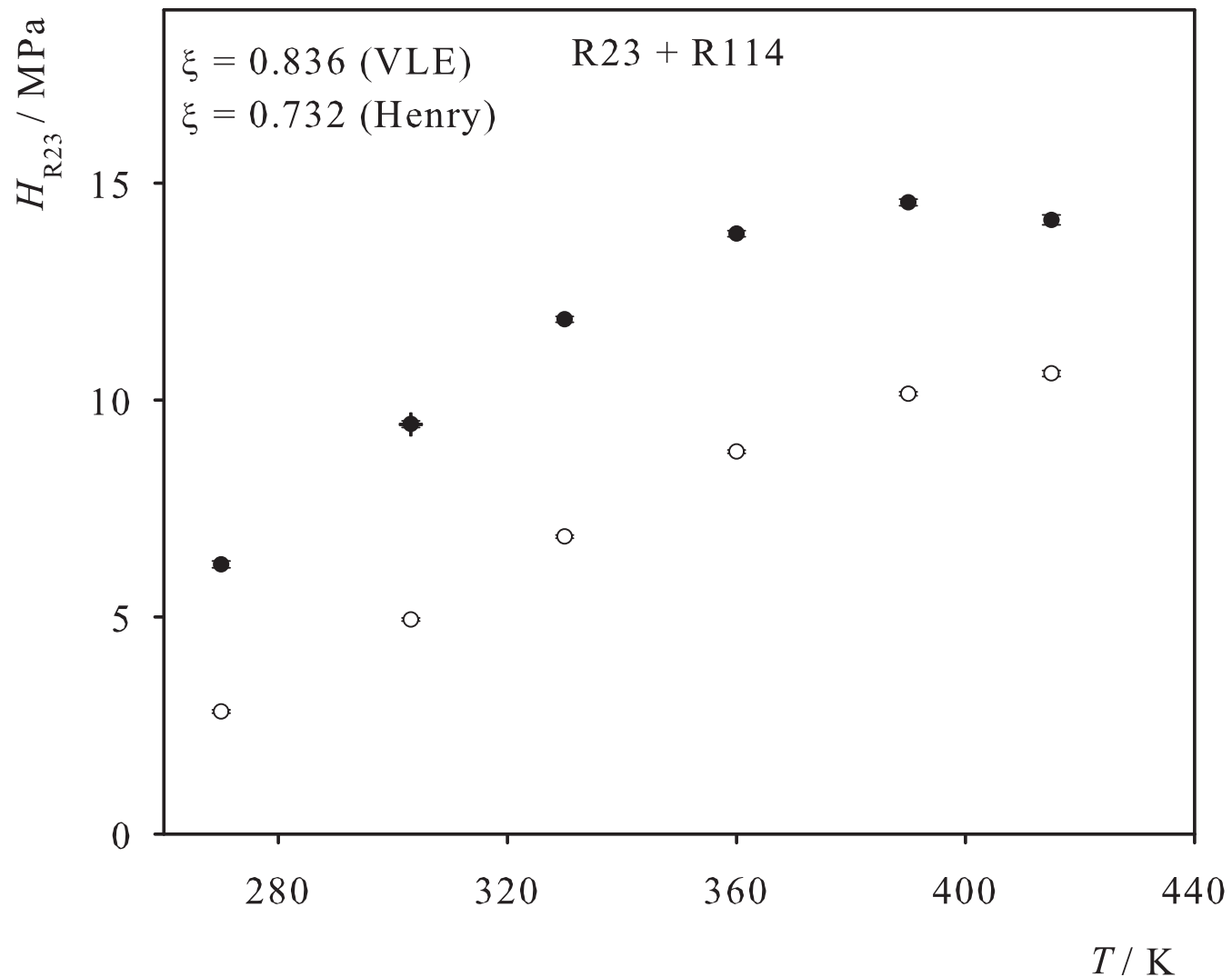


Fig. 73. Henry's law constant of  $\text{Cl}_2$  in liquid R130a. Simulation data: ●; experimental data: + [68].

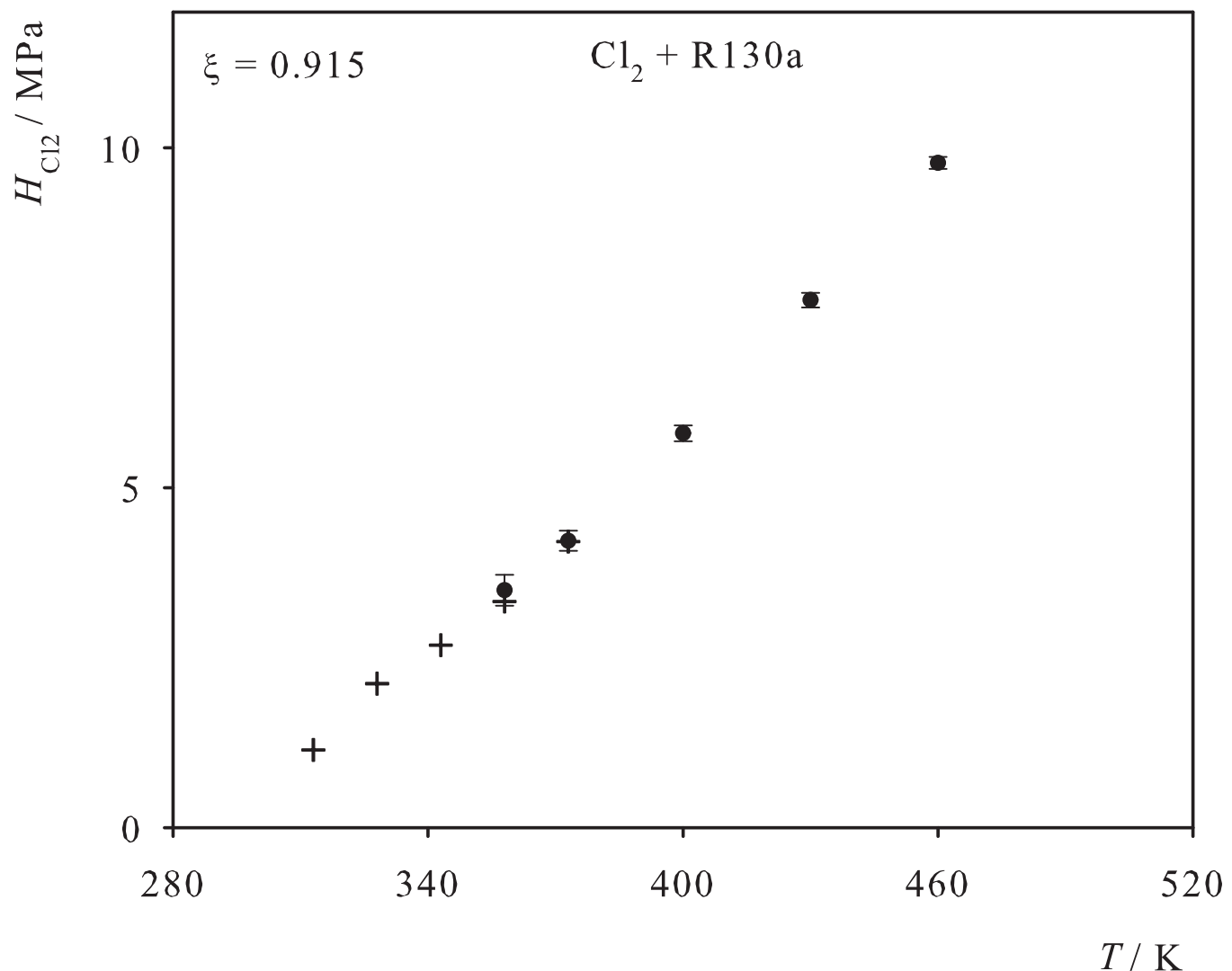


Fig. 74. Henry's law constant of  $\text{Cl}_2$  in liquid R140. Simulation data: ●; experimental data: + [68].

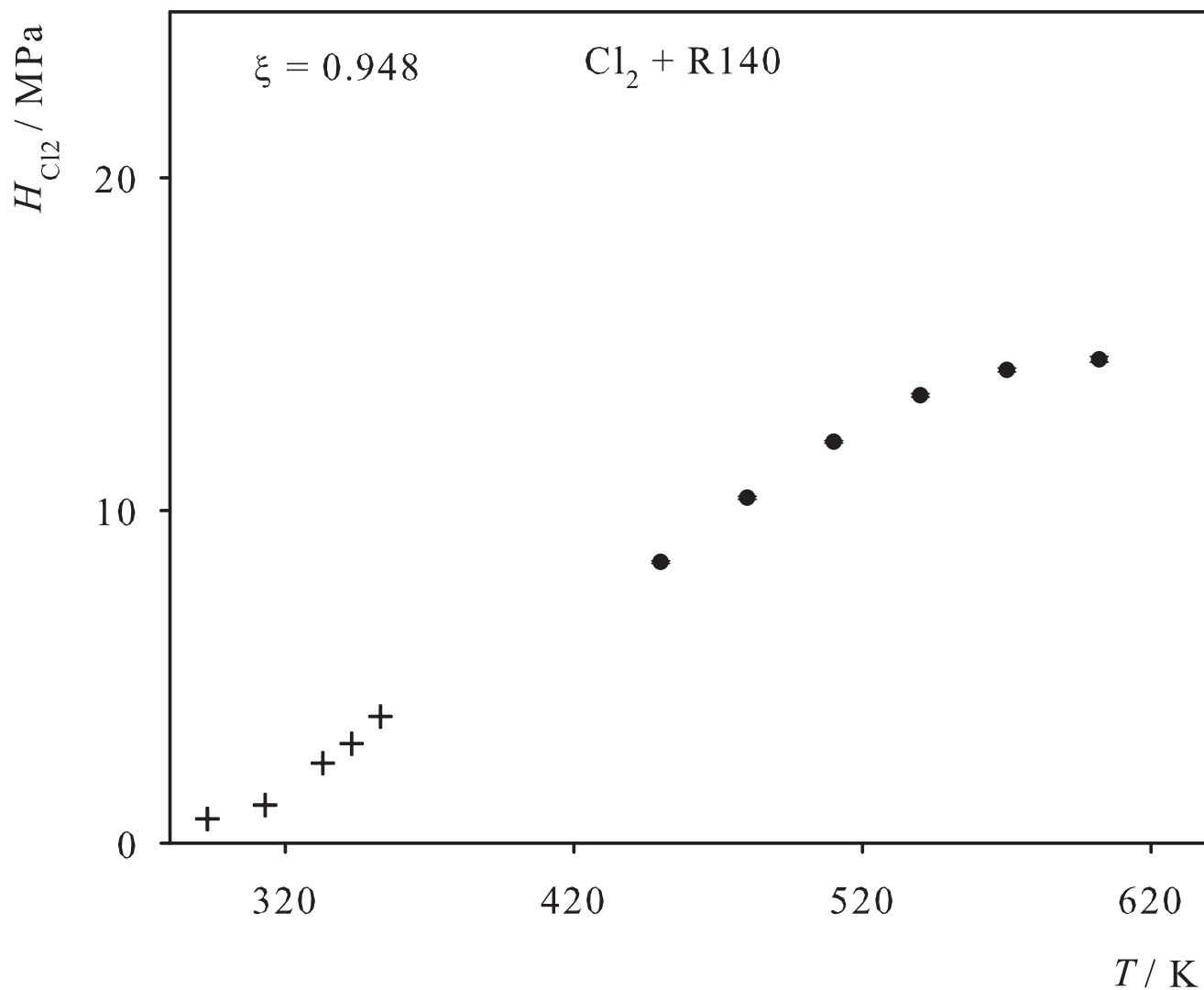


Fig. 75. Henry's law constant of C<sub>2</sub>H<sub>2</sub> in liquid R140. Simulation data: ●; experimental data: + [69].

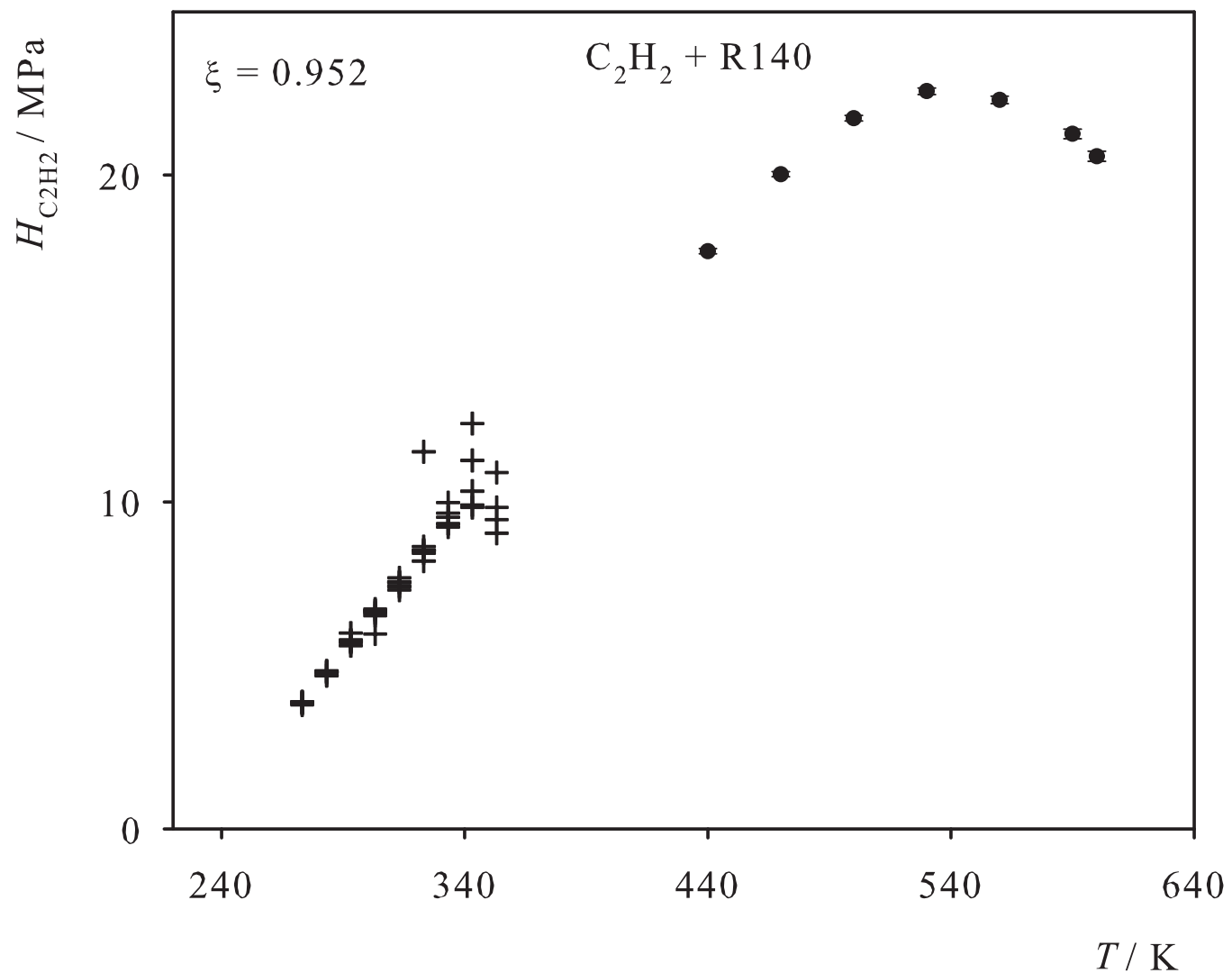


Fig. 76. Henry's law constant of R1140 in liquid R140. Simulation data: ●; experimental data: + [70].

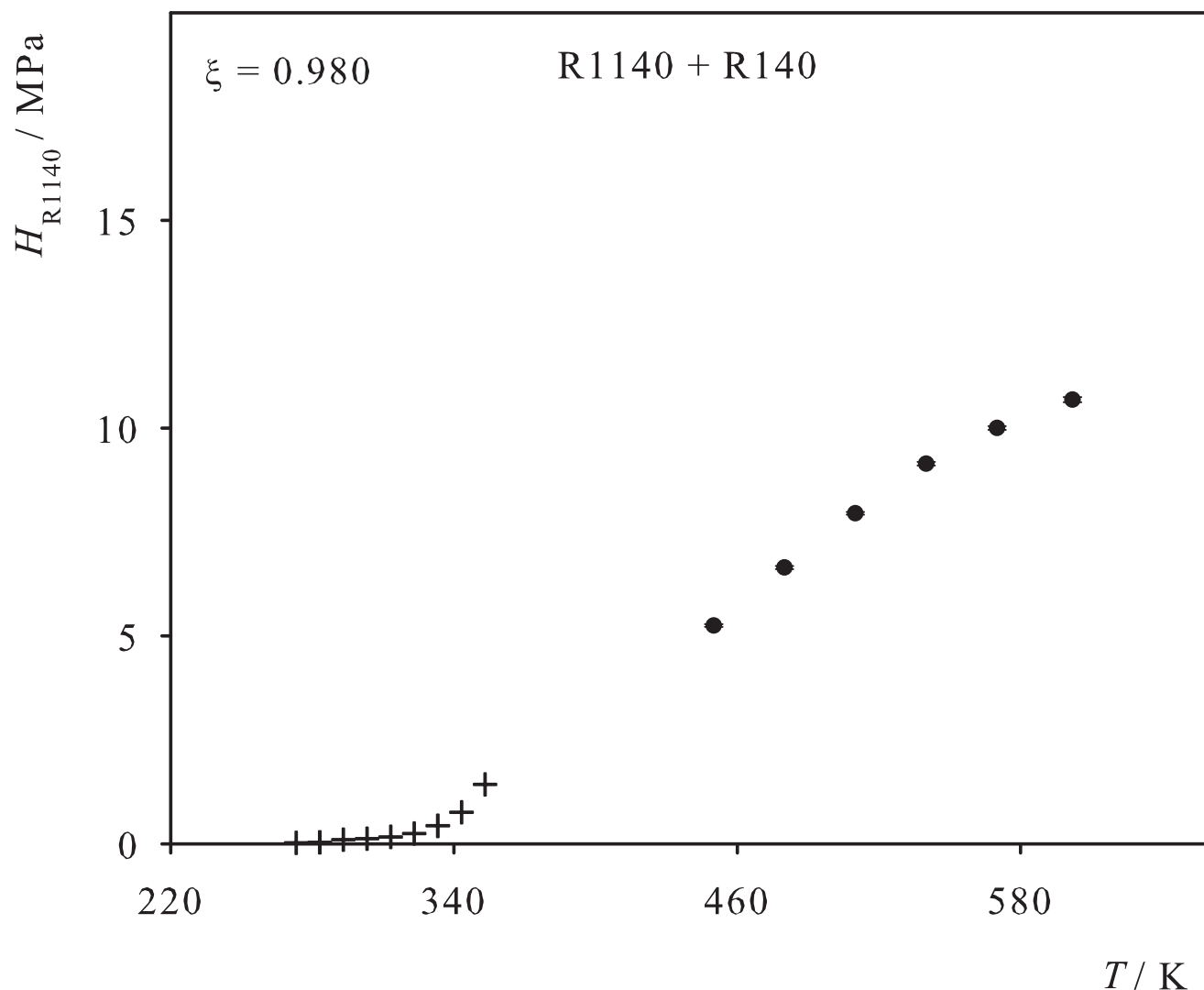


Fig. 77. Henry's law constant of  $\text{Cl}_2$  in liquid R140a. Simulation data: ●; experimental data: + [68].

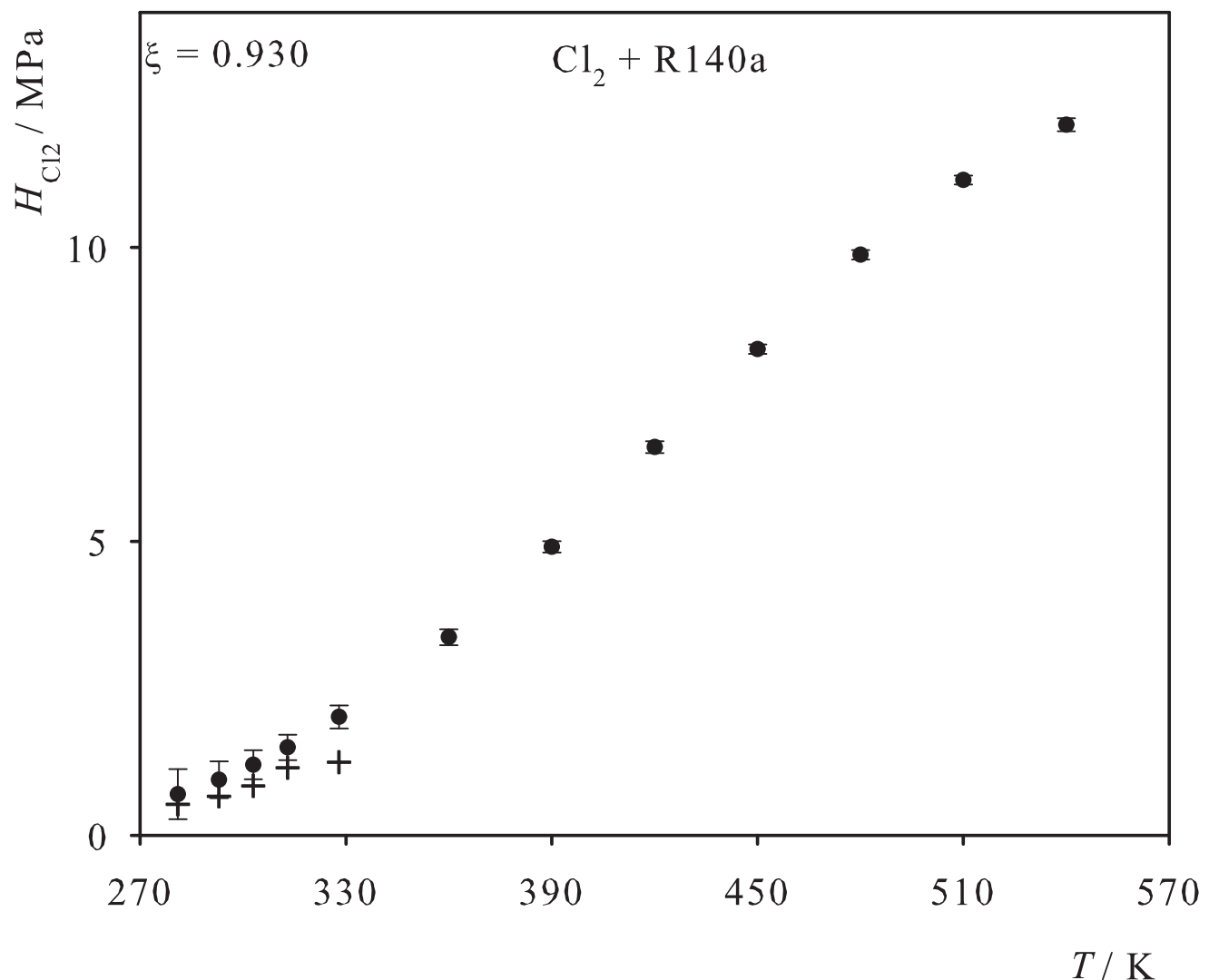


Fig. 78. Henry's law constant of CO<sub>2</sub> in liquid R140a. Simulation data: ●; experimental data: + [37].

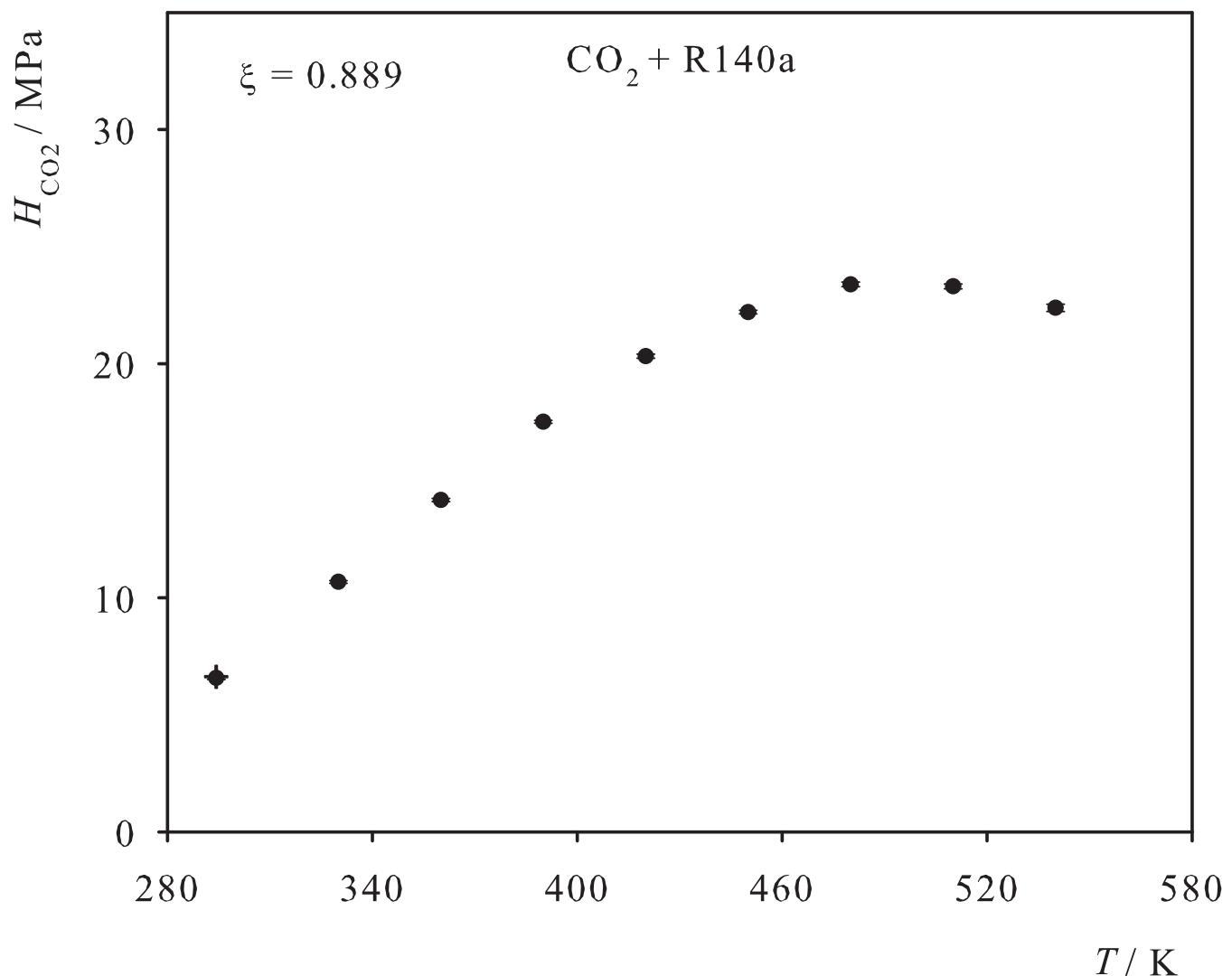


Fig. 79. Henry's law constant of C<sub>2</sub>H<sub>2</sub> in liquid R140a. Simulation data: ●; experimental data: + [69].

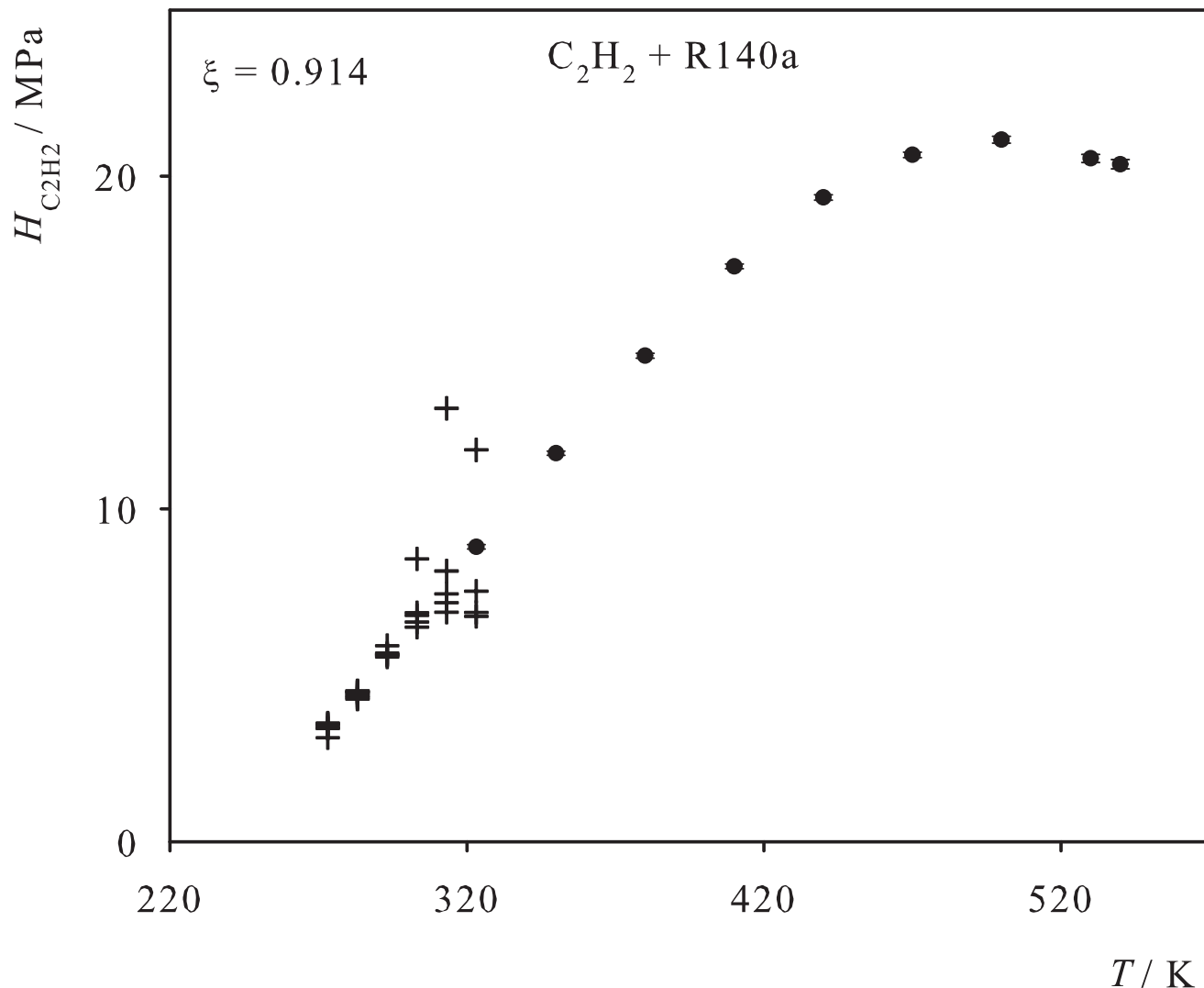


Fig. 80. Henry's law constant of R1140 in R140a. Simulation data: ●; experimental data: + [69].

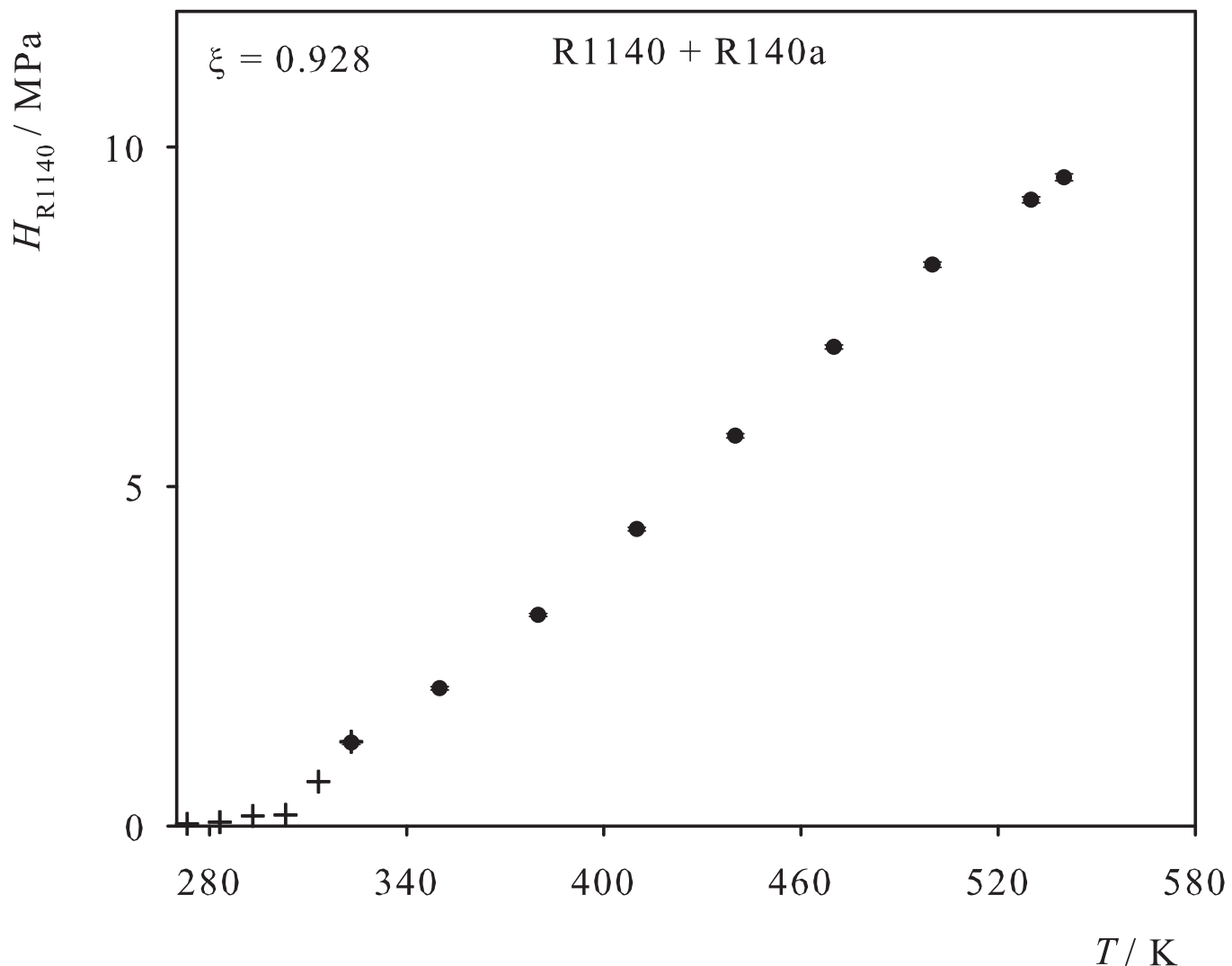


Fig. 81. Henry's law constant of  $\text{Cl}_2$  in liquid R150a. Simulation data: ●; experimental data: + [68].

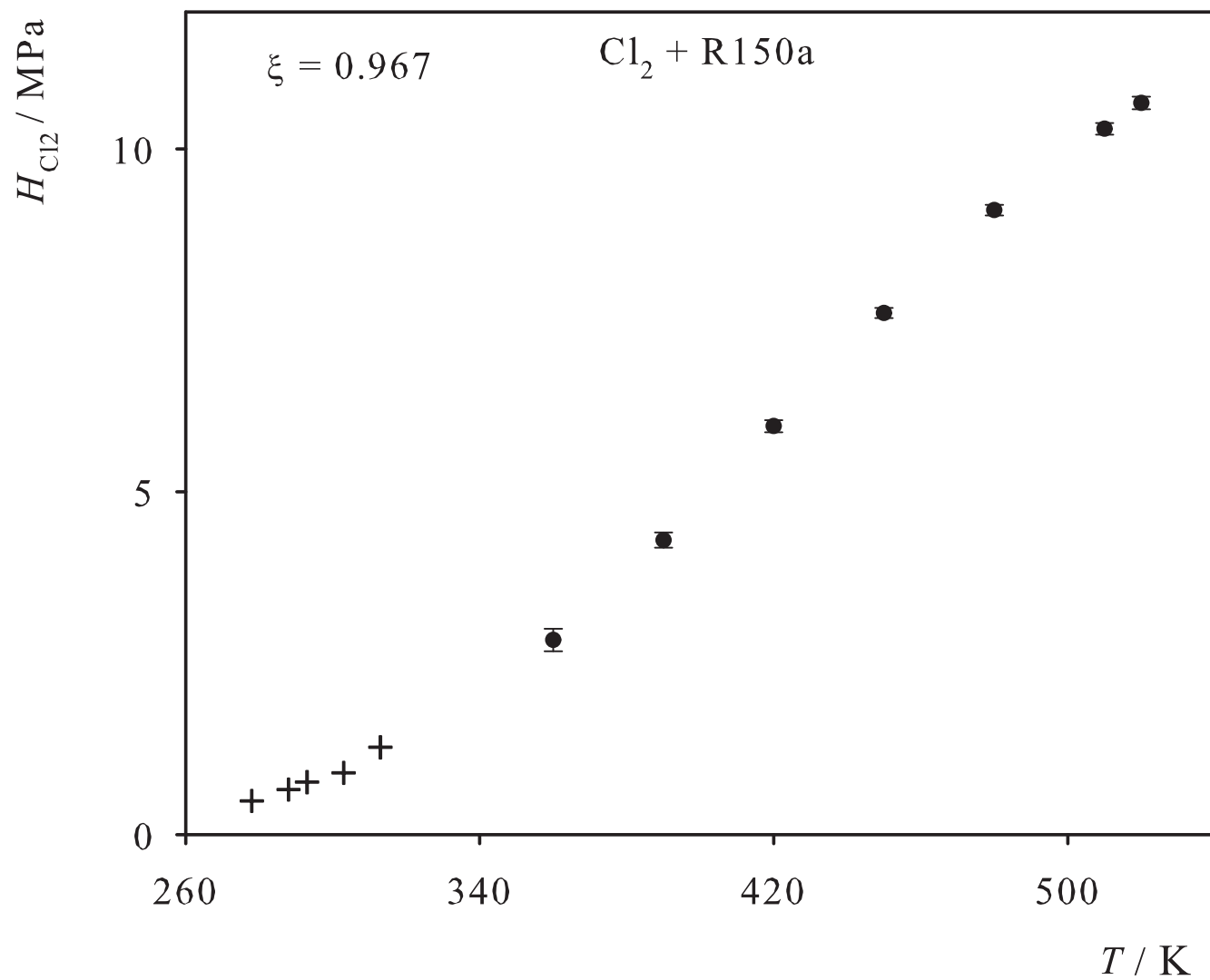


Fig. 82. Henry's law constant of C<sub>2</sub>H<sub>2</sub> in liquid R150a. Simulation data: ●; experimental data: + [71].

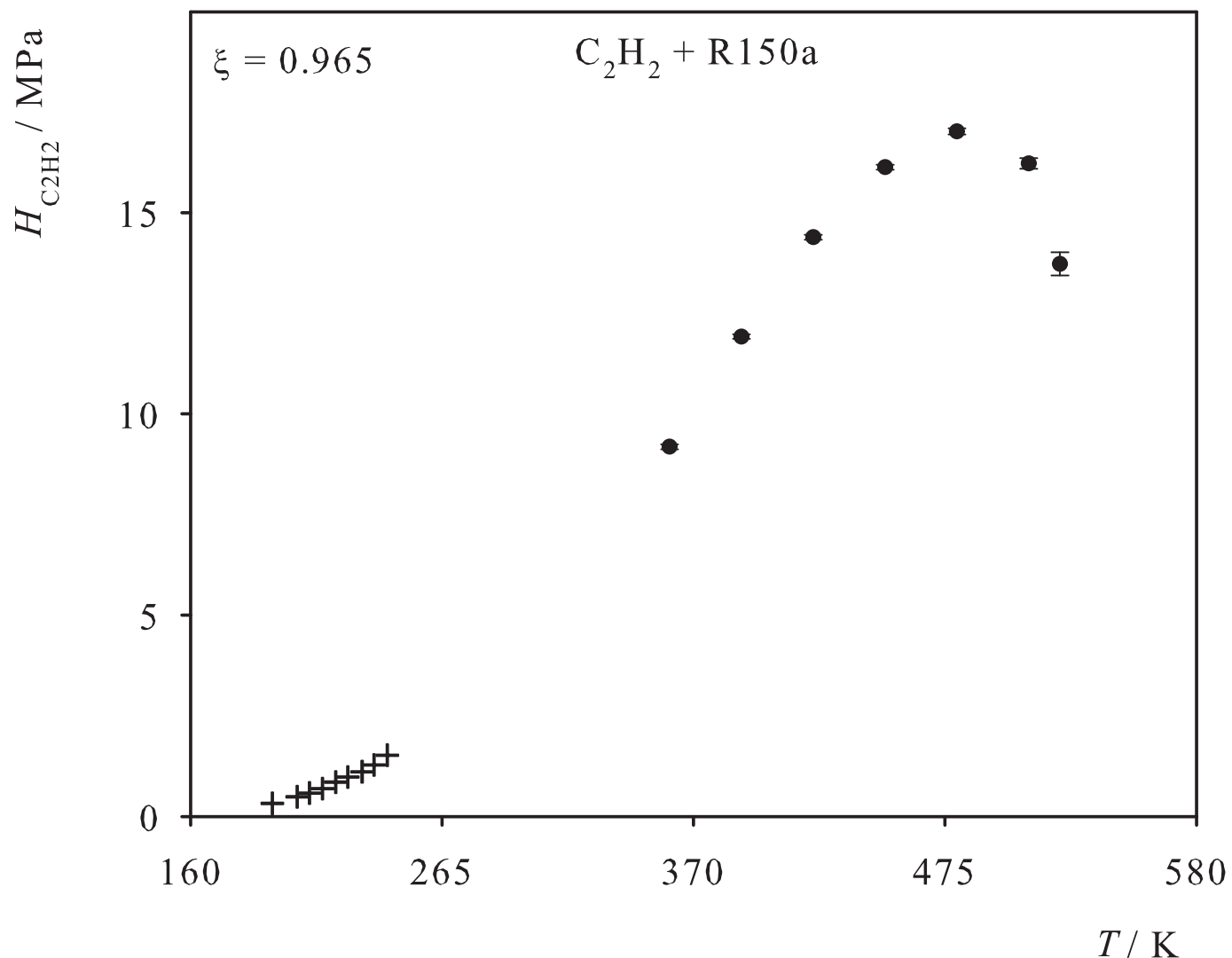


Fig. 83. Henry's law constant of  $\text{Cl}_2$  in liquid R150B2. Simulation data: ●; experimental data: + [34].

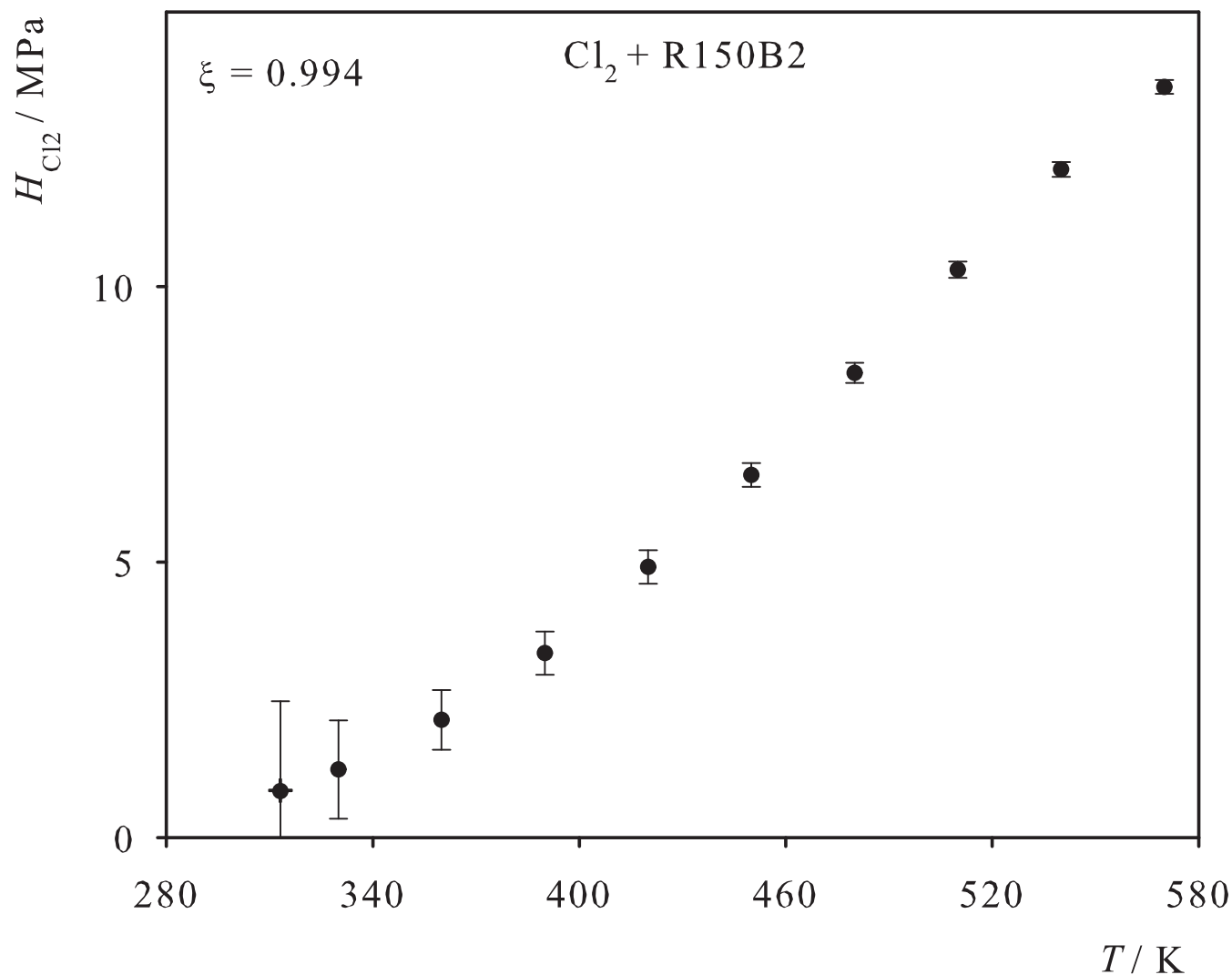


Fig. 84. Henry's law constant of CO in liquid R150B2. Simulation data: ●; experimental data: + [72].

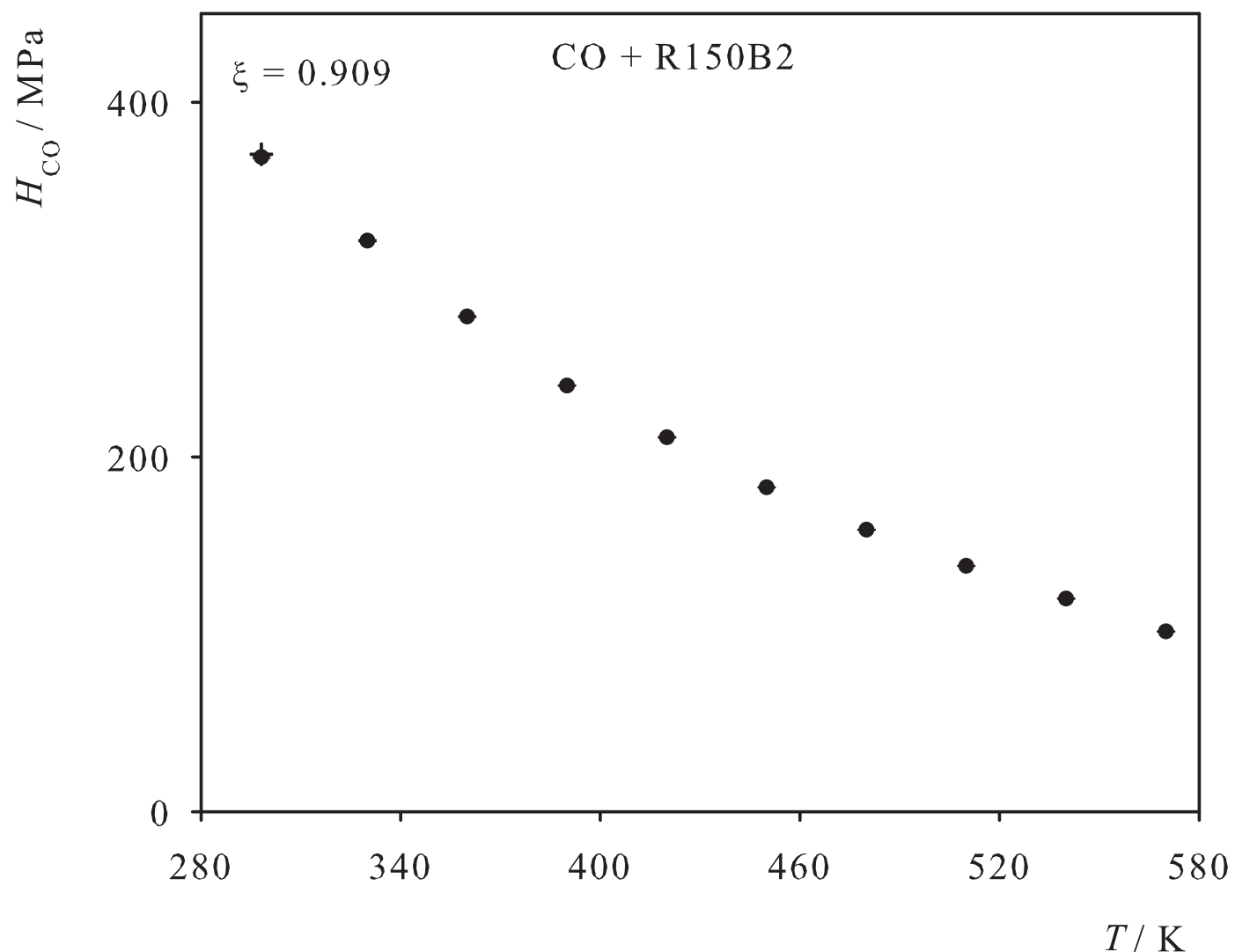


Fig. 85. Henry's law constant of O<sub>2</sub> in liquid R1110. Simulation data: ●; experimental data: + [29], ■ [28].

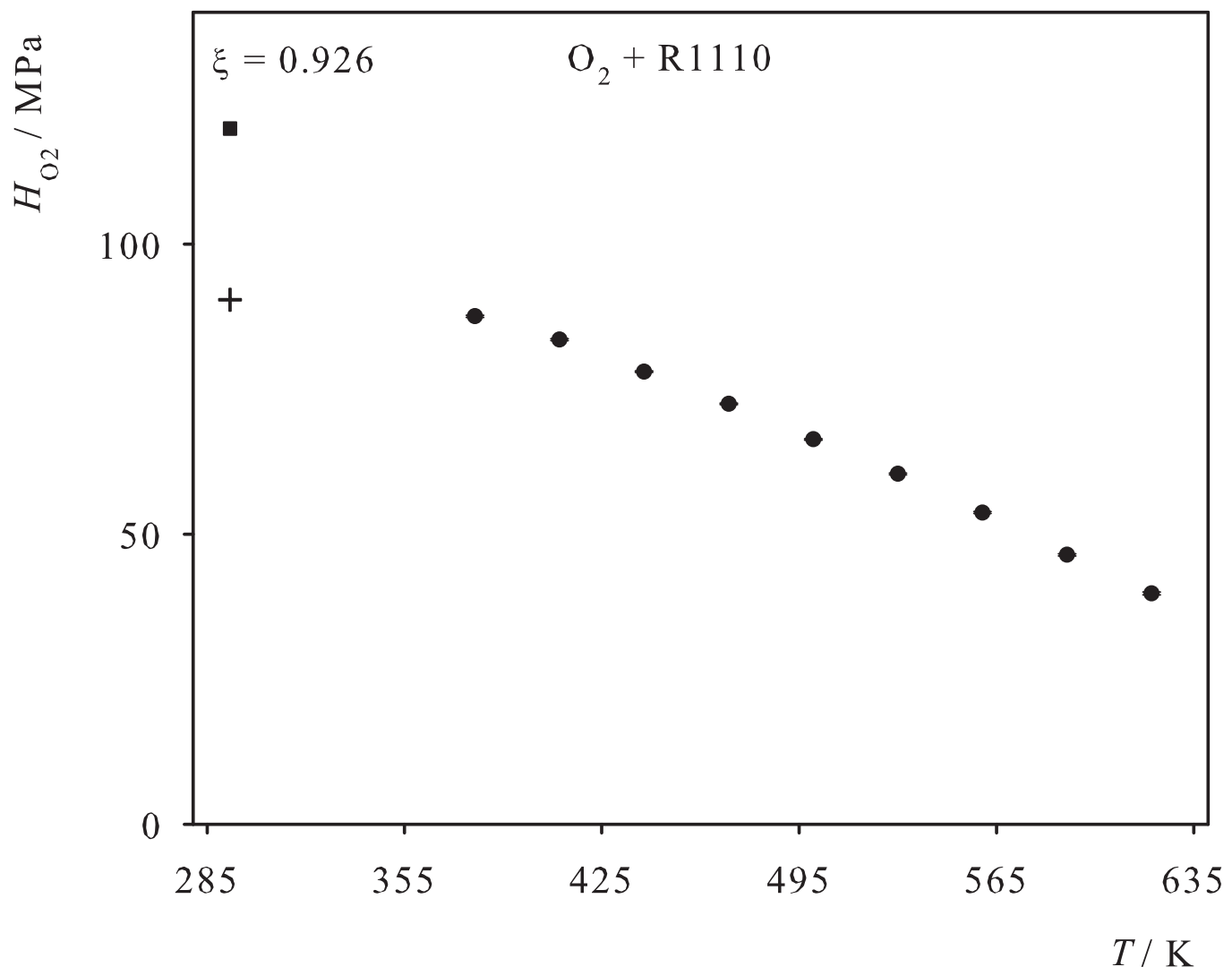


Fig. 86. Henry's law constant of Propylene in liquid R1110. Simulation data: ●; experimental data: + [41].

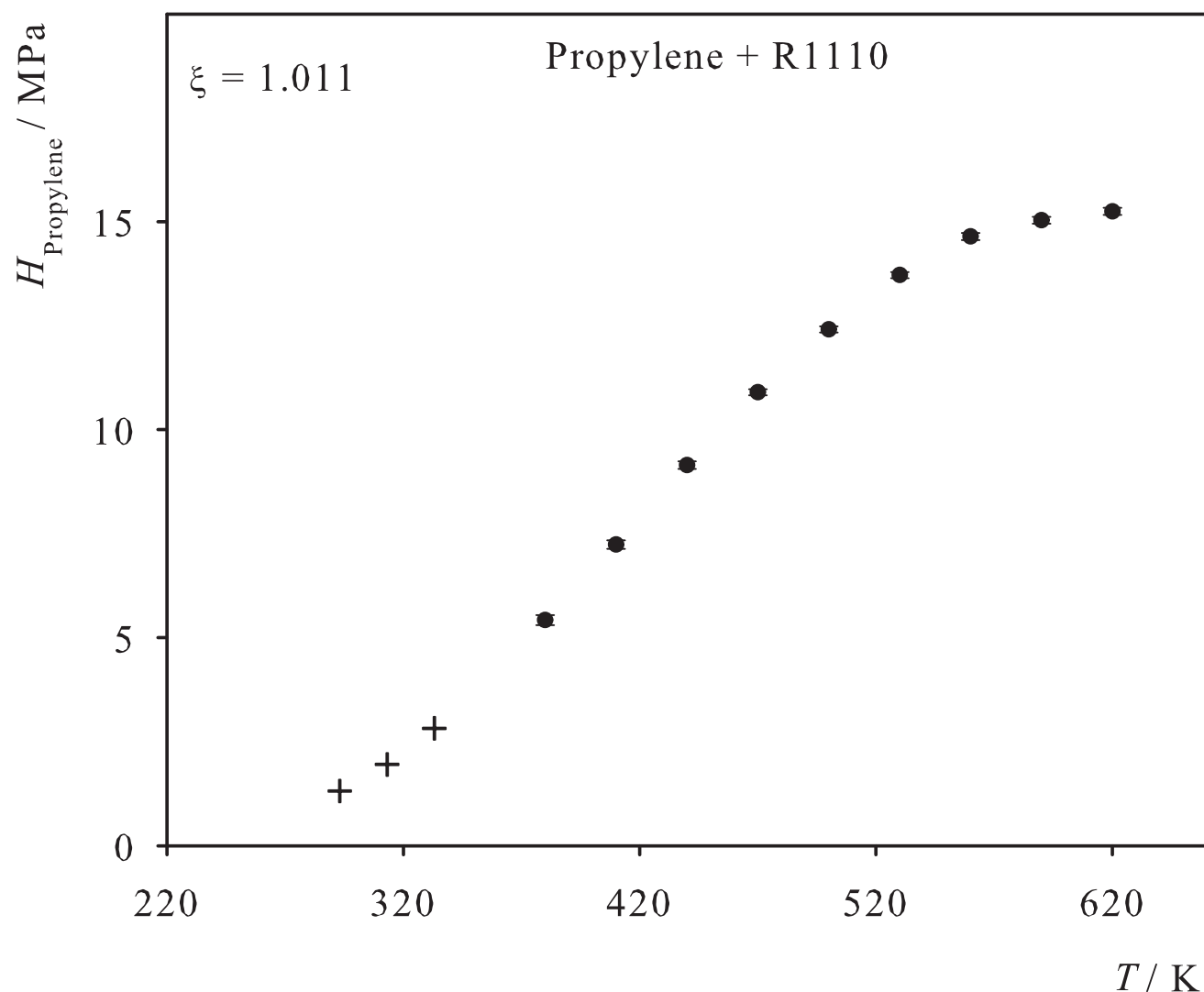


Fig. 87. Henry's law constant of R23 in liquid R1110. Simulation data: ●; experimental data: + [45], ■ [46].

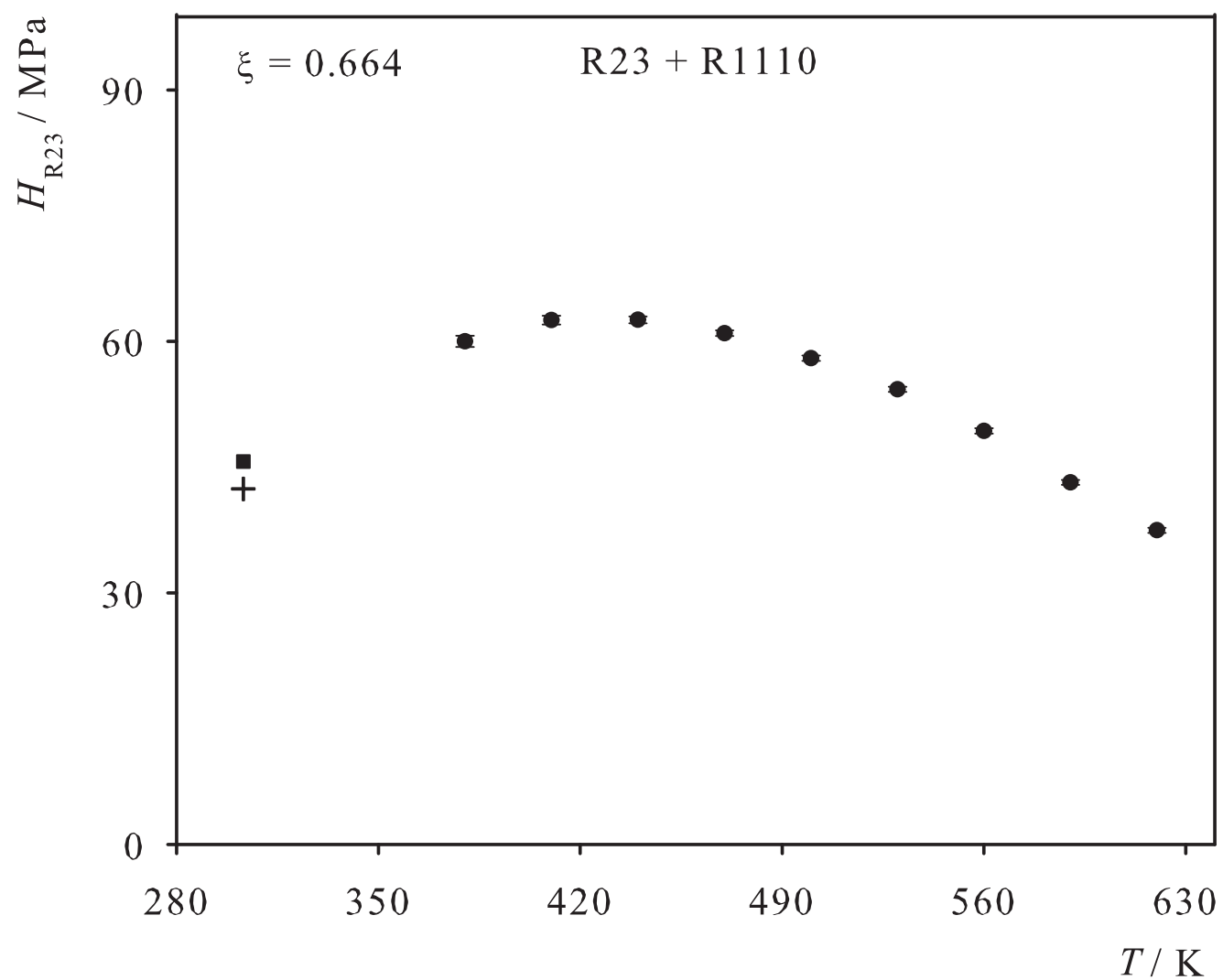


Fig. 88. Henry's law constant of O<sub>2</sub> in liquid R1120. Simulation data: ●; experimental data: + [29].

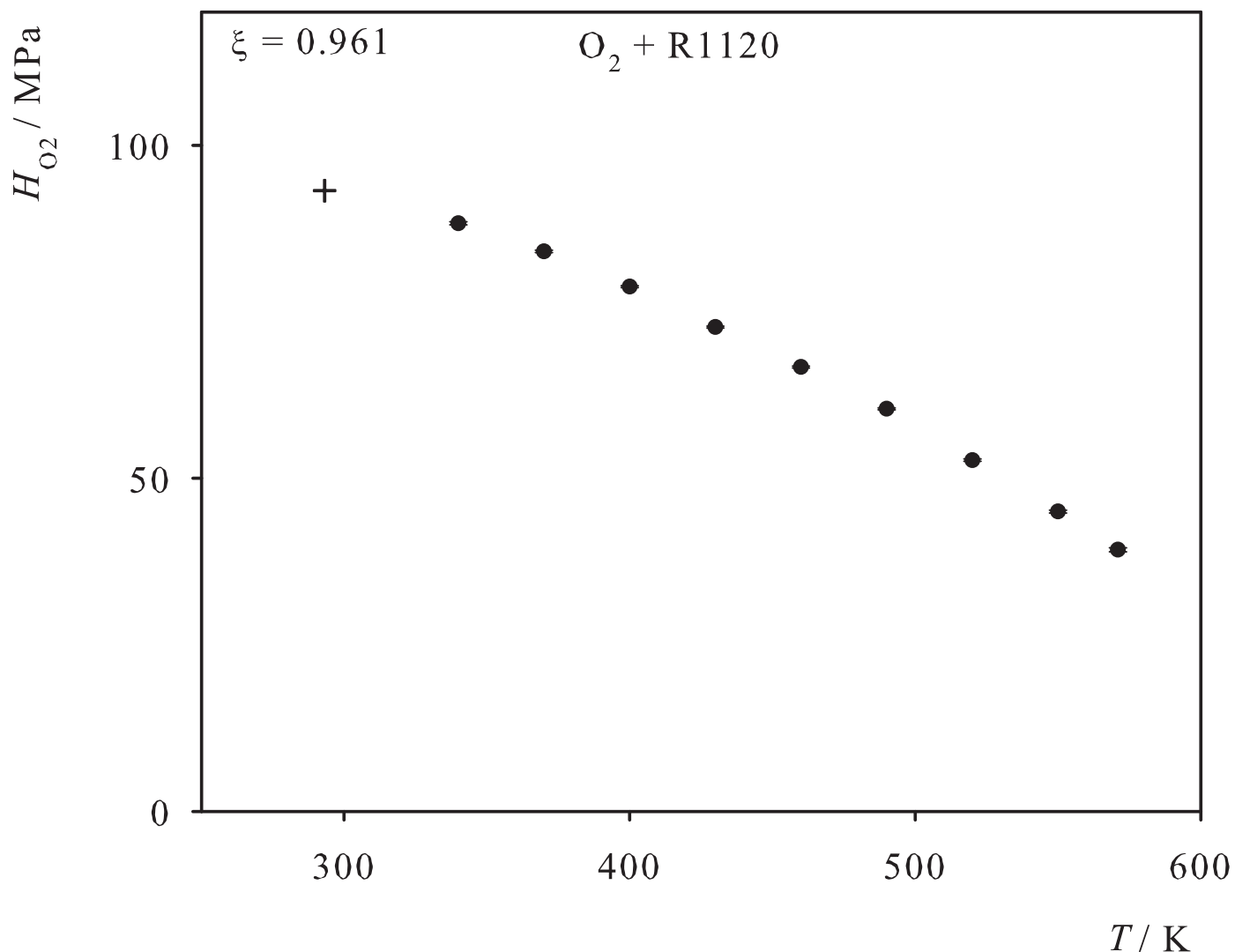


Fig. 89. Henry's law constant of CO<sub>2</sub> in liquid R1120. Simulation data: ●; experimental data: + [74].

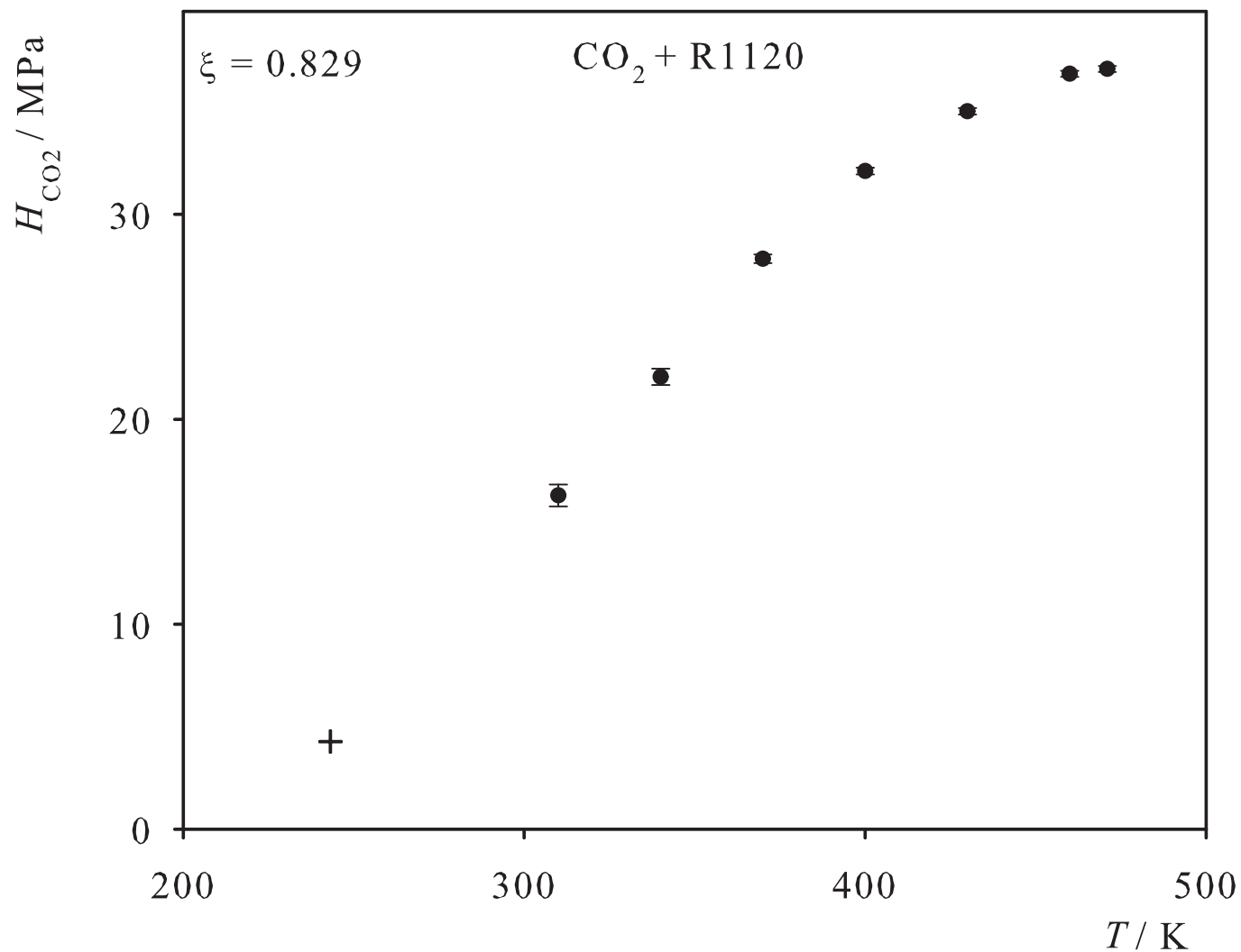


Fig. 90. Henry's law constant of C<sub>2</sub>H<sub>2</sub> in liquid R1120. Simulation data: ●; experimental data: + [74].

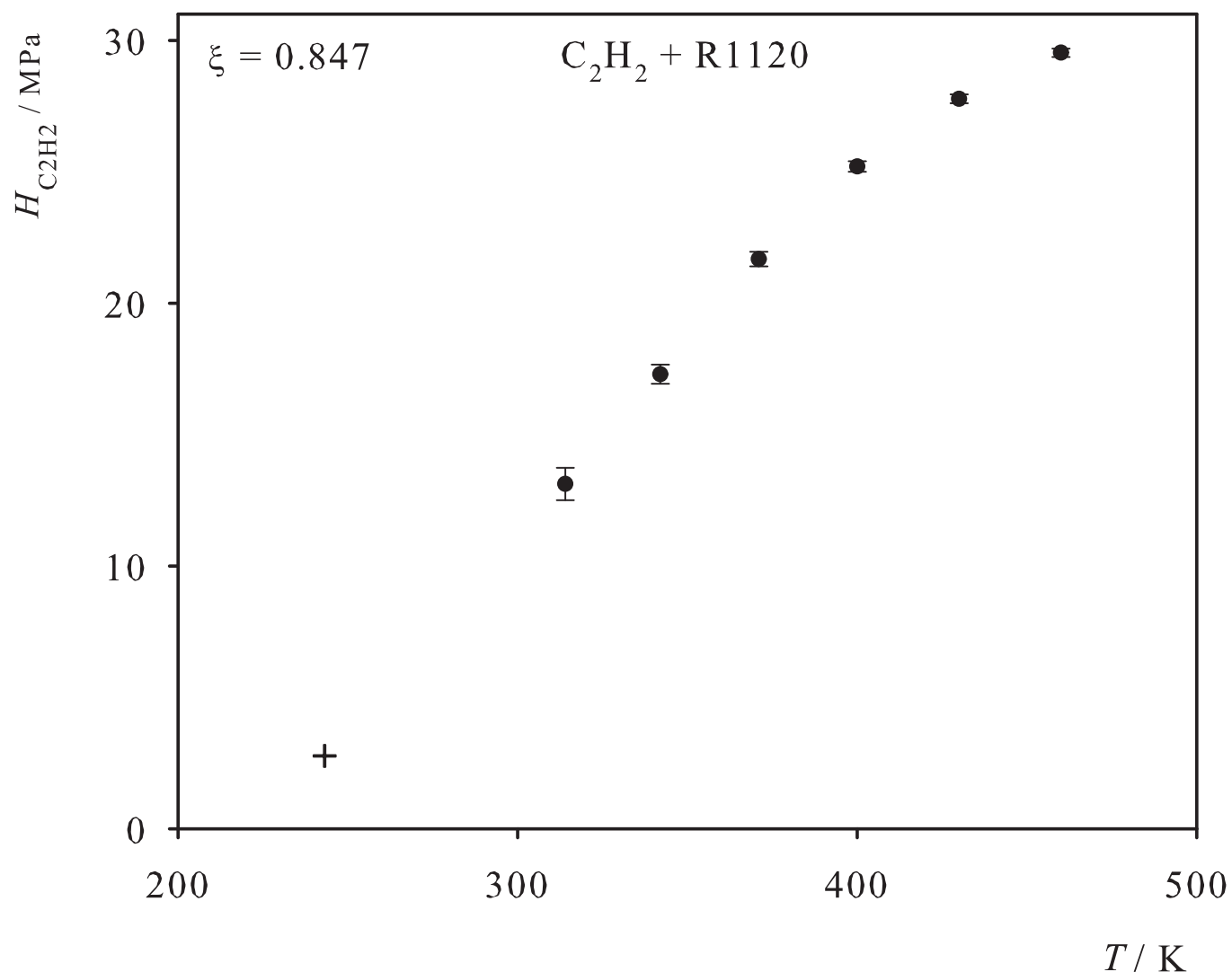


Fig. 91. Henry's law constant of Propylene in liquid R1120. Simulation data: ●; experimental data: + [75], ■ [41].

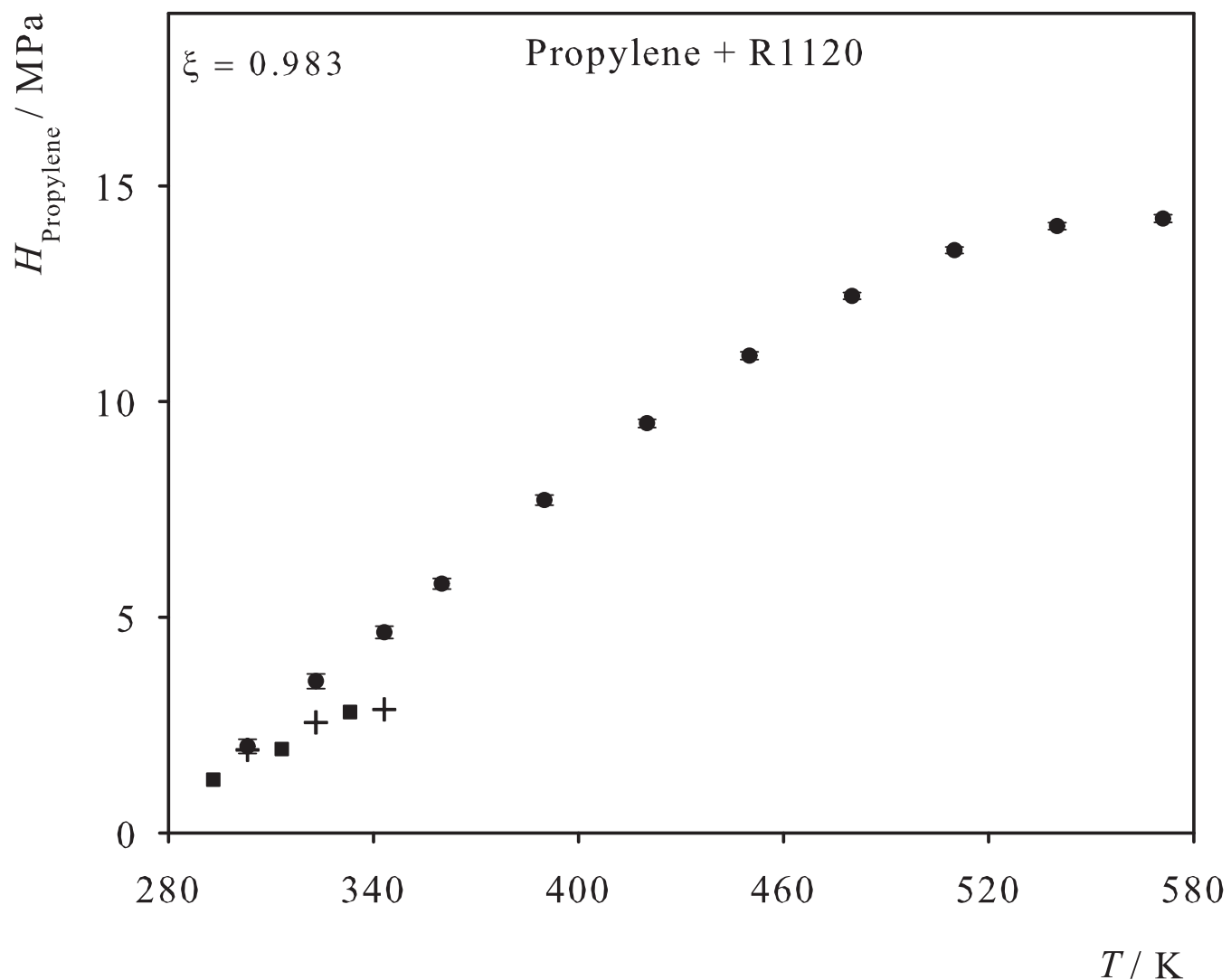
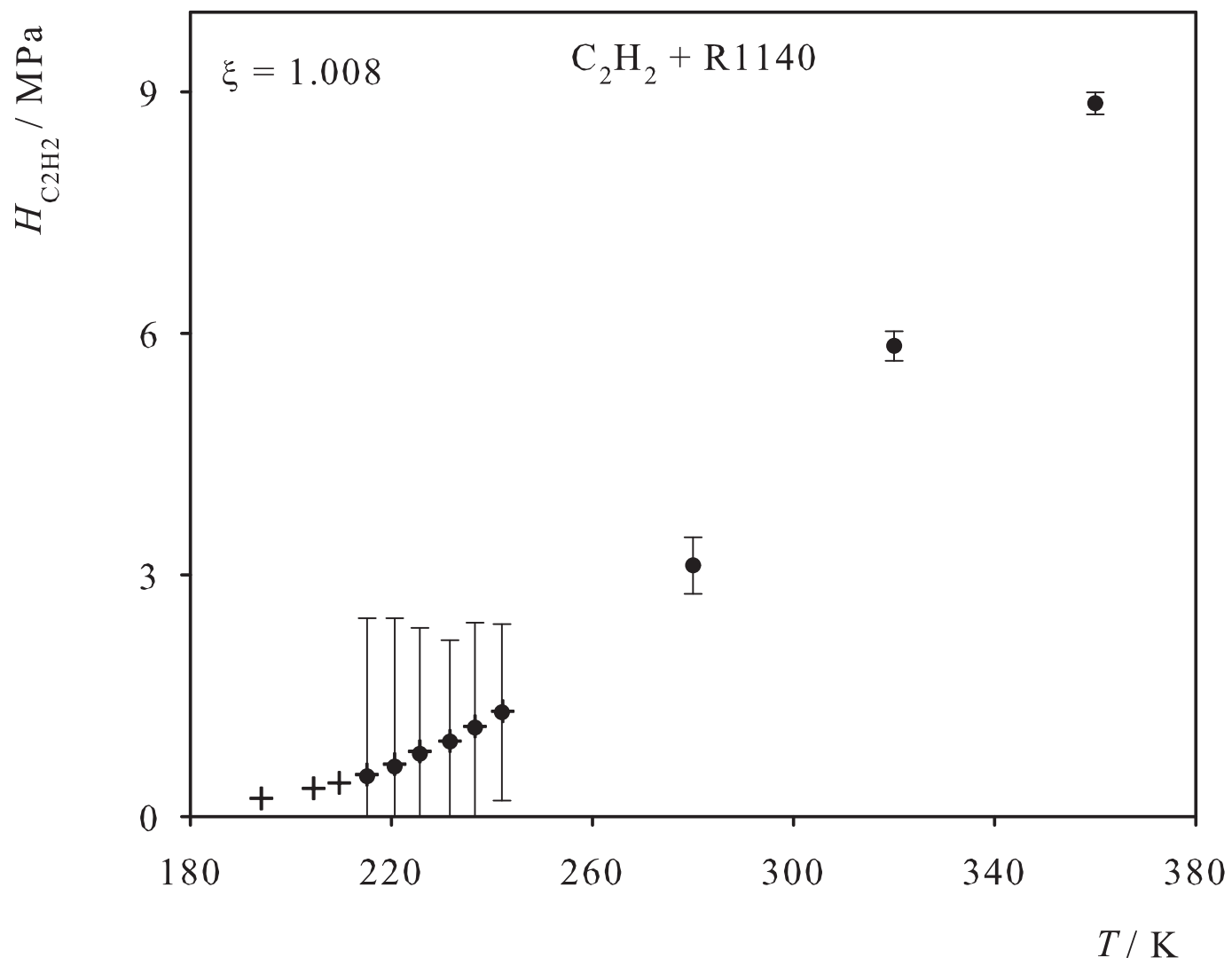


Fig. 92. Henry's law constant of C<sub>2</sub>H<sub>2</sub> in liquid R1140. Simulation data: ●; experimental data: + [71].



## References

- [1] Vrabec J., Huang Y. L. and Hasse H., "Molecular models for 267 binary mixtures validated by vapor-liquid equilibr.: A systematic approach", *Fluid Phase Equilibria* **279**, 120-135 (2009).
- [2] Gmehling J., Rarey J. and Menke J., *Dortmunder Datenbank, Mixture Properties*, Version 1.3.0.211 (2004).
- [3] Krieve W. F. and Mason D. M., "The soulubility of chlorine in titanium tetrachlorine and of carbon dioxine and oxygen in chlorine", *J. Phys. Chem.* **60**, 374-374 (1956).
- [4] Ackley R. D. and Notz K. J., "Distribution of xenon between gaseous and liquid CO<sub>2</sub>", Technical Report ORNL-5122, Oak Ridge National Lab. TN (USA), 1-35 (1976).
- [5] Fredenslund A., Mollerup J. and Persson O., "Gas-Liquid Equilibrium of Oxygen-Carbon Dioxide System", *J. Chem. Eng. Data* **17**, 440-443 (1972).
- [6] Gjaldbaek J. C. and Niemann H., "The Solubility of Nitrogen, Argon and Ethane in Alcohols and Water", *Acta Chem. Scand.* **12**, 611-614 (1958).
- [7] Reeves L. W. and Hildebrand J. H., "The Solubility and Entropy of Solution of Argon in Five Selected Non-polar Solvents", *J. Am. Chem. Soc.* **79**, 1313-1314 (1957).
- [8] Powell R. J., "Solubility of 16 gases in (C<sub>4</sub>H<sub>9</sub>)<sub>3</sub>N and CS<sub>2</sub>", *J. Chem. Eng. Data* **17**, 302-304 (1972).
- [9] Kobatake Y. and Hildebrand J. H., "Solubility and entropy of solution of He, N<sub>2</sub>, Ar, O<sub>2</sub>, CH<sub>4</sub>, C<sub>2</sub>H<sub>6</sub>, CO<sub>2</sub> and SF<sub>6</sub> in various solvents", *J. Phys. Chem.* **65**, 331-334 (1961).
- [10] Gjaldbaek J. C. and Hildebrand J. H., "The Solubility of Nitrogen in Carbon Disulfide, Benzene, Normal- and Cyclo-hexane, and in Three Fluorocarbons", *J. Am. Chem. Soc.* **71**, 3147-3150 (1949).
- [11] Gjaldbaek J. C., "The solubility of hydrogen, oxygen, and carbon monoxide in some non-polar solvents", *Acta Chem. Scand.* **6**, 623-633 (1952).
- [12] Raskina A. D., Zetkin V. I., Zakharov E. V., Kolesnikov I. M. and Kosorotov V. I., "Solubility of chlorine in carbon disulfide and products of its chlorination", *J. Appl. Chem. (USSR)* **45**, 1374-1375 (1972).
- [13] Gjaldbaek J. C., "The Solubility of Carbon Dioxide in Perfluoro-n-heptane, Normal Heptane, Cyclo-hexane, Carbon Tetrachloride, Benzene, Carbon Disulphide and Aqueous Solution of Aerosol", *Acta Chem. Scand.* **7**, 537-544 (1953).
- [14] Miyano Y. and Hayduk W., "Solubility of acetylene in several polar and non-polar solvents and solvent mixtures", *Can. J. Chem. Eng.* **59**, 746-751 (1981).
- [15] Sahgal A., La H. M. and Hayduk W., "Solubility of ethylene in several polar and non-polar solvents", *J. Chem. Eng.* **56**, 354-357 (1978).
- [16] Archer G. and Hildebrand J. H., "The soulbility and entropy of solution of carbon tetrafluorine and sulfur hexaflourine in nonpolar solvents", *J. Phys. Chem.* **67**, 1830-1833 (1963).

- [17] Blagoi Yu. P. and Orobinskii N. A., "Liquid-vapor phase equilibrium in the propylene-nitrogen system", Russ. J. Phys. Chem. **39**, 1073-1074 (1965).
- [18] Miller H. C., Verdelli L. S. and Gall J. F., "Some Physical Properties of Sulfur Hexafluoride", Ind. Eng. Chem. **43**, 1126-1129 (1951).
- [19] Tominaga T., Battino R., Gorowara H. K., Dixon R. D. and Wilhelm E., "Solubility of gases in liquids. 17. The solubility of helium, neon, argon, krypton, hydrogen, nitrogen, oxygen, carbon monoxide, methane, carbon tetrafluoride, and sulfur hexafluoride in tetrachloromethane at 283 to 318 K", J. Chem. Eng. Data **31**, 175-180 (1986).
- [20] Graham E. B. and Weale K. E., "The solubility of compressed gases in nonpolar liquids", Prog. Int. Res. Therm. Trans. Prop., 153-158 (1962).
- [21] Körösy F., "Two rules concerning solubility of gases and crude data on solubility of krypton", Trans. Faraday Soc. **33**, 416-425 (1937).
- [22] Lannung A. and Gjaldbaek J. C., "Solubility of methane in hydrocarbons, alcohols, water and other solvents", Acta Chem. Scand. **14**, 1124-1128 (1960).
- [23] Akimoto T., Nitta T. and Katayama T., "Nitrogen solubility and vapor pressure of binary mixed solvents containing benzene, carbon tetrachloride, cyclohexane and 1-hexane", J. Chem. Eng. (Japan) **17**, 637-641 (1984).
- [24] Gorbachev V. M. and Tretyakov T. V., "Determination of the Solubility of Oxygen and Nitrogen in  $\text{CH}_3\text{SiCl}_3$ ,  $\text{SiCl}_4$  and  $\text{GeCl}_4$  using Gas-Liquid Chromatography", Zavod. Lab. (USSR) **32**, 796-798 (1966).
- [25] Wolfe J. K., "Solubility of Air in Freon-12 and Freon-22", Refrig. Eng. **59**, 704-706 (1951).
- [26] Luehring P. and Schumpe A., "Gas Solubilities in organic liquids at 293.2 K", J. Chem. Eng. Data **34**, 250-252 (1989).
- [27] Naumenko N. K., "Investigation on the Solubility of Oxygen in Organic Solvents", Thesis, 3-11 (1970).
- [28] Schlaepfer P., Audykowski T. and Bukowiecki A., "Über die Lösungsgeschwindigkeit des Sauerstoffs in verschiedenen Flüssigkeiten", Schweizer Archiv für Wiss. u. Technik **15**, 299-307 (1949).
- [29] Sinn E., Matthes K. and Naumann E., "Experimentelle Untersuchungen über die Löslichkeit von Sauerstoff in flüssigen organischen Substanzen", Wiss. Z. Friedrich-Schiller-Univ. Jena, Math.-Naturwiss. R. **16**, 523-529 (1967).
- [30] Vdovichenko V. T. and Kondratenko V. I., "Solubilities of chlorine and hydrogen chloride in chloromethanes and of methyl chloride in anisole", Khim. Prom. (USSR) **43**, 290-291 (1967).
- [31] Kogan L. M., Koltsov N. S. and Litvinov N. D., "Apparatus for Determining Solubility of Chlorine and other Gas in Liquids", Russ. J. Phys. Chem. **37**, 1040-1042 (1963).
- [32] Smith T. L., "The Solubility of Chlorine in Carbon Tetrachloride", J. Phys. Chem. **59**, 188-189 (1955).

- [33] Blair C. M. and Yost D. M., "The Thermodynamic Constants of Iodine Monochloride, Iodine Monobromide and Bromine Monochloride in Carbon Tetrachloride", *J. Am. Chem. Soc.* **55**, 4489-4496 (1933).
- [34] Taylor N. W. and Hildebrand J. H., "Solubility. VIII. Solubility Relations of Certain Gases", *J. Am. Chem. Soc.* **45**, 682-694 (1923).
- [35] Just G., "Löslichkeit von Gasen in organischen Lösungsmitteln", *Z. Phys. Chem. (Leipzig)* **37**, 342-367 (1901).
- [36] Takahashi M., Kobayashi Y. and Takeuchi H., "Diffusion coefficients and solubilities of carbon dioxide in binary mixed solvents", *J. Chem. Eng. Data* **27**, 328-331 (1982).
- [37] Hsu H. and Campbell D., "Formulations With Soluble Gas Propellants", *Aerosol Age* **9**, 34-139 (1964).
- [38] Takeuchi H., Fujine M., Sato T. and Onda K., "Simultaneous Determination of Diffusion Coefficient and Solubility of Gas in Liquid by a Diaphragm Cell", *J. Chem. Eng. (Japan)* **8**, 252-253 (1975).
- [39] Brueckl N. and Kim J. I., "Gibbs free energies of solute-solvent interactions for He, Ne, Ar, Kr, Xe, H<sub>2</sub>, O<sub>2</sub>, N<sub>2</sub>, CH<sub>4</sub>, SF<sub>6</sub>, C<sub>2</sub>H<sub>4</sub>", *Z. Phys. Chem., Neue Folge* **126**, 133-150 (1981).
- [40] Jadot R., "Determination of Henry constants by chromatography", *J. Chim. Phys. Phys.-Chim. Biol.* **6**, 1036-1040 (1972).
- [41] Konobeev B. I. and Lyapin V. V., "Solubility of Ethylene and Propylene in Organic Solvents", *Khim. Prom. (USSR)* **43**, 114-116 (1967).
- [42] Hayduk W. and Cheng S. C., "Solubilities of ethane and other gases in normal paraffin solvents", *Can. J. Chem. Eng.* **48**, 93-99 (1970).
- [43] Wilhelm E. and Battino R., "The solubilities of gases in liquids", *J. Chem. Thermodyn.* **3**, 379-392 (1971).
- [44] Makitra R. G., Pirig Ya. N., Politanskaya T. I. and Moin F. B., "Effect of properties of solvents on solubility of Freon 22", *Russ. J. Phys. Chem.* **55**, 424-426 (1981).
- [45] Anonymous, "Löslichkeit von F23 und HCl in verschiedenen Lösungsmitteln", *Confident. Comp. Res. Rep.*, Rep. No. LC4912 (1970); cf. [2].
- [46] Anonymous, "Löslichkeit von HCl und F23 in verschiedenen Lösungsmitteln", *Confident. Comp. Res. Rep.*, Rep. No. LC4914 (1970); cf. [2].
- [47] Sies P. and Krafczyk J., Unpublished Data, (1992); cf. [2].
- [48] Krafczyk J., Unpublished Data, (1991); cf. [2].
- [49] Mamedaliev Yu. G. and Musakhanly S., "The solubility of chloromethane in some solvents", *Zh. Prikl. Khim. (USSR)* **13**, 735-737 (1940).
- [50] Horiuti J., "The Solubility of Gas and Coefficient of Dilution by Absorption", *Sci. Pap. Inst. Phys. Chem. Res. (Japan)* **17**, 125-256 (1931).

- [51] Makitra R. G., Politanskaya T. I., Moin F. B., Pirig Y. N. and Politanskaya T. S., "Solubility of ethyl fluoride in organic solvents", *J. Appl. Chem. (USSR)* **56**, 2048-2051 (1984).
- [52] Makitra R. G., Moin F. B. and Politanskaya T. I., "Solubility of Fluoroethane in Toluene, Tetrachloromethane and N-Methylpyrrolidone", *J. Phys. Chem. (USSR)* **53**, 572-573 (1979).
- [53] Kriebel M. and Loeffler H. J., "Löslichkeit von gasförmigem F13, F22 und F23 in flüssigem F11", *Kältetechnik* **18**, 34-38 (1966).
- [54] Anonymous, "Löslichkeit von gasförmigem F13, F22 und F23 in flüssigem F11", *Confident. Comp. Res. Rep.*, Rep. No. LC4994 (1969); cf. [2].
- [55] Nitta T., Nakamura Y., Ariyasu H. and Katayama T., "Solubilities of nitrogen in binary solutions of acetone with cyclohexane, benzene, chloroform and 2-propanol", *J. Chem. Eng. (Japan)* **13**, 97-103 (1980).
- [56] Fischer F. and Pfleiderer G., "Über die Löslichkeit von Sauerstoff in verschiedenen organischen Lösungsmitteln", *Z. Anorg. Chem.* **124**, 61-69 (1922).
- [57] Giles N. F., Wilson L. C., Wilson G. M. and Wilding W. V., "Phase equilibria on eight binary mixtures", *J. Chem. Eng. Data* **42**, 1067-1074 (1997).
- [58] Vonderheiden F. H. and Eldridge J. W., "The system carbon dioxide - methylene chloride", *J. Chem. Eng. Data* **8**, 20-21 (1963).
- [59] Doering K. E., "Solubility of methane in methyl chloride", *FIZ Report*, 1201 (1965).
- [60] Linford R. G. and Hildebrand J. H., "Solubility and entropy of solution of gases in  $\text{CCl}_2\text{F}-\text{CClF}_2$ ", *Trans. Faraday Soc.* **66**, 577-581 (1970).
- [61] Hiraoka H. and Hildebrand J. H., "The solubility and entropy of the solution of certain gases in  $(\text{C}_4\text{H}_9)_3\text{N}$ ,  $\text{CCl}_2\text{F}-\text{CCl}_2\text{F}_2$ , and  $2,2,4-(\text{CH}_3)_3\text{C}_5\text{H}_9$ ", *J. Phys. Chem.* **68**, 213-214 (1964).
- [62] Sokolov Y. P. and Konshin A. I., "Study of solubility of ethylene and tetrafluoroethylene in perhalogenated solvents under pressure", *J. Appl. Chem. (USSR)* **62**, 1310-1312 (1989).
- [63] Armitage D. A., Linford R. G. and Thornhill D. G. T., "Appratus for accurately and rapidly measuring the solubility of gases in liquid mixtures", *Ind. Eng. Chem. Fundam.* **17**, 362-364 (1978).
- [64] Linford R. G. and Hildebrand J. H., "Solubility of gases in mixtures of nonpolar liquids", *J. Phys. Chem.* **73**, 4410-4411 (1969).
- [65] Jaster H. and Kosky P. G., "Solubility of sulphur hexafluoride in fluorocarbon liquids", *J. Chem. Eng. Data* **21**, 66-71 (1976).
- [66] Sokolov Yu. A., Konshin A. I. and Sokolov S. V., "Study of solubility of tetrafluoroethylene and vinylidene fluoride in Freon 113 under pressure", *J. Appl. Chem. (USSR)* **60**, 2523-2525 (1988).
- [67] Williams V. D., "Solubility of Nitrogen in Freon-144", *J. Chem. Eng. Data* **4**, 92-93 (1959).

- [68] Efstigneev O. V., Santimova M. B., Dunaev S. G. and Levanova S. B., "Solubility of chlorine in polychloroalkanes", Khim. Prom. (USSR) **6**, 342-343 (1985).
- [69] Makitra R. G., Moin F. B., Pirig Ya. N. and Politanskaya T. I., "Solubility of acetylene in some haloethanes", J. Appl. Chem. (USSR) **60**, 663-665 (1987).
- [70] Makitra R. G., Moin F. B., Pirig Ya. N. and Politanskaya T. I., "Solubility of vinyl chloride in tri- and tetrachloroethanes", J. Appl. Chem. (USSR) **62**, 2567-2571 (1990).
- [71] Danov S. M. and Golubev Yu. D., "Solubility of acetylene and hydrogen chloride in vinyl chloride, 1,1-dichloroethane, and trans-1,2-dichloroethylene", Khim. Prom. (USSR) **44**, 116-120 (1968).
- [72] Gjaldbaek J. C. and Anderson E. K., "The solubility of carbon dioxide, oxygen, carbon monoxide, and nitrogen in polar solvents", Acta Chem. Scand. **8**, 1398-1413 (1954).
- [73] Begley J. W., Maget H. J. R. and Williams B., "Solubility of Carbon Dioxide in Cyclohexanol, 1,2-Dibromoethane, a Mixture of 1-Chloro-2-bromopropane and 2-Chloro-1-bromopropane, and Mineral Oil", J. Chem. Eng. Data **10**, 4-8 (1965).
- [74] Otsuka E. and Takada M., "Purification of acetyls formed in combustion gases by partial oxidation of methane. I. Investigation of the solubility of acetylene and carbon dioxide in methanol and selectivity for carbon dioxide", Nenryo-Kyokai-shi **42**, 229-237 (1963).
- [75] Guzechak O. Y., Sarancha V. N., Romanyuk I. M., Yavorskaya O. M. and Churik G. P., "Gasometric method for studying liquid-phase epoxidation of propylene by organic peroxides", J. Appl. Chem. (USSR) **57**, 1662-1665 (1985).